GEOLOGICAL SURVEY OF CANADA
COMMISSION GÉOLOGIQUE DU CANADA

CURRENT RESEARCH 1994-B
INTERIOR PLAINS AND ARCTIC CANADA

RECHERCHES EN COURS 1994-B
PLAINES INTÉRIEURES ET RÉGION ARCTIQUE DU CANADA

1994

Natural Resources Canada Ressources naturelles Canada

Canada

NOTICE TO LIBRARIANS AND INDEXERS

The Geological Survey's Current Research series contains many reports comparable in scope and subject matter to those appearing in scientific journals and other serials. Most contributions to Current Research include an abstract and bibliographic citation. It is hoped that these will assist you in cataloguing and indexing these reports and that this will result in a still wider dissemination of the results of the Geological Survey's research activities.

AVIS AUX BIBLIOTHÉCAIRES ET PRÉPARATEURS D'INDEX

La série Recherches en cours de la Commission géologique contient plusieurs rapports dont la portée et la nature sont comparables à ceux qui paraissent dans les revues scientifiques et autres périodiques. La plupart des articles publiés dans Recherches en cours sont accompagnés d'un résumé et d'une bibliographie, ce qui vous permettra, on l'espère, de cataloguer et d'indexer ces rapports, d'où une meilleure diffusion des résultats de recherche de la Commission géologique.

GEOLOGICAL SURVEY OF CANADA
COMMISSION GÉOLOGIQUE DU CANADA

CURRENT RESEARCH 1994-B

INTERIOR PLAINS AND ARCTIC CANADA

RECHERCHES EN COURS 1994-B

PLAINES INTÉRIEURES ET RÉGION ARCTIQUE DU CANADA

1994

Available in Canada through
authorized bookstore agents and other bookstores

or by mail from

Canada Communication Group - Publishing
Ottawa, Canada K1A 0S9

and from

Geological Survey of Canada offices:

601 Booth Street
Ottawa, Canada K1A 0E8

3303-33rd Street N.W.,
Calgary, Alberta T2L 2A7

100 West Pender Street
Vancouver, B.C. V6B 1R8

A deposit copy of this publication is also available for reference
in public libraries across Canada

Cat. No. M44-1994/2
ISBN 0-660-58986-9

Price subject to change without notice

Cover description

The main 49th Parallel minette dyke, looking northeast with the Milk River valley and Oldman and Foremost formations in the background. For more information on potassic magmatism in the Milk River area, see paper by Kjarsgaard, p. 59-68. (photo by B.A. Kjarsgaard. GSC 1993-305E)

Description de la photo couverture

Photo prise vers le nord-est montrant le principal dyke de minette présent au niveau du 49^{e} parallèle et, à l'arrière-plan, la vallée de la rivière Milk ainsi que les formations d'Oldman et de Foremost. Le lecteur intéressé à obtenir plus d'information sur le magmatisme potassique dans la région de la rivière Milk est renvoyé à l'article de Kjarsgaard, à la page 59-68. (photo de B.J. Kjarsgaard, GSC 1993-305E)

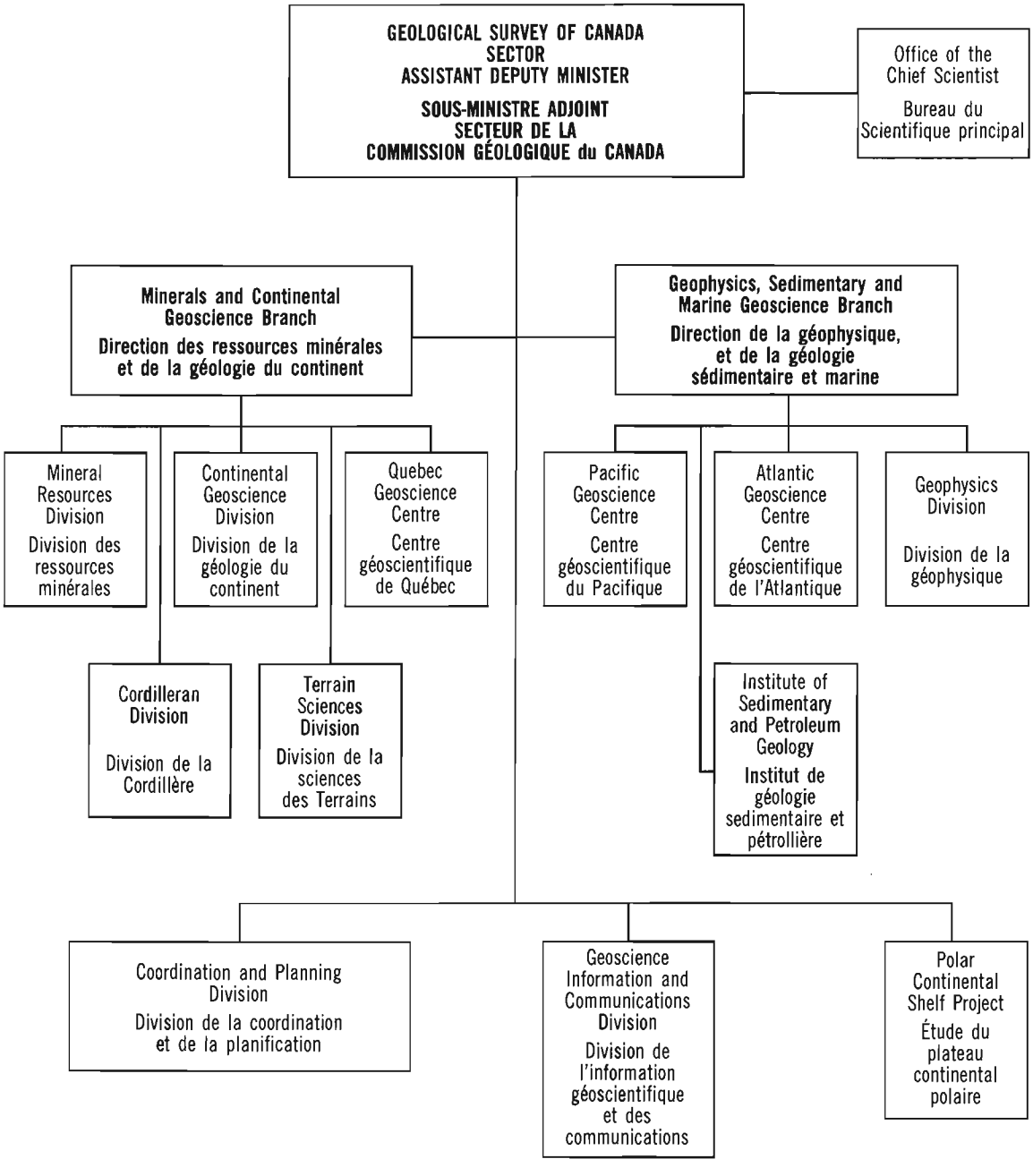
GEOLOGICAL SURVEY OF CANADA
SECTOR
ASSISTANT DEPUTY MINISTER
SOUS-MINISTRE ADJOINT
SECTEUR DE LA
COMMISSION GÉOLOGIQUE du CANADA
Office of the Chief Scientist
Bureau du Scientifique principal
Minerals and Continental Geoscience Branch
Direction des ressources minérales et de la géologie du continent
Geophysics, Sedimentary and Marine Geoscience Branch
Direction de la géophysique, et de la géologie sédimentaire et marine
Mineral Resources Division
Division des ressources minérales
Continental Geoscience Division
Division de la géologie du continent
Quebec Geoscience Centre
Centre géoscientifique de Québec
Pacific Geoscience Centre
Centre géoscientifique du Pacifique
Atlantic Geoscience Centre
Centre géoscientifique de l'Atlantique
Geophysics Division
Division de la géophysique
Cordilleran Division
Division de la Cordillère
Terrain Sciences Division
Division de la sciences des Terrains
Institute of Sedimentary and Petroleum Geology
Institut de géologie sedimentaire et pétrollière
Coordination and Planning Division
Division de la coordination et de la planification
Geoscience Information and Communications Division
Division de l'information géoscientifique et des communications
Polar Continental Shelf Project
Étude du plateau continental polaire

Separates

A limited number of separates of the papers that appear in this volume are available by direct request to the individual authors. The addresses of the Geological Survey of Canada offices follow:

601 Booth Street
OTTAWA, Ontario
K1A 0E8
(FAX: 613-996-9990)

Institute of Sedimentary and Petroleum Geology
3303-33rd Street N.W.
CALGARY, Alberta
T2L 2A7
(FAX: 403-292-5377)

Cordilleran Division
100 West Pender Street
VANCOUVER, B.C.
V6B 1R8
(FAX: 604-666-1124)

Pacific Geoscience Centre
P.O. Box 6000
9860 Saanich Road
SIDNEY, B.C.
V8L 4B2
(Fax: 604-363-6565)

Atlantic Geoscience Centre
Bedford Institute of Oceanography
P.O. Box 1006
DARTMOUTH, N.S.
B2Y 4A2
(FAX: 902-426-2256)

Québec Geoscience Centre
2700, rue Einstein
C.P. 7500
Ste-Foy (Québec)
G1V 4C7
(FAX: 418-654-2615)

When no location accompanies an author's name in the title of a paper, the Ottawa address should be used.

Tirés à part

On peut obtenir un nombre limité de «tirés à part» des articles qui paraissent dans cette publication en s'adressant directement à chaque auteur. Les adresses des différents bureaux de la Commission géologique du Canada sont les suivantes:

601, rue Booth
OTTAWA, Ontario
K1A 0E8
(facsimilé : 613-996-9990)

Institut de géologie sédimentaire et pétrolière
3303-33rd St. N.W.,
CALGARY, Alberta
T2L 2A7
(facsimilé : 403-292-5377)

Division de la Cordillère
100 West Pender Street
VANCOUVER, British Columbia
V6B 1R8
(facsimilé : 604-666-1124)

Centre géoscientifique du Pacifique
P.O. Box 6000
9860 Saanich Road
SIDNEY, British Columbia
V8L 4B2
(facsimilé : 604-363-6565)

Centre géoscientifique de l'Atlantique
Institut océanographique Bedford
B.P. 1006
DARTMOUTH, Nova Scotia
B2Y 4A2
(facsimilé : 902-426-2256)

Centre géoscientifique de Québec
2700, rue Einstein
C.P. 7500
Ste-Foy (Québec)
G1V 4C7
(facsimilé : 418-654-2615)

Lorsque l'adresse de l'auteur ne figure pas sous le titre d'un document, on doit alors utiliser l'adresse d'Ottawa.

Contents

Persistent organic compounds in the Barents Sea: Canada-Russia collaboration on arctic pollutants

D.N. Skibo and W.W. Nassichuk
Institute of Sedimentary and Petroleum Geology, Calgary

Skibo, D.N. and Nassichuk, W.W., 1994: Persistent organic compounds in the Barents Sea: Canada-Russia collaboration on arctic pollutants; in Current Research 1994-B; Geological Survey of Canada, p. 1-9.

Abstract: In 1991, Project 10, a new initiative on anthropogenic contaminants in the Arctic Ocean, commenced within the Canada-Russia Agreement on Cooperation in the Arctic and the North. The purpose of the project is to determine the distribution and concentration of trace and heavy metals, radionuclides, persistent organic toxins, and mutagenic and carcinogenic compounds in seafloor sediments off Arctic Canada and Siberia. During 1992 and 1993, several hundred samples were taken from the Barents Sea. Forty samples, representing an areal distribution and several depth profiles in the sediments, have been analyzed for: 1) polychlorinated biphenyls (PCBs); 2) organochlorine pesticides [chlorobenzenes, hexachlorocyclohexanes (HCHs), chlordanes, nonachlors, DDTs, Mirex]; and 3) polycyclic aromatic hydrocarbons (PAHs). Total PAHs and total organic carbon (TOC) from sediments at or near the seabed are found to be positively correlated to water column depth. However, purely anthropogenic contaminants (PCBs and OC pesticides) show no such correlation.

Résumé : En 1991, le projet 10, nouvelle initiative portant sur les contaminants anthropogènes dans l'océan Arctique, a débuté dans le cadre de l'Accord canado-russe de coopération dans l'Arctique et le Nord. Le but du projet est de déterminer la distribution et la concentration des métaux traces et lourds, des radionucléides, des toxines organiques persistantes, et des composés mutagènes et carcinogènes dans les sédiments du fond marin au large des côtes arctiques du Canada et de la Sibérie. En 1992 et 1993, plusieurs centaines d'échantillons ont été prélevés dans la mer de Barents. La composition de 40 échantillons, représentatifs de la distribution spatiale et de plusieurs profils de concentration dans les sédiments, a été analysée : (1) polychlorobiphényles (PCB); (2) pesticides organochlorés [chlorobenzènes, hexachlorocyclohexanes (HCH), chlordanes, nonachlores, DDT, Mirex]; et (3) hydrocarbures aromatiques polycycliques (HAP). Il existe une corrélation positive entre les HAP totaux et le carbone organique total (COT) dans les sédiments ou près du fond marin et la profondeur de la tranche d'eau. Toutefois, les contaminants purement anthropogènes (PCB et pesticides OC) ne présentent pas une telle corrélation.

INTRODUCTION

In 1984, the Canada-Russia Agreement on Cooperation in the Arctic and the North was initiated for collaborative projects on geology, geophysics, and geochemistry. A number of important maps and reports, co-authored by Russian and Canadian scientists have resulted from the Agreement. Increasing concerns about the environmental consequences of exploration for and exploitation of oil, gas, and mineral resources, particularly in Siberia, led to the initiation of the environmental project discussed herein. Indeed, the entire Arctic has become a focus for studies of global climate and environmental contamination.

The United States has also initiated activities dealing with contamination of the Arctic environment. The U.S. Arctic Research and Policy Act of 1984 led to the formation of the Interagency Arctic Research Policy Committee (IARPC) composed of fourteen United States Federal agencies that conduct or manage research in the Arctic. Presently, the major issue of concern to IARPC member agencies is contamination in the Arctic. This has been expressed in the Policy Statement on Arctic Contamination (August 27, 1992) and the Agenda for Action to Implement the Policy Statement on Arctic Contamination (November 25, 1992). Both documents were presented in May, 1993 at the IARPC-convened Workshop on Arctic Contamination, in Anchorage, Alaska. The main contaminant categories of concern were radionuclides, trace and heavy metals, and chronic organic and organochlorine compounds. The workshop marked the first wide-scale distribution of the full-text English translation of the Yablokov Commission Report, Facts and Problems Related to Radioactive Waste Disposal in Seas Adjacent to the Territory of the Russian Federation, prepared for Russian President Boris N. Yeltsin, (Yablokov et al., 1993). In recognition of the global significance of the Arctic environment, the workshop participants represented agencies from many countries including several member countries of the Arctic Monitoring and Assessment Program (AMAP).

AMAP was established in 1991 by the "Circum-Polar 8" nations-Canada, Denmark, Finland, Iceland, Norway, Russia, Sweden, and the United States – with the primary objective of measuring levels of anthropogenic pollutants and assessing their effects on the Arctic environment and ecosystem. It was noted in the draft policy statement (AMAP, 1993) that, with few exceptions, pollution data available from the Arctic region are based on national programmes, carried out within limited areas, and not by bilateral or international co-operation. To implement the AMAP, the eight countries have established an Arctic Monitoring and Assessment Task Force (AMATF) and invited, as observers to the Task Force, the international agencies that are involved in significant research and monitoring relevant to the Arctic – IASC, UNEP, UN ECE, ICES, Paris Commission, United Kingdom, Poland, Germany, the Netherlands, and Japan. Representatives from indigenous people have also been nominated as observers – The Inuit Circumpolar Conference, The Nordic Saami Council, and the Russian Association of Small Peoples of the North.

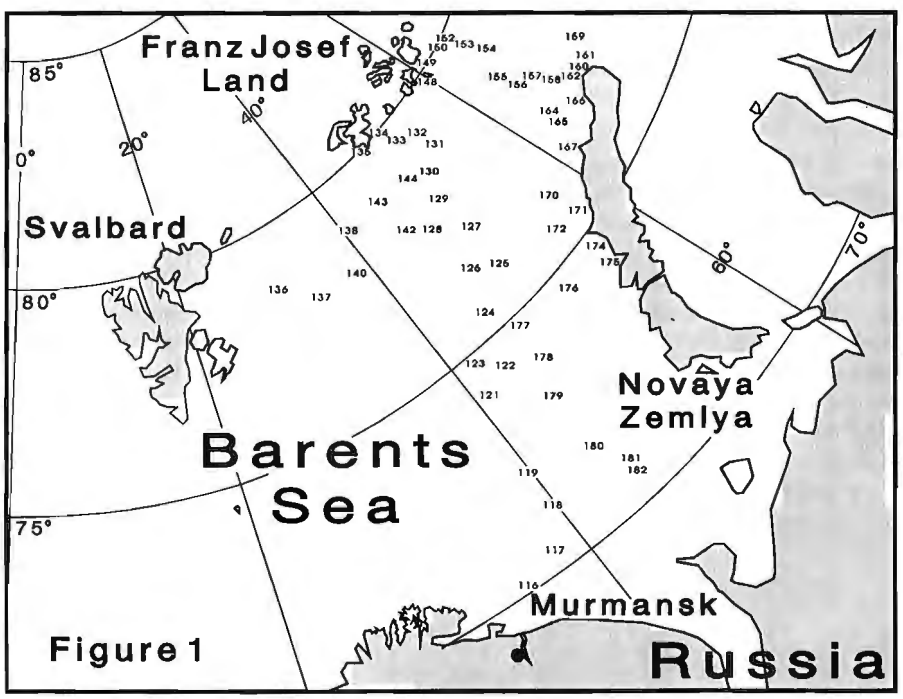

Figure 1. Map showing location of sites in the Barents Sea where samples were collected from the research vessel "Geolog Fersman" (1992).

The Arctic Ocean has become a particular focus for issues of global climate change. The World Climate Research Programme has instituted plans for an international program on the Arctic, the Arctic Climate System Study (ACSYS). In the problem areas of climate and contaminants in the Arctic, there is an obvious overlap in the controlling physical, chemical, and biological processes involved, in their time scales, and indeed, in areas of knowledge necessary for development of quantitative predictive capabilities. The joint Canadian/ American Trans-Arctic Section, which will cross the Polar Basin from the Chukchi Sea to Fram Strait in 1994, will involve a wide variety of global change programs supporting both climate and contaminant investigation.

Our main purpose in Project 10, therefore, is to determine the level of anthropogenic contaminants in the shelf areas adjacent to Russia and Canada in a manner that is consistent with marine environmental strategies prepared by AMAP. Further, our data will be employed to monitor contaminant levels and to develop transport, accumulation and dispersal models. During 1992 and 1993, the project acquired drill core and grab seabed samples from the eastern Barents Sea. Samples were collected from the Russian research vessel "Geolog Fersman" (Nassichuk et al., 1993). Samples from the sites shown in Figure 1 have been analyzed for heavy metals (52 samples analyzed at AGC, Dartmouth, Nova Scotia), for total organic carbon (TOC) by Rock-Eval pyrolysis (120 samples analyzed at ISPG, Calgary, Alberta), for PAHs, PCBs and other chlorinated hydrocarbons and pesticides (40 samples analyzed at Axys Laboratories, Sidney, B.C.), and for radionuclides (in progress, Department of Fisheries and Oceans, Bedford Institute of Oceanography, Dartmouth, Nova Scotia).

In this report we provide preliminary data on polychlorinated biphenyls (PCBs), organochlorine pesticides (mainly chlorobenzenes), and polycyclic aromatic hydrocarbons (PAHs) derived from forty samples from the Barents Sea (Tables 1, 2).

BARENTS SEA PHYSICAL CHARACTERISTICS

The Barents Sea, covering approximately 1.2 x 10^6 km^2 and underlain by glaciated continental shelf, is relatively deep and cut by undersea valleys and troughs. Major riverine flow comes from the Northern (Severnaya) Dvina (110 km^3/a) and Pechora (130 km^3/a) rivers although flow from the Ob (530 km^3/yr) and Yenisei (603 km^3/yr) farther east in Siberia probably also provide significant input (mean annual runoff figures are from Aagaard and Carmack, 1989). The circulation pattern of the Barents Sea (AMAP, 1993, Annex 1) shows, at the northern end of Novaya Zemlya, a convergence of westward flow (from the Kara Sea) with northward flow

Table 1. GC/MS analysis for organic compounds in Barents Sea sea floor samples (ng/g). Total PCBs: sum of 9 compounds (see Table 2); total chlorobenzenes (organochlorine pesticides): sum of 3 compounds (see text); total PAHs: sum of 17 compounds (see Appendix 1).

Sample	Water depth (m)	Sediment interval (cm)	Total PCBs (includes aroclor)	Total chloro-benzenes	Total PAHs (A)
116	189	0-10	0.9	0.04±0.02	57±2.5*
117	192	0-20	ND	0.035±0.005*	115±3%
118-4	356	20-21	2.3	0.5	467±2%
124-4	316	0-2	2.3	0.5	402
124-5	316	2-5	2.2	0.5	408
124-14	316	5-10	3.9	0.2	494
124-15	316	10-15	2.6	0.2	432
124-18	316	25-30	4.4	ND	266
133-7	456	2-10	0.4	0.03	348±9%*
133-43	456	70-80	3.2	0.03	2026 526 (B)
136-1	228	0-2	4.0	0.4	381
137-1	227	0-1	2.5	0.3	573
137-2	227	1-8	0.55±0.01*	0.1	604
153-39	465	0-10	0.04	0.1	244
153-41	465	30-40	0.1	0.01	311
153-43	465	50-60	0.3	0.04	290
153-45	465	70-80	0.1	0.03	317±10*
153-47	465	90-100	0.15±0.05*	0.045±0.01*	300
153-49	465	110-120	0.2	0.05	121
159-27	276	0-5	0.6	0.4	231
159-31	276	40-50	2.0	0.08	154
159-34	276	70-80	ND	0.07	154
159-36	276	90-100	ND	0.03	158
161-30	200	0-10	7.7±0.33	0.3±0.04	185±29
161-31	200	10-20	0.7±0.36	0.03±0.07	244±2*
161-32	200	20-30	0.2	ND	155±3
161-35	200	50-60	0.1	ND	172±10
161-39	200	90-100	0.1	ND	182±5%
170-1	56	0-5	ND	0.1	35±15
171-10	71	0-2	0.6	0.4	142±26
171-11	71	2-10	2.3	0.6	162±17
171-12	71	10-20	0.9	0.7	193±19
171-13	71	20-30	ND	0.07	205±12*
171-16	71	50-60	0.1	0.07	180±13
171-35	71	100-110	ND	0.05	160±20
171-25	71	150-160	0.3	0.04	144±15
179-9	356	0-1	4.0	0.3	494±23
179-8	356	1-10	0.5	0.1	351±11
182-1	115	0-2	3.5	0.1	80±9
182-9	115	2-8	4.55±0.20*	0.135±0.007*	89±6

*Duplicate analyses
(A) Perylene included (B) Perylene excluded

Table 2. PCB analyses for selected samples.

Sample:	116	118-4	124-4	136-1
Water depth (m)	189	356	316	228
Sediment interval (cm)	0-10	20-21	0-2	0-1
Dry weight (g)	10.04	10.05	10.01	9.05
Tri-PCB	0.2 (0.01)	0.2 (0.01)	0.5 (0.01)	1.9 (0.01)
Tetra-PCB	0.09 (0.02)	0.3 (0.01)	0.4 (0.01)	1.8 (0.01)
Penta-PCB	0.1 (0.01)	0.4 (0.01)	0.4 (0.02)	0.2 (0.02)
Hexa-PCB	0.1 (0.03)	0.3 (0.02)	0.2 (0.02)	ND (0.03)
Hepta-PCB	ND (0.03)	0.06 (0.02)	0.03 (0.03)	0.09 (0.04)
Octa-PCB	ND (0.04)	ND (0.03)	ND (0.04)	ND (0.06)
Nona-PCB	ND (0.05)	ND (0.03)	ND (0.04)	ND (0.07)
Deca-PCB	ND (0.04)	ND (0.03)	ND (0.03)	ND (0.04)
Total PCB	0.5	1.3	1.5	4.0
AROCLOR 1254/1260	0.4 (0.20)	1.0 (0.20)	0.8 (0.20)	ND (0.03)
ROCK-EVAL MEASUREMENTS				
TOC (weight %)	0.64±0.2	2.78±0.12	3.47±0.07	1.10±0.08
Tmax (°C)	394±4	410±2	387±2	475±5
Concentration in ng/g; (detection limit); ND, not detected				

along the west side of the island. This latter current is a continuation of flow entering the Barents Sea between Norway and the Svalbard Bank (south end of Spitsbergen). This flow pattern indicates possible areas of concentration in the central Barents Sea and between the northern end of Novaya Zemlya and FranzJosef Land.

An important feature for pollutant transport into seabed sediments is the permanent stratification of the deep Arctic basins by a cap of low salinity water. However, in general, shelf waters, although stratified in summer by caps of low salinity water, are relatively well mixed in winter. The residence time of waters on the shelf, and of their dissolved materials, is 2 to 4 years in the Barents and Kara seas (Hanzlick and Aagaard, 1980; Schlosser et al., in press). Tritium and helium distributions suggest a time scale of about ten years for the spread of injected shelf waters (and their dissolved contaminants) within the upper Arctic Ocean (Östlund, 1982; Schlosser et al., 1990). Although detailed understanding of the process is lacking, many studies, including those studies of natural radionuclide disequilibria (Moore and Smith, 1986), indicate transfer of physical and chemical properties of shelf water to the interior Arctic basin.

The Yablokov Commission Report (Yablokov et al., 1993) estimates that river runoff to the Barents Sea between 1961 and 1989 supplied about 6 kCi (kiloCuries) of radioactivity. Over the same period, atmospheric input from global fallout of nuclear testing was estimated to be 100 kCi (radioactivity is mainly from the isotopes ^{137}Cs and ^{90}Sr). Without additional study, no meaningful conclusions can be made on the relative concentrations of atmospheric versus riverborne organic pollutants. Of additional interest, however, the Commission Report estimates that 200 kCi from nuclear reprocessing plants at Sellafield, England and La Hague, France, were transported from the Atlantic flow into the Barents Sea.

PERSISTENT ORGANIC CONTAMINANTS IN THE ARCTIC ENVIRONMENT

Organochlorine pesticides and PCBs

Organochlorine compounds and PCBs are semi-volatile, toxic, entirely anthropogenic compounds which are not readily broken down by natural processes. Organochlorine contaminants in Arctic marine and freshwater ecosystems raise concerns that aboriginal peoples, whose traditional diet includes marine mammals and fish, may be adversely affected by chronic exposure to these pollutants (Kinloch et al., 1991; Dewailly et al., 1989). Many studies have been conducted, utilizing data from Arctic locations (especially Svalbard) in order to make comparisons with more polluted marine environments. Ottar (1981) raised the concern that polar regions could be a sink for semi-volatile organics and metals, such as mercury, emitted in the mid-latitudes. Wania and Mackay (1992, 1993) developed a simple global meridional box model to evaluate the "cold-condensation" effect further. They concluded that this effect does exist for volatile organochlorines such as hexachlorobenzene (HCB) and hexachlorocyclohexanes (HCH). Further support for the cold condensation hypothesis comes from recent estimates that the net flux of PCBs from the atmosphere to the oceans is greater at high latitudes (Iwata et al., in press).

Another area for concern is bioconcentration (partitioning from water to organisms) of toxins. Particulate matter, under certain circumstances, can adsorb dissolved organochlorine compounds (OCs) and polycyclic aromatic hydrocarbons (PAHs), making them available for sedimentation and consumption by grazing organisms such as zooplankton. Bioaccumulation factors from water to zooplankton are about 2×10^6 (Muir et al., 1992).

Pathways for the transport of semi-volatile organics (such as gases and particulate matter) to the Arctic regions include the troposphere, as well as ocean currents (Barrie et al., 1992). HCH isomers and HCB are among the most prominent organochlorines in Arctic air and seawater (Patton et al., 1989; Bidleman et al., 1989) as well as freshwater (Lockhart et al., 1992). Concentrations of total HCHs ranging from about 1 to 6 ng/L in the Arctic Ocean were measured by Muir et al. (1992). Concentrations are highest in surface waters and decline rapidly with depth in the Arctic Ocean, indicating inputs are mainly from gas exchange with the atmosphere, as well as from river flows and melt water. In seawater, more highly chlorinated OCs such as DDT and PCBs (Cl_4-Cl_{10}) are associated with particles while more water soluble compounds such as HCH are mainly in the dissolved phase.

PAHs

Polycyclic aromatic (or more simply polyaromatic) hydrocarbons are in another group of organic contaminants in the Arctic. Levels of PAHs in freshwater and marine sediments, water, and biota have been discussed by Muir et al. (1992) and Lockhart et al. (1992). Yunker et al. (1991, 1993) studied PAHs in the Mackenzie River-Beaufort Sea deltaic system.

There are also important natural sources for PAHs in freshwater and marine environments in the Arctic (Yunker et al., 1993). PAHs are important toxic components of Arctic haze (Daisey et al., 1981). In general, because of natural and anthropogenic sources, interpretation of PAH data is more difficult than for PCBs and OC pesticides, which are entirely anthropogenic. Furthermore, PAHs do not bioaccumulate to the same extent as most organochlorines in freshwater and marine food chains.

Present data concerning both the kinds and amounts of natural and pollutant hydrocarbons in marine and terrestrial Arctic environments are often limited in space and time, and levels of precision and accuracy are often unknown. Nevertheless, the available information shows that anthropogenic, as well as natural hydrocarbons occur widely in the Arctic environment (Hites et al., 1980; Venkatesan and Kaplan, 1982; Barrie, 1986; Yunker et al., 1993). Natural sources include peat deposits, coal outcrops, and oil seeps. Anthropogenic sources include spills, leaks and wastage associated with human habitations and resource exploitation (i.e., petroleum, mineral production, and transport) as well as long range atmospheric transport of combustion derived hydrocarbons. A characteristic suite of polycyclic aromatic hydrocarbons is produced during incomplete combustion of all carbon-containing fuels and is released as gases and fine particulates. Study of sediments has shown that these hydrocarbons are globally distributed as a result of atmospheric transport (Blumer and Youngblood, 1975; LaFlamme and Hites, 1978; Wakeham et al., 1980a, b; Heit et al., 1981; Wickstrom and Tolonen, 1987; McVeety and Hites, 1988; Patton et al., 1991).

BARENTS SEA SAMPLES

Organochlorine Pesticides and PCBs

Table 1 is a summary of measurements of total PCBs (∑PCB) including aroclor 1254/1260 and total chlorobenzenes (organochlorine pesticides; ∑OCp). An example of the specific types of PCBs encountered in analysis is given in Table 2. Included in ∑OCp are tetra-, penta-, and hexachlorobenzene. A complete listing of individual values will be presented in subsequent publications. Of the three organochlorine pesticides, hexachlorobenzene is generally the dominant species, with concentrations greater than or equal to tetrachlorobenzene. In addition, the organochlorine pesticides – alpha HCH, beta HCH, gamma HCH – were detected only in samples 124-4 and 171-10 to 171-12 (at the 1 ng/g level). Cis- and trans-chlordane; cis- and trans-nonachlor; o,p' -DDE; p,p' -DDE; o,p' -DDD; p,p' -DDD; o,p' -DDT; p,p' -DDT and Mirex were not detected at the 0.05 ng/g level.

Total chlorobenzene values may be separated into two groupings: those with values between 0.2 and 0.5 ng/g and those between 0.01 and 0.1 ng/g. The highest values occur in the deeper, more central parts of the basin (stations 124 and 179), although station 136, nearest Svalbard, also has a high value.

PAHs

The list of seventeen PAH compounds in the 40 samples analyzed by Axys Analytical Services (Sidney, B.C.) is given in the Appendix. The totals of these compounds are given in Table 1 for every sample analyzed. The forty samples were also analyzed for 11 additional compounds: C1-C4 napthalenes, C1-C4 phenanthrenes, dibenzothiophene, and C1 and C2 dibenzothiophene. Total amounts for these alkylated PAHs and thiophenes are often from 25 to 50% of the PAH totals given in Table 1.

From the data presented in Table 1, it can be noted that in general, ∑PAH increases toward the center of the Barents Sea (Fig. 1, stations 179, 124, and 137). While Rock-Eval pyrolysis measurements of TOC (total organic carbon) are not presented here (see Nassichuk et al., 1993), it has been observed that ∑PAH tends to correlate positively with TOC. In addition, both TOC and ∑PAH tend to increase with an increase in water depth – although there are some exceptions (e.g., station 137).

A correlation between PAH and TOC is illustrated in the following consideration of data for perylene which is widely distributed and instead of having solely anthropogenic origins, may instead be derived from early-diagenic transformations of biogenic precursors. Figure 2 is a plot of perylene concentration (ng/g, dry) in seafloor sediment samples from the uppermost sediment interval of the samples listed in Table 1 versus their TOC (weight %). There are two trends apparent for perylene versus TOC as shown by the two smooth dashed curves. The curves are derived from a least squares fit on measurements of samples from the shallowest sediment interval (0-20 cm, Table 1). The lower curve is given by the equation:

$$[\text{perylene(ng/g)}] = 35.43 * \ln[\text{TOC(wt.\%)}] + 27.64$$

For the uppermost of the two trends, the relationship is given by the equation:

$$[\text{perylene(ng/g)}] = 45.18 * \ln[\text{TOC(wt.\%)}] + 71.18$$

These two equations provide an excellent fit to all but two of the observations (samples 117 and 136-1).

So far, discussion has been concerned only with the samples highest in the sedimentary column and nearest to the sea bed. Where available (samples from sites 153, 171, 161, 159, and 124), perylene/TOC analyses are also plotted in Figure 2. Another correlation in Figure 2 shows that perylene generally increases in concentration with increasing depth in the sediment core while TOC decreases in concentration by amounts varying between 0 and about 50% (site 153). The increase in concentration of perylene, often with little or no change in TOC, further supports proposals for the microbially mediated generation of perylene in an anaerobic environment (Wakeham et al., 1980b).

It seems reasonable that any changes in TOC with depth in the sediment column mainly reflect changes in concentration or preservation at the time of deposition since the anaerobic condition of the sediments should generally act to preserve TOC. For example, sample 133-43 (sediment interval 70-80 cm, not plotted here) has a perylene concentration of 1500 ng/g and a TOC of 2.16 wt.%. The shallower sediment sample from the same core, 133-7 (sediment interval 2-10 cm) has a perylene concentration of 98 ng/g and a TOC of 1.74 wt.%. Thus, for a TOC increase of only 24%, suggesting relatively constant conditions of deposition, perylene concentration has increased by over 1400%. Aizenshtat (1973), Orr and Grady (1967), Brown et al. (1972), and Wakeham (1977) all report sediment core studies where perylene concentrations increase with depth, suggesting an in situ formation mechanism. Also, it has been demonstrated by some of these sediment core studies that perylene concentration eventually decreases for increasing sediment depth. This is illustrated by our results, plotted in Figure 2, for sites 171 and 153 (Fig. 1) at sediment depth of 150 to 160 cm and 110 to 120 cm respectively. Ishiwatari and Hanya (1975) report no increase in perylene concentration in a core ranging from 11 to 196 m in depth suggesting a completion of perylene synthesis by the 11 m depth. The above discussion suggests completion within the first few metres of sediment depth.

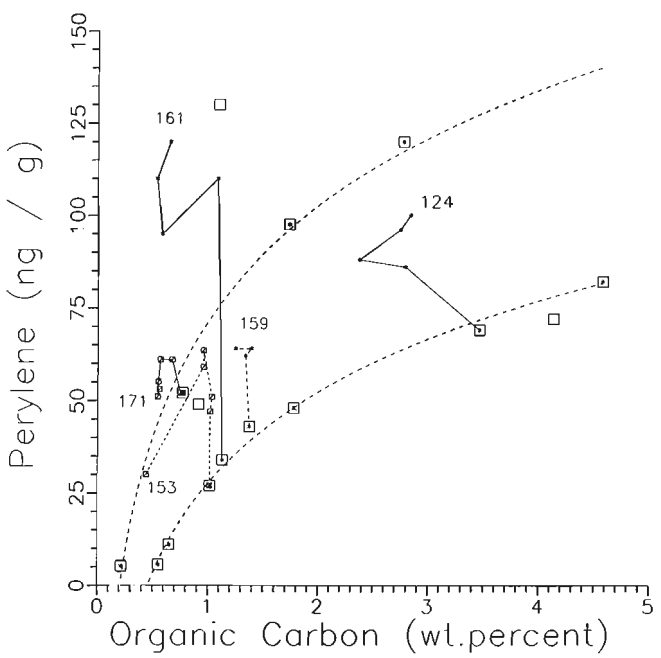

Figure 2. *Perylene versus organic carbon (TOC by Rock-Eval pyrolysis) for Barents Sea samples. "Lower trend" (curved dashed line) samples: 182-1, 116, 153-39, 161-30, 159-27, 137-1, 124-4, 179-8, 179-9 ; "upper trend" samples: 170-1, 171-10, 133-7, 118-4 (all samples are listed in order of increasing concentration along respective trends). Samples 117, 136-1, and 179-8 are not included in the derived least squares fit curve. "Vertical trends" (mainly parallel to y-axis) are perylene vs. TOC for the remainder of the samples in Table 1, sediment intervals are given in Table 1.*

This completion of perylene synthesis suggests a rapid, microbially mediated synthesis. Wakeham (1977) has calculated rates of formation of 4 ppb/year, based on core analyses and sedimentation rates in sediments from Lake Washington, Washington. For the core sample from site 133 discussed above, such a rate of formation would give an age for the 70 to 80 cm horizon (sample 133-43) of 350 years. This is a sedimentation rate of about 2 mm/year, comparable to the Recent lake sedimentation rates reported by Wakeham et al. (1980a). Interesting comparisons and new data on perylene rates of formation will be possible when radionuclide measurements are available for these Barents Sea samples to independently determine sedimentation rates.

DISCUSSION

The above discussion of PAH/TOC correlations was presented to illustrate the following points. First, there appears to be a remarkable correlation between PAH, perylene and total organic carbon amounts (measured quantities differing in absolute value by seven orders of magnitude). This correlation may well vanish as more data become available and the mathematical functions which fit the data have no underlying physical or chemical model justification. Further, no obvious reason for the two ("upper" and "lower") trends shown in Figure 2 is immediately apparent from the data given here. The four "upper trend" samples are not distinguished from the nine "lower trend" samples by either location or water depth. The only consistent analytical factor noted was that the "lower trend" samples tend to have lower Tmax values, between 300 and 400°C, while the "upper trend" samples have Tmax values of 400°C to 582°C. Tmax is the Rock-Eval pyrolysis analysis parameter: the temperature at maximum hydrocarbon generation for the S2 peak where hydrocarbons are being generated from kerogen in the sample (see Nassichuk et al., 1993). Preliminary inspection of the analytical data suggests that several of the 17 measured PAHs and alkyl-PAHs may follow similar trends. For example, in a comparison of sample 133-7, at a 2 to 10 cm sediment interval, with sample 133-43, at a 70 to 80 cm interval, only phenanthrene, fluoranthene, C1 naphthalenes, and C2 naphthalenes showed a decrease in concentration with increased depth; all other compounds showed varying degrees of increase. Also, as seen in Table 1, total PCBs and total chlorobenzenes often increase with increasing sediment depth. Accordingly, there may be other factors involved, such as bioturbation or variable sedimentation or variable organic compound input rates and types.

Examination of values in Table 1 shows that the anthropogenic contaminants correlate neither with water depth nor with TOC concentration. These values tend to cluster in three groupings: 0.03 to 1.5, 0.3 to 1.0, and 2 to 8 ng/g independent of water depth or TOC concentration. This observation may

indicate fundamental differences in sedimentary uptake or deposition for purely anthropogenic contaminants and for PAH compounds.

While this report has focused primarily on a general overview of organic contaminants in the Barents Sea, subsequent papers will deal with a more complete reporting of the data, more detailed analysis including factor analysis and correspondence analysis (ANOVA), and global comparisons with other data sets from the Arctic including those of our Russian colleagues (V.I. Popova and A.I. Daniushevskaya, VNIIOkeanologia, St. Petersburg).

ACKNOWLEDGMENTS

We are indebted to Russell Shearer from the Environmental Services and Research Division of the Department of Indian Affairs and Northern Development who contributed financial resources for chemical analyses completed by Axys Analytical Services Ltd. of Sidney, British Columbia. We thank J.S. Bell and R.W. Macqueen (ISPG, Calgary) for constructive reviews of this paper. Laurie Phillips of Axys Laboratories, Sidney, B.C. is also thanked for her help in timely transmission of data and for supplying reference material.

REFERENCES

Aagaard, K. and Carmack, E.C.
1989: The role of sea ice and other fresh water in the Arctic Circulation; Journal of Geophysical Research, v. 94, p. 18163-18175.

Aizenshtat, Z.
1973: Perylene and its geochemical significance; Geochimica Cosmochimica Acta, v. 37, p. 559-567.

AMAP (Arctic Monitoring and Assessment Program)
1993: The updated monitoring program for AMAP; Oslo, Norway.

Barrie, L.A.
1986: Arctic air pollution: an overview of current knowledge; Atmospheric Environment, v. 20, p. 643-663.

Barrie, L.A., Gregor, D., Hargrave, B., Lake, R., Muir, D.C.G., Shearer, R., Tracey, B., and Bidleman, T.
1992: Arctic contaminants: sources, occurrence and pathways; Science of the Total Environment, v. 122, p. 1-74.

Bidleman, T.F., Patton, G.W., Walla, M.D., Hargrave, B.T., Vass, W.P., Erickson, P., Fowler, B., Scott, V., and Gregor, D.G.
1989: Toxaphene and other organochlorines in Arctic Ocean fauna: evidence for atmospheric delivery; Arctic, v. 42, p. 307-313.

Blumer, M. and Youngblood, W.W.
1975: Polycyclic aromatic hydrocarbons in soils and recent sediments; Science, v. 188, p. 53-55.

Brown, F.S., Baedecker, M.J., Nissenbaum, A., and Kaplan, I.R.
1972: Early diagenesis in a reducing fjord, Saanich Inlet, British Columbia - III. Changes in organic constituents of sediment; Geochimica et Cosmochimica Acta, v. 36, p. 1185-1203.

Daisey, J.M., McCaffrey, R.J., and Gallagher, R.A.
1981: Polycyclic aromatic hydrocarbons and total extractable particulate aromatic matter in Arctic aerosol; Atomospheric Environment, v. 15, p. 1353-1364.

Dewailly, E., Nantel, A., Weber, J-P., and Meyer, F.
1989: High levels of PCBs in breast milk of women from Arctic Quebec; Bulletin of Environmental Contamination Toxicology, v. 43, p. 641-646.

Hanzlick, D. and Aagaard, K.
1980: Freshwater and Atlantic water in the Kara Sea; Journal of Geophysical Research, v. 85, p. 4937-4942.

Heit, M., Tan, Y.L., Klusek, C.S., and Burke, J.C.
1981: Anthropogenic trace elements and polycyclic aromatic hydrocarbons in sediment cores from two lakes in the Adirondack acid lake region; Water Soil Air Pollution, v. 15, p. 441-464.

Hites, R.A., LaFlamme, R.E., and Windsor, J.G.
1980: Polycyclic aromatic hydrocarbons in marine/aquatic sediments: Their ubiquity; in Petroleum in the Marine Environment, (ed.) L. Petrakis and F.T. Weiss; Advances in Chemistry Series, v. 185, p. 289-311.

Ishiwatari, R. and Hanya, T.
1975: Organic geochemistry of a 200-metre core sample from Lake Biwa - II. Vertical distribution of mono- and di-carboxlyic acids and polynuclear aromatic hydrocarbons; Proceedings of the Japan Academy, v. 51, p. 436-441.

Iwata, H., Tanabe, S., Sakai, N., and Tatsukawa, R.
in press: Distribution of persistent organochlorines in the oceanic air and surface seawater, and the role of the ocean on the global transport and fate; Environmental Science Technology.

Kinloch, D., Kuhnlein, H., and Muir, D.C.G.
1991: Inuit foods and diet. A preliminary assessment of benefits and risks; Science of the Total Environment, v. 122, p. 247-278.

LaFlamme, R.E. and Hites, R.A.
1978: The global distribution of polycyclic aromatic hydrocarbons in recent sediments; Geochimica Cosmochimica et Acta, v. 42, p. 289-303.

Lockart, W.L., Wagemann, R., Tracey, B., Sutherland, D., and Thomas, D.J.
1992: Presence and implications of chemical contaminants in the freshwaters of the Canadian Arctic; Science of the Total Environment, v. 122, p. 165-246.

McVeety, B.D. and Hites, R.A.
1988: Atmospheric deposition of polycyclic aromatic hydrocarbons to water surfaces: a mass balance approach; Atmospheric Environment, v. 22, p. 511-536.

Moore, R.M. and Smith, J.N.
1986: Disequilibria between ^{226}Ra, ^{210}Pb and ^{210}Po in the Arctic Ocean and the implications for chemical modification of the Pacific water inflow; Earth and Planetary Science Letters, v. 77, p. 285-292.

Muir, D.C.G., Ford, C.A., Grift, N.P., Stewart, R.E.A., and Bidleman, T.F.
1992: Arctic marine ecosystem contamination; Science of the Total Environment, v. 122, p. 75-134.

Nassichuk, W.W., Skibo, D.N., Fowler, M.G., Stewart, K.R., and Snowdon, L.R.
1993: Update of Canada-Russia collaboration on Arctic Pollutants; in Current Research, Part E; Geological Survey of Canada, Paper 93-1E, p. 113-121.

Orr, W.L. and Grady, J.R.
1967: Perylene in basin sediments of Southern California; Geochimica et Cosmochimica Acta, v. 31, p. 1201-1209.

Östlund, H.G.
1982: The residence time of the freshwater component in the Arctic Ocean; Journal of Geophysical Research, v. 87, p. 2035-2043.

Ottar, B.
1981: The transfer of airborne pollutants to the Arctic region; Atmospheric Environment, v. 15, p. 1439-1445.

Patton, G.W., Hinckley, D.A., Walla, M.D., Bidleman, T.F., and Hargrave, B.T.
1989: Airborne organochlorines in the Canadian high Arctic; Tellus, v. 41B, p. 243-255.

Patton, G.W., Walla, M.D., Bidleman, T.F., and Barrie, L.A.
1991: Polycyclic aromatic and organochlorine compounds in the atmosphere of northern Ellesmere Island, Canada; Journal of Geophysical Research, v. 96D, p. 10867-10879.

Schlosser, P., Bönisch, G., Kromer, B., Münnich, K.O., and Kolterman, K.P.
1990: Ventilation rates of waters in the Nansen Basin of the Arctic Ocean derived by a multi-tracer approach; Journal of Geophysical Research, v. 95, p. 3265-3272.

Schlosser, P., Grabitz, D., Fairbanks, R., and Bönisch, G.
in press: Mean residence time on the shelves and in the halocline; Deep-Sea Research.

Venkatesan, M.I. and Kaplan, I.R.
1982: Distribution and transport of hydrocarbons in surface sediments of the Alaskan Outer Continental Shelf; Geochimica et Cosmochimica Acta, v. 46, p. 2135-2149.

Wakeham, S.G.
1977: Synchronous fluorescence spectroscopy and its application to indigenous and petroleum-derived hydrocarbons in lacustrine sediments; Environmental Science Technology, v. 11, p. 272-276.
Wakeham, S.G., Schaffner, C., and Giger, W.
1980a: Polycyclic aromatic hydrocarbons in Recent lake sediments - I. Compounds having anthropogenic origins; Geochimica et Cosmochimica Acta, v. 44, p. 403-413.
1980b: Polycyclic aromatic hydrocarbons in Recent lake sediments - II. Compounds derived from biogenic precursors during early diagenesis; Geochimica et Cosmochimica Acta, v. 44, p. 415-429.
Wania, F. and Mackay, D.
1992: Revisiting the cold condensation effect. Presented: 5th International Symposium on Arctic Air Chemistry; Copenhagen, Denmark, September 1992.
1993: Global fractionation and cold condensation of low volatility organochlorine compounds in polar regions; Ambio, v. 22, p. 10-18.
Wickstrom, K. and Tolonen, K.
1987: The history of airborne polycyclic aromatic hydrocarbons (PAH) and perylene as recorded in dated lake sediments; Water Air Soil Pollution, v. 32, p. 155-175.
Yablokov, A.V., Karasev, V.K., Rumyantsev, V.M., Kokeyev, M.Ye., Petrov, O.I., Lystsov, V.N., Yemelyenenkov, A.F., and Rubtsov, P.M.
1993: Facts and Problems Related to Radioactive Waste Disposal in Seas Adjacent to the Territory of the Russian Federation (Materials for a Report by the Government Commission on Matters Related to Radioactive Waste Disposal at Sea, Created by Decree No. 613 of the Russian Federation President, October 24, 1992); Translated by P. Gallager and E. Bloomstein; Small World Publishers, Inc., Albuquerque, New Mexico.
Yunker, M.B., Macdonald, R.W., Fowler, B.R., Cretney, W.J., Dallimore, S.R., and McLaughlin, F.A.
1991: Geochemistry and fluxes of hydrocarbons to the Beaufort Sea shelf: A multivariate comparison of fluvial inputs and shoreline erosion of peat using principal components analysis; Geochimica et Cosmochimica Acta, v. 55, p. 255-273.
Yunker, M.B., Macdonald, R.W, Cretney, W.J., Fowler, B.R., and McLauaghlin, F.A.
1993: Alkane, terpene and polycyclic aromatic hydrocarbon geochemistry of the Mackenzie River and Mackenzie Shelf: riverine contributions to Beaufort Sea coastal sediment; Geochimica et Cosmochimica Acta, v. 57, p. 3041-3061.

Geological Survey of Canada Project 840081

APPENDIX

PAH compounds analyzed

Compound	Chemical Formula	Molecular Weight	Comments/use
Naphthalene	$C_{10}H_8$	128.16	(1a) Most abundant single constituent. (2) Appreciably volatile at room temperature (mothballs). Use: manufacture of compounds used in dye industry, synthetic resins, solvents, lubricants. Former use as insecticide/repellant supplanted by chlorinated compounds (e.g., p-dichlorobenzene).
naphthalin; naphthene; tar camphor.			
Acenaphthylene	$C_{12}H_8$	152.20	(2)
Acenaphthene.			
Acenaphthene	$C_{12}H_{10}$	154.21	(1a) (3) Use: dye intermediate; plastics manufacture; insecticide; fungicide.
1,2-Dihydroacenaphthylene; periethylenenaphthalene; 1-8 ethylenenaphthalene.			
Fluorene	$C_{13}H_{10}$	166.21	(1a) (1b)
o-biphenylenemethane; diphenylenemethane; 2-2-'methylenebiphenyl			
Phenanthrene	$C_{14}H_{10}$	178.22	(1a) (2) Isomeric with anthracene; toxic.
Anthracene	$C_{14}H_{10}$	178.22	(1a) Source for dyestuffs; chemical manufacture; alizarin dyes.
Fluoranthene	$C_{16}H_{10}$	202.24	(1a) (2-minor)
1,2-benzacenaphthene.			
Pyrene (1a) (2)	$C_{16}H_{10}$	202.24	(1a) (2)
Benzo[def]phenanthrene.			
Benz(a)anthracene	$C_{18}H_{12}$	228.28	(1a) Listed as a carcinogen by the U.S. EPA (1981).
1,2-Benzanthracene; 2,3-benzphenanthrene; tetraphene; benzanthrene; naphthanthracene.			
Chrysene	$C_{18}H_{12}$	228.28	(1a) Occurs in very small amounts during distillation or pyrolysis of many fats and oils.
1,2-Benzphenanthrene.			
Benzofluoranthenes	$C_{20}H_{12}$	252.32	(2-minor).
3,4-benzofluoranthene; 10,11-benzofluoranthene; 11,12-benzofluoranthene.			
Benzo(e)pyrene	$C_{20}H_{12}$	252.30	(1a) (2)
1,2-Benzpyrene; 4,5-Benzpyrene.			
Benzo(a)pyrene	$C_{20}H_{12}$	252.30	(1a) (2) Listed as a carcinogen by the U.S. EPA.
3,4-Benzpyrene.			
Perylene	$C_{20}H_{12}$	252.30	(1a) (1c)
Dibenz[*de,kl*]anthracene; *peri*-dinaphthalene.			
Dibenz(ah)anthracene	$C_{22}H_{12}$	276	
Ideno(1,2,3-cd)pyrene	$C_{22}H_{12}$	276	(2-minor)
Benzo(ghi)perylene	$C_{22}H_{12}$	276	(2-minor)

(1a) Occurs in coal tar or coal tar derivatives.
(1b) Occurs in coke oven tar.
(1c) Occurs in pitch distillate.
(2) Occurs in hydrocarbon combustion products.
(3) Occurs in petroleum residues.

Geophysical studies of massive ground ice, Fosheim Peninsula, Ellesmere Island, Northwest Territories

Stephen D. Robinson[1]
Terrain Sciences Division

Robinson, S.D., 1994: Geophysical studies of massive ground ice, Fosheim Peninsula, Ellesmere Island, Northwest Territories; in Current Research 1994-B; Geological Survey of Canada, p. 11-18.

Abstract: Three geophysical techniques were employed to study massive ground ice found as a component of the raised marine sediments of the Fosheim Peninsula, Ellesmere Island, N.W.T. The EM-31 terrain conductivity meter was hampered by the highly variable overburden salt content, especially in the vicinity of thaw disturbances. The heterogeneous surface terrain also hindered ground penetrating radar surveys, however some reflectors noted at 10 to 15 m depth could represent the base of massive ice. Gravity surveying showed several of the flat-topped hills in the area to be cored with massive ice up to 17 m thick. Materials encountered in shallow boreholes agreed with geophysical interpretations.

Although evidence of past thermokarst is abundant over much of the region, the large amount of deep and shallow ice still remaining suggests that there is the potential for severe terrain disturbance in the future.

Résumé : On a employé trois techniques géophysiques pour étudier les masses de glace de sol qui font partie des sédiments marins soulevés de la péninsule Fosheim, dans l'île d'Ellesmere (T.N.-O.). Le fonctionnement du conductimètre de terrain EM-31 a été gêné par la teneur en sel très variable des terrains de couverture, surtout à proximité des perturbations causées par le dégel. Le terrain superficiel hétérogène a aussi été un obstacle aux levés au géoradar, mais certains réflecteurs signalés à entre 10 et 15 m de profondeur pourraient représenter la base de la glace massive. Les levés gravimétriques ont montré que plusieurs des collines à sommet plat de la région avaient un noyau de glace massive pouvant atteindre 17 m d'épaisseur. Les matériaux rencontrés dans les trous de forage peu profonds confirment les interprétations géophysiques.

Dans une grande partie de la région, les indices d'un ancien thermokarst abondent, mais les importantes quantités résiduelles de glace profonde et peu profonde suggèrent qu'il pourrait se produire à l'avenir de sérieuses perturbations du terrain.

[1] Department of Geography, Queen's University, Kingston, Ontario K7L 3N6

INTRODUCTION

Massive ground ice has been noted as an important component of fine grained, raised marine sediments of the western Fosheim Peninsula, Ellesmere Island, N.W.T. (Edlund et al., 1989; Hodgson et al., 1991; Pollard, 1991; Barry, 1992). Thickness and distribution of ground ice bodies away from sites of exposure is unknown. Mapping the areal distribution and characteristics of massive ground ice is fundamental to a better understanding of the climatic and hydrological conditions under which the ice formed. Ground ice with a thin sediment overburden has the potential for thermokarst development following natural or anthropogenic disturbance. The processes influencing the periglacial landscape today and in the future can also be examined.

Geophysical methods have successfully been used as an aid in the mapping of massive ground ice and other permafrost features (Scott et al., 1990). The majority of geophysical studies in Canada targeting massive ground ice have been conducted in the western Arctic (i.e., Rampton and Walcott, 1974; Sartorelli and French, 1982; Dallimore and Davis, 1987, 1992; Dallimore et al., 1988; Robinson et al., 1993). Seismic (Gagne and Hunter, 1975) and ground penetrating radar (Barry, 1992) studies of limited scope have been attempted previously on the Fosheim Peninsula, although little geophysical research has been conducted in combination with studies of periglacial geomorphology.

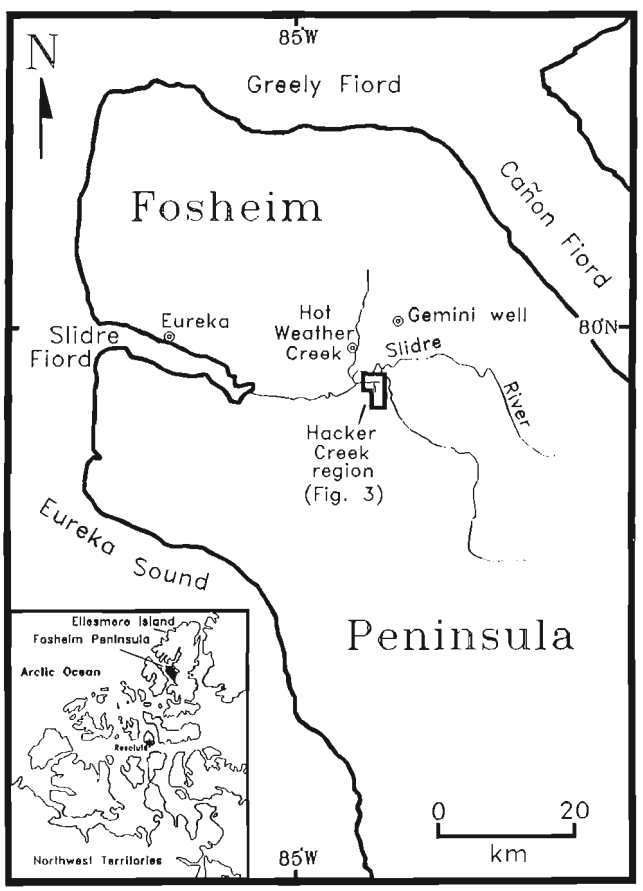

Figure 1. Location map of Fosheim Peninsula, Ellesmere Island, showing Hot Weather Creek camp and the Hacker Creek (unofficial name) study region.

During the summers of 1991 and 1992, a joint geophysical and geomorphological study of massive ground ice was conducted. This study was undertaken as part of the Geological Survey of Canada's global change monitoring program in the High Arctic, based since 1988 at Hot Weather Creek, west-central Ellesmere Island (79°58′N, 84°28′W; Fig. 1). The aim of this paper is to present the findings of geophysical surveys conducted at the Hacker Creek (unofficial name) site, utilizing terrain conductivity, ground penetrating radar, and gravity techniques.

REGIONAL BACKGROUND AND STUDY SITE

West-central Fosheim Peninsula is a broad, rolling intermontane lowland. The surrounding mountain ranges protect the area from the incursion of cold air masses during the summer, resulting in temperatures which are anomalously high for this latitude. Taylor et al. (1982) calculate a permafrost thickness of 500 m from thermal measurements in Gemini well, 8 km from the study site and near the limit of early Holocene marine inundation. Below local marine limit (approx. 145 m a.s.l.), ice-rich marine sandy silts and silty clays form a veneer over poorly consolidated bedrock. Massive ground ice in the region appears to be exclusively overlain by these fine marine sediments (Pollard, 1991; Barry, 1992; Robinson, unpub. data), with the rare exception of ice sills within bedrock (Robinson, 1993). Tabular ice bodies are found up to 8 m thick in exposure (Fig. 2a), and are likely of segregated origin (Pollard, 1991). Exposed ice bodies approach 100% ice by volume in many sections (Pollard, 1991; Robinson, unpub. data).

Geophysical surveys targeting massive ice were confined to a 3.5 km^2 area near Hacker Creek (79°55.5′N, 84°18′W), about 6 km southeast of Hot Weather Creek. Numerous active and stabilized retrogressive thaw slumps indicate a widespread distribution of ground ice in the Hacker Creek region (Fig. 2b). Intensive slope gullying is magnified by the ice-rich nature of the surficial sediments (Robinson, unpub. data). The majority of ice degradation has occurred on slopes, and although most interfleuve areas remain undisturbed, they are also thought to be underlain by massive ground ice. The sparse vegetation cover is in part due to the slope processes. An evaporitic salt crust develops most prominently during the summer on disturbed sediments, and is generally absent over undisturbed terrain. Elevation within the study area ranges from 55 to 110 m a.s.l.

METHODS

Three nondestructive geophysical instruments were employed for shallow subsurface surveying in this study. The EM-31 and ground penetrating radar (GPR) record the response of electromagnetic (EM) induction and transmission respectively to determine the electrical properties of the shallow subsurface. The gravity meter detects subsurface density differences

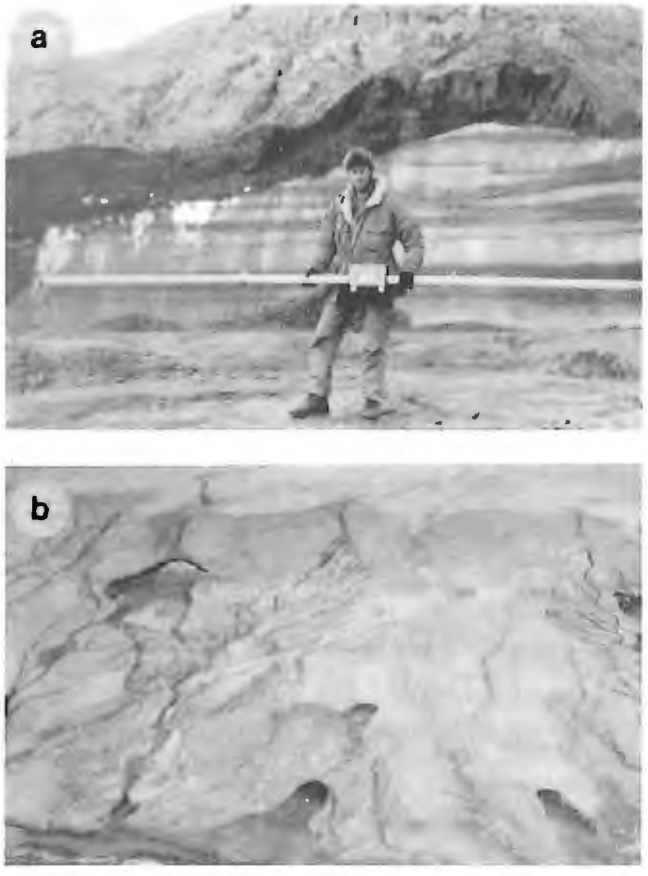

Figure 2. *(a) Massive ground ice exposure at the Slidre River site near the 970 position of the gravity profile (Fig. 8B). Maximum thickness of exposed ice reached 6.8 m in 1991. The author is shown with the EM-31 terrain conductivity meter. (**b**) Active and stabilized retrogressive thaw slumps indicate a widespread distribution of ground ice in the Hacker Creek region.*

attributable to the presence of massive ice. A series of shallow boreholes were drilled to verify the geophysical surveys. Both borehole lithology and observations of ground ice in exposure aided geophysical interpretations.

Terrain conductivity (EM-31)

The terrain conductivity technique utilizes a transmitter coil to induce circular eddy currents in the shallow subsurface. Secondary eddy currents will then be induced within any conductors within the ground. The combination of these two fields is measured at the receiver coil and the output voltage is linearly related to the apparent terrain conductivity (Geonics, 1984). Apparent conductivity is an integrated value of true conductivities at different depths within the effective depth of penetration. The Geonics EM-31 is capable of detecting changes in terrain conductivity as small as 5%.

Measurements in both vertical and horizontal dipole orientations are useful for diagnosing and defining a layered earth, typical of relatively nonconductive ice overlain by more conductive sediments. In addition to measurements being taken at each station in both vertical and horizontal dipole orientations, measurements were taken with the antenna boom parallel and perpendicular to the survey line. Assuming isotropic electrical conditions in the immediate vicinity of the instrument, conductivity readings should be independent of instrument orientation with respect to the earth.

A total of 6 km of EM-31 surveys were conducted in July and August 1992 at several sites in the Hacker Creek region in grid patterns and along surveyed lines. More complete details of terrain conductivity survey methodology are given in McNeill (1980) and Geonics (1984). Sartorelli and French (1982), Sinha and Stephens (1983), Washburn and Phukan (1988), and Dyke (1988) discuss the application of terrain conductivity techniques to the mapping of permafrost.

Ground penetrating radar (GPR)

Ground penetrating radar technique involves the transmission of short pulses of high frequency electromagnetic (EM) energy into the ground. Reflections occur at depth from interfaces with contrasting electrical properties caused by changes in material, temperature, moisture, and density. Measurement of the two-way travel time of electrical returns from these interfaces allows the interpretation of subsurface characteristics. Propagation velocities can be determined in situ by conducting common mid-point (CMP) surveys. Continuous profiling allows the construction of an electromagnetic cross-section with a vertical depth axis and the horizontal axis representing survey position. Approximately 5 km of GPR surveys were conducted in May and June 1992 with the pulseEKKO IV GPR system.

Permafrost generally represents ideal transmission media due to the low electrical conductivities causing very little attenuation and enabling deep signal penetration. More complete details of survey methodology and GPR theory are given in Ulriksen (1982) and Davis and Annan (1989). Annan and Davis (1976), Davis et al. (1976), and Judge et al. (1991) provide details of GPR surveying in permafrost environments, while Dallimore and Davis (1987, 1992) and Robinson et al. (1993) used GPR to specifically map massive ground ice.

Gravity

The gravity technique has been utilized for decades in geological prospecting, and more recently as a tool in engineering and environmental studies to determine lateral subsurface density variations (Hinze, 1990). Density differences exist between massive ground ice (0.9 t/m^3) and the enclosing frozen sediments (likely between 1.6 and 2.4 t/m^3), and therefore massive ice should be amenable to detection by gravity methods (Rampton and Walcott, 1974).

Survey sites were chosen based on ground-ice exposures or evidence of ground-ice thaw on multiple slope aspects indicating the presence of massive ice beds underlying the topography. Field gravity data were corrected for instrument drift, station elevation, latitude, and topography of the surrounding terrain to give the resultant Bouguer anomaly. Gravity profiles often contain signals from mass heterogeneities outside the survey area (Rampton and Walcott, 1974), which can be removed as the

linear trend between the ends of the profile. Excess ice along the profile is reflected by Bouguer anomaly values below the linear trend due to the lack of gravitational attraction from mass deficiency. Approximately 3.5 km of gravity lines were run using a Scintrex gravimeter with a sensitivity of 0.01 mGal was used for the surveys. Topographic profiles were made using a Wild T2 theodolite.

Rampton and Walcott (1974) provide details of the survey and interpretation methods used in this study, proven successful for mapping massive ice bodies near Tuktoyaktuk, Northwest Territories. Topographic corrections follow the method outlined by Hammer (1939). Complete details of gravity survey methods, data reduction, and interpretation techniques can be found in Telford et al. (1990).

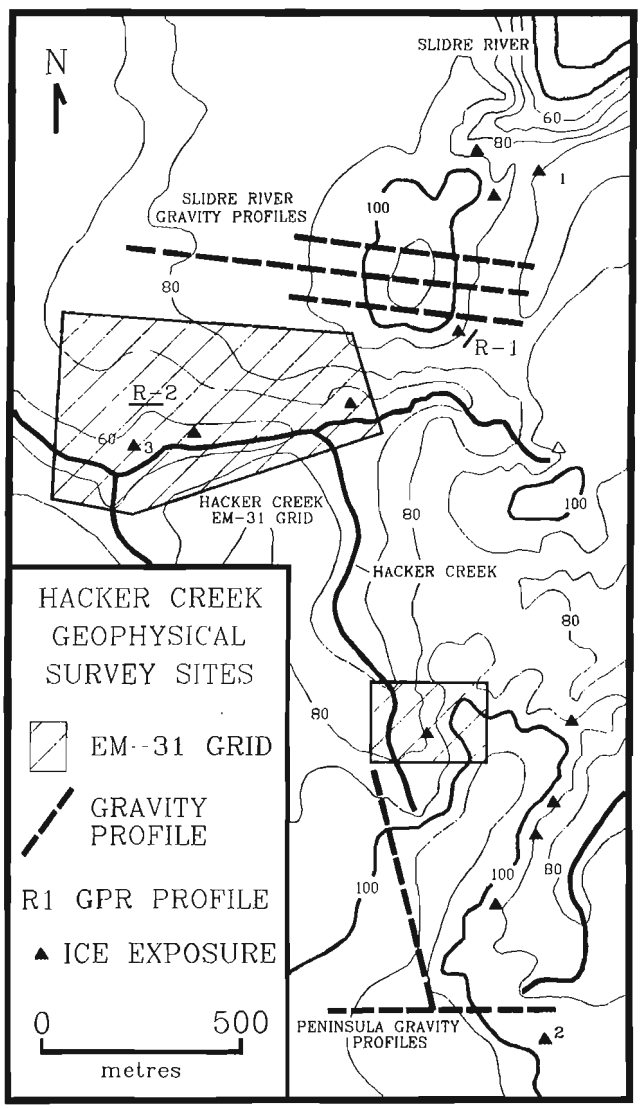

Figure 3. Hacker Creek geophysical survey region showing the locations of surveys conducted in 1992. As numerous individual GPR surveys were conducted, only the locations of GPR profiles discussed in the text are shown. Numbers beside some ice exposures refer to EM-31 profile locations shown in Figure 5.

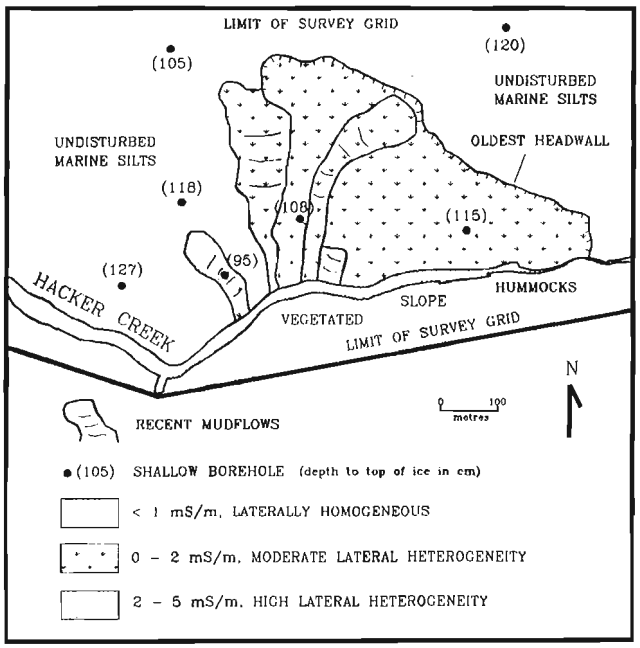

Figure 4. EM-31 survey grid at Hacker Creek. Boreholes locations and depths to the top of massive ground ice are also shown. Low, homogeneous conductivities occur over undisturbed marine sediments. Recent thaw flows show higher conductivities and lateral heterogeneity.

RESULTS

Figure 3 shows the Hacker Creek geophysical study region, with the locations of terrain conductivity, GPR, and gravity surveys conducted during the 1992 field season. Selected survey results are presented and discussed below. Except where noted, these results are considered as typical for the region.

Terrain conductivity

The EM-31 terrain conductivity surveys were conducted with the aim of delineating the presence of low conductivity ice (about 1.0 mS/m) overlain by variable thicknesses of more conductive sediments. Figure 4 shows the results of a survey grid conducted at the Hacker Creek site. Thickness of sediment overlying the ice was found to be between 0.95 and 1.27 m in the 7 shallow boreholes drilled within the grid area. The base of the massive ice is below the bottom of all boreholes (maximum depth 2.87 m). This survey grid is considered to represent overburden thicknesses found across the study region, but without the extensive surficial salt crust that affected the electrical methods over other marine sediments.

Negative conductivity readings were found in all boom orientations across the entire area of undisturbed marine silts. Negative conductivities are a theoretical impossibility, and suggest the instrument has drifted out of absolute calibration. All readings therefore cannot be considered as absolute values, but are still useful for comparison between regions as relative conductivities (J.D. McNeill, pers. comm., 1993). These negative values should be considered as extremely low (<1 mS/m) conductivities.

Profiles crossing areas disturbed by past slumping events now stabilized, dry, and frozen, were of slightly higher conductivities (instrument readings between 0 and 2 mS/m), although the depth to massive ice remained similar. Readings taken in different boom orientations also varied, suggesting an increase in lateral and vertical soil heterogeneity. The mudflows of more recently active slumping events showed higher conductivities (2-5 mS/m). These mudflows had a more continuous salt crust and were often saturated near the surface. Even though conductivities were slightly higher, drilling confirmed the thickness of sediment overlying the ice remained similar to other regions. Lateral variations were greatest in this environment, with a comparision between readings taken both parallel and perpendicular to the survey line in the vertical dipole orientation showing a correlation of only r^2=0.42.

Mudflows of active ground ice slumps displayed the greatest lateral and vertical inhomogeneities. Figure 5 shows the results of three surveys conducted in vertical dipole orientation over different slumps in the Hacker Creek area. In all cases, the massive ice is known to be overlain by 0.95 to 1.5 m of mudflow sediment. Regression coefficients between r^2=0.18 and r^2=0.77 demonstrate the extreme lateral anisotropy

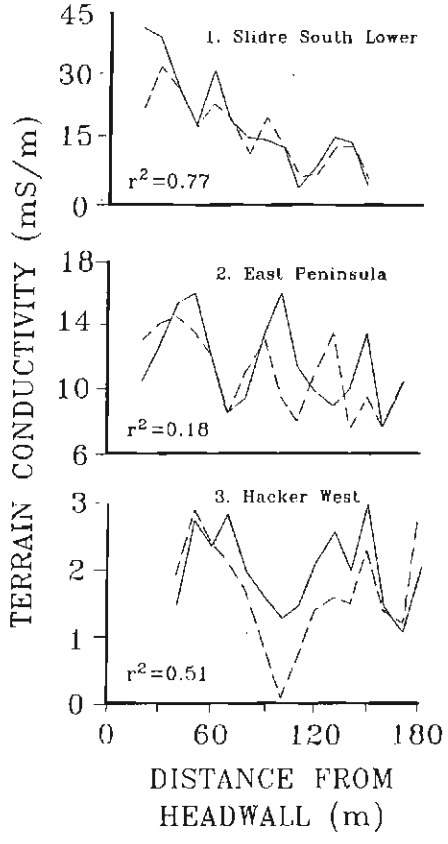

Figure 5. EM-31 surveys in vertical dipole orientation across the mudflows of active ground ice slumps. A high degree of lateral heterogeneity within the mudflow sediments is shown by the differences between readings taken parallel (solid line) and perpendicular (dotted line) to the flow direction. Site numbers refer to locations shown in Figure 3.

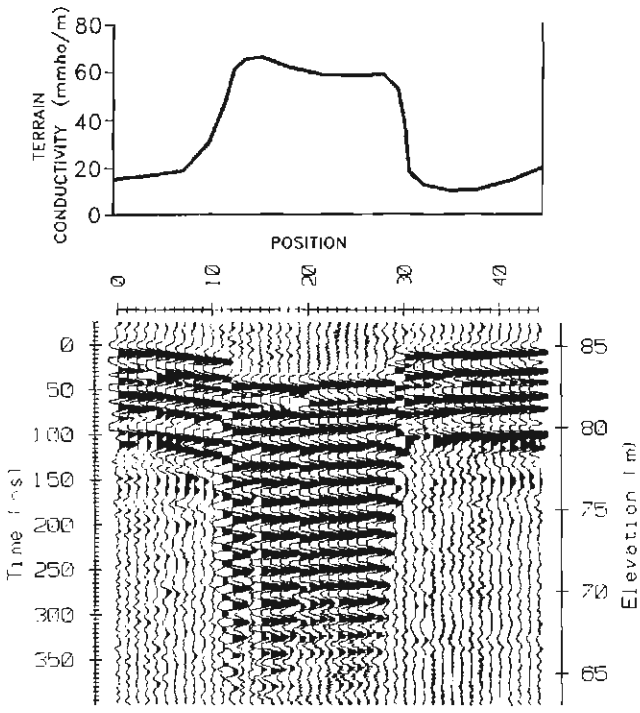

Figure 6. Ground penetrating radar (100 MHz) and EM-31 (upper) profiles across the active mudflow of a ground ice slump. Note the increase in both terrain conductivity and GPR signal noise as the profile crosses mudflow with a salt crust.

present within the electrical properties of the slumped sediments. As noted previously, this effect was not seen within undisturbed sediments of the same lithology.

Survey lines crossing terrain with an extensive evaporitic salt crust on the surface were also conducted. Passing over the salt, instrument readings jumped from background levels of less than 5 mS/s to over 100 mS/m, even though drilling confirmed the depth to massive ice remained essentially constant.

Ground penetrating radar

The GPR technique is generally of limited success when profiling over terrain with a soil conductivity higher than 10-15 mS/m due to rapid signal attenuation. Additionally, a sediment-rich snowpack or a wet active layer can present signal noise that confuses returns from depth. Surveys were initiated in mid-May prior to active layer development. Three days of high winds (May 25-27) resulted in severe snow drifting and eolian sediment beds within the snow, drastically limiting radar effectiveness. Subsequent equipment problems forced the postponement of radar surveying until mid-June when the moist active layer approached 20 cm depth.

Although approximately 5 km of GPR surveys were eventually conducted, most were strongly affected by the same highly conductive thawed sediments and salt crust that hampered the EM-31 surveys. Figure 6 shows both GPR and EM-31 profiles across a slump mudflow at site R-1, with

increased radar interference directly on the mudflow corresponding with a rise in conductivity. The profile consists of incoherent noise without indication of underlying structure, although the site is known to be underlain by massive ice.

Sporadic "windows" of low soil conductivity yielded reflectors at depths of up to 15 m. Figure 7 shows the results of a profile conducted at site R-2, across a mudflow of an abandoned slump with much lower terrain conductivities than at R-1. Reflectors parallel topography in the first 125 ns of each trace. Amongst these reflectors may be the base of the active layer and the top of the ice, indistinguishable due to the poor near-surface resolution of the 50 MHz antennas. A major reflector located between 7 and 12 m below the surface indicates a major structural change not associated with topography. This reflector, beyond the limit of shallow drilling, likely represents either the base of the massive ice body or the upper contact with bedrock.

Gravity

From the five gravity survey lines conducted, the central profile from the Slidre River site best illustrates a gravity anomaly caused by massive ice. A steep-sided, flat-topped hill with approximate basal dimensions of 450 x 600 m rises 30 m above the surrounding terrain. The profile starts and ends on bedrock tors assumed not to be underlain with ice. Along the line between the tors are unconsolidated marine sediments with unknown volumes of ground ice. Massive ground ice exposures and abandoned thaw slumps are found on all flanks of the hill, suggesting an ice core.

Figures 8A and 8B show the Bouguer anomaly and topography above datum respectively for the Slidre gravity survey. The Bouguer anomaly profile shows a negative correlation with

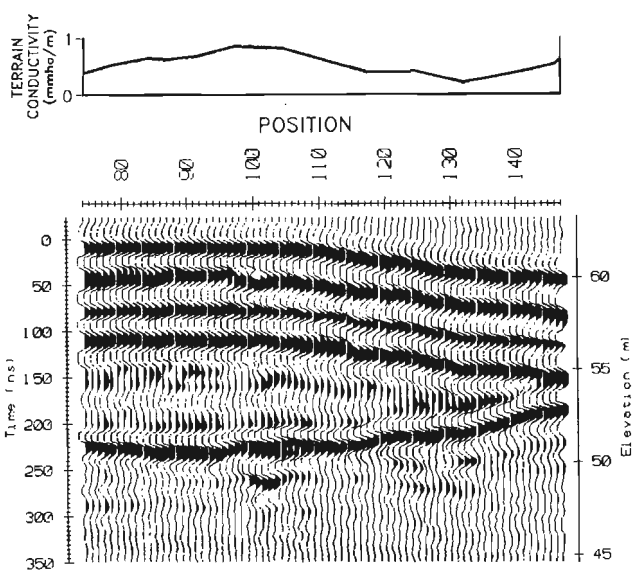

Figure 7. *GPR profile (50 MHz)(lower) across abandoned mudflow with much lower terrain conductivity. The deepest reflector (between 7 and 12 m depth) is interpreted as either the base of the massive ice or the contact between marine silts and sandstone bedrock. Such "windows" of signal penetration were rare within the survey area. CMP surveying indicated a radar propagation velocity of 0.11 m/ns.*

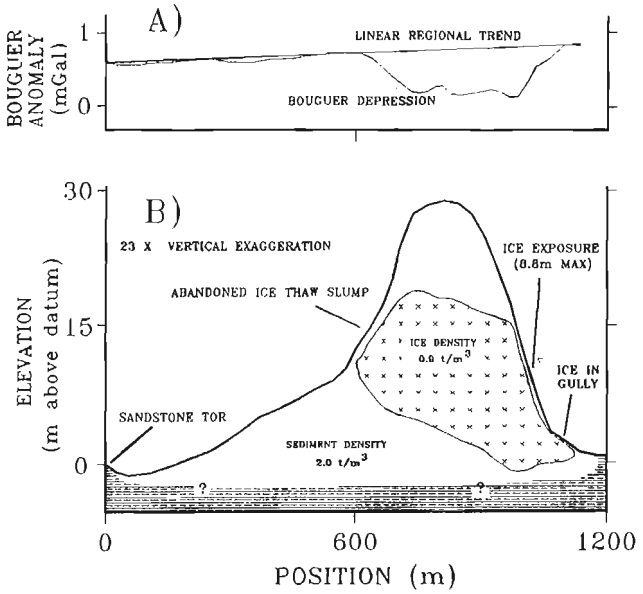

Figure 8. *The calculated Bouguer anomaly (A) and the topography and interpreted model of ice distribution (B) for a gravity profile across a hill at the Slidre River site. The occurrence of ice in exposure (Fig. 2a) and in shallow boreholes aided in interpretation.*

elevation, suggesting that a large proportion of the relief is due to the presence of a massive ground-ice body. Figure 8B also shows the interpreted ice thickness underlying the hill using an assumed sediment density of 2.0 t/m^3. Ice thickness reaches a maximum of almost 17 m beneath the hill. Surveying along parallel lines 60 m north and south of the central lines revealed slightly thinner ice. A survey perpendicular to this profile was not possible due to steep bluffs at the north and south ends of the hill preventing accurate surveying.

Drilling at the slope foot revealed segregated ice lensing only between 0.71 and 1.78 m. Large thicknesses of massive ice were not found in this borehole, an observation consistent with the gravity results. Another borehole on the hilltop did not reveal any massive ice before completion at 2.6 m. Massive ice up to 6.8 m thick in exposure (Fig. 2a) occurs slightly south of the 970 m position. Massive ground ice has also been exposed in a meltwater gully 14 m below the top of the ice at this location. The minor Bouguer anomaly depressions between 50 and 500 m possibly indicate smaller thicknesses of ground ice. Drilling was not conducted along this section and there is no morphological evidence to support this.

DISCUSSION

It became evident early in the surveys that the electrical influence from the sediment was overwhelming the GPR and EM-31 results, masking any signal from the underlying massive ice. As the thickness of sediment over ice remained essentially constant along the EM-31 profiles, variations in results can be attributed to a high degree of overburden heterogeneity, which in turn prevented any modelling of ice distribution.

Inkster et al. (1989) noticed the loss of radar reflectors along a profile as terrain conductivity increased, and suggested that GPR and EM-31 are highly complementary sensors. That general trend is also noted in this study, although the relationship between terrain conductivity and GPR survey success seems more complicated. Radar transmits a poorly focused pulse, and thus local soil variations result in variations in the propagation and return of individual portions of each pulse. This likely contributed to the often incoherent nature of the profiles, even in sections with terrain conductivities of less than 10 mS/m. Some areas of low conductivity were noted with much improved radar penetration, although poor resolution and confusing reflectors prevented the delineation of the top of the ice body. Without information from deep boreholes, the origin of reflectors at greater depths cannot be interpreted with confidence.

The magnitude of lateral electrical anisotropy correlates well with the degree and timing of soil disturbance, as does the pattern of salt crust development. The recently disturbed thaw slump mudflows displayed the greatest degree of anisotropy and the most extensive salt crust. A lower degree of anisotropy was noted within the stabilized mudflows, drier and now frozen with a sporadic salt crust. Electrical responses from the undisturbed marine sediments were far less variable, and the salt crust was generally absent. This suggests that mudflows associated with thaw disturbance could act to preferentially align conductive salts within the mudflow. Evaporitic salt is also more extensive across recent mudflows because the flow process mixes the soil, presenting a fresh salt source from the sediment. Undisturbed marine sediments are likely more depleted of available salt within the active layer, however a thaw slump event or active layer deepening would mix the deeper layers and release salts trapped deeper within the soil. Vegetation was common in areas without the salt crust and generally absent where salt was extensive. The salt could represent a toxicity to vegetation, with recolonization not possible until salts are depleted.

If air bubbles within the ice can be neglected, the ice density of ρ_i=0.9 t/m^3 can be assumed with some certainty. The density of enclosing sediments cannot be determined without analysis of samples from deep boreholes. Therefore, the sediment density, ρ_s=2.0 t/m^3, incorporated into the Bouguer anomaly calculations represents an estimation based on published densities for unconsolidated silts and sands (Telford et al., 1990). An underestimated sediment density results in an overestimated excess ice content. Substituting an assumed sediment density of 1.7 and 2.3 t/m^3 yields a maximum ice thickness of approximately 23 and 13 m respectively. An elevation error of 10 cm yields an error of approximately 45 cm in ice thickness.

Gravity profiling cannot predict whether the ice occurs as a single massive body or as multiple ice lenses. GPR is much more useful as a stratigraphic tool, often revealing information on the nature of the ice which may be used to infer ice origin (Robinson et al., 1993). If only small ice bodies are present, high resolution GPR is a far more appropriate instrument for their detection, but only under optimal electrical conditions in the soil. An ice body less than 5 m thick is probably beyond the resolution of conventional gravity surveying. Microgravimeters sensitive to 0.001 mGal have recently become available and would greatly improve this resolution; however, the accuracy of gravity corrections (i.e., instrument drift, elevation, density, reading error) would still limit survey confidence. As is the case for most geophysical surveying, the need for ground truthing is paramount. Although numerous shallow boreholes were drilled for this study, deeper boreholes would have permitted determination of accurate values for sediment density and ice thicknesses.

The ice thickness and distribution calculated from the gravity surveys suggests that, if the ice were to melt, most of the hill would disappear. The presence of numerous retrogressive thaw slumps, intensive gullying, and other melt-out features (Pollard, 1991; Robinson, unpub. data) indicate that this may have already occurred over much of the Hacker Creek region. The shallow occurrence of massive ground ice in boreholes in the Hacker Creek vicinity indicates a widespread distribution of remaining ground ice in the near-surface (Robinson, unpub. data). The scattered flat-topped hills and interfluve areas, such as that shown to be ice-cored, may contain the last remnants of deeper buried ice bodies formerly of much greater extent. The relationship between the deep and shallow ice bodies is unclear. As large volumes of shallow massive ground ice remain, there is the potential for severe terrain disturbance from thermokarst.

Massive ground ice is known to occur at other locations on the Fosheim Peninsula (Pollard, 1991; Barry, 1992); yet the large number of exposures and geomorphic indications of past and present buried ice distribution suggest that the Hacker Creek area is anomalous for the region.

CONCLUSIONS

Of the three geophysical techniques used in the Hacker Creek region, only gravity surveying was successful in delineating massive ground ice. Flat-topped, steep-sided hills were shown to be cored with massive ground ice with a maximum thickness of almost 17 m. This thickness is an estimate based upon the magnitude of Bouguer anomaly depression and assumed values for the density of enclosing sediments.

The electrical geophysical methods were severely affected by the highly variable electrical conductivities of the overburden. The magnitude of soil heterogeneity correlated well with the degree and timing of thaw disturbance of the ice-rich marine sediments, suggesting that mudflows associated with thaw disturbance could act to align preferentially conductive salts within mudflows. These conditions prevented the use of EM-31 for layered-earth modelling of ice distribution and limited the effectiveness of GPR to areas of low terrain conductivity. Even in areas of low terrain conductivity, radar returns were affected by soil heterogeneity and reverberations within the active layer.

Widespread shallow massive ground ice underlies much of the Hacker Creek region as shown through geophysical surveying and the presence of ice in exposure and in boreholes. Although evidence of past thermokarst is abundant in

the Hacker Creek region, the large amount of ice still remaining suggests that there is the potential for severe terrain disturbance in the future.

ACKNOWLEDGMENTS

Sylvia Edlund, Terrain Sciences Division, graciously provided employment, equipment, and friendship at Hot Weather Creek. Alan Judge, Terrain Sciences Division, arranged for the loan of the GPR unit. Robert Gilbert is expertly advising this work at Queen's University. Field assistance was capably provided by Roger Edgecombe and Chris North. The Polar Continental Shelf Project (PCSP), the Science Institute of the Northwest Territories, and the Northern Science Training Program assisted both financially and logistically. Doug Hodgson provided helpful comments on an earlier manuscript version. J.D. McNeill provided useful comments on EM-31. Thanks are also extended to Wayne Pollard, Antoni Lewkowicz, and all researchers at Hot Weather Creek and Queen's University who have helped greatly in one way or another.

REFERENCES

Annan, A.P. and Davis, J.L.
1976: Impulse radar sounding in permafrost; Radio Science, v. 11, no. 4, p. 383-394.

Barry, P.
1992: Ground ice characteristics in permafrost on the Fosheim Peninsula, Ellesmere Island, N.W.T.; a study utilizing ground probing radar and geomorphological techniques; M.Sc. thesis, Department of Geography, McGill University, Montreal, Quebec.

Dallimore, S.R. and Davis, J.L.
1987: Ground probing radar investigations of massive ground ice and near surface geology in continuous permafrost; in Current Research, Part A; Geological Survey of Canada, Paper 87-1A, p. 913-918.
1992: Ground penetrating radar investigations of massive ground ice; in Ground penetrating radar, (ed.) J. Pilon; Geological Survey of Canada, Paper 90-4, p. 41-48.

Dallimore, S.R., Hunter, J.A., Kurfurst, P.J., and Pullan, S.E.
1988: Evaluation of geotechnical and geophysical methods used for permafrost and ground ice detection; in Proceedings, 41st Canadian Geotechnical Conference, Waterloo, Ontario, p. 106-112.

Davis, J.L. and Annan, A.P.
1989: Ground-penetrating radar for high-resolution mapping of soil and rock stratigraphy; Geophysical Prospecting, v. 37, p. 531-551.

Davis, J.L., Scott, W.J., Morey, R.M., and Annan, A.P.
1976: Impulse radar experiments on permafrost near Tuktoyaktuk, Northwest Territories; Canadian Journal of Earth Sciences, v. 13, p. 1584-1590.

Dyke, L.D.
1988: Permafrost aggradation along an emergent coast, Churchill, Manitoba; in Proceedings, Fifth International Conference on Permafrost, Trondheim, Norway, p. 138-142.

Edlund, S.A., Alt, B.T., and Young, K.L.
1989: Interaction of climate, vegetation, and soil hydrology at Hot Weather Creek, Fosheim Peninsula, Ellesmere Island, Northwest Territories; in Current Research, Part D; Geological Survey of Canada, Paper 89-1D, p. 125-133.

Gagne, R.M. and Hunter, J.A.
1975: Hammer seismic studies of surficial materials, Banks Island, Ellesmere Island, and Boothia Peninsula, N.W.T.; in Report of Activities, Part B, Geological Survey of Canada, Paper 75-1B, p. 13-17.

Geonics
1984: Operating manual for EM31-D non-contacting terrain conductivity meter; Geonics Ltd., Mississauga, Canada.

Hammer, S.
1939: Terrain corrections for gravimeter stations; Geophysics, v. 4, p. 184-194.

Hinze, W.J.
1990: The role of gravity and magnetic methods in engineering and environmental studies; in Geotechnical and Environmental Geophysics, Volume I – Review and Tutorial (ed.) S.H. Ward, Society of Exploration Geophysicists.

Hodgson, D.A., St-Onge, D.A., and Edlund, S.A.
1991: Surficial materials of Hot Weather Creek basin, Ellesmere Island, Northwest Territories; in Current Research, Part E; Geological Survey of Canada, Paper 91-1E, p. 157-163.

Inkster, D.R., Rossiter, J.R., Goodman, R., Galbraith, M., and Davis, J.L.
1989: Ground penetrating radar for subsurface environmental applications; Proceedings of the Seventh Thematic Conference on Remote Sensing for Exploration Geology, Calgary, Alberta, Canada, October 1989, p. 127-140.

Judge, A.S., Tucker, C.M., Pilon, J.A., and Moorman, B.J.
1991: Remote sensing of permafrost by ground pentrating radar at two airports in arctic Canada; Arctic, v. 44, Supplement 1, p. 40-48.

McNeill, J.D.
1980: Electromagnetic terrain conductivity measurements at low induction numbers; Technical Note TN-6, Geonics Ltd., Mississauga, Canada.

Pollard, W.H.
1991: Observations on massive ground ice on Fosheim Peninsula, Ellesmere Island, Northwest Territories; in Current Research, Part E; Geological Survey of Canada, Paper 91-1E, p. 223-231.

Rampton, V.N. and Walcott, R.I.
1974: Gravity profiles across ice-cored topography; Canadian Journal of Earth Sciences, v. 11, p. 110-122.

Robinson, S.D.
1993: Massive ground ice in the vicinity of Hot Weather Creek, Fosheim Peninsula, Ellesmere Island, N.W.T., Canada; 23rd Annual Arctic Workshop Program and Abstracts, 1993, Byrd Polar Research Center Miscellaneous Series Publications No. 322, Byrd Polar Research Center, The Ohio State University, Columbus, p. 102.

Robinson, S.D., Moorman, B.J., Judge, A.S., and Dallimore, S.R.
1993: The characterization of massive ground ice at Yaya Lake, Northwest Territories using radar stratigraphy techniques; in Current Research, Part B; Geological Survey of Canada, Paper 93-1B, p. 23-32.

Sartorelli, A.N. and French, R.B.
1982: Electro-magnetic induction methods for mapping permafrost along northern pipeline corridors; in Proceedings, Fourth Canadian Permafrost Conference, Calgary, Alberta, National Research Council of Canada, p. 283-295.

Scott, W.J., Sellmann, P.V., and Hunter, J.A.
1990: Geophysics in the study of permafrost; in Geotechnical and Environmental Geophysics, Volume 1 – Review and Tutorial (ed.) S.H. Ward; Society of Exploration Geophysicists, p. 355-384.

Sinha, A.K. and Stephens, L.E.
1983: Permafrost mapping over a drained lake using electrical induction methods; in Current Research, Part A; Geological Survey of Canada, Paper 83-1A, p. 213-220.

Taylor, A.E., Burgess, M., Judge, A.S., and Allen, V.S.
1982: Canadian geothermal data collection-northern wells, 1981; Ottawa, Energy, Mines and Resources Canada, Geothermal Series 13, Earth Physics Branch, 153 p.

Telford, W.M., Geldart, L.P., and Sheriff, R.E.
1990: Gravity methods; Chapter 2 in Applied Geophysics, Second edition, Cambridge University Press, Cambridge.

Ulriksen, C.P.F.
1982: Application of impulse radar to civil engineering; Ph.D. thesis, Lund University of Technology, Lund, Sweden, 175 p.

Washburn, D.S. and Phukan, A.
1988: Discontinuous permafrost mapping using the EM-31; in Proceedings, Fifth International Conference on Permafrost, Trondheim, Norway, p. 1018-1023.

Geological Survey of Canada Project 920047

Effective porosity of shale samples from the Beaufort-Mackenzie Basin, northern Canada

D.R. Issler[1] and T.J. Katsube
Mineral Resources Division

Issler, D.R. and Katsube, T.J., 1994: Effective porosity of shale samples from the Beaufort-Mackenzie Basin, northern Canada; in Current Research 1994-B; Geological Survey of Canada, p. 19-26.

Abstract: Porosity (ϕ) was determined for 41 shale core samples from 9 petroleum exploration wells in the Beaufort-Mackenzie Basin of northern Canada using the helium porosimetry technique. The samples span a broad depth range (1-4.9 km) and were obtained from regions which experienced significantly different sedimentation rates during their burial/compaction history. These porosity (ϕ) values show good agreement with previous measurements (mercury porosimetry method) on a subset of the same samples, and support the suggestion that both helium and water penetrate pores smaller than 3 nm in diameter. The observed trend of decreasing ϕ with depth is drastically reduced or reversed in zones of excess pore pressure at depths greater than 2.4-3.4 km. The laboratory-based ϕ measurements compare favourably with porosity values predicted from sonic logs and verify the correlation that exists between undercompaction, excess pore pressure, and high sedimentation rate, as inferred from well log analysis.

Résumé : La porosité (ϕ) de 41 échantillons de carottes de shales provenant de neuf puits d'exploration pétrolière dans le bassin de Beaufort-Mackenzie du nord canadien a été déterminée par la technique de la porosimétrie à l'hélium. Les échantillons ont été prélevés dans un intervalle de profondeurs étendu (de 1 à 4,9 km) dans des régions ayant connu des taux de sédimentation très différents au cours de leur enfouissement/tassement. Les résultats correspondent bien aux mesures effectuées antérieurement (méthode de porosimétrie au mercure) sur un sous-ensemble des mêmes échantillons, et ils indiquent que l'hélium et l'eau s'infiltrent dans des pores de moins de 3 nm de diamètre. La tendance observée, selon laquelle ϕ diminue avec la profondeur, est fortement atténuée, voire inversée, dans les zones de pression interstitielle excessive à des profondeurs dépassant 2,4 à 3,4 km. Les mesures de ϕ effectuées en laboratoire se comparent favorablement aux prévisions des diagraphies soniques et vérifient la corrélation qui existe entre le sous-tassement, la pression interstitielle excessive et le taux de sédimentation élevé, comme l'indique l'analyse des diagraphies de puits.

[1] Institute of Sedimentary and Petroleum Geology, Calgary

INTRODUCTION

Following earlier studies (Issler, 1992; Katsube and Best, 1992; Katsube and Issler, 1993), this paper reports results from multi-disciplinary physical property studies of shales from the Beaufort-Mackenzie Basin (Fig. 1). The main purpose of this study is to obtain geochemical/petrophysical information for constraining models of shale compaction. Discussion of the regional framework and rationale for the study can be found in Issler (1992) and Katsube and Issler (1993). In a previous paper, mercury porosimetry data were presented to show how shale pore-size distributions vary with burial depth (Katsube and Issler, 1993). In this paper, we present and compare porosity data for Beaufort-Mackenzie Basin shale core samples obtained by three different methods: helium porosimetry, mercury porosimetry, and sonic porosity. The two main objectives of this phase of the study are, to (1) test the predictions of porosity from independently-calibrated sonic logs and thereby provide confirmation of log-predicted porosity trends in the Beaufort-Mackenzie Basin (Issler, 1992), and (2) provide an independent check on porosity values determined by mercury porosimetry in phase 1 (Katsube and Issler, 1993) of the study. Only basic experimental results are reported in this paper with minimal interpretation.

EXPERIMENTAL METHODS

Sample selection and preparation

Forty-one shale core samples from 9 wells in 4 different compaction zones of the Beaufort-Mackenzie Basin (Fig. 1) were selected for a variety of physical property measurements

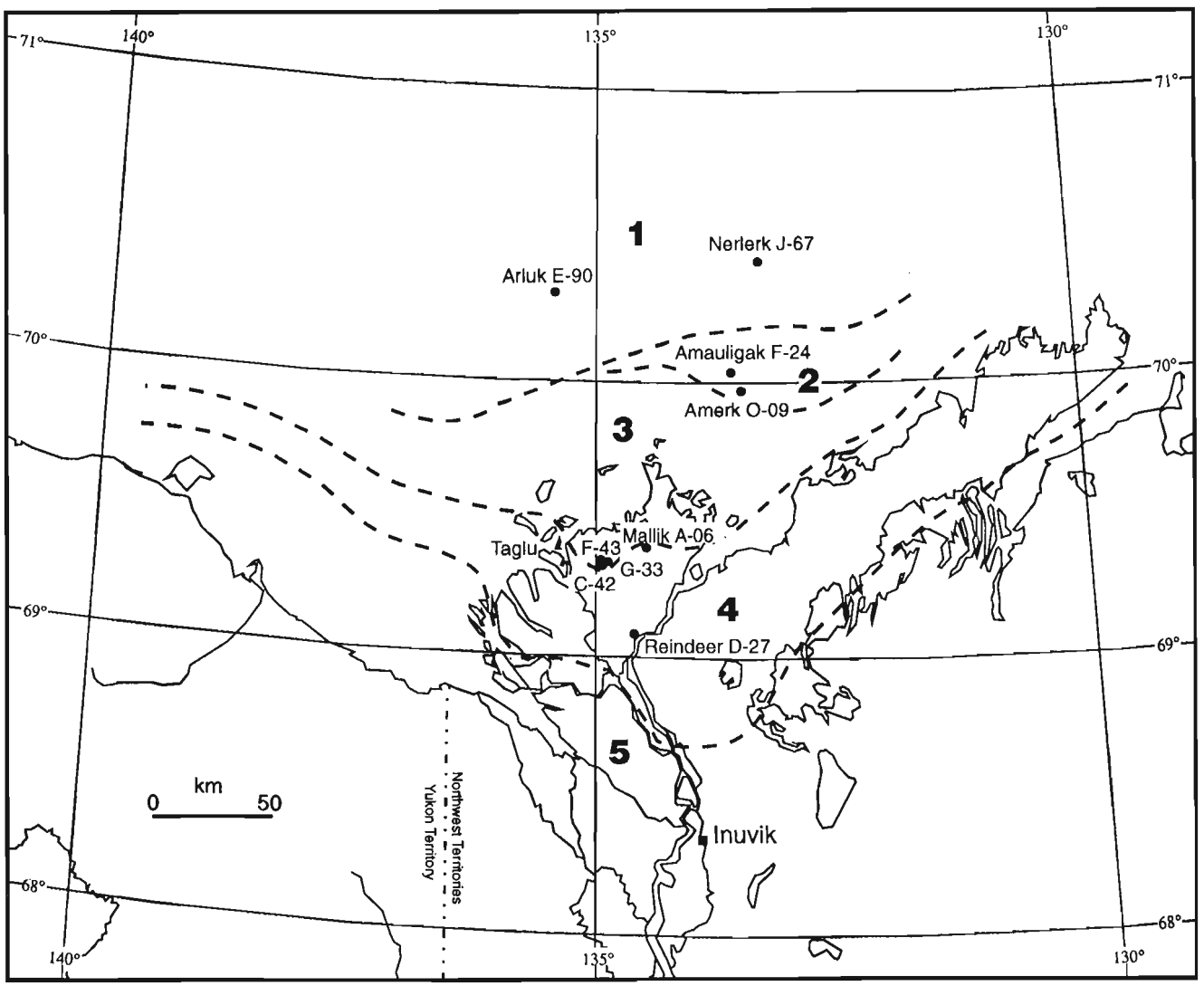

Figure 1. *Map showing the location of 9 wells in the Beaufort-Mackenzie Basin, northern Canada, from which the shale core samples were obtained (from Katsube and Issler, 1993). Approximate boundaries for 5 shale compaction zones (Issler, 1992) are shown by the heavy dashed lines.*

Table 1. Sample identification and sedimentation rates of zones (Issler, 1992) from which the samples were taken, in the Beaufort-MacKenzie Basin (offshore Northwest Territories), northern Canada.

Zone	Characteristics	Pliocene-Pleistocene Sedimentation Rates (m/m.y.)	Wells	Sample Series
1	High sedimentation rates	380-660	Arluk E-90 Nerlerk J-67	B-AK- B-NR-
2	Intermediate sedimentation rates	190-380	Amauligak F-24 Amerk O-09	B-AM- B-AR-
3	Low sedimentation rates	40-190	Taglu C-42 Taglu F-43 Taglu G-33	B-TA-1 B-TA-2 B-TG-
4	Eroding and uplifting	negative	Mallik A-06 Reindeer D-27	B-ML- B-RE-

as part of a multidisciplinary study. Approximately 5-10 g fractions were cut from these core samples and these specimens were used for porosity determination. Information on well names, sample numbers, and depths are given in Tables 1 and 2. Additional well information can be found in Katsube and Issler (1993). The shale compaction zones in which the samples are located are characterized by distinctive porosity-depth trends (Issler, 1992) that correlate with Pliocene-Pleistocene sedimentation rates (Table 1). Shales are least compacted in zone 1 where Pliocene-Pleistocene sedimentation rates were the highest and become progressively more compacted toward zone 4 where sedimentation rates declined and the amount of erosion is greater (Fig. 1; Table 1).

Experimental approach

Porosity was determined for these 41 shale samples using 3 different techniques: helium porosity, ϕ_{he}, and mercury porosity, ϕ_{gm1}, ϕ_{gm2}, determined by laboratory methods; and sonic porosity, ϕ_s, determined from sonic logs. The methods and procedures used for porosity measurement are briefly described below.

Helium porosity, ϕ_{he}

Helium porosity values (ϕ_{he}) were determined in two steps: first the sample grain volume was determined using a Boyles' Law double-celled helium porosimeter, and then the sample bulk volume was obtained using the mercury immersion technique. Descriptions of these measurement techniques and procedures, which generally follow the recommended practices of the American Petroleum Institute (API, 1960), are given in Loman et al. (1993).

Mercury porosity, ϕ_{gm1}, ϕ_{gm2}

Mercury porosity values (ϕ_{gm1} and ϕ_{gm2}) for these shale samples are by-products of the pore-size distribution measurements (Katsube and Issler, 1993). The pore-size distribution of these shale samples was determined by mercury intrusion porosimetry, following the procedures described in previous publications (e.g., Katsube, 1981; Katsube and Walsh, 1987; Katsube and Hume, 1987; Katsube and Best, 1992). The pore-size distribution of a shale sample is represented by the distribution of partial porosity values, ϕ_a, contributed by different pore-size ranges. Mercury porosity, ϕ_{gm1} is the sum of partial porosity values for pore-sizes from 3 nm to 10 μm, and ϕ_{gm2} is the same for partial porosity values from 3 nm to 250 μm. Both ϕ_{gm1} and ϕ_{gm2} represent effective porosity (Katsube et al., 1992; Katsube, 1992), that is, the porosity of interconnected pores in a rock. However, ϕ_{gm1} is more likely to represent a true sample porosity, compared to ϕ_{gm2} which may include measurement errors such as those originating from the space between the specimen and the sample container. Further details of this measuring method and procedure can be found in Katsube and Issler (1993).

Sonic porosity, ϕ_s

Issler (1992) previously established a correlation between shale porosity and sonic transit-time (from sonic logs) for the Beaufort-Mackenzie Basin. The correlation function was determined by comparing core porosity values with average sonic transit-time values recorded at depths in the wells where the cores were recovered. These core porosities were previously determined by use of the helium porosimeter (Issler, 1992), but not necessarily under the same conditions as ϕ_{he} was determined. Sonic porosity (ϕ_s) values for the 41 shale

Table 2. Porosity (ϕ) measured by different methods.

Sample Number	Depth (TVD, km)	δ (g/mL)	ϕ_s	ϕ_{gm1} (%)	ϕ_{gm2} (%)	ϕ_{he} (%)
(Zone-1)						
B-AK-1*	3.45	2.40	21	12.7	13.1	14.2
B-AK-2*	3.94	2.40	19	14.0	16.8	17.3
B-NR-1*	3.66	2.30	18-20	15.9	16.9	19.5
B-NR-2*	3.67	2.28	18-20	16.2	16.7	17.2
B-NR-3*	4.01	2.32	16-18	14.0	15.4	21.9
(Zone-2)						
B-AM-1	3.11	2.50	12	9.76	10.0	14.0
B-AM-2	3.12	2.40	12	10.8	12.0	11.9
B-AM-3	3.34	2.44	10-12	9.4	10.1	9.6
B-AR-1	1.32	1.73	30-31	31.5	31.6	39.3
B-AR-2	1.53	1.99	28-31	25.8	29.2	30.5
B-AR-3	1.77	1.78	25-29	28.3	30.0	33.9
B-AR-4*	3.87	2.43	10-13	10.3	11.5	11.6
B-AR-5*	4.38	2.47	10-12	8.46	9.6	-
B-AR-6*	4.61	2.50	11-14	8.35	8.8	10.0
B-AR-7*	4.86	2.50	10	8.16	8.6	11.5
(Zone-3)						
B-TA-1	2.88	2.10	10-13	6.29	7.0	6.8
B-TA-2*	3.25	2.56	6-9	7.65	8.0	11.4
B-TG(33)-1	0.95	1.87	22-29	29.5	30.6	29.5
B-TG(33)-2	1.35	2.07	24	22.8	23.5	24.5
B-TG(33)-3	1.64	2.28	18-23	18.6	19.2	18.4
B-TG(33)-4	2.08	2.38	13-16	12.6	14.2	17.3
B-TG(33)-5	2.46	2.46	12-17	7.54	8.3	9.8
B-TG(33)-6	2.46	2.55	12-17	6.92	7.8	10.6
B-TG(33)-7	2.53	2.46	11	9.95	10.7	10.0
(Zone-4)						
B-ML-1	1.36	2.05	20	21.3	22.9	23.7
B-ML-2*	3.18	2.61	2	5.09	5.4	7.4
B-ML-3*	3.55	2.61	4-5	5.80	6.4	5.8
B-RE-1	1.46	2.34	15-17	15.0	15.5	15.1
B-RE-2	1.47	2.34	15-17	12.1	12.8	11.1
B-RE-3	2.02	2.57	7-8	5.9	6.7	7.1
B-RE-4	2.09	2.61	7-10	7.04	7.6	7.0
B-RE-5	2.10	2.53	7-10	6.23	6.7	7.3
B-RE-6*	2.21	2.56	10-11	6.58	7.0	8.2
B-RE-7*	2.39	2.50	11-13	8.66	9.1	10.6
B-RE-8*	2.42	2.48	11-13	7.93	8.5	8.0
B-RE-9*	2.55	2.47	11-15	8.90	9.4	9.8
B-RE-10*	2.73	2.48	14-16	9.25	9.5	10.9
B-RE-11*	2.92	2.46	13-15	8.47	8.9	10.3
B-RE-12*	3.15	2.53	9-11	6.61	7.1	8.1
B-RE-13*	3.48	2.55	10	5.58	5.7	6.7
B-RE-14*	3.63	2.58	9-15	7.04	7.4	9.1

* : Overpressured.
TVD : True vertical depth (Katsube and Issler, 1993).
δ : Bulk density (Katsube and Issler, 1993).
ϕ_s : Sonic porosity determined from sonic logs.
ϕ_{gm1} : Total porosity measured by mercury porosimetry for pore sizes up to 10 μm (Katsube and Issler, 1993).
ϕ_{gm2} : Total porosity measured by mercury porosimetry for pore sizes up to 250 μm (Katsube and Issler, 1993).
ϕ_{he} : Porosity measured by helium porosimetry.

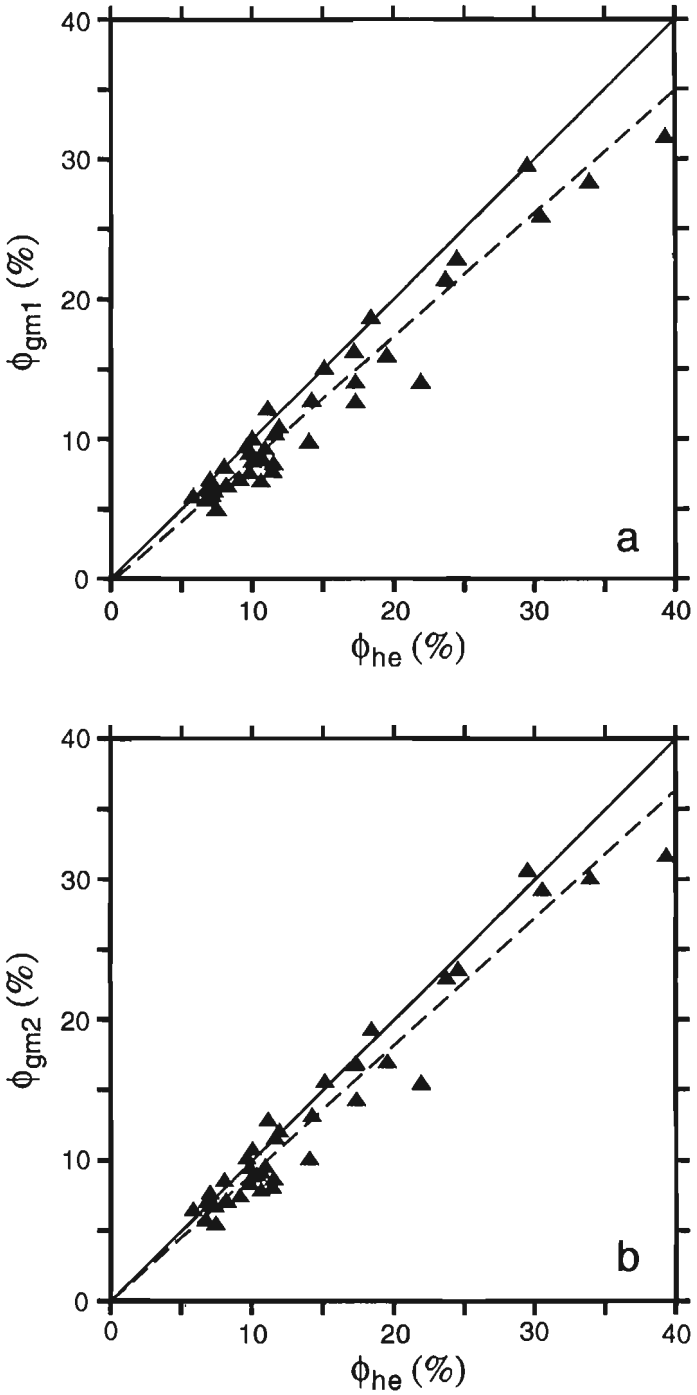

Figure 2. *Comparison between helium porosity (ϕ_{he}) and (**a**) mercury porosity, ϕ_{gm1} (includes pore-sizes less than 10 μm) and (**b**) mercury porosity, ϕ_{gm2} (includes pore-sizes less than 250 μm). The solid lines represent a 1:1 relation between the two different porosity measurements, and the dashed lines represent the reduced major axis (RMA) of the regression analysis.*

core samples discussed in this paper were determined by converting average sonic transit-time readings of the sonic logs, at core recovery depths, into porosity using that equation (Issler, 1992). These sonic porosity values are then compared with independent sets of other porosity values (e.g., ϕ_{he}, ϕ_{gm1}, and ϕ_{gm2}).

EXPERIMENTAL RESULTS

Results for the measurement of sonic porosity (ϕ_s), helium porosity (ϕ_{he}), and mercury porosity (ϕ_{gm1} and ϕ_{gm2}) are listed in Table 2 for all 41 samples. The data for ϕ_{gm1} and ϕ_{gm2} have been obtained from the pore-size distribution data in Katsube and Issler (1993). Bulk density (δ) values are also from the same source. The data for ϕ_s and ϕ_{he} have not been previously published. Measurements are complete for all samples except sample B-AR-5 which lacks ϕ_{he} data (Table 2).

The correlation of ϕ_{he} with ϕ_{gm1} and ϕ_{gm2} is generally very good. Figure 2 shows crossplots of both ϕ_{gm1} and ϕ_{gm2} versus ϕ_{he}. The solid curves in Figures 2a and b represent a 1:1 relationship between mercury and helium porosity values. The dashed lines represent the reduced major axis, (RMA) (Davis, 1986; Katsube and Agterberg, 1990), for the regression lines that take the form:

$$y = Ax + B, \qquad (1)$$

where x and y are variables and A and B are coefficients. Substituting ϕ_{he} for x, and ϕ_{gm1} and ϕ_{gm2} for y (equation 1) produces the following values for the regression coefficients A and B:

ϕ_{gm1}/ϕ_{he}:	A = 0.88	B = -0.29	r = 0.97
ϕ_{gm2}/ϕ_{he}:	A = 0.91	B = -0.03	r = 0.97,

where r is the correlation coefficient. Although both relationships produce good results with correlation coefficient values close to unity, it is clear that there are systematic differences between these measurement techniques which cause A and B to depart from unity and zero, respectively. Superficially, it appears that the ϕ_{gm2} to ϕ_{he} relationship is slightly better because its values of A and B are closer to unity and zero.

Figure 3 shows a comparison of all the measured core porosity data (ϕ_{he}, ϕ_{gm1}, ϕ_{gm2}) with sonic porosity (ϕ_s) values estimated from sonic logs. The solid line represents a 1:1 correlation between core porosity and ϕ_s. The resolution of the sonic log tool (approximately 0.5 m) is much coarser than the scale of core porosity measurements (approximately 1 cm). Furthermore, many of the shale cores were obtained from thinly interbedded sandstones and shales where sonic transit-times can vary significantly. For these reasons, ϕ_s values are given as a range (Table 2) representative of sonic transit-times at core recovery depths. Plot symbols are arbitrarily centred in the middle of the ϕ_s range for ease of

comparison (Fig. 3). In general, ϕ_{he} values are more uniformly distributed around the 1:1 correlation line whereas most of the ϕ_{gm1} and ϕ_{gm2} values tend to fall below this line.

DISCUSSION AND CONCLUSIONS

The laboratory porosity values (Table 2, Fig. 2) determined by two different methods show good agreement, and are therefore considered reliable. The ϕ_{gm2} values are slightly closer to the ϕ_{he} values in comparison with ϕ_{gm1}, although this may be fortuitous. The ϕ_{gm2} values which encompass a broader range of pore-sizes may also include measurement artifacts, and thus may be less accurate. Both sets of mercury porosity data are systematically lower than the ϕ_{he} values (Fig. 2).

It has been suggested that water can penetrate shale pores smaller than 3 nm (Katsube, 1992), the lower pore-size limit for mercury penetration for these mercury porosity measurements. If helium also penetrates pores smaller than 3 nm, then ϕ_{he} values will be larger than the mercury porosity values. We believe that ϕ_{gm1} values are accurate for the pore-size range they represent (3 nm to 10 μm) but that ϕ_{he} values may be more representative of the total interconnected porosity (effective porosity).

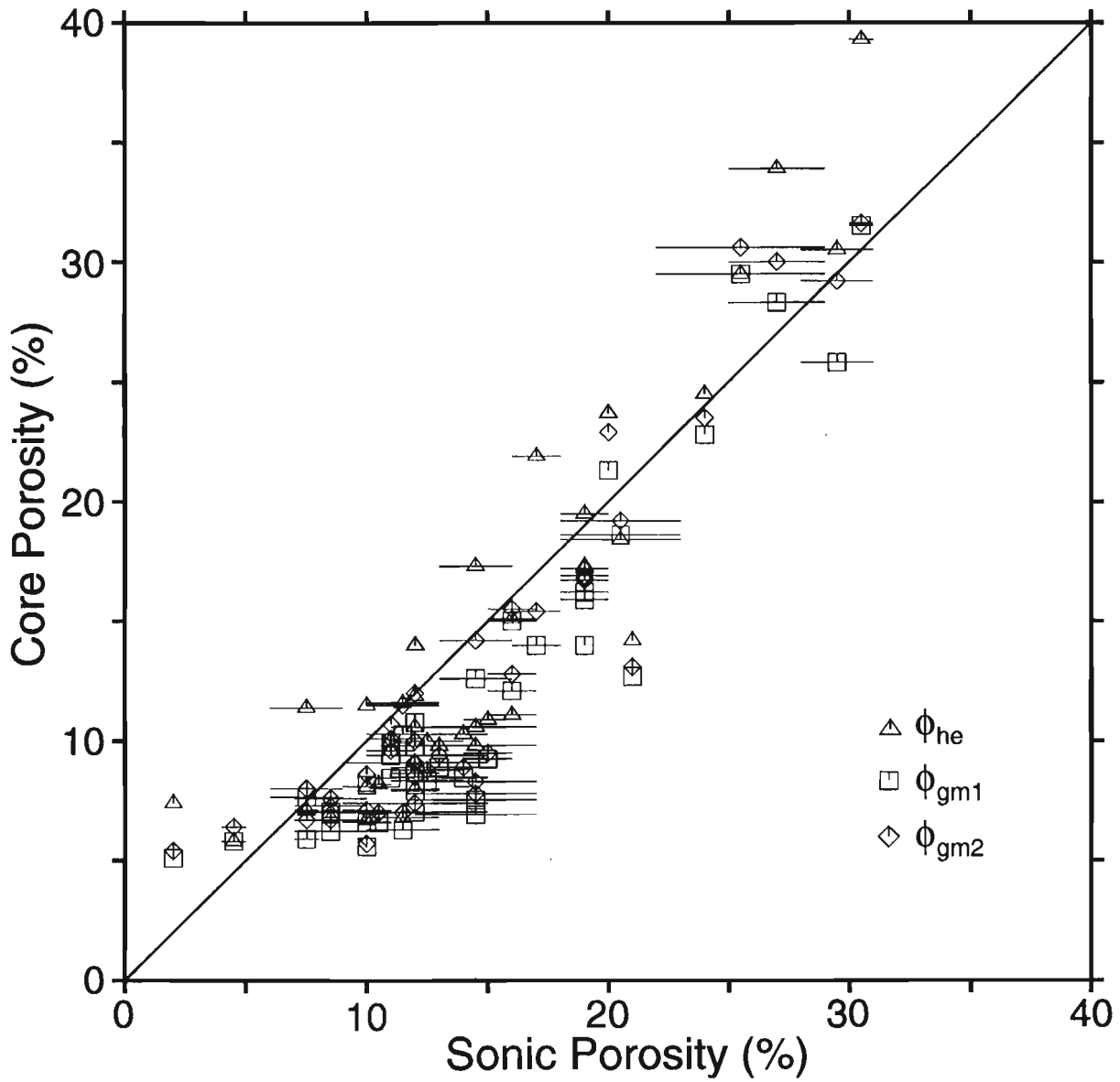

Figure 3. *Comparison between laboratory measured core porosity values (ϕ_{he}, ϕ_{gm1}, ϕ_{gm2}) and porosity values estimated from sonic logs (ϕ_s). The solid line represents a 1:1 relation between laboratory porosity values and ϕ_s values.*

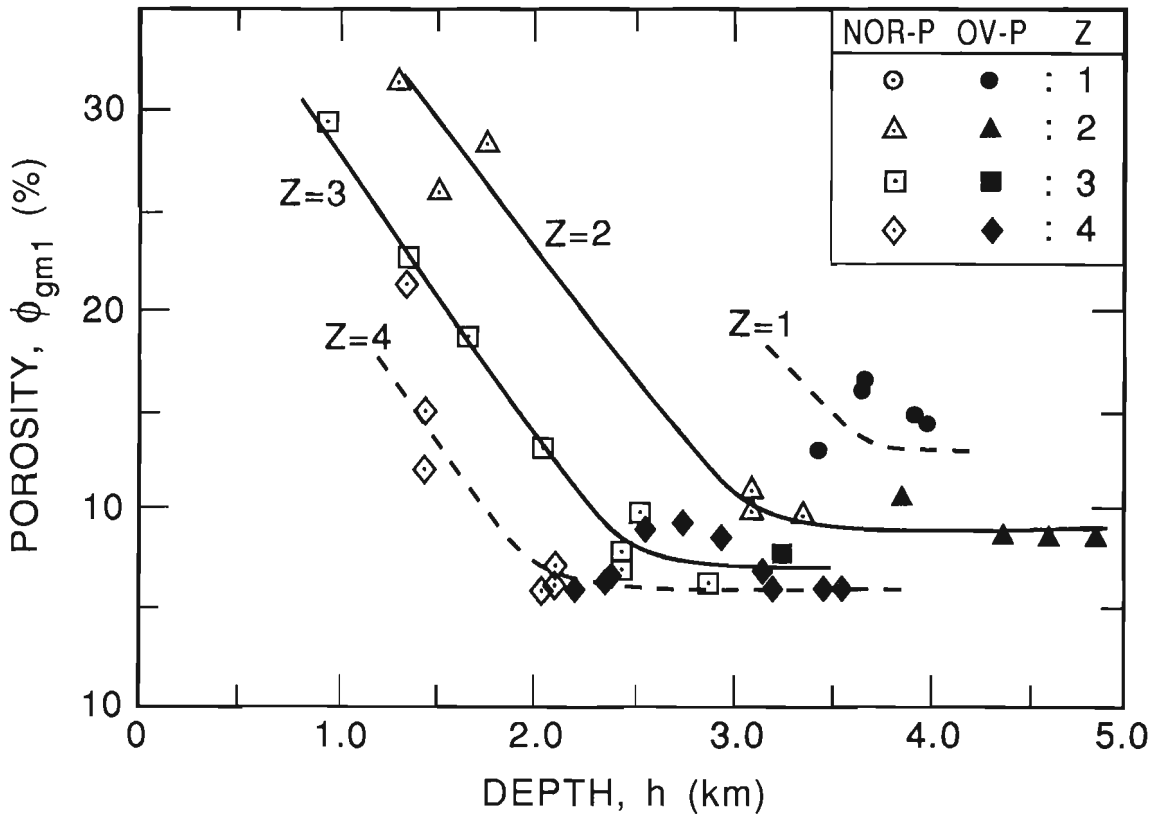

Figure 4. Mercury porosity (ϕ_{gm1}) as a function of depth (h) for 4 different compaction zones with different sedimentation rates (Table 1; Issler, 1992). (Z – zone; NOR-P – normally pressured; OV-P – overpressured).

Laboratory porosity data compare favourably with sonic porosity (ϕ_s) values (Fig. 3), thereby supporting the porosity-sonic transit-time relationship established by Issler (1992). With the exception of the two highest ϕ_{he} values, ϕ_{he} data show the best agreement with ϕ_s values, whereas ϕ_{gm1} and ϕ_{gm2} values tend to be systematically lower than the ϕ_s values. It should be noted that all laboratory porosity measurements were made on unstressed samples. Sample coring and the elimination of overburden stresses can produce microfractures which could adversely affect porosity measurements (Annor and Katsube, 1983; Katsube et al., 1991; Katsube and Mareschal, 1993). Future studies will determine whether this has a significant effect on these samples.

Figure 4 shows a plot of ϕ_{gm1} versus depth for samples from 4 different compaction zones in the Beaufort-Mackenzie Basin (Table 1). The solid and dashed curves in Figure 4 are intended to illustrate general trends in the data. Porosity generally decreases with increasing depth as previously indicated (Katsube and Best, 1992; Katsube and Issler, 1993) for samples from this area; however, the rate of porosity (ϕ_{gm1}) decrease with depth is dramatically reduced or reversed within overpressured zones (Table 2) at depths greater than 2.4-3.4 km across the study area. In addition, porosity values are highest in regions with the highest sedimentation rates (zone 1), and decrease towards regions with the lowest sedimentation rates. These porosity trends support the relationship between shale compaction, pore fluid pressure and sedimentation rate, as determined by Issler (1992) on the basis of sonic logs.

ACKNOWLEDGMENTS

J. Correia of K & A Laboratories (Tulsa, Oklahoma) made the helium porosity measurements. Core samples were collected from the core repository at the Institute of Sedimentary and Petroleum Geology (Calgary). Funding for this study was provided through the Office of Energy Research and Development (OERD). The authors thank G. Stockmal (GSC, Calgary) for critically reviewing this paper and making useful suggestions. The authors also thank K.A. Richardson (Geological Survey of Canada, Ottawa) for his comment on this paper.

REFERENCES

American Petroleum Institute
1960: Recommended practice for core analysis procedure; American Petroleum Institute, API RP 40, 55 p.

Annor, A. and Katsube, T.J.
1983: Nonlinear elastic characteristics of granite rock samples from Lac du Bonnet batholith; in Current Research, Part A; Geological Survey of Canada; Paper 83-1A, p. 411-416.

Davis, J.C.
1986: Statistics and Data Analysis in Geology; John Wiley & Sons, p. 200-204.

Issler, D.R.
1992: A new approach to shale compaction and stratigraphic restoration, Beaufort-Mackenzie Basin and Mackenzie Corridor, Northern Canada; American Association of Petroleum Geologists, v. 76, p. 1170-1189.

Katsube, T.J.
1981: Pore structure and pore parameters that control the radionuclide transport in crystalline rocks; Proceedings of the Technical Program, International Powder and Bulk Solids Handling and Processing, Rosemont, Illinois, p. 394-409. (Available from: CAHNERS Exposition Group, 222 West Adams Street, Chicago, Illinois 60606 U.S.A.).
1992: Statistical analysis of pore-size distribution data of tight shales from the Scotian Shelf; in Current Research, Part E; Geological Survey of Canada, Paper 92-1E, p. 365-372.

Katsube, T.J. and Agterberg, F.P.
1990: Use of statistical methods to extract significant information from scattered data in petrophysics; in Statistical Applications in the Earth Sciences, (ed.) F.P. Agterberg and G.F. Bonham-Carter; Geological Survey of Canada, Paper 89-9, p. 263-270.

Katsube, T.J. and Best, M.E.
1992: Pore structure of shales from the Beaufort-MacKenzie Basin, Northwest Territories; in Current Research, Part E; Geological Survey of Canada, Paper 92-1E, p. 157-162.

Katsube, T.J. and Hume, J.P.
1987: Pore structure characteristics of granitic rock samples from Whiteshell Research Area: in Geotechnical Studies at Whiteshell Research Area (RA-3), CANMET, Report MRL 87-52, p. 111-158.

Katsube, T.J. and Issler, D.R.
1993: Pore-size distribution of shales from the Beaufort-MacKenzie Basin, northern Canada; in Current Research, Part E; Geological Survey of Canada, Paper 93-1E, p.123-132.

Katsube, T.J. and Mareschal, M.
1993: Petrophysical model of deep electrical conductors; graphite lining as a source and its disconnection due to uplift; Journal of Geophysical Research, v. 98, no. B5, p. 8019-8030.

Katsube, T.J. and Walsh, J.B.
1987: Effective aperture for fluid flow in microcracks; International Journal of Rock Mechanics and Mining Sciences and Geomechanics Abstracts, v. 24, p. 175-183.

Katsube, T.J., Best, M.E., and Mudford, B.S.
1991: Petrophysical characteristics of shales from the Scotian shelf; Geophysics, v. 56, p. 1681-1689.

Katsube, T.J., Scromeda, N., and Williamson, M.
1992: Effective porosity of tight shales from the Venture Gas Field, offshore Nova Scotia; in Current Research, Part D; Geological Survey of Canada, Paper 92-1D, p. 111-119.

Loman, J.M., Katsube, T.J., Correia, J., Best, M.E., and Williamson, M.A.
1993: Effect of compaction on porosity and formation factor for tight shales from the Scotian Shelf; in Current Research, Part E; Geological Survey of Canada, Paper 93-1E, p. 331-335.

Geological Survey of Canada Project 870057

Active layer monitoring in natural environments, Mackenzie Valley, Northwest Territories

F.M. Nixon and A.E. Taylor
Terrain Sciences Division

Nixon, F.M. and Taylor, A.E., 1994: Active layer monitoring in natural environments, Mackenzie Valley, Northwest Territories; in Current Research 1994-B; Geological Survey of Canada, p. 27-34.

Abstract: Relict active layers in permafrost regions have been interpreted as indicators of past changes in climate. The present active layer above the permafrost should respond to enhanced warming in Arctic areas predicted by global circulation models for the next several decades. A multi-instrumented transect has been established along the Mackenzie Valley, between Fort Simpson and San Sault Rapids, Northwest Territories, to monitor changes in the active layer over this period. Seventeen sites have been chosen in diverse natural environments and instrumented with thaw tubes, ground temperature cables and probes, air temperature screens, and automatic data loggers.

Résumé : Les paléomollisols dans les régions pergélisolées ont été interprétés comme des indicateurs de changements climatiques passés. Le mollisol actuel au-dessus du pergélisol devrait réagir à un réchauffement climatique dans les régions arctiques comme le prévoient les modèles de circulation globale pour les prochaines décennies. Un transect a été établi au moyen de plusieurs instruments le long de la vallée du Mackenzie, entre Fort Simpson et San Sault Rapids (Territoires du Nord-Ouest), pour surveiller les modifications du mollisol au cours de cette période. Pour ce faire, 17 sites ont été choisis dans différents milieux naturels, et l'on y a installé des tubes de dégel, des câbles et des sondes de température du sol, des écrans de la température de l'air et des enregistreurs automatiques de données.

INTRODUCTION

Global circulation models (GCMs) indicate that the predicted increase in air temperatures over the next several decades due to increasing CO_2 concentrations may be greatest in Arctic regions, particularly in winter; predictions are less certain for other climate parameters such as precipitation and snow cover (e.g., Mitchell et al., 1990). These predictions raise concern for the impact on permafrost in Canada's Arctic.

One scenario for environmental change is an increased active layer depth resulting from global warming of several degrees during the next few decades. Under such conditions, a likely impact will be on slope stability, resulting in more active layer detachment slides and retrogressive thaw flows. This, in turn will change sediment loads in hydrological systems. Active layer thickening and melting of ground ice will affect active layer hydrology and discharge, potentially altering channel stability, and sediment load conditions (Kane et al., 1991). Where slopes are gentle or flat, penetration of thaw into ice-rich permafrost may change the capacity to support traffic. Knowledge of how the active layer responds in many situations and how the response is related to widely available or easily measured parameters, may enable a more reliable estimation of impact for the proposed changes.

This report describes the rationale for, and the details of, a long-term multi-parameter active layer monitoring program along the Mackenzie Valley from latitude 61° to 66°N. This transect trends northwest across the discontinuous permafrost zone in the western Canadian Arctic (Brown, 1978). Seventeen sites have been established in 1992 and 1993 between Fort Simpson and Sans Sault Rapids, Northwest Territories (Fig. 1). An additional 20 sites, where measurements are restricted to maximum active layer thickness, were established further north in 1990-92 (Nixon, unpub. data, 1992).

Regional setting

The Mackenzie River flows northwestward across the Great Slave Plain and into the narrow Mackenzie Plain flanked by Mackenzie Mountains in the west and Franklin Mountains to the east (Bostock, 1970). The underlying geology consists of middle Palaeozoic rocks of the interior platform in the south and deformed Palaeozoic to Cenozoic sediments in the Cordilleran Orogen (Douglas, 1970). All installations of the present study are in late Wisconsinan and Holocene sediments, usually on low alluvial terraces of the Mackenzie River or its tributaries that cut into, or are deposited on, glacial or proglacial sediments (Dyke and Prest, 1987; Hughes, 1987; Hawes, 1980a, b, c; Hanley and Hughes, 1973; Duk-Rodkin and Hughes, 1993). Materials comprise alluvial and lacustrine silt, deltaic and eolian sands, and diamictons of colluvial and glacial origin. The area is covered by varying thickness of organic material (e.g., Aylsworth et al., 1993; Duk-Rodkin and Hughes, 1993) and is generally forested (Environment Canada, 1974), traversing the Boreal forest and the Boreal-Tundra transition (Edlund, 1992).

The study area is entirely within the zone of discontinuous permafrost (Brown, 1978; Heginbottom and Radburn, 1992; Heginbottom, unpub. data, 1993); the area is permafrost-prone, as the -4°C annual mean daily air temperature isotherm passes near Fort Simpson (Fig. 1), and the -7°C isotherm crosses the valley between Norman Wells and Sans Sault (Burns, 1973, Fig. 4.18). Mean surface temperatures are, however, some 2 K to 5 K higher than mean air temperatures in the area, a reflection of the influence of winter snow cover and vegetation in moderating the ground thermal regime; positive mean annual surface temperatures are widespread south of the Root and Willowlake rivers (Fig. 1), and negative mean annual surface temperatures occur to the north (Judge, 1973, 1975). The few sites where permafrost thicknesses have been measured suggest it varies between a few metres to 143 m (Judge, 1975; Taylor et al., 1982).

SITE SELECTION CRITERIA

In this zone of discontinuous permafrost, sites were chosen in areas underlain by permafrost, as determined by probing. As the development of the active layer is affected by meteorological, biological, and geological factors, sites have been chosen to reflect the diversity of these environments, by reference to available surficial geology (Hawes, 1980a, b, c; Hanley and Hughes, 1973; Duk-Rodkin and Hughes, 1993) and forestry maps (Environment Canada, 1974). Emphasis was placed on finding representative natural areas remote from recent disturbance. Logistic considerations required ease of foot access from either the Mackenzie River or from the winter road, and availability of a small quantity of water for jet-drilling some of the installations. Every effort was made to minimize surficial disturbance to the vegetation, mosses, and soils during the installations, because of the effect of terrain disturbance on the thermal regime. Holes for thaw tubes, temperature cables, and soil probes were jet drilled with a light, back-packable water pump, using 2.5 cm diameter pipe and a maximum flow rate of 70 litres per minute. Figure 2 is a photo taken a year after jet-drilling at a typical site. Figure 1 shows site locations, and Table 1 includes a site description and list of instrumentation.

DESCRIPTION OF SITE INSTRUMENTATION

General site description

Permafrost temperatures and the thickness of the active layer integrate the effects of air temperatures, snow cover, vegetation, soil properties, and drainage (e.g., Judge, 1973, 1975), underlining the importance of a description or measure of these parameters at each site. The landform and surface morphology were described, slope and aspect were estimated, and elevation measured with an aneroid barometer relative to the Mackenzie River. A characterization of vegetation included identification, and estimation of height of shrubs, and chest diameter of trees in the immediate vicinity of the installations. Estimates of percentage ground cover were made and plants identified, approximating species level for vascular plants.

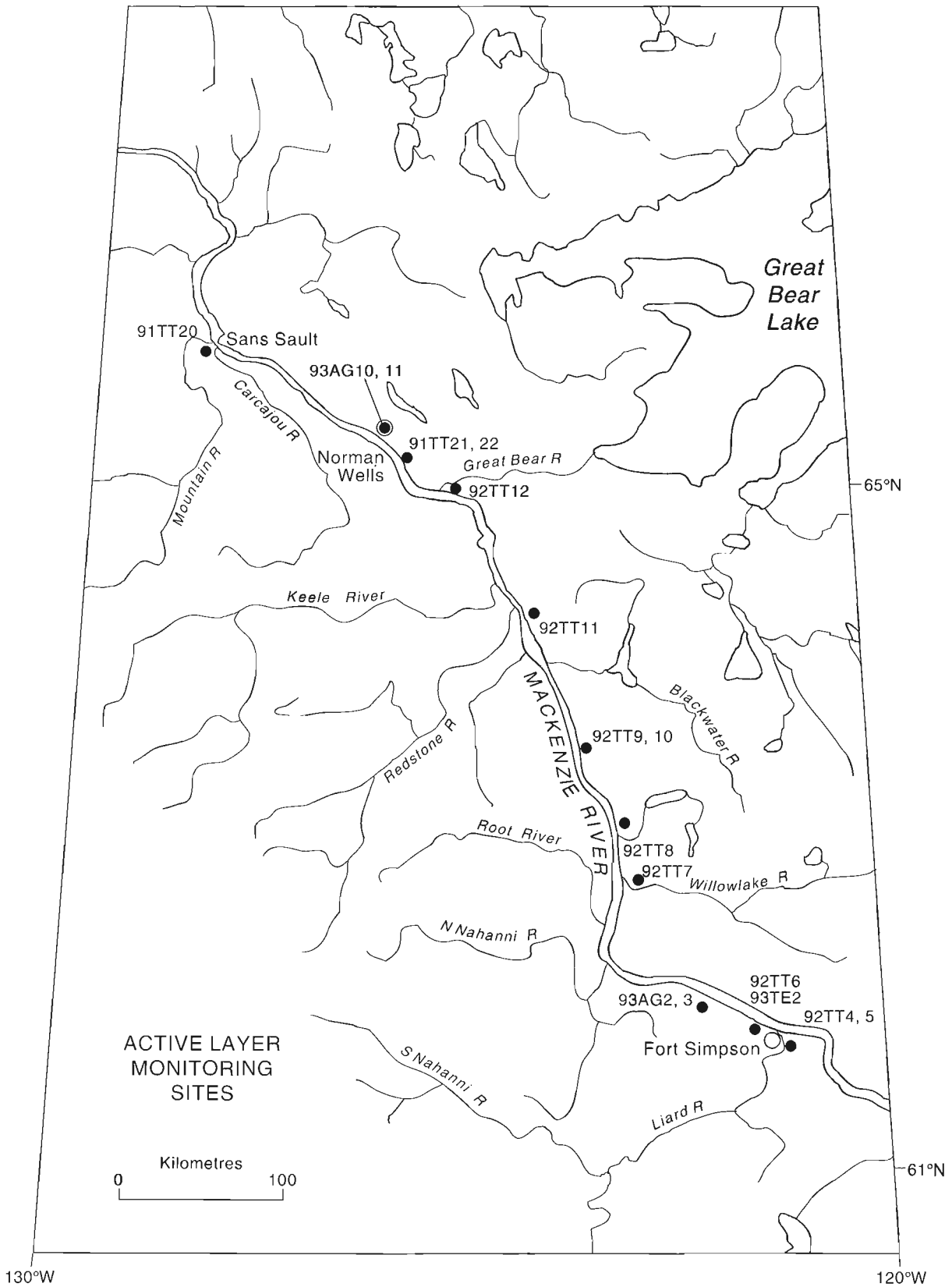

Figure 1. *Location of the instrumented sites in the zone of discontinuous permafrost, Mackenzie Valley, Northwest Territories. Sites are named according to year and first type of principal instrumentation installed, e.g., 92 TT 6, and keyed to Table 1.*

Figure 2. View of site 92 TT 7, Willowlake River, one year after jet-drilling two holes for the thaw tube with heave scriber (foreground) and the ground temperature cable (not visible, but near two logger silos, right of centre). The air temperature screen can be identified by the 45° guy ropes (background).

installations. Estimates of percentage ground cover were made and plants identified, approximating species level for vascular plants.

Installations were made in late July-August 1991-1993. A 1.2 m stainless steel frost probe was used about each site to measure the depth of the active layer at that time. A pit was dug to the frost table and the materials were described, and soil samples were taken for laboratory moisture content and texture determinations. At some sites, spot readings of surface and subsurface temperatures were taken.

Thaw tubes (TT) and heave/subsidence recorder (12 sites)

Multi-tiered ice wedges have been observed in near-surface permafrost, suggesting that the maximum depth of the active layer above permafrost has changed substantially in the past in response to climate changes (Mackay, 1975, 1976). The effect of the predicted global warming should be measurable in the active layer through a long-term monitoring program.

Maximum annual depth of thaw is measured using a modified version of frost tubes developed by Mackay (1973). These consist of nested plastic tubes: an outer 2.5 cm diameter PVC tube is anchored in permafrost to a depth of about 4 m below surface, and an inner clear tube, containing water, and extending below maximum thaw depth, slips into the outer tube and is held at a reference height by a collar (Fig. 3). The principle is simple: after the water in the inner tube freezes to the frost table above maximum thaw depth, a coloured glass bead of 3 mm diameter is dropped through the water column to rest on the ice surface. As thaw progresses downward the bead follows the water/ice interface until maximum depth is reached. On refreezing, it is incorporated into the ice and records the maximum depth of the active layer that year. Next season prior to maximum thaw, the installation is visited and the inner tube raised to measure the depth of the bead and to introduce a bead of different colour (silicone fluid in the outer tube prevents the tubes from freezing together).

To measure the maximum ground surface heave and subsidence over the year, a grill supporting a scribing sleeve is set on the ground surface such that it encircles, but is free of, the outer tube (Fig. 3) that is anchored in permafrost. As the

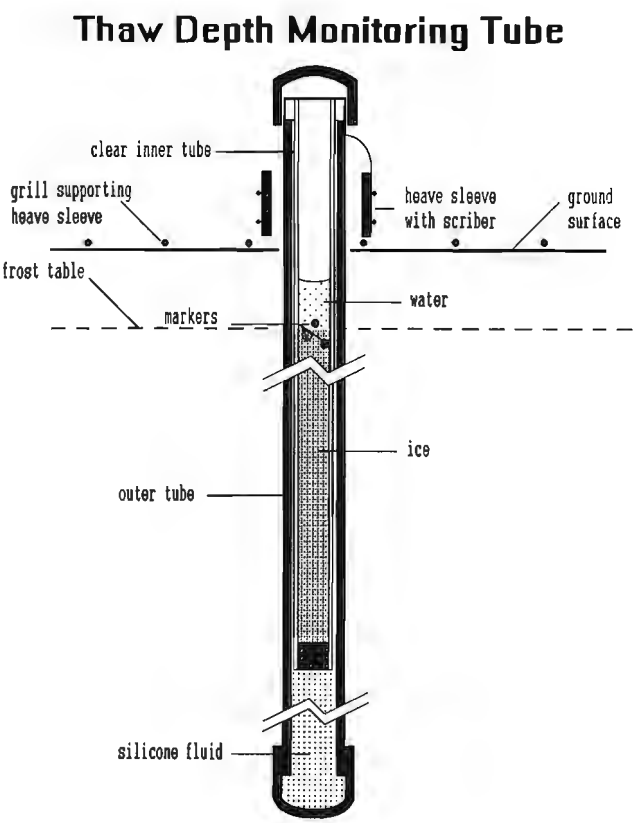

Figure 3. Schematic of the thaw depth monitoring tube, adapted from Mackay (1973).

Table 1. Location and description of active layer monitoring sites

Site	Location	Installations	Depth of Installation	Situation
Manners Creek mouth (92 TT 4)	61°46'13" 121°11'33"	TT, 1992 AG, 1993		-top of bank at confluence of Manners Crk. and Liard R., organic silt on alluvial terrace[1] -open upland hardwood forest[7]
Manners tributary (92 TT 5)	61°45'58" 121°11' 6"	TT, 1992 AG, 1993 TDR, 1993	TDR @ 60,90,120 cm	-south bank of NHRI tributary east of pipeline ROW, on slope cut into silt of lacustrine plain[1] -open upland spruce feather moss with hardwoods; site in aspen thicket[7]
Martin R. crossing (92 TT 6)	61°53'13" 121°35'59"	TT, 1992 SP, 1992 TDR, 1992 TE, 1993 AG, 1993	SP to 1.5 metres TDR @ 60,90,120 cm TE array to 48 cm	-broad thermokarst depression in sand of lacustrine - eolian complex[1] -spruce feather moss; site more open on edge of fen[7]
Martin R. Basin (93 TE 2)	61°53'14" 121°36'44"	4xTE, 1993 2xAG, 1993 2xTDR, 1993	TE array to maximum 90 cm TDR east 61,90,98 cm TDR s. 60,90,120 cm	-narrow flood plain of lower Martin R. poorly sorted sand[1] -spruce feather moss; site in clearing at edge of fen[7]
Wrigley Hwy. km 504.7 (93 AG 3)	61°58' 121°49'	AG, 1993		-on silt of lacustrine plain[1] -upland hardwood spruce forest[7]
Wrigley Hwy. km 507.6 (93 AG 2)	61°58' 121°52'	AG, 1993		-bog developed on lacustrine plain[1] -small bog between fen and open upland mixed forest[7]
Willow Lake River (92 TT 7)	62°41'48" 123°3'46"	TT, 1992 TC, 1992 TDR, 1992 TDR, 1993 TE, 1993 AG, 1993	TC to 4.3 metres TE array to 48 cm TDR @ 60,90,120 cm	-silt on low terrace bar, in flood plain[2] -tall open spruce hardwood forest[7] (AG in open succession vegetation of burn)
River Between Two Mts. (92 TT 8)	62°57'40" 123°12'32"	TT, 1992 AG, 1993 TDR, 1992		-silt on alluvial terrace above Mackenzie[2] -tall open hardwood spruce upland forest[7]
Ochre River (92 TT 9,10)	63°27'59" 123°41'35"	TT, 1992 SP, 1992 TDR, 1992 TE, 1993 AG, 1993 TDR, 1993	SP 1.8 metres TDR @ 57,88,110 cm TE array to 48 cm TDR @ 60,90,120 cm	-organics and silt on low alluvial terrace cut in lacustrine deposits; AG on higher stoney terrace[3] -open upland spruce with hardwoods (AG in tall upland mixed forest)[7]
Saline River (92 TT 11)	64°17'20" 124°31'28"	TT, 1992 TC, 1992 TDR, 1992 TE, 1993 AG, 1993	TC to 3 metres TDR @ 60,90,100 cm TE array to 72 cm	-silt veneer over stony colluvium in low alluvial terrace, AG up stream on spur cut in higher stony alluvial terrace[4] -pioneer steep slope open spruce with hardwoods[7] (AG in open aspen grove)
Fort Norman (92 TT 12)	64°54'40" 125°34'32"	TT, 1992		-organics over silt on alluvial terrace at base of steep slope[4] -low open black spruce sphagnum transition[7]
Francis Creek (91 TT 21, 22)	65°11'52" 126°27'56"	TT, 1991 AG, 1993 2xTDR, 1993	TDR @ 60,90,94 cm TDR @ 61,91,121 cm	-alluvial terrace cut into stony silt till[6] -open mixed forest, birch willow thicket
Norman Wells AES (93 AG 10)	65°17'35" 126°45'40"	AG, 1993		-till plain between Discovery Ridge and River[5] -low, open black spruce and hardwoods over moss plus cleared AES compound
Norman Wells, IPL (93 AG 11)	65°17'35" 126°53'08"	AG, 1993		-alluvial terrace above modern river[5] -open black spruce and hardwoods over moss
Mountain River (91 TT 20)	65°40'29" 128°49'37"	TT, 1991 AG, 1993 TDR, 1993	TDR @ 60,90,114 cm	-low terrace in stony sand on alluvial plain[6]

[1] (after Hawes, 1980a)
[2] (after Hawes, 1980b)
[3] (after Hawes, 1980c)
[4] (after Hanley and Hughes, 1973)
[5] (after Duk-Rodkin and Hughes, unpub. data, 1993)
[6] (after Duk-Rodkin and Hughes, 1993)
[7] (after Environment Canada, 1974)

Temperature cables (TC) and soil probes (SP) (4 sites)

Ground temperatures and thermal properties are central parameters for analyses of the ground thermal regime and heat transfer, and for any quantitative reconciliation of maximum active layer development measured by the thaw tube installations (e.g., Lunardini, 1981). Multithermistor temperature cables were installed at sites 92 TT 7 and 92 TT 11, and soil probes at 92 TT 6 and 92 TT 10 (Fig. 1; Table 1). Cables are 8 m long, but in the field were doubled back as required by the maximum depth of the holes. Soil probes are 1.6 m long and designed such that the upper 0.5 m of the probe with 2 sensors is above ground surface; this enables a measure of air and snow temperatures simultaneously with active layer and permafrost temperatures. Each cable or soil probe is connected to an automatic data logger recording temperatures at intervals of 8 hours. The loggers were left in 10 cm PVC "silos" dug into the active layer to reduce exposure to extreme winter air temperatures while ensuring year-round access (Fig. 2). Similar instrumentation is used in the Norman Wells Pipeline Monitoring Program (see Burgess and Allen, 1991).

Temperature-electrical potential probes (TE) (5 sites)

The magnitude and rate of heat transfer across the ground surface can be significantly affected by nonconductive processes in the soil (e.g., Oke, 1987). Hinkel et al. (1993) have shown that some nonconductive processes may be separated from the total heat flux by measurement of soil water ionic concentration; the soil electrical potential is considered a surrogate of the latter parameter. Instrumentation was developed from a design used by Hinkel et al. (1993) and installed in soil pits at sites 92 TT 6, 92 TT 7, 92 TT 10, and 92 TT 11 (Fig. 1, Table 1); an intensive site (93 TE 2), consisting of 4 pits within an area a few tens of metres in diameter, is located in the Martin River Basin study area.

Each temperature-electrical potential sensor consists of a thermistor probe around which is wrapped a length of copper wire such that temperature and electrical potential are measured at the same location in the soil column. Seven of these composite sensors comprise a set, and were inserted horizontally in the side wall of a carefully dug pit, to make a vertical profile (Fig. 4). Probe units are equally spaced in the active layer, the top probe being near the surface and the lowest probe just above the frozen ground; this spacing ranged from 5-8 cm. Soil electrical potential is referenced to a 3 m copper-clad steel ground spike. Another temperature sensor is used to record temperatures in a radiation shield (see below) and automatic temperature and voltage loggers were installed at each site.

TDR moisture content rods (13 sites)

Soil moisture is a major controlling factor in the maximum development of the active layer because of the mobilization of a large quantity of latent heat in the ice/water phase change. While soil samples were taken for laboratory water content determination, stainless steel rod pairs were installed at all sites except 93 AG 2, 93 AG 3, 93 AG 10, and 93 AG 11 to measure the average moisture content in the active layer by the TDR (time domain reflectometry) technique (Table 1). In this method, a precision digital electrical cable tester measures the soil dielectric constant, which is related to unfrozen water content through empirical relations (e.g., Smith and Tice, 1988).

Figure 4. *The ground temperature-electrical potential probes (TE system) inserted in a vertical profile in the side wall of a soil pit; the second and third probes are particularly visible. The white oblique line is a tape measure.*

Air temperature-ground temperature sensors (AG) (all sites)

To monitor for direct evidence of climate change, and for future analysis of the air-ground interaction, an air temperature time-series is required. Also, an overall thermal transfer function between air and ground is useful in regional studies needing an engineering-level quantification of the influence of various vegetation, forest types, and snow cover on the ground thermal regime. One such function, the n-factor, is defined in terms of an air temperature and ground temperature time series; currently, there are few n-factors published for natural areas, as the emphasis has been more on pavements and cleared areas (Lunardini, 1978).

A 6-plate 12 cm diameter radiation shield was mounted 1.5 m above the ground surface at each site. Air temperatures are measured by a thermistor in the screen that is connected to a data logger used for the TC, SP, or TE instrumentation (sites 92 TT 6, 93 TE 2, 92 TT 7, 92 TT 10, 92 TT 11; Fig. 1, Table 1). At

sites without such ground temperature instrumentation (92 TT 5, 93 AG 2, 93 AG 3, 92 TT 8, 91 TT 21, 93 AG 10, 93 AG 11, 91 TT 20; Fig. 1, Table 1), a thermistor and a single channel miniature data logger is used in the air screen and two similar loggers are buried at a nominal depth of 10 cm, one near the base of the air screen and the other several tens of metres away in a distinctly different vegetation or forest environment. To capture the diversity of vegetation at three sites (92 TT 7, 92 TT 10, 92 TT 11), a second air/ground setup using the single channel loggers is located several hundred metres from the main site.

DISCUSSION

Outside of general site description, there is no quantitative data available at present. Sites will be revisited at least annually for data collection and servicing. In summer, the depth of thaw will be probed and photos taken; in early spring, snow depth will be measured. Changes in site features can be captured in the photographic record of each visit. In a few years, the spatial variability of active layer development should be established; in later years, any temporal variability should emerge and provide the opportunity to correlate with air temperatures and prediction from global circulation models.

This project is undertaken under the umbrella of the Integrated Research and Monitoring Area program of Terrain Sciences Division, GSC and is a member of the Mackenzie Basin Impact Study, Environment Canada (Cohen, 1991). Site selection and instrumentation has been co-ordinated with these and other studies already underway in this region. In particular, this natural area transect complements the permafrost monitoring program of Indian and Northern Affairs Canada along the Mackenzie Valley pipeline (e.g., Burgess and Harry, 1990; Tarnocai and Kroetsch, 1990); also, sites around Fort Simpson have been located in areas where the National Hydrological Research Institute has been conducting permafrost-hydrologic interactions (T. Prowse, pers. comm., 1992).

CONCLUSIONS

1. Seventeen sites on a 700 km transect in the discontinuous permafrost zone of the Mackenzie River valley have been instrumented to monitor changes in the active layer due to climate change over the next two decades. Sites were established in natural areas in a manner to make minimal impact on the soil, moss, and vegetation.
2. Instrumentation consists of 12 thaw tubes (TT), 4 ground temperature cables or probes (TC, SP), 8 temperature-electrical potential sets (TE), 17 air temperature screens with ground surface temperatures (AG), and 13 moisture content rods (TDR).
3. The variety of instrumentation will contribute to a quantitative analysis of active layer development and processes, and permafrost-climate and climate change interaction.

ACKNOWLEDGMENTS

Invaluable advice and logistic assistance was provided by Pat Wood and staff, Water Resources Branch, Environment Canada, and B. Gauthier, Indian and Northern Affairs Canada, both in Fort Simpson, N.W.T. Vic Allen assisted with design of site instrumentation and provided data loggers; Anne Wilkinson co-ordinated equipment preparation. Prof. Ken Hinkel, University of Cincinnati, kindly provided specifications for his soil temperature-ionic concentration system, and Murray Mitchell designed similar cables and probes for our use. Funding was provided by Geological Survey of Canada under the Green Plan, and by the Panel on Energy Research and Development, Natural Resources Canada.

REFERENCES

Aylsworth, J.M., Kettles, I.M., and Todd, B.J.
1993: Peatland distribution in the Fort Simpson area, Northwest Territories with a geophysical study of peatland-permafrost relationships at Antoine Lake; in Current Research, Part E; Geological Survey of Canada, Paper 93-1E, p. 141-148.

Bostock, H.S.
1970: Physiographic Regions of Canada; Geological Survey of Canada, Map 1254A, scale 1:5 000 000.

Brown, R.J.E.
1978: Permafrost map of Canada; in, Hydrological Atlas of Canada, Fisheries and Environment Canada, Ottawa, plate no. 32.

Burgess, M.M. and Allen, V.S.
1991: Notes on the use and performance of thermal instrumentation: experience from the Norman Wells pipeline ground temperature monitoring program; in Current Research, Part E; Geological Survey of Canada, Paper 91-1E, p. 337-345.

Burgess, M.M. and Harry, D.G.
1990: Norman Wells pipeline permafrost and terrain monitoring: geothermal and geomorphic observations, 1984-1987; Canadian Geotechnical Journal, v. 27, p. 233-244.

Burns, R.M.
1973: The climate of the Mackenzie Valley-Beaufort Sea; Atmospheric Environment Service, Environment Canada, Climatological Studies No. 24, 227 p.

Cohen, S.J.
1991: Regional impacts of projected global warming: a research proposal for the Mackenzie Basin; in Proceedings, 2nd Symposium on global change studies, American Meteorological Society.

Douglas, R.J.W.
1970: Geological Map of Canada; Geological Survey of Canada, Map 1250A, scale 1:5 000 000.

Duk-Rodkin, A. and Hughes, O.L.
1993: Surficial geology, Sans Sault Rapids, District of Mackenzie, Northwest Territories; Geological Survey of Canada, Map 1784A, scale 1:250 000.

Dyke, A.S. and Prest, V.K.
1987: Late Wisconsinan and Holocene history of the Laurentide ice sheet; Géographie physique et Quaternaire, v. XLI, no. 2, p. 237-263.

Edlund, S.A.
1992: Climate change and its effect on Canadian Arctic plant communities; in Proceedings: Arctic Environment, Past Present and Future symposium, (ed.) M. Woo and D.J. Gregor, McMaster University, Hamilton, Ontario, Canada, p. 121-133.

Environment Canada
1974: Vegetation types of the Mackenzie corridor; Environmental-Social Program, Northern Pipelines, report no. 73-46, Canadian Forestry Service, Environment Canada, 85 p., appendices, maps.

Hanley, P.T. and Hughes, O.L.
1973: Surficial geology and geomorphology of Fort Norman, Carcajou Canyon, Norman Wells and Sans Sault Rapids map areas, District of Mackenzie, Northwest Territories; Geological Survey of Canada, Open File 155, scale 1:125 000.

Hawes, R.J. (comp.)
1980a: Surficial geology and geomorphology of Fort Simpson, District of Mackenzie; Geological Survey of Canada, Map 3-1978, scale 1:125 000.
1980b: Surficial geology and geomorphology of Camsell Bend, District of Mackenzie; Geological Survey of Canada, Map 9-1978, scale 1:125 000.
1980c: Surficial geology and geomorphology of Wrigley Lake, District of Mackenzie; Geological Survey of Canada, Map 13-1978, scale 1:125 000.

Heginbottom, J.A. and Radburn, L.K. (comp.)
1992: Permafrost and ground ice conditions of northwestern Canada; Geological Survey of Canada, Map 1691A, scale 1:1 000 000.

Hinkel, K.M., Outcalt, S.I., and Nelson, F.E.
1993: Near-surface summer heat-transfer regimes at adjacent permafrost and non-permafrost sites in central Alaska; in Permafrost, Sixth International Conference, Beijing, China, Proceedings, v. 1, p. 261-266.

Hughes, O.L.
1987: Late Wisconsinan Laurentide glacial limits of northwestern Canada: the Tutsieta Lake and Kelley Lake phases; Geological Survey of Canada, Paper 85-25, 19 p.

Judge, A.S.
1973: The thermal regime of the Mackenzie Valley: observations of the natural state; Environmental-Social Program, Northern Pipelines, report no. 73-38, Earth Physics Branch, Energy, Mines and Resources Canada, 177 p.
1975: Geothermal studies in the Mackenzie Valley by the Earth Physics Branch; Energy, Mines and Resources Canada, Earth Physics Branch, Geothermal Series no. 2, 12 p.

Kane, D.L., Hinzman, L.D., and Zarling, J.P.
1991: Thermal response of the active layer to climatic warming in a permafrost environment; Cold Regions Science and Technology, v. 19, p.111-122.

Lunardini, V.J.
1978: Theory of n-factors and correlation of data; in Proceedings, Third International Conference on Permafrost, Natural Research Council of Canada, v. 1, p. 40-46.

Lunardini, V.J. (cont.)
1981: Heat transfer in cold climates; Van Nostrand Reinhold, New York, 704 p.

Mackay, J.R.
1973: A frost tube for the determination of freezing in the active layer above permafrost; Canadian Geotechnical Journal, v. 10, p. 392-396.
1975: The stability of permafrost and recent climatic change in the Mackenzie Valley, N.W.T.; in Geological Survey of Canada, Paper 75-1, Part B, p. 173-176.
1976: Ice wedges as indicators of recent climatic change, western Arctic coast; in Geological Survey of Canada, Paper 76-1, Part A, p. 233-234.

Mitchell, J.F.B., Manabe, S., Meleshko, V., and Tokioka, T.
1990: Equilibrium climate change – and its implications for the future; in Climate change, The IPCC Assessment, (ed.) J.T. Houghton, G.J. Jenkins, and J.J. Ephraums; Cambridge Press, New York, p. 131-172.

Oke, T.R.
1987: Boundary layer climates; Methuen, New york, 435 p.

Smith, M.W. and Tice, A.R.
1988: Measurement of the unfrozen water content of soils: comparison of NMR and TDR techniques; U.S. Army Cold Regions Research and Engineering Laboratory, CRREL report 88-18, 11 p.

Tarnocai, C. and Kroetsch, D.J.
1990: Site and soil descriptions for the Norman Wells pipeline soil temperature study; Agriculture Canada, Land Resources Research Centre, Contribution no. 89-56, 46 p.

Taylor, A.E., Burgess, M., Judge, A.S., and Allen, V.S.
1982: Canadian geothermal data collection – northern wells 1981; Energy, Mines and Resources Canada, Earth Physics Branch, Geothermal Series no. 13, 153 p.

Geological Survey of Canada Project 920046

Physical properties of Canadian kimberlites, Somerset Island, Northwest Territories, and Saskatchewan[1,2]

T.J. Katsube and N. Scromeda
Mineral Resources Division

Katsube, T.J. and Scromeda, N., 1994: Physical properties of Canadian kimberlites, Somerset Island, Northwest Territories and Saskatchewan; in Current Research 1994-B; Geological Survey of Canada, p. 35-42.

Abstract: Physical properties (density, magnetic susceptibility, electrical resistivity, porosity, formation factor, surface resistivity) were measured on 26 Canadian kimberlite samples for information required in exploration of kimberlite-hosted diamond deposits. Following previous studies on fewer samples and parameters, this paper provides a more complete set of measurements to link geophysical parameters to geological characteristics.

Results suggest that porosity is a major factor controlling density, formation factor and electrical resistivity of these kimberlites, with additional factors of significance influencing resistivity. There are indications of porous kimberlites being altered, and nonporous ones being fresh. Magnetic susceptibilities seem unrelated to other parameters. Archie's coefficients may show characteristics unique to kimberlites.

This is primarily a documentation of physical properties of some kimberlite samples. Continuing studies on quantitative relationships between mineralogy (primary and secondary), petrographic textural type (crater, diatreme, or hypabyssal facies), and physical properties are expected to provide geophysical signatures unique to kimberlites.

Résumé : Les propriétés physiques (densité, susceptibilité magnétique, résistivité électrique, porosité, facteur de formation, résistivité superficielle) de 26 échantillons de kimberlites canadiennes ont été mesurées afin d'obtenir les renseignements requis pour la prospection des gisements de diamants logés dans des kimberlites. Ces travaux suivent d'autres études menées sur un nombre moins élevé d'échantillons et de paramètres. Le rapport présente une série plus complète de mesures permettant de relier les paramètres géophysiques aux caractéristiques géologiques.

Les résultats semblent indiquer que la porosité est un facteur de contrôle majeur de la densité, du facteur de formation et de la résistivité électrique de ces kimberlites; d'autres facteurs importants influent sur la résistivité. Certaines indications font croire que les kimberlites poreuses sont altérées et que les kimberlites non poreuses sont fraîches. Les susceptibilités magnétiques ne semblent pas être liées à d'autres paramètres. Les coefficients d'Archie pourraient révéler des caractéristiques particulières aux kimberlites.

Le présent rapport documente les propriétés physiques de certains échantillons de kimberlite. L'étude continue des liens quantitatifs entre la minéralogie (primaire et secondaire), le type textural pétrographique (faciès de cratère, de diatrème ou hypabyssal) et les propriétés physiques fournira des signatures géophysiques particulières aux kimberlites.

[1] Contribution to Canada-Northwest Territories Mineral Initiatives (1991-1996), an initiative under the Canada-Northwest Territories Economic Development Cooperation Agreement.
[2] Contribution to Canada-Saskatchewan Partnership Agreement on Mineral Development (1990-1995), a subsidiary agreement under the Canada-Saskatchewan Economic and Regional Development Agreement.

INTRODUCTION

There is considerable exploration activity in progress related to kimberlite-hosted diamond deposits in Saskatchewan, Alberta, Ontario, and the Northwest Territories (Kjarsgaard and Peterson 1992; Northern Miner, March 30, 1992). Use of airborne magnetics and electromagnetics as exploration tools for kimberlites has been demonstrated in various parts of the world (summarized in Atkinson, 1989). Basic physical rock property information is required in exploration (planning and interpretation of geophysical data), and to provide the opportunity for further development of geophysical methods with improved detecting capabilities for kimberlites below overburden. For this reason, a physical rock property study on kimberlites consisting of electrical resistivity, formation factor, magnetic susceptibility, density, and porosity measurements has been carried out.

Results of part of this study have previously been reported (Katsube et al., 1992a). It includes magnetic susceptibility and density measurements on kimberlite samples from Somerset Island, Northwest Territories, and Sturgeon Lake, Saskatchewan (Fig. 1), in addition to electrical resistivity and porosity measurements for Sturgeon Lake. The purpose of this paper is to complete the reporting of the results for electrical resistivity, formation factor, magnetic susceptibility, density, and porosity for these two areas (Fig. 1); that is, the new data in this paper are electrical resistivity, formation factor, and porosity data for Somerset Island samples, formation factor data for Sturgeon Lake samples, and data for all five parameters for several Somerset Island samples. This is primarily a documentation of physical properties of some kimberlite samples, with studies currently continuing on quantitative relationships between mineralogy (primary and secondary), petrographic textural type (crater, diatreme or hypabyssal facies), and physical properties.

While rock property data on electrical resistivity, magnetic susceptibility, and density can be used directly for interpretation of surface and airborne geophysical methods, formation factor and porosity are used to analyze the physical structure of the rocks, and help link the geophysical parameters (electrical resistivity, magnetic susceptibility, and density) to the geological characteristics of the kimberlites. Examples of such analysis using these parameters can be found in the literature (Katsube and Kamineni, 1983; Katsube and Hume, 1987a, b; Katsube et al., 1991; Katsube and Mareschal, 1993).

METHOD OF INVESTIGATION

Samples and sample preparation

Twenty six drill core and hand samples of kimberlite were collected from the two areas in Canada for this study. The sample numbers used in the laboratory, sampling locations and field identification numbers used by the geologists who collected them are all listed in Table 1. First, magnetic susceptibility measurements were made on these samples. Then, rectangular specimens were cut from these core and hand samples for electrical resistivity, formation factor, porosity, and bulk density measurements. The geometric characteristics of the specimens used for electrical and bulk density measurements, for samples not previously reported (Katsube et al., 1992a), are listed in Table 2. The specimen dimensions are in the range of (1.2-2.3)x(1.3-2.7) cm for the cross-section, and 0.6-1.1 cm for thickness, dimensions similar to those previously reported. Remaining chips, instead of the rectangular specimens, were used for effective porosity measurements of some of the samples. Two or more rectangular specimens were cut from each sample. Further details of the sample preparation were described previously (Katsube et al., 1992a).

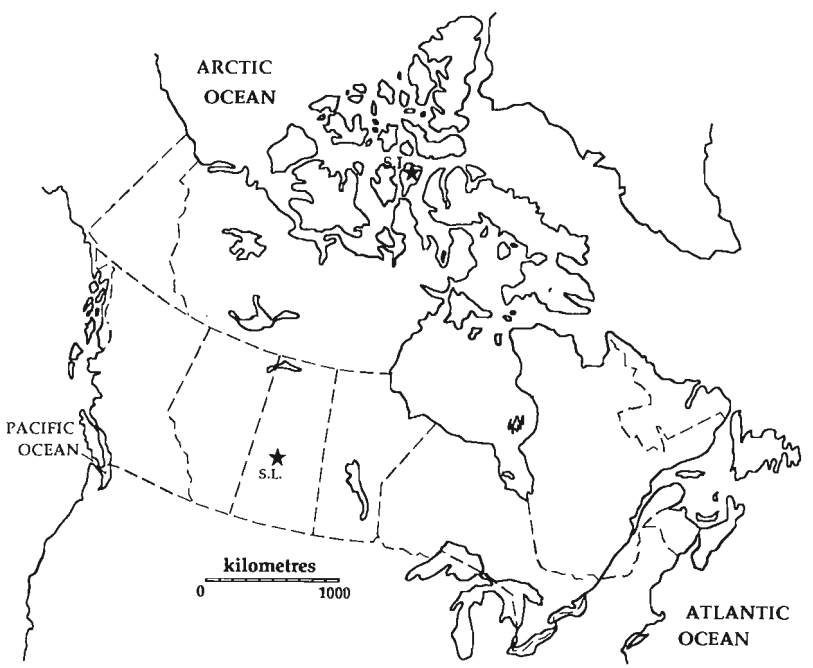

Figure 1.

Locations of the sites from which the two sample suites have been obtained. Detailed map of the sampled sites for the Somerset Island suite can be found in Kjarsgaard and Peterson (1992); S.I. and S.L. on the map represent the Somerset Island (Northwest Territories) and Sturgeon Lake (Saskatchewan) sites.

Bulk density and effective porosity measurements

The caliper method (American Petroleum Institute, 1960) has been used to determine the bulk density, δ, of the samples, by measuring the dimensions and weight of the rectangular specimens. This measurement constitutes part of the porosity determining procedure. Effective porosity, ϕ_E, in principle represents the pore volume of all interconnected pores. In this study, it is determined from the difference in weight between the oven-dried and water-saturated rock specimen. The API Recommended Practice for Core-Analysis Procedures (American Petroleum Institute, 1960) has generally been followed in these measurements. The procedures routinely used in our measurements are described in the literature (Katsube and Scromeda, 1991; Katsube et al., 1992b).

Magnetic susceptibility measurements

Magnetic susceptibility measurements were made on the hand samples using the hand-held JH-8 magnetometer manufactured by Geoinstruments (Finland). This instrument is an analog type which is used to scan the surface of a sample to determine the range of magnetic susceptibility (MS) values.

Table 1. Kimberlite sample information (sample numbers used in the laboratory, sampling locations, and field identification numbers used by the geologists who collected them).

Sample Number	Sampling Location	Sample I.D.
SI-1	Somerset Island, N.W.T.	PHA90-HD
SI-2	Somerset Island, N.W.T.	PHA90-K4A
SI-3	Somerset Island, N.W.T.	PHA90-K10D
SI-4	Somerset Island, N.W.T.	PHA90-K10E
SI-5	Somerset Island, N.W.T.	PHA90-K15B
SI-6	Somerset Island, N.W.T.	PHA90-K22A
SI-7	Somerset Island, N.W.T.	PHA90-K23A
SI-8	Somerset Island, N.W.T.	PHA90-PC-1
SI-9	Somerset Island, N.W.T.	PHA90-J1A
SI-10	Somerset Island, N.W.T.	PHA92-KLC14-M730
SI-11	Somerset Island, N.W.T.	PHA92-KLC14-D260
SI-12	Somerset Island, N.W.T.	PHA92-KLC14-D560
SL-1	Sturgeon Lake, Saskatchewan	SEM-KIM-2
SL-2	Sturgeon Lake, Saskatchewan	KIA91-MP-SLPJ2
SL-3	Sturgeon Lake, Saskatchewan	SEM-KIM-3
SL-4	Sturgeon Lake, Saskatchewan	SEM-KIM-4
SL-5	Sturgeon Lake, Saskatchewan	SEM-KIM-5
SL-6	Sturgeon Lake, Saskatchewan	SEM-KIM-6
SL-7	Sturgeon Lake, Saskatchewan	SEM-KIM-7
SL-9	Sturgeon Lake, Saskatchewan	SEM-KIM-9
SL-10	Sturgeon Lake, Saskatchewan	HDB-89-2
SL-11	Sturgeon Lake, Saskatchewan	HDB-89-3a
SL-12	Sturgeon Lake, Saskatchewan	HDB-89-3b
SL-13	Sturgeon Lake, Saskatchewan	HDB-89-8
SL-14	Sturgeon Lake, Saskatchewan	HDB-89-10
SL-15	Sturgeon Lake, Saskatchewan	HDB-89-11b

Bulk resistivity measurements

The bulk resistivity, ρ_r, is determined from the complex electrical resistivity, ρ^*, measurements made by methods described in recent publications (e.g., Katsube et al., 1991; Katsube and Salisbury, 1991). It (ρ^*) is measured over a frequency range of $1\text{-}10^6$ Hz, with ρ_r representing an electrical resistivity at a frequency of about $10^2\text{-}10^3$ Hz. It is a function of the pore structure and pore fluid resistivity, and is understood to exclude any other effects, such as pore surface, dielectric, or any other polarizations (Katsube, 1975; Katsube and Walsh, 1987).

Specific details of density, magnetic susceptibility, electrical resistivity, and porosity measurements used for these kimberlite samples are found in a previous publication (Katsube et al., 1992a).

Formation factor determination

The formation factor, F, is a parameter representing the pore structure characteristics specifically related to the flow of fluids and electrical current through the rock. In principle, it is determined by taking the ratio of the bulk rock resistivity (ρ_r) over the pore fluid resistivity, ρ_w (Archie, 1942). Actually, in order to eliminate the pore surface electrical conductivity or surface resistivity, ρ_c, effect (Patnode and Wyllie, 1950), F is determined by measuring the bulk resistivity (ρ_m) of the rock for solutions of different salinities (NaCl: 0.02-0.50 N), and then inserting the results into the Patnode and Wyllie equation. Note that a symbol (ρ_m) different from the previous one (ρ_r) is used for these bulk resistivity measurements. Further details of the procedures used for these measurements can be found elsewhere (Katsube, 1981; Katsube and Walsh, 1987; Katsube et al., 1991; Katsube and Salisbury, 1991).

Table 2. Dimensions of specimens cut out from the kimberlite samples for electrical measurements.

Sample	a_1 (cm)	a_2 (cm)	ℓ (cm)	W (g)	K_g (10^{-2}m)	δ (g/mL)
SI-2	1.330	2.263	0.643	5.6818	4.68	2.94
SI-3	2.240	2.502	0.823	11.9193	6.81	2.58
SI-4	1.513	2.051	0.746	6.6607	4.16	2.88
SI-5	2.062	2.683	0.701	10.5647	7.89	2.72
SI-6	1.797	2.091	0.588	6.3177	6.39	2.86
SI-7	1.213	1.388	0.737	3.7071	2.29	2.99
SI-8	1.759	2.298	0.675	7.8859	5.99	2.89
SI-9	1.642	2.113	0.763	8.1318	4.55	3.07
SI-10	1.938	2.343	0.686	8.8148	6.62	2.83
SI-11	2.048	2.291	0.815	9.0167	5.76	2.36
SI-12	1.708	2.305	0.999	8.9166	3.94	2.27

a_1, a_2 : Length of the two sides of the rectangular specimen.
ℓ : Thickness of specimen.
W : Weight of specimen under room dry conditions.
K_g : Geometric factor.
δ : Bulk density

EXPERIMENTAL RESULTS

The results of the new bulk density (δ) determinations are listed in Table 2, and are in the range of 2.3-3.1, results similar to those previously reported for these kimberlites (Katsube et al., 1992a). The larger values resemble those of basic rocks, and the smaller ones resemble those for sedimentary rocks (Daly et al., 1966).

The results of the magnetic susceptibility measurements are listed in Table 6. Only the data for samples SI-10 to SI-12 are new. The rest have been reported previously (Katsube et al., 1992a). The magnetic susceptibilities are in the range of 10^{-3} to $3x10^{-2}$ SI units, values generally on the larger side of the previously reported results, but within the range of those for ultramafic intrusive rocks (Grant and West, 1965).

Table 3. Results of the effective porosity measurements.

Sample	δ (g/mL)	W_W (g)	W_D (g)	S_{Ir} (%)	ϕ_E (%)
SI-2	2.94	9.0106	8.9045	34.8	3.50
SI-3	2.58	6.9251	6.6194	11.0	11.92
SI-4	2.88	5.0195	4.8877	31.1	7.77
SI-5	2.72	5.7782	5.6740	16.2	5.00
SI-6	2.86	8.6377	8.5812	52.4	1.88
SI-7	2.99	5.6928	5.6112	29.4	4.35
SI-8	2.89	3.9241	3.8013	27.4	9.34
SI-9	3.07	11.3180	11.2245	39.4	2.56
SI-10	2.83	5.2649	5.1872	25.6	4.24
SI-11	2.36	18.1805	16.7449	6.8	20.23
SI-12	2.27	21.0006	18.7464	3.1	27.30

W_w = wet weight; W_D = dry weight; S_{Ir} = irreducible water saturation; δ = bulk density; ϕ_E = effective porosity

Table 4. Results of electrical resistivity measurements.

Sample	ρ_r (10^3 Ωm) Mes. #1	Mes. #2	Mean
SI-2	31.93	33.85	33. ±1.
SI-3	0.66	0.74	0.70 ±0.04
SI-4	8.29	8.99	8.6 ±4.
SI-5	3.10	3.28	3.2 ±0.1
SI-6	57.50	60.91	59. ±2.
SI-7	21.55	21.55	21.6 ±0.05
SI-8	16.87	18.93	17.9 ±0.04
SI-9	21.26	22.78	22. ±1.
SI-10	6.76	6.84	6.8 ±0.04
SI-11	0.19	0.21	0.20 ±0.01
SI-12	0.13	0.15	0.14 ±0.01

ρ_r =Bulk Electrical Resistivity.
Mes. (#1) =Measurement after 24 hours of saturation.
Mes. (#2) =Measurement after 48 hours of saturation.

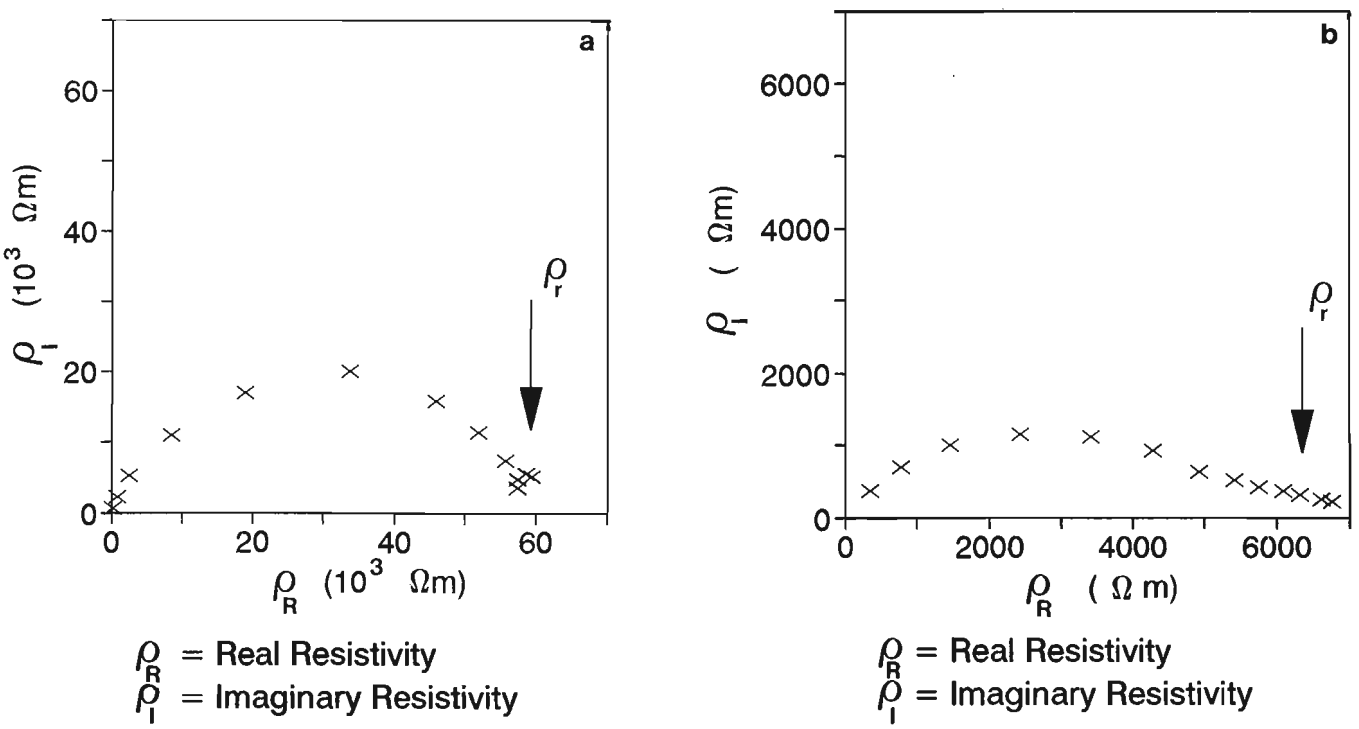

Figure 2. Typical examples of complex resistivity plots used to determine bulk resistivity (ρ_r), a) for sample SI-6 displaying a normal arc, and b) for sample SI-10 displaying a suppressed arc.

The new results of the effective porosity (ϕ_E) measurements are listed in Table 3, values in the range of 1.9-27%. The lower values are similar to those reported previously for these kimberlites, but the range extends to values considerably larger than those of earlier measurements. This range of values resembles that of sedimentary rocks (Daly et al., 1966), with the larger values similar to those of sandstones, and the smaller ones resembling those of shales and carbonates.

The new electrical resistivity (ρ_r) values are listed in Table 4. Determinations have been made at 24 and 48 hours after saturation, to ensure that they represent ρ_r values stable with time. Examples of the complex resistivity measurements used to determine ρ_r are shown in Figure 2. The ρ_r values are in the range of 10^2 to 5.9×10^4 Ω-m, the lower end being smaller and the higher end being similar to the previously reported results (Katsube et al., 1992a) for these kimberlites. This represents a wide range of ρ_r values, the smaller ones resembling those of Paleozoic and Precambrian sedimentary and volcanic rocks (Keller, 1982), and the larger ones resembling those of crystalline rocks (Katsube and Hume, 1987a, 1989). The possibility of increased error when measuring samples with high resistivity (e.g., SI-6), is eliminated by maintaining small thicknesses of the specimens, a technique previously discussed (Katsube et al., 1992a, c).

Results of the resistivity measurements (ρ_m) used for formation factor (F) determination are listed in Table 5. The results for the three samples SL-1, SL-4, and SL-7 were published previously (Katsube et al., 1992a) and are not repeated here. The results of the F and surface resistivity (ρ_c) determinations using the Patnode and Wyllie Equation (Katsube and Scromeda, 1993) are listed in the last two

Table 5. Formation-factor, surface resistivity and bulk resistivities for different NaCl solutions for the kimberlite samples.

Sample	ρ_m ($\times 10^3$ Ω-m)					F ±%	ρ_o ±%
ρ_w (Ω-m) NaCl (N)	0.27 ±0.02 0.5	0.62 ±0.04 0.2	1.08 ±0.003 0.1	2.01 ±0.08 0.05	5.21 ±0.08 0.02	($\times 10^2$)	($\times 10^3$) (Ω-m)
SI-1/1	0.48	1.16	1.96	4.49	11.5	6.2 ±1	-
			X	X	X	17.1 ±1	-
SI-2	0.71	1.82	4.12	7.76	12.3	23.6 ±1	-
			X	X	X	44.4 ±1	33.6 ± 4
SI-3	0.072	0.15	0.26	0.32	0.41	2.76±1	0.87± 3
SI-4	0.64	1.33	2.39	3.30	11.1	2.25±1	31.6 ± 3
SI-5	0.48	0.89	1.50	1.80	2.30	1.92±1	3.58± 1
SI-6	0.69	1.71	3.76	9.67	20.9	22.5 ±1	-
SI-7	0.44	1.07	2.18	9.52	8.78	14.4 ±1	-
SI-8	0.46	1.15	1.95	3.17	7.19	15.9 ±1	-
		X	X	X	X	19.7 ±1	20.5 ± 1
SI-9	0.52	1.05	2.36	4.00	11.7	17.2 ±1	-
			X	X	X	21.8 ±1	165. ±16
SI-10	0.73	1.36	2.57	3.72	9.79	25.8 ±1	18.0 ± 3
SI-11	0.038	0.062	0.088	0.12	0.14	1.67±1	0.17± 1
SI-12	0.015	0.027	0.041	0.061	0.077	0.60±1	0.11± 1
SL-2/1	0.049	0.10	0.15	0.21	0.22	1.98±1	0.40± 2
SL-3/1	0.040	0.074	0.11	0.14	0.15	1.70±1	0.22± 1
SL-5/1	0.011	1.58	2.57	8.03	18.0	-	-
		X	X	X	X	23.3 ±1	-
SL-6/1	0.082	0.13	0.16	0.19	0.22	4.27±1	0.25± 1
SL-9/1	0.091	0.20	0.30	0.47	0.61	3.43±1	1.40± 2
SL-10/1	0.71	1.31	3.34	7.31	17.3	23.1 ±1	-
			X	X	X	29.9 ±1	-
SL-11/2	0.80	1.49	3.38	8.02	18.2	26.3 ±1	-
			X	X	X	29.8 ±1	-
SL-12/1	0.72	1.85	4.30	9.98	27.5	23.4 ±1	-
SL-13/1	0.43	1.14	1.61	2.15	9.06	15.2 ±1	-
SL-14/1	0.81	1.20	2.14	5.90	27.0	26.4 ±4	-
SL-15/3	0.74	1.45	2.68	5.42	14.1	25.3 ±1	207. ±18

ρ_w = Pore fluid resistivity
ρ_m = Bulk resistivity of the rock for solutions of different salinities
F = Formation factor
ρ_c = Surface resistivity
- = Data not available

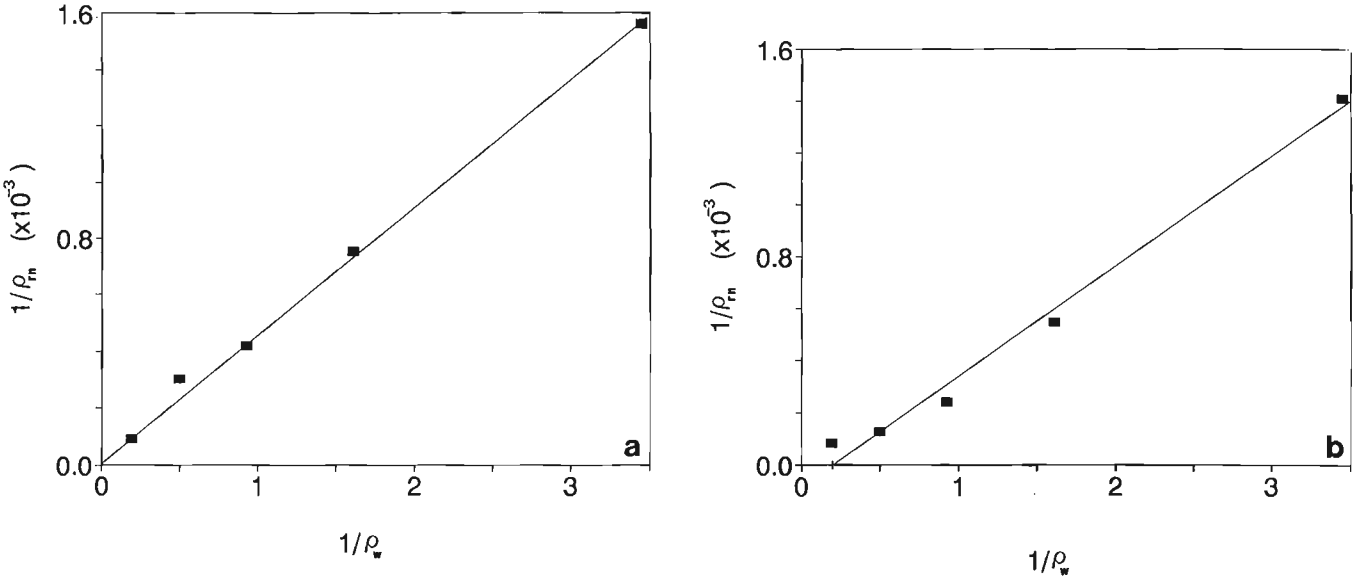

*Figure 3. Typical examples of the ($1/\rho_m$) versus ($1/\rho_w$) relationship observed when determining formation factor (F) and surface resistivity (ρ_c), **a)** for sample SI-4 displaying normal results, and **b)** for sample SI-2 displaying an abnormal result where the ρ_c is negative.*

columns of Table 5. The percentage errors, listed in these columns, are determined by taking the differences in the F and ρ_c values obtained by using the different regression lines: the reduced major axis (RMA) and the normal regression lines (NRL). Typical examples of the $1/\rho_{rn}$ versus $1/\rho_w$ relationships observed when determining F and ρ_c are shown in Figure 3. The principles of the reduced major axis are described in Davis (1986), and examples of related applications are found in Katsube and Agterberg (1990). In cases where the deviation from linearity of a data point is the cause of negative values for $1/\rho_c$ (Fig. 3b), that data point is eliminated from the regression analysis performed to determine F and ρ_c (Katsube et al., 1992c; Katsube and Scromeda, 1993). In such cases, the data points used to determine the two parameters are identified by the symbol "X" in Table 5. According to the Patnode and Wyllie equation, the $1/\rho_{rn}$ versus $1/\rho_w$ relationship is linear (Patnode and Wyllie, 1950) and both F and $1/\rho_c$ should be positive, as displayed in Figure 3a. The symbol "-" in the last column, indicating no available data, implies either that the ρ_c values were negative or the error range was extremely large. The negative ρ_c values, in this case, are usually interpreted to be extremely large resistivity values approaching infinity, indicating little surface conduction.

Table 6. Summary of petrophysical and physical properties.

Samples	δ (g/mL)	MS (10^{-3})	ϕ_E (%)	F (x10^2)	ρ_r ($10^3\Omega$ m)	ρ_c ($10^3\Omega$ m)
SI-1	2.68	20.	3.1	16.7 ± 0.5	38. ± 1.2	-
SI-2	2.94	8.0	3.5	44. ± 21.	33. ± 1.	33.6 ± 1.3
SI-3	2.58	25.	12.	2.76 ± 0.03	0.70 ± 0.04	0.87 ± 0.03
SI-4	2.88	4.0	7.8	2.25 ± 0.03	8.6 ± 4.	31.6 ± 0.95
SI-5	2.72	24.	5.0	1.92 ± 0.02	3.2 ± 0.1	3.58 ± 0.04
SI-6	2.86	5.0	1.9	22.5 ± 0.3	59. ± 2.	-
SI-7	2.99	12.	4.4	14.4 ± 0.2	21.6 ± 0.05	-
SI-8	2.89	3.0	9.3	20. ± 5.	17.9 ± 0.04	20.5 ± 0.5
SI-9	3.07	15.	2.6	22. ± 5.	22. ± 1.	165. ± 27.
SI-10	2.83	30. *	4.2	25.8 ± 0.6	6.8 ± 0.04	18.3 ± 0.6
SI-11	2.36	1.6*	20.	1.67 ± 0.02	0.20 ± 0.01	0.17 ± 0.002
SI-12	2.27	5.5*	27.	0.60 ± 0.01	0.14 ± 0.01	0.11 ± 0.002
SL-1	3.11	2.6	1.8	23. ± 7.	45. ± 5.5	37. ± 33.
SL-2	2.46	1.5	19.	1.96 ± 0.02	0.58 ± 0.04	0.56 ± 0.01
SL-3	2.37	0.9	18.	1.70 ± 0.02	0.35 ± 0.001	0.22 ± 0.005
SL-4	2.49	1.7	16.	6.5 ± 0.4	0.95 ± 0.01	1.95 ± 0.2
SL-5	3.08	1.9	2.0	23. ± 0.3	52. ± 3.	-
SL-6	2.60	1.8	14.	4.3 ± 0.04	0.42 ± 0.01	0.25 ± 0.003
SL-7	2.64	1.6	10.7	0.72 ± 0.01	0.39 ± 0.02	0.35 ± 0.004
SL-9	2.53	1.5	14.1	3.4 ± 0.04	1.50 ± 0.01	1.40 ± 0.03
SL-10	3.09	2.5	5.5	27. ± 4.	32. ± 2.	-
SL-11	2.86	2.0	4.1	28. ± 2.	56. ± 2.1	-
SL-12	2.95	2.1	4.0	23. ± 0.3	82. ± 3.1	-
SL-13	3.01	1.7	3.2	15. ± 0.2	27. ± 2.3	-
SL-14	3.23	2.4	1.83	26. ± 1.	58.6 ± 0.3	-
SL-15	3.00	1.7	3.5	25. ± 0.5	51.4 ± 0.4	207. ± 38.

MS =Mean MS in SI units
* = New data supplied by G. Bernius (Geological Survey of Canada)

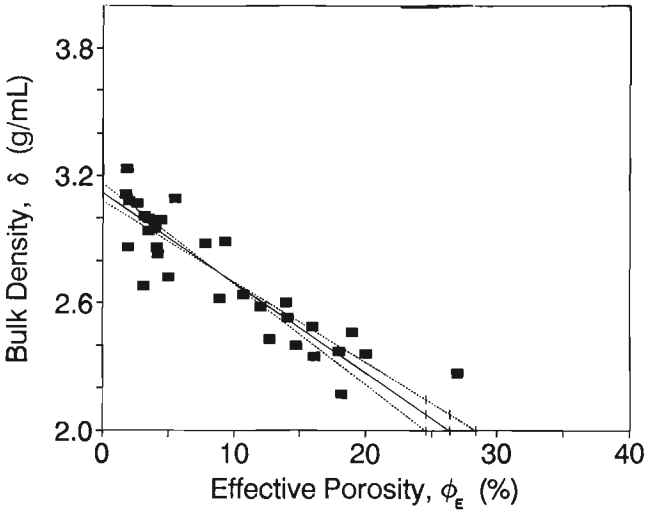

Figure 4. *Bulk density (δ) as a function of effective porosity (ϕ_E) for the kimberlite samples (r=-0.90). The solid line is the reduced major axis, and the two broken lines are the normal regression lines.*

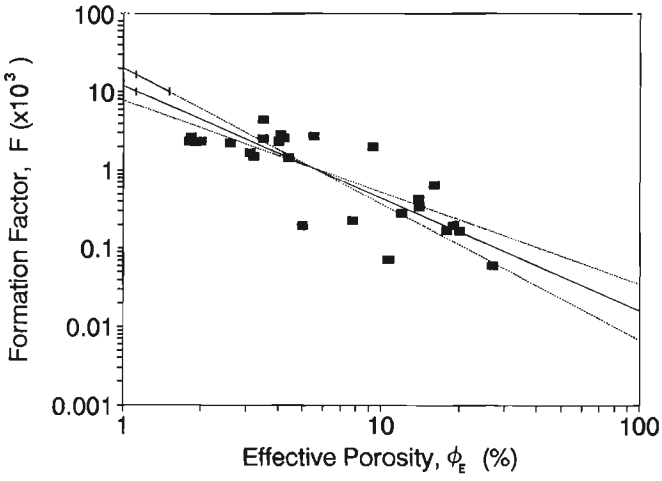

Figure 5. *Formation factor (F) as a function of effective porosity (ϕ_E) for the kimberlite samples (r=-0.82). The solid line is the reduced major axis, and the two broken lines are the normal regression lines.*

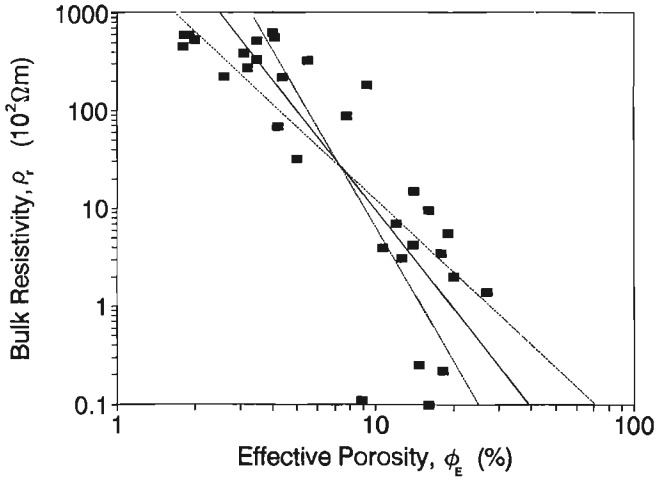

Figure 6. *Bulk resistivity (ρ_r) as a function of effective porosity (ϕ_E) for the kimberlite samples (r=-0.74). The solid line is the reduced major axis, and the two broken lines are the normal regression lines.*

The formation factor (F) and surface resistivity (ρ_c) values show a wide range of variation for these samples, that is 60-4400 and 110-207 000 Ω-mm, respectively. The smaller values for F resemble those of sedimentary rocks (Keller, 1982) and the larger values resemble those of crystalline rocks (Katsube and Hume, 1987b, 1989). The larger values of ρ_c resemble those of crystalline rocks (Katsube and Hume, 1989).

DISCUSSION AND CONCLUSIONS

Results for all six parameters, bulk density (δ), magnetic susceptibility (MS), effective porosity (ϕ_E), formation factor (F), bulk resistivity (ρ_r), and surface resistivity (ρ_c), are compiled in Table 6 for all 26 kimberlite samples, including those previously published (Katsube et al., 1992a). The "SL" samples show low magnetic susceptibility values and the "SI" samples show both high and low magnetic susceptibility values. Little characterization by sample suite is possible for the rest of the data. Similar to the previous study on kimberlites (Katsube et al., 1992a), where there was a lack of correlation between magnetic susceptibility (MS) and bulk density (δ), little correlation can be seen between magnetic susceptibility (MS) and any of the other four parameters (ϕ_E, F, ρ_r, and ρ_c) used in this study, indicating its independence from the other parameters.

A relatively good correlation exists between bulk density (δ) and effective porosity (ϕ_E), as shown in Figure 4. A somewhat similar correlation between formation factor (F) and ϕ_E (Fig. 5), and a poorer correlation between bulk resistivity (ρ_r) and ϕ_E (Fig. 6) exist. The correlation coefficient (r) for these three relationships are -0.90, -0.82, and -0.74, respectively. These relationships indicate that ϕ_E changes are associated with those of δ, F, and ρ_r, and that ϕ_E may have a major influence on the values of these three parameters. However, there are indications that further analysis could reveal other factors that affect ρ_r, these being the reason for the rather poor correlation of between ρ_r and ϕ_E. The tortuosity factor, a, and cementation factor, m, of the Archie's equation ($F=a/\phi_E$-m) which are determined from the F versus ϕ_E relationship (Fig. 5), are 16.6 and 1.43, respectively for these kimberlites. While the value of "m" is within the usual range for igneous and sedimentary rocks (Katsube and Hume, 1987c), that of "a" is considerably larger.

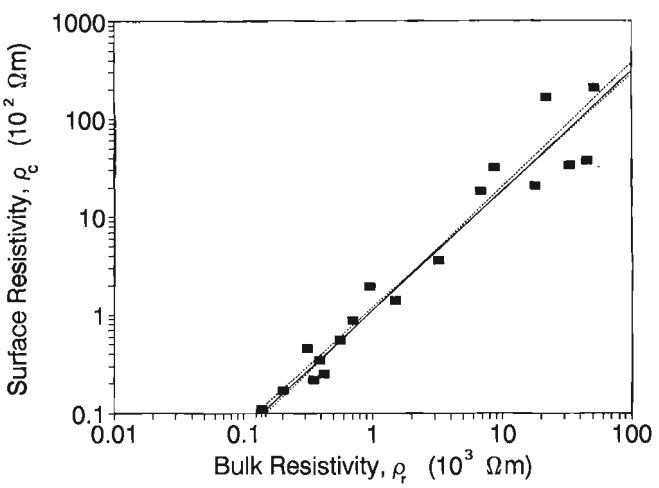

Figure 7. Surface resistivity (ρ_c) as a function of bulk resistivity (ρ_r) for the kimberlite samples (r=0.97). The solid line is the reduced major axis, and the two broken lines are the normal regression lines.

A good correlation exists between ρ_c and ρ_r (r=0.97, Fig. 7), with a slope of 1.22. Considering the facts that the slope is larger than unity and that many of the ρ_c values may be infinite as indicated above, it is possible that while the lower values of ρ_r may be a result of low values of ρ_c, there may be little or no surface conduction in the high ρ_r samples. Since low ρ_c values are an indication of clay lining of the pores and that the ρ_r versus ϕ_E relationship is negative (Fig. 6), it is implied that the pore surfaces of the high porosity kimberlites are likely to be altered, and those of the low porosity kimberlites are probably fresh.

Katsube et al. (1992a) indicated that the physical properties in Table 6 show a range of values that may relate to variations in mineralogy (primary and secondary) and petrographic textural type (crater, diatreme, or hypabyssal facies). Generally, crater and diatreme facies rocks appear to be relatively porous as compared to the hypabyssal facies (Clement and Skinner, 1979), and as a result probably tend to be more susceptible to alteration (secondary clay minerals and carbonates). These trends are consistent with the porosity-alteration relationship implied from the porosity-resistivity relationship discussed above. Further studies are underway to determine the quantitative relationship between the mineralogy and the physical properties.

ACKNOWLEDGMENTS

The authors acknowledge support from the Canada-Northwest Territories 1991-1996 Mineral Initiative, and from the Canada-Saskatchewan Mineral Development Agreement for Kimberlite Studies (1990-1995) for this study. The authors are grateful to the mining companies that provided the Sturgeon Lake (Saskatchewan) samples used in this study, and to B.A. Kjarsgaard (Geological Survey of Canada) for making the arrangements to obtain the samples, in addition to his advice on this study. The authors thank G. Bernius (Geological Survey of Canada) for providing new magnetic susceptibility measurements for three SI- series samples. The authors acknowledge the encouragement provided by P.G. Killeen (Geological Survey of Canada) regarding this study, and are thankful for the critical review of this paper by K.A. Richardson (Geological Survey of Canada).

REFERENCES

American Petroleum Institute
1960: Recommended practices for core-analysis procedure: API Recommended Practice 40 (RP 40) First Edition, American Petroleum Institute, Washington, D.C., p. 55.

Archie, G.E.
1942: The electrical resistivity log as an aid in determining some reservoir characteristics; Transactions of the American Institute of Mining, Metallurgical and Petroleum Engineers, v. 146, p. 54-67.

Atkinson, W.J.
1989: Diamond exploration philosophy, practice and promises; a review; in Proceedings of the Forth International Kimberlite Conference, Kimberlites and Related Rocks, Volume 2, (ed.) J. Ross; Geological Society of Australia, Special Publication no. 14, p. 1075-1107.

Clement, C.R. and Skinner, E.M.W.
1979: A textural genetic classification of kimberlite rocks (extended abstract); in Proceedings of the Kimberlite Symposium II, Cambridge, p. 14.

Daly, R.A., Manger,E.G., and Clark, S.P., Jr.
1966: Density of rocks; Sec. 4 (p. 23); in Handbook of Physical Constants; The Geological Society of America, Inc., Memoir 97, p. 19-26.

Davis, J.C.
1986: Statistics and Data Analysis in Geology; John Wiley & Sons, p. 200-204.

Grant, F.S. and West, G.F.
1965: Interpretation Theory in Applied Geophysics; McGraw-Hill, p. 355-381.

Katsube, T.J.
1975: The electrical polarization mechanism model for moist rocks; in Report of Activities, Part C; Geological Survey of Canada Paper 75-1C, p. 353-360.
1981: Pore structure and pore parameters that control the radionuclide transport in crystalline rocks; Proceedings of the Technical Program, International Powder and Bulk Solids Handling and Processing, Rosemont, Illinois, p. 394-409.

Katsube, T.J. and Agterberg, F.P.
1990: Use of statistical methods to extract significant information from scattered data in petrophysics; in Statistical Applications in the Earth Sciences, (ed.) F.P. Agterberg and G.F. Bonham-Carter; Geological Survey of Canada, Paper 89-9, p. 263-270.

Katsube, T.J. and Hume, J.P.
1987a: Electrical properties of granitic rocks in Lac du Bonnet batholith; in Geotechnical Studies at Whiteshell Research Area (RA-3), CANMET, Report MRL 87-52, p. 205-220.
1987b: Pore structure characteristics of granitic rock samples from Whiteshell Research Area; in Geotechnical Studies at Whiteshell Research Area (RA-3), CANMET, Report MRL 87-52, p. 111-158.
1987c: Permeability determination in crystalline rocks by standard geophysical logs; Geophysics, v. 52, p. 343-352.
1989: Electrical resistivity of rocks from Chalk River; in Workshop Proceedings on "Geophysical and Related Geoscientific Research at Chalk River, Ontario", Atomic Energy of Canada Limited Report AECL-9085, p. 105-114.

Katsube, T.J. and Kamineni, D.C.
1983: Effect of alteration on pore structure of crystalline rocks: core samples from Atikokan, Ontario; Canadian Mineralogist, v. 21, p. 637-646.

Katsube, T.J. and Salisbury, M.
1991: Petrophysical characteristics of surface core samples from the Sudbury structure; in Current Research, Part E; Geological Survey of Canada, Paper 91-1E, p. 265-271.

Katsube, T.J. and Scromeda, N.
1991: Effective porosity measuring procedure for low porosity rocks; in Current Research, Part E; Geological Survey of Canada, Paper 91-1E, p. 291 -297.
1993: Formation factor determination procedure for shale sample V-3; in Current Research, Part E; Geological Survey of Canada, Paper 93-1E, p. 321-330.

Katsube, T.J. and Walsh, J.B.
1987: Effective aperture for fluid flow in microcracks; International Journal of Rock Mechanics and Mining Sciences and Geomechanics Abstracts, v. 24, p. 175-183.

Katsube, T.J., Best, M.E., and Mudford, B.S.
1991: Petrophysical characteristics of shales from the Scotian shelf; Geophysics, v. 56, p. 1681-1689.

Katsube, T.J., Scromeda, N., Bernius, G., and Kjarsgaard, B.A.
1992a: Laboratory physical property measurements of kimberlites; in Current Research, Part E; Geological Survey of Canada, Paper 92-1E, p. 357-364.

Katsube, T.J., Scromeda, N., and Williamson, M.
1992b: Effective porosity of tight shales from the Venture Gas Field, offshore Nova Scotia; in Current Research, Part D; Geological Survey of Canada, Paper 92-1D, p. 111-119.

Katsube, T.J., Scromeda, N., Mareschal, M., and Bailey, R.C.
1992c: Electrical resistivity and porosity of crystalline rock samples from the Kapuskasing Structural Zone; in Current Research, Part E; Geological Survey of Canada, Paper 92-1E, p. 225-236.

Katsube, T.J. and Mareschal, M.
1993: Petrophysical model of deep electrical conductors; Graphite lining as a source and its disconnection due to uplift; Journal of Geophysical Research, v. 98, no. B5, p. 8019-8030.

Keller, G.V.
1982: Electrical properties of rocks and minerals; in Handbook of Physical Properties of Rocks, Volume I; (ed.) R.S. Carmichael; CRC Press, Inc., Florida, p. 217-293.

Kjarsgaard, B.A. and Peterson, T.D.
1992: Kimberlite-derived ultramafic xenoliths from the diamond stability field; a new Cretaceous geotherm for Somerset Island, Northwest Territories; in Current Research, Part B; Geological Survey of Canada, Paper 92-1B, p. 1-6.

Patnode, H.W. and Wyllie, M.R.J.
1950: The presence of conductive solids in reservoir rocks as a factor in electric log interpretation; Transactions of the American Institute of Mining, Metallurgical and Petroleum Engineers, v. 189, p. 47-52.

Geological Survey of Canada Project 870057

Diagenetic paragenesis of Middle Devonian Presqu'ile Barrier, northeastern British Columbia

H. Qing, M. Teare[1], H. Abercrombie, J. Reimer[1], and C. Riediger[2]
Institute of Sedimentary and Petroleum Geology, Calgary

Qing, H., Teare, M., Abercrombie, H., Reimer, J., and Riediger, C., 1994: Diagenetic paragenesis of Middle Devonian Presqu'ile Barrier, northeastern British Columbia; in Current Research 1994-B; Geological Survey of Canada, p. 43-48.

Abstract: The Middle Devonian Presqu'ile Barrier complex in northeastern British Columbia is host to large natural gas reserves. Much of the gas is reserved in massive, coarsely crystalline, replacement dolostones, which occur as a widespread diagenetic facies throughout the barrier. Preliminary core and thin section studies suggest that the Presqu'ile Barrier has experienced diagenesis in submarine, subaerial, and subsurface environments. Submarine diagenesis includes micrite envelopes, plus syntaxial, micritic, microspar, and fibrous cements infilling interparticle pores. These phases have significantly reduced primary porosity in the barrier limestones. Subaerial diagenesis has had only a minor influence on the barrier, primarily as localized meteoric dissolution which occurred immediately beneath the Watt Mountain unconformity. In contrast, subsurface diagenesis has had a significant effect on the barrier, frequently transforming otherwise tight limestones into highly porous and permeable dolostone reservoirs. The products of subsurface diagenesis include blocky sparry calcite, stylolites, dissolution vugs and collapse breccias, coarsely crystalline and saddle dolomites, sulphides, late-stage coarsely crystalline calcite, elemental sulphur, quartz, illite, pyrobitumen, methane, and carbon dioxide gas.

Résumé : Le complexe de la barrière de Presqu'ile du Dévonien moyen, dans le nord-est de la Colombie-Britannique, renferme de vastes réserves de gaz naturel. Une grande partie du gaz est contenue dans des dolomies de substitution massives et à grands cristaux qui forment un faciès diagénétique étendu dans toute la barrière. Les études préliminaires de carottes et de lames minces indiquent que la barrière de Presqu'ile a subi une diagenèse dans des milieux sous-marins, subaériens et subsuperficiels. La diagenèse sous-marine a produit des enveloppes de micrite, ainsi que des ciments interstitiels syntaxiaux, micritiques, microspathiques et fibreux. Ces phases ont réduit considérablement la porosité primaire des calcaires de la barrière. La diagenèse subaérienne n'a eu sur la barrière qu'un effet mineur de dissolution météorique localisée qui s'est produite immédiatement sous la discordance de Watt Mountain. Par ailleurs, la diagenèse subsuperficielle a eu un effet important, transformant souvent des calcaires autrement conpacts en roches réservoirs dolomitiques très poreuses et très perméables. La diagenèse subsuperficielle a produit de la calcite spathique blocailleuse, des stylolites, des druses de dissolution et des brèches d'effondrement, des dolomies en selle à gros cristaux, des sulfures, de la calcite tardive à gros cristaux, du soufre élémentaire, du quartz, de l'illite, du pyrobitume, du méthane et du dioxyde de carbone gazeux.

[1] Home Oil Company Limited, 1600 Home Oil Tower, 324 8th Ave. S.W., Calgary, Alberta T2P 2Z5
[2] Department of Geology and Geophysics, University of Calgary, Calgary, Alberta T2N 2N4

INTRODUCTION

The Middle Devonian Presqu'ile Barrier of northeastern British Columbia is host to natural gas reserves of 12 710 x 10^6 m^3 of marketable gas (Reinson et al., 1993). This gas is typically reserved in a massive, coarsely crystalline, replacement dolomite which occurs as a widespread diagenetic facies throughout the barrier complex (Reimer and Teare, 1992; Qing and Mountjoy, 1992, in press). This facies is frequently referred to as the Presqu'ile dolostone. Understanding the origin of this dolostone is crucial for the petroleum industry because dolomitization creates diagenetic gas reservoirs in otherwise tight limestones. Most of the known hydrocarbon pools within the barrier (e.g., Helmet, Kotcho Lake, Clarke Lake, Hossitl, and Adsett gas fields) occur within these coarsely crystalline dolomite reservoirs (Fig. 1).

Previous studies have suggested that the coarsely crystalline replacement dolomite in the Presqu'ile Barrier was formed by hydrothermal fluids during burial (Qing and Mountjoy, 1992, in press). It has been further proposed that these hydrothermal fluids triggered a coupled organic-inorganic reaction involving dolomitization, sulphate reduction, and hydrocarbon oxidation, to simultaneously form both the replacement dolostones and the natural gas (Reimer and Teare, 1992). The purpose of this project is to develop a fundamental understanding of coupled organic-inorganic diagenetic reactions and their possible role in localizing hydrocarbon accumulations. Because dolomitization associated with hydrothermal fluids has been reported in other parts of the Western Canada Sedimentary Basin – e.g., the Keg River Formation in Rainbow and Zama areas (Aulstead and Spencer, 1985; Qing and Mountjoy, 1989) and Middle Devonian Manetoe Facies in Northwest Territories (Morrow et al., 1986; Aulstead et al., 1988) – the results of this project should have implications elsewhere in the basin. This report presents preliminary observations concerning carbonate diagenetic paragenesis of the Presqu'ile Barrier complex. These observations are based on core examination and thin section studies from the producing gas fields (e.g., Helmet, Kotcho Lake, Yoyo, Clark Lake, and Adsett; Fig. 1) and from wells drilled in areas between these gas fields.

GEOLOGICAL SETTING

The Middle Devonian Presqu'ile Barrier consists of two stacked carbonate barrier complexes (Fig. 2). The lower barrier developed within the upper Keg River Formation. It rests conformably on the regionally extensive lower Keg River platform. Muskeg evaporites fill regional depressions and subbasins behind this barrier to the south and east. Shales of the Klua and Evie formations fill various embayments along the northern and western edges of the barrier system (e.g., Cordova and Klua embayments; Fig. 1). Numerous upper Keg River patch reefs occur within these shale embayments and immediately in front of the barrier (e.g., Yoyo; Fig. 1)

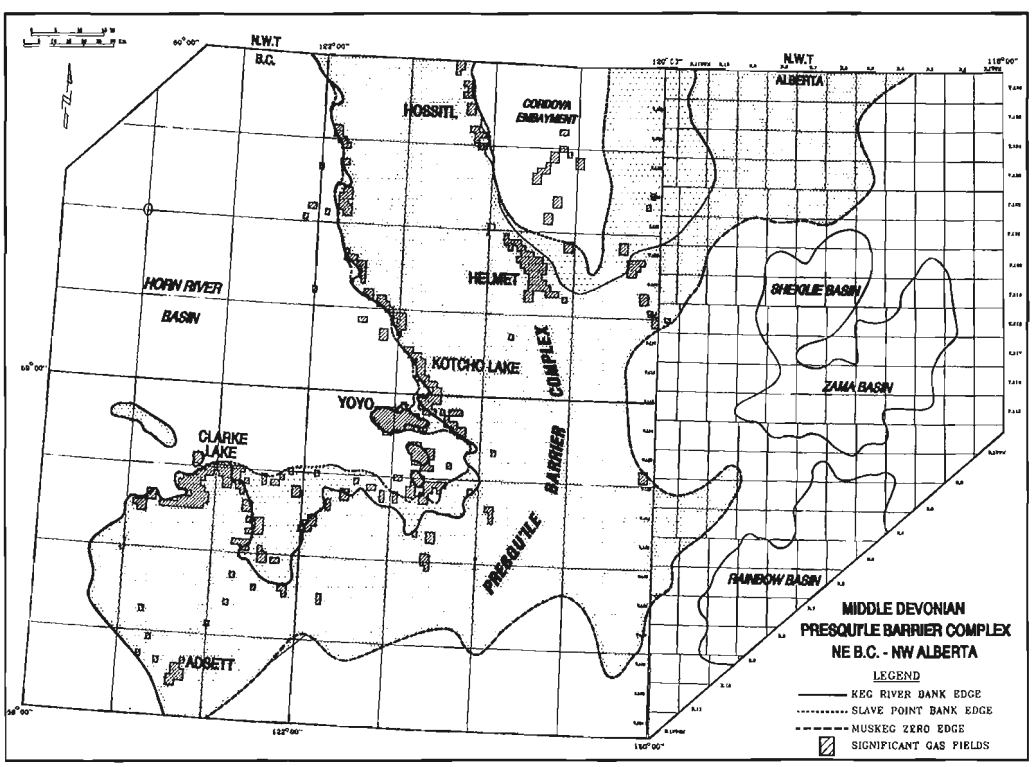

Figure 1. Paleogeographic and location map for the Middle Devonian Presqu'ile Barrier in northeastern British Columbia and northwestern Alberta.

The Sulphur Point Formation represents a prograding platform facies that conformably overlies the upper Keg River and Klua Formations. Sulphur Point deposition was terminated by a period of subaerial exposure, represented by the Watt Mountain unconformity.

The upper barrier developed within the Slave Point Formation, immediately overlying the Watt Mountain unconformity. Its northwestern limit is generally coincident with the lower barrier edge, except in the vicinity of the Klua and Cordova embayment areas, where it progrades out to the edge of the Klua shale clinoform. The Slave Point Formation may be coarsely divided into lower and upper intervals. The lower interval is regionally continuous through the back-barrier platform; the upper interval is discontinuous. Areas of non-deposition in the upper Slave Point are commonly filled by shales of the Otter Park Formation (Fig. 2). The Slave Point and Otter Park are, in turn, disconformably overlain by the Muskwa Formation (shale), which represents a regional drowning event that terminated Middle Devonian carbonate deposition in northeastern British Columbia (Reimer and Teare, 1992).

DIAGENETIC PARAGENESIS

The Presqu'ile Barrier has undergone diagenetic alteration in submarine, subaerial, and subsurface environments. Petrographic evidence suggests that the Keg River barrier was periodically inundated by evaporitic brines from the Elk Point Basin to the southeast, and also by meteoric water during Watt Mountain exposure. Both the Slave Point and Keg River barriers have been affected by basinal and hydrothermal fluids during burial. Many of the diagenetic features associated with these burial processes have been described by Jackson and Beales (1967), Skall (1975), Kyle (1981, 1983), Rhodes et al. (1984), Krebs and Macqueen (1984), and Qing and Mountjoy (1989, 1992, in press). Most of these studies, however, were based mainly on information from open pits and outcrops in the Pine Point area, with an emphasis on Pb-Zn mineralization. This study specifically describes the diagenetic features in correlative carbonate reservoirs in the subsurface. These diagenetic features are discussed according to their paragenetic sequence (Fig. 3). Overlapping phases are listed according to their first appearance.

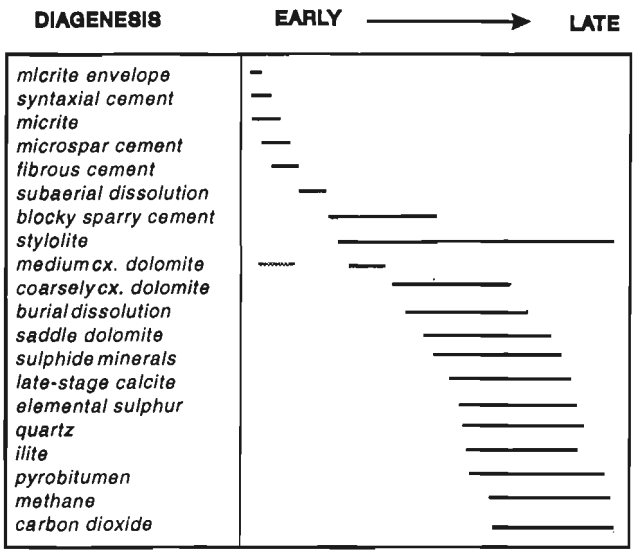

Figure 3. Diagenetic paragenesis of the carbonates from Middle Devonian Presqu'ile Barrier, northeastern British Columbia.

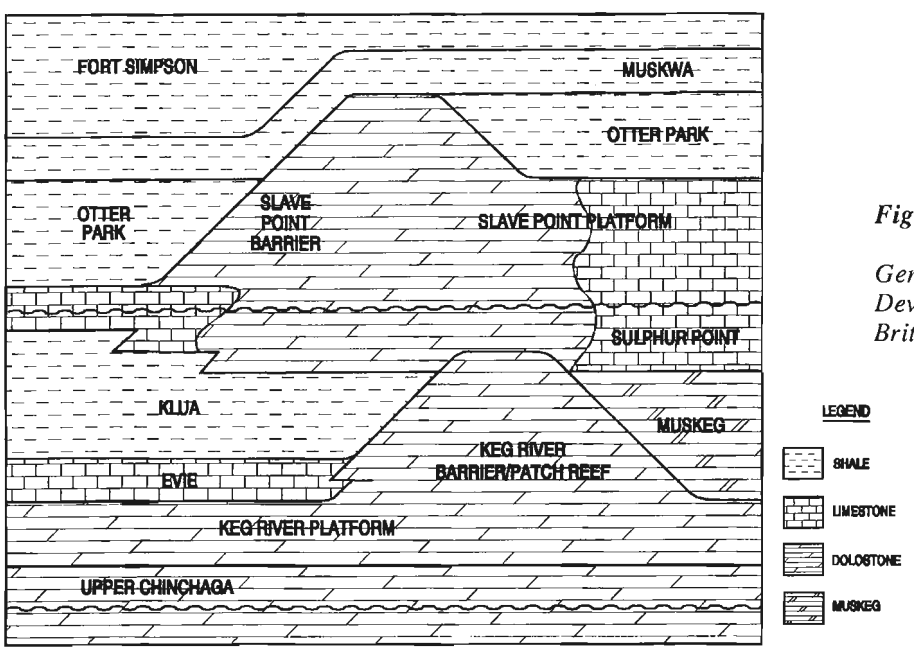

Figure 2.

Generalized stratigraphy of the Middle Devonian Presqu'ile Barrier, northeastern British Columbia.

SUBMARINE DIAGENESIS

Submarine diagenetic features are best preserved in the Sulphur Point and Slave Point limestones. Submarine diagenesis has produced a variety of marine cements, including syntaxial, micritic, microspar, and fibrous phases. These cements commonly occlude or partly fill interparticle pores, thereby significantly reducing the primary porosity in these carbonates.

Micrite envelopes

Micrite envelopes form a relatively thin rim (40-100 μm) on fossil fragments, especially on gastropod and/or brachiopod shells. Micrite envelopes are most abundant in skeletal floatstones.

Syntaxial cement

Syntaxial cement occurs as calcite overgrowths on echinoderm fragments. The cement has the same crystallographic orientation as the host calcite crystal. It precipitated prior to micritic, microspar, and fibrous cement in interparticle pores.

Micrite

Micrite occurs as a cement and/or a lime matrix in the pore spaces of peloidal wackestones, packstones, and some skeletal wakestones. It is the most abundant pore filling carbonate cement in the barrier.

Microspar cement

Microspar cement (equant and anhedral crystals 10-30 μm) is common in the barrier limestones. It precipitated after micrite, but before fibrous cement. It fills the primary pore spaces in peloidal wackestones, packstones, and skeletal wackestones.

Fibrous cement

Fibrous cement (elongate calcite crystals 100-600 μm long and 25-100 μm wide) occurs locally in shelter and interparticle pores in skeletal packstones. Most fibrous cements are nonferroan, but some have ferroan bands about 15 μm along the crystal terminations.

SUBAERIAL DIAGENESIS

Minor dissolution vugs, many of which contain geopetal fabrics of green sediment, occur at the top of the Sulphur Point Formation. The scale of dissolution for these vugs appears to be small and is restricted to a few metres immediately below the Watt Mountain unconformity. Pendant cement, which was reported in equivalent settings within the barrier in Northwest Territories (Qing, 1991), has not been observed in northeastern British Columbia.

SUBSURFACE DIAGENESIS

Diagenetic features attributed to subsurface diagenesis include blocky sparry calcite cement, stylolites, medium crystalline dolomite, coarsely crystalline dolomite, dissolution vugs and collapse breccias, saddle dolomite, sulphides, elemental sulphur, late stage coarsely crystalline calcite, quartz, illite, pyrobitumen, methane, and carbon dioxide gas.

Blocky sparry calcite cement

Blocky sparry calcite cement forms limpid to translucent, equant, and usually anhedral crystals of 100 to 1000 μm in size, and postdates the micritic, microspar and fibrous cements, filling the remaining pore spaces in the skeletal floatstones, peloidal packstones, and fenestrae. Most blocky sparry cement is nonferroan. Minor amounts of ferroan blocky sparry cement occur locally in the barrier.

Stylolites

Both low and high amplitude stylolites are common in the barrier carbonates. Although low amplitude stylolites may start to develop at burial depths of about 300 to 500 m, the high amplitude stylolites probably formed at burial depths greater than 1000 m. Vertical stylolites are also observed in the barrier, and presumably developed in response to local structure or regional tectonic events.

Fabric-preserving, medium crystalline dolomite

Massive, medium crystalline, replacement dolomite is brown or grey, with fossils and sedimentary textures generally well preserved. This fabric-preserving, medium crystalline dolomite occurs mostly in the lower part of the barrier and the platform of the Keg River Formation. Petrographic examination reveals that the medium crystalline dolomite is composed of anhedral to subhedral crystals (150-250 μm, average 200 μm), with well defined crystal boundaries. No undulatory extinction is observed. Some medium crystalline dolomite crystals have a cloudy centre and clear rim, suggesting neomorphism and/or overprinting by later diagenetic fluids.

Fabric-destructive, coarsely crystalline dolomite

Massive, coarsely crystalline, replacement dolomite is grey. The original sedimentary features, early diagenetic cements, and organic fabrics are mostly destroyed. At dolomite/limestone contacts, coarsely crystalline dolomite clearly replaces limestone, precluding the possibility that coarsely crystalline dolomite is a neomorphic modification of earlier dolomite. In thin section, it consists of subhedral to anhedral dolomite crystals ranging from 500 μm to 2 mm. Under cross-polarized light, it exhibits undulatory extinction. Coarsely crystalline dolomite is most abundant in the Sulphur Point and Slave Point formations. In partly dolomitized rocks, coarsely crystalline dolomite has precipitated along stylolites, suggesting

a burial origin. Coarsely crystalline dolomite contains a large variety of vugs and fractures, which creates excellent hydrocarbon reservoirs in otherwise tight barrier limestones.

Burial dissolution

The Presqu'ile Barrier has a strong overprint of burial dissolution fabrics including the pinpointing of cavernous porosities and collapse breccias (Skall, 1975; Krebs and Macqueen, 1984; Qing and Mountjoy, in press; Reimer and Teare, 1992). Many of the vugs are filled with saddle dolomite, sulphide minerals, pyrobitumen, and late stage calcite. Since evidence for large-scale dissolution, brecciation, and associated saddle dolomitization occurs continuously across the Watt Mountain unconformity from the Sulphur Point into the Slave Point, these diagenetic events must have occurred after sub-Watt Mountain exposure. Furthermore, some Slave Point collapse breccias contain indurated clasts of Muskwa shale, further constraining timing of this burial process to postdate the Middle Devonian.

Saddle dolomite

In hand specimen, saddle dolomite is a white, coarsely crystalline (millimetre-sized) phase. It occurs mainly as a cement in vugs and fractures within the grey, coarsely crystalline dolomite. It is most abundant in the Sulphur Point and Slave Point Formations.

Sulphide minerals

Sulphide minerals occur in both the dolostones and limestones of the barrier complex. The most common sulphide mineral is pyrite, which occurs as aggregates of fine grains. Locally scattered coarsely crystalline sphalerite and euhedral galena crystals are also observed. The sulphides occur as replacements of the host rock, as vug-filling phases, and as intercrystalline cements in the grey, coarsely crystalline dolomites, particularly in the upper part of the barrier. These textural relationships suggest that sulphide mineralization overlapped with the formation of the coarse grey dolomite and saddle dolomite phases.

Late-stage coarsely crystalline calcite

Late-stage coarsely crystalline calcite usually forms semi-translucent or white, rhombohedra or hexagonal scalenodedra. It is commonly observed in large vugs and caves, fractures or breccia, lining the walls and encrusting the earlier saddle dolomite and sulphide minerals. The crystal size varies from a few millimetres to about 20 cm. Late stage, coarsely crystalline calcite postdates sulphide minerals and saddle dolomite.

Elemental sulphur

Minor amounts of elemental sulphur occur in vugs and fractures at Pine Point (Qing, 1991). Significant volumes of sulphur also occur in two wells in the Minnaker area (immediately south of the Adsett Field; Fig. 1), where solid elemental sulphur was recovered from the Middle Devonian

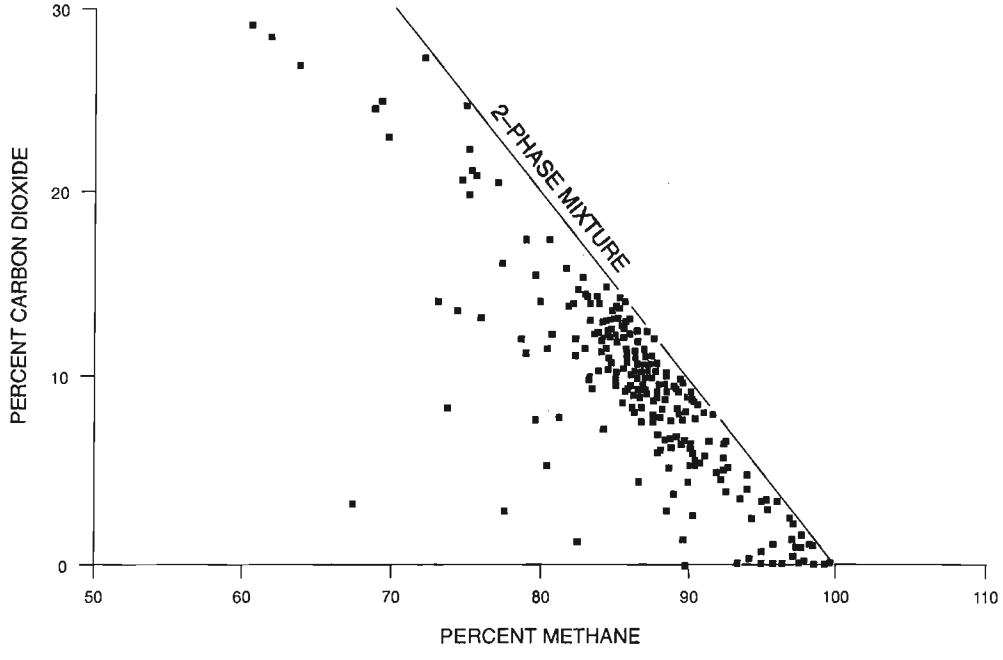

Figure 4. The gas compositions from gas pools in the Middle Devonian Presqu'ile Barrier. These gases consists primarily of a mixture of methane and carbon dioxide.

carbonates on drill stem tests. At Pine Point the elemental sulphur postdates saddle dolomite and late stage, coarsely crystalline calcite.

Quartz

Euhedral quartz crystals that range in size from 1 to 3 mm occur in the dissolution vugs in the coarsely crystalline dolomite. The quartz crystals postdate saddle dolomite cement.

Illite

Microscopic illite occurs locally as an authigenic filamentous phase associated with pyrobitumen and late stage calcite.

Pyrobitumen

Pyrobitumen is abundant in the barrier. It occurs in a variety of morphological forms, and coats saddle and coarsely crystalline dolomites and sulphide minerals. Some grey colouration of the coarsely crystalline and saddle dolomites may be attributed to pyrobitumen situated in the intercrystalline pores.

Methane and carbon dioxide gas

The Presqu'ile Barrier gases are primarily a volumetric mixture of methane and carbon dioxide (Fig. 4). Minor amounts of nitrogen and hydrogen sulphide are also present.

SUMMARY AND CONCLUSIONS

The diagenetic features of the Presqu'ile Barrier are interpreted to have developed in submarine, subaerial, and subsurface environments. The main diagenetic products developed in a submarine environment are various cements, including syntaxial, micritic, microspar, and fibrous cements, all of which are best preserved in the Sulphur Point and Slave Point limestones. The submarine cements filled interparticle pores, significantly reducing the primary porosity in these carbonate rocks.

Subaerial diagenesis has little influence on the barrier. A few small dissolution vugs occur immediately beneath the Watt Mountain unconformity. These were probably formed by meteoric action during the Watt Mountain emergence.

Subsurface diagenesis products and textures include blocky sparry calcite, stylolites, dissolution vugs and collapse breccias, medium crystalline, coarsely crystalline, and saddle dolomites, sulphides, late stage, coarsely crystalline calcite, elemental sulphur, quartz, illite, pyrobitumen, methane, and carbon dioxide gas. The formation of the coarsely crystalline dolomite, associated dissolution features, and saddle dolomites have produced the most important diagenetic modifications in the Presqu'ile Barrier, and are the subject of continuing studies.

ACKNOWLEDGMENTS

This project is jointly funded by the Geological Survey of Canada and Home Oil Ltd. as Industrial Partners Program project 93-046. Dr. R.W. Macqueen (Geological Survey of Canada) kindly reviewed the manuscript.

REFERENCES

Aulstead, K.L. and Spencer, R.J.
1985: Diagenesis of the Keg River Formation, northeastern Alberta: fluid inclusion evidence; Bulletin of Canadian Petroleum Geology, v. 33, p. 167-183.

Aulstead, K.L., Spencer, R.J., and Krouse, H.R.
1988: Fluid inclusion and isotopic evidence on dolomitization, Devonian of Western Canada; Geochimica et Cosmochimica Acta, v. 52, p. 1027-1035.

Jackson, S.A. and Beales, F.W.
1967: An aspect of sedimentary basin evolution: the concentration of Mississippi Valley-type ores during late stages of diagenesis; Bulletin of Canadian Petroleum Geology, v. 15, p. 383-433.

Krebs, W. and Macqueen, R.
1984: Sequence of diagenetic and mineralization events: Pine Point lead-zinc property, NWT, Canada; Bulletin of Canadian Petroleum Geology, v. 32, p. 434-464.

Kyle, J.R.
1981: Geology of Pine Point lead-zinc district; in Handbook of stratabound and stratiform ore deposits, (ed.) K.H. Wolf; Elsevier, New York, v. 9, p. 643-741.
1983: Economic Aspects of subaerial carbonates; in Carbonate depositional environments, (ed.) P.A. Scholle, D.G. Bebout, and C.H. Moore; American Association of Petroleum Geologists, Memoir 33, p. 73-92.

Morrow, D.W., Cumming, G.L., and Koepnick, R.B.
1986: Manetoe Facies - a gas-bearing, megacrystalline, Devonian dolomite, Yukon and Northwest Territories, Canada; Bulletin of American Association of Petroleum Geologists, v. 70, p. 702-720.

Qing, H.
1991: Petrography and geochemistry of Middle Devonian Presqu'ile dolomite, Pine Point, NWT and adjacent subsurface; Ph.D. thesis, McGill University, Montreal, Quebec, 292 p.

Qing, H. and Mountjoy, E.
1989: Multistage dolomitization in Rainbow buildups, Middle Devonian Keg River Formation, Alberta, Canada; Journal of Sedimentary Petrology, v. 59, p. 114-126.
1992: Large-scale fluid flow in the Middle Devonian Presqu'ile Barrier, Western Canada Sedimentary Basin; Geology, v. 20, p. 903-906.
in press: Formation of coarse-crystalline, hydrothermal dolomite reservoirs in the Presqu'ile Barrier, Western Canada Sedimentary Basin; Bulletin of American Association of Petroleum Geologists.

Reimer, J.D. and Teare, M.R.
1992: Deep burial diagenesis and porosity modification in carbonate rocks by thermalorganic sulphate reduction and hydrothermal dolomitization: TSR-HTD; in Subsurface dissolution porosity in carbonates: recognition, causes and implications, Canadian Society of Petroleum Geologists, Short Course Notes, 1992, CSPB-AAPG Convention, Calgary, 26 p.

Reinson, G.E., Lee, P.J., Warters, W., Osadetz, K.G., Bell, L.L., Price, P.R., Trollope, F., Campbell, R.I., Barclay, J.E., Dallaire, S.M., Waghmare, R.R., and Conn, R.F.
1993: Devonian Gas Resources of the Western Canada Sedimentary Basin; Geological Survey of Canada, Bulletin 452, 157 p.

Rhodes, D., Lantos, E.A., Lantos, J.A., Webb, R.J., and Owens, D.C.
1984: Pine Point orebodies and their relationship to the stratigraphy, structure, dolomitization, and karstification of the Middle Devonian barrier complex; Economic Geology., v. 79, p. 991-1055.

Skall, H.
1975: The paleoenvironment of the Pine Point lead-zinc district; Economic Geology, v. 70, p. 22-45.

Geological Survey of Canada Project 890058

Paleolimnology and global change on the southern Canadian prairies[1]

R.E. Vance and W.M. Last[2]
Terrain Sciences Division, Calgary

Vance, R.E. and Last, W.M., 1994: Paleolimnology and global change on the southern Canadian prairies; in Current Research 1994-B; Geological Survey of Canada, p. 49-58.

Abstract: Field and laboratory work over the past two years has produced an extensive collection of sediment core data from lakes in southern Alberta, Saskatchewan, and Manitoba. Preliminary analyses, including physical description, photography and radiography, isolation of plant macrofossils, development of chronostratigraphy and lithostratigraphy, as well as documentation of current lake chemistry, morphology and drainage basin characteristics, indicate that significant water level and chemical variations have occurred during the Holocene over this broad geographic area. Because historic hydrological fluctuations in these prairie watersheds are closely related to the balance between evaporation and precipitation, climate is considered the driving force behind Holocene lake-level dynamics. Continued analyses are directed at producing a detailed reconstruction of long-term hydrological and climatic dynamics for the southern Canadian prairies.

Résumé : Le travail effectué sur le terrain et en laboratoire au cours des deux dernières années s'est traduit par un imposant ensemble de données sur des carottes de sédiments lacustres prélevées dans le sud de l'Alberta, de la Saskatchewan et du Manitoba. Les analyses préliminaires, qui comprennent une description physique, des photographies et des radiographies, l'isolement de macrofossiles végétaux, l'établissement de la chronostratigraphie et de la lithostratigraphie, ainsi que la documentation des caractéristiques chimiques, morphologiques et hydrographiques actuelles des lacs, indiquent que d'importantes variations du chimisme et du niveau de l'eau se sont produites pendant l'Holocène dans cette vaste région géographique. Comme les fluctuations hydrologiques historiques dans ces bassins hydrographiques des prairies sont étroitement liées à l'équilibre évaporation-précipitation, le climat est considéré comme la force qui a régi la dynamique du niveau des eaux durant l'Holocène. Les efforts continus d'analyse visent à reproduire en détail la dynamique hydrologique et climatique à long terme du sud des prairies canadiennes.

[1] Palliser Triangle Global Change Contribution no. 15
[2] Department of Geological Sciences, University of Manitoba, Winnipeg, Manitoba R3T 2N2

INTRODUCTION

In 1860, after four years surveying what was to become the heartland of Canada's wheat production, Cpt. John Palliser returned to Ottawa with the view that the semi-arid grassland of the western Canadian interior would be "forever and comparatively useless" (Spry, 1968). Ignoring Palliser's view, the Canadian government built the national railroad across Palliser's Triangle (Fig. 1), bringing a wave of settlement at the turn of this century (a time of abundant moisture, quite unlike the drought conditions that prevailed at the time of Palliser's expedition). The area has since become one of the world's most productive agricultural regions, despite enduring severe social and economic hardships during two decades of hot, dry weather in the 1930s and 1980s. These unusually warm, dry episodes, combined with global climate model (GCM) predictions of increased aridity in the North American interior due to increased greenhouse gas concentrations (Karl and Heim, 1991), have raised concern for the area's economic future. Although one hundred years of temperature records from the Canadian prairies support the view that the region is warming (Fig. 2), it is impossible to assess how this historic trend and computer model predictions compare to long-term climatic variability without consulting proxy climate records. Recognizing the importance of this perspective, the Geological Survey of Canada established the Palliser Triangle Integrated Research Monitoring Area (IRMA) to both produce a high resolution paleoclimatic record for the region and document the nature of landscape responses to a variety of past climatic regimes (Lemmen et al., 1993). This report summarizes progress to date on the paleoclimatic component of the Palliser IRMA.

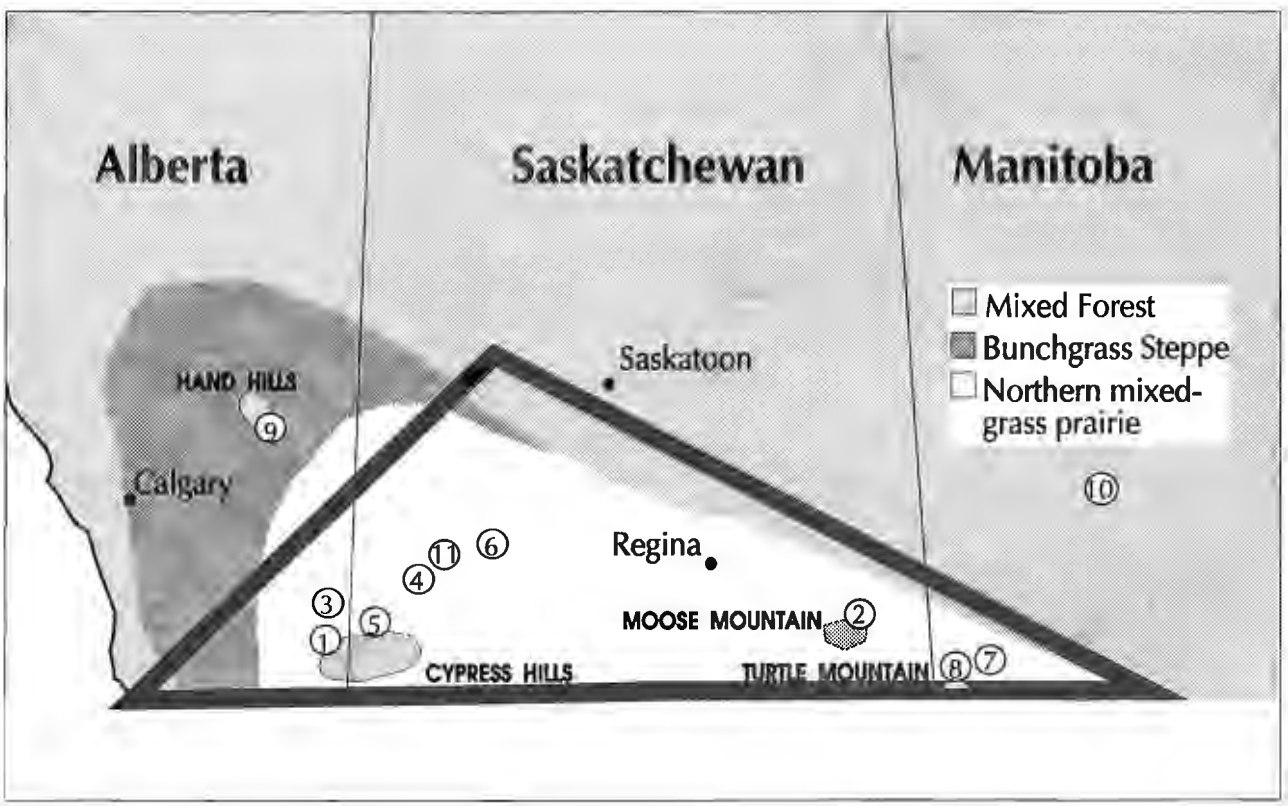

Figure 1. *Palliser Triangle IRMA and study site locations discussed in text. Extent of Palliser Triangle as described in Spry (1968), although in ecological terms this semi-arid region corresponds to the extent of northern mixed-grass prairie and brown soil zone in western Canada.*

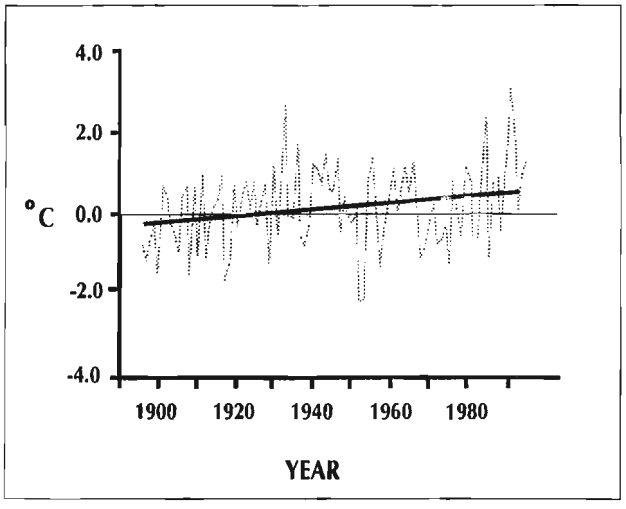

Figure 2. Prairie region temperature trend expressed as annual temperature departures from mean: 1895-1991 (adapted from Gullett and Skinner, 1992). Solid line indicates best-fit linear trend for the last century (trend significantly different from 0°C at the 95% level).

METHODS

With few of the most commonly used sources of proxy climate information available (for example, lengthy tree ring records, ice cores, etc.), development of a paleoclimatic record for Palliser's Triangle relies exclusively on sedimentary records from a select few of the numerous lakes in the region. The many saline and hyposaline lakes residing in poorly integrated drainages of recently deglaciated terrain (Last and Slezak, 1988), many displaying rapid responses to recent climate change (Hammer, 1990), contain archives of detailed proxy climate data within their sedimentary records. However, the ephemeral nature of most of these lakes, mineral-rich sediments typical of many of the basins and till containing carbonaceous shale, lignite and limestone produce significant problems in sediment sampling, developing accurate chronologies and obtaining uninterrupted stratigraphic sequences. These long-standing difficulties have hindered paleoeclimatic investigations in the entire Great Plains region of western Canada and northern United States (Barnosky et al., 1987; Last, in press b). To circumvent these problems, we have targeted spring-fed lakes on the prairie floor and large lakes on forested uplands for study, employed power assisted vibracoring techniques (Smith, 1992) to ensure collection of complete sedimentary records, and are relying solely on accelerator mass spectrometry (AMS) radiocarbon ages on seeds of upland and shoreline plants for chronological control. Where possible, we have arranged study sites in a series of transects emanating from the Cypress Hills (considered the hub of the Palliser Triangle), crossing climatically sensitive elevation, hydrological and vegetation gradients, ultimately linking our study sites with more extensively studied portions of surrounding regions.

Climate reconstructions will be based on regional lake-level and chemical responses to changes in the hydrological balance. The strategy used to reconstruct the paleohydrology of individual lake basins follows Digerfeldt's (1986) guidelines, utilizing multiple sensors in multiple cores from each lake. To accomplish these goals, a multi-disciplinary, co-operative approach to data collection and analyses has been adopted. GSC resources have been devoted to core collection, description, photography and X-ray imagery, as well as development of preliminary chronostratigraphies, lithostratigraphies and plant macrofossil stratigraphies for each core (Table 1). Remaining funds have been directed to graduate students working on specific paleoenvironmental parameters of the cores, under supervision of Canadian university collaborators with long-standing research interests in the study area. Others, although not receiving direct funding from the GSC, have accepted invitations to collaborate, increasing the breadth of data collected. In addition to the geochronology and lithostratigraphy described here, plant macrofossil, ostracode, diatom and gastropod stratigraphies will be developed at selected sites. Detailed study of the paleohydrology of the Great Sand Hills in southwestern Saskatchewan will also be undertaken. Investigation of the groundwater hydrodynamics of one study site (Chappice Lake) has recently begun, a venture that should serve as a launching point for additional hydrogeological research of other lakes in this study.

STUDY SITES

1. Elkwater Lake

Elkwater Lake straddles the climatically sensitive forest-grassland transition on the northwestern margin of the Cypress Hills. This relatively large (2.3 km^2) lake is fed by surface runoff and groundwater. A weir, built in 1908 (Mitchell and Prepas, 1990), regulates stream outflow resulting in stable, freshwater conditions that have established the lake as a popular resort. Irregular basin morphometry (Fig. 3.1), with two deep sharply contoured basins, mirrors the hummocky topography surrounding the basin.

Four sedimentary cores have been collected. Detailed studies on three of these cores, forming a transect from the deepest point of the main basin to its southern shoreline (Fig. 3.1), are currently underway. Cores EW1 and EW2 consist entirely of massive to crudely bedded silt and clay. Clay content increases with depth. Preliminary macrofossil analysis of core EW1 indicates that early lake history (ca. 5000-4000 BP) included a period of increased salinity, compared to present. This high-salinity phase was followed by a prolonged fresh, high-water stand. An attempt to date the onset of this high stand has been unsuccessful (the uppermost date on core EW1 is clearly too old, Fig. 3.1), presumably due to sampling ancient shoreline remains that were redeposited when lake-level increased.

In contrast to cores EW1 and EW2, near-shore core EW3 consists of sands interbedded with massive mud and organic-rich layers. Deposition rates are evidently much more rapid in the littoral zone than in the central lake area, particularly during the period from 550 to 325 BP. Rapid deposition here

Table 1. Summary of core information and analytical parameters at Palliser Triangle IRMA study sites.

	Elkwater	Kenosee	Chappice	Antelope	Harris	Clearwater	Killarney	Max	Little Fish	Manitoba	Freefight
Core Description	X	X	X	X	X	X	X	X	X	X	X
Photography	X	X	X	X	X	X	X	X	X	X	X
Radiography	X	X	X	X	X	X	X	X	X	X	X
% H_2O	X	X	X	X	X	X	X	X	X	X	X
% Organic	X	X	X	X	X	X	X	X	X	X	X
% Carbonate	X	X	X	X	X	X	X	X	X	X	X
Particle Size	X	X	X	X	X	X	X	X	X	X	X
Mineralogy:											
Bulk	X	X	X	X	X	X	X	X	X	X	X
Detailed Carbonate & Evaporite	X	X	X	X	X		X			X	X
Detailed Clay			X	X						X	X
Geochemistry:											
Inorganic			X	X						X	X
Organic			X	X			X			X	X
^{13}C & ^{18}O			X		X					X	X
AMS ^{14}C	X	X	X	X	X	X	X	X	X	X	
Biostratigraphy:											
Plant Macro.	X	X	X	X	X	X	X	X	X		
Diatom	X	X			X		X			X	X
Ostracode	X	X	X	X	X					X	X

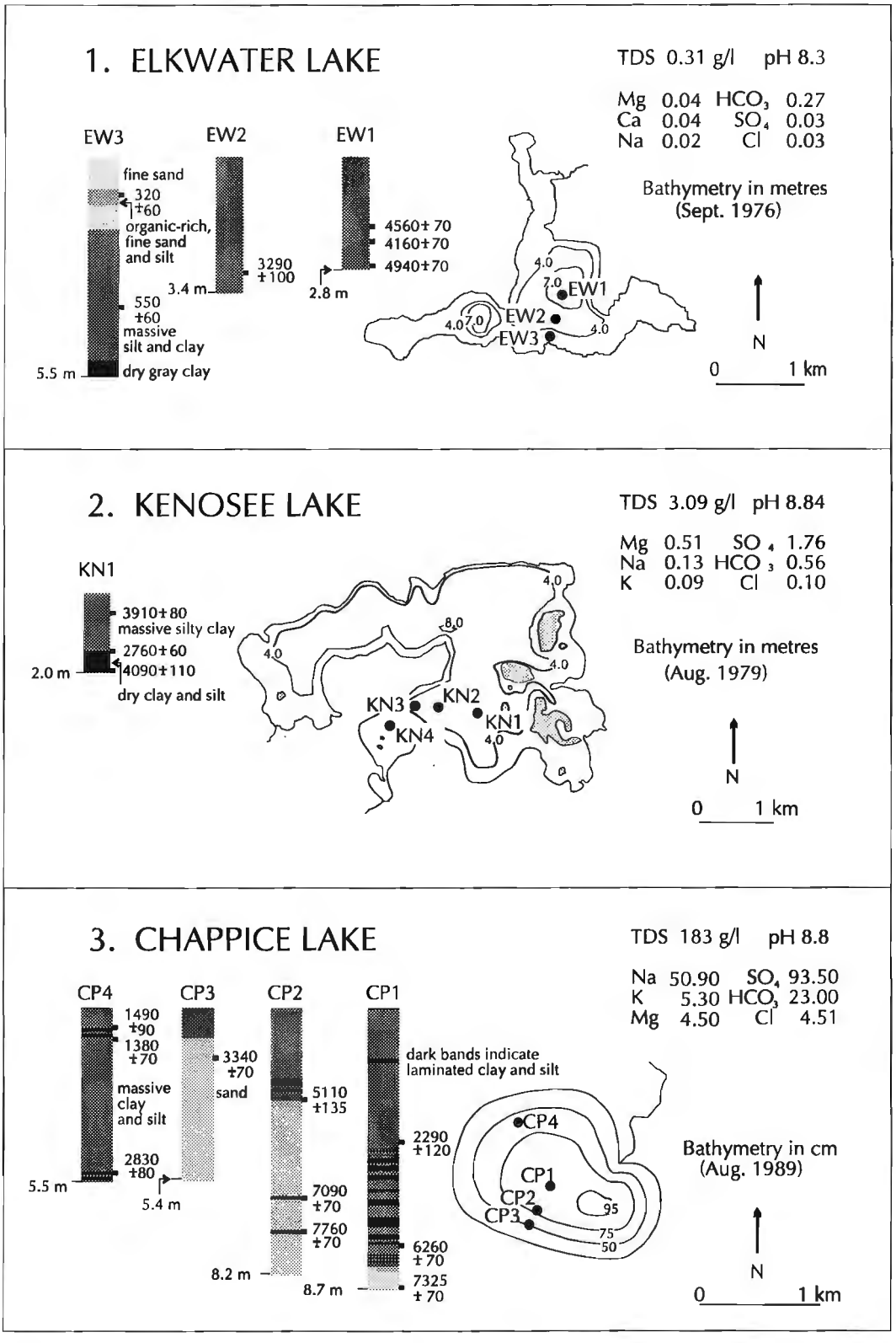

Figure 3. Bathymetry, water chemistry (where available), sediment stratigraphy, and geochronology of study sites discussed in text. Shaded areas within lake basins indicate islands.

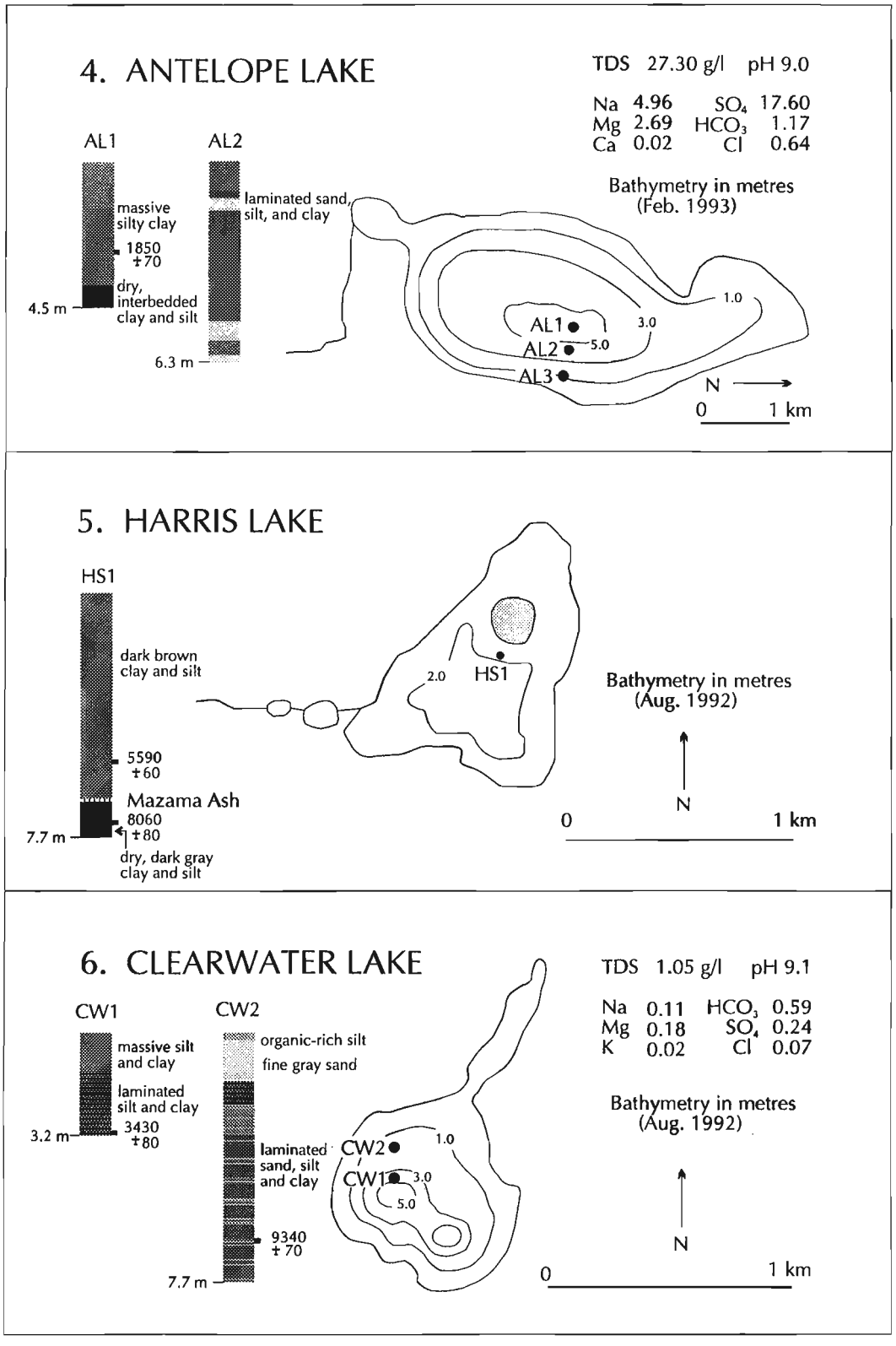

Figure 3. *(cont.)*

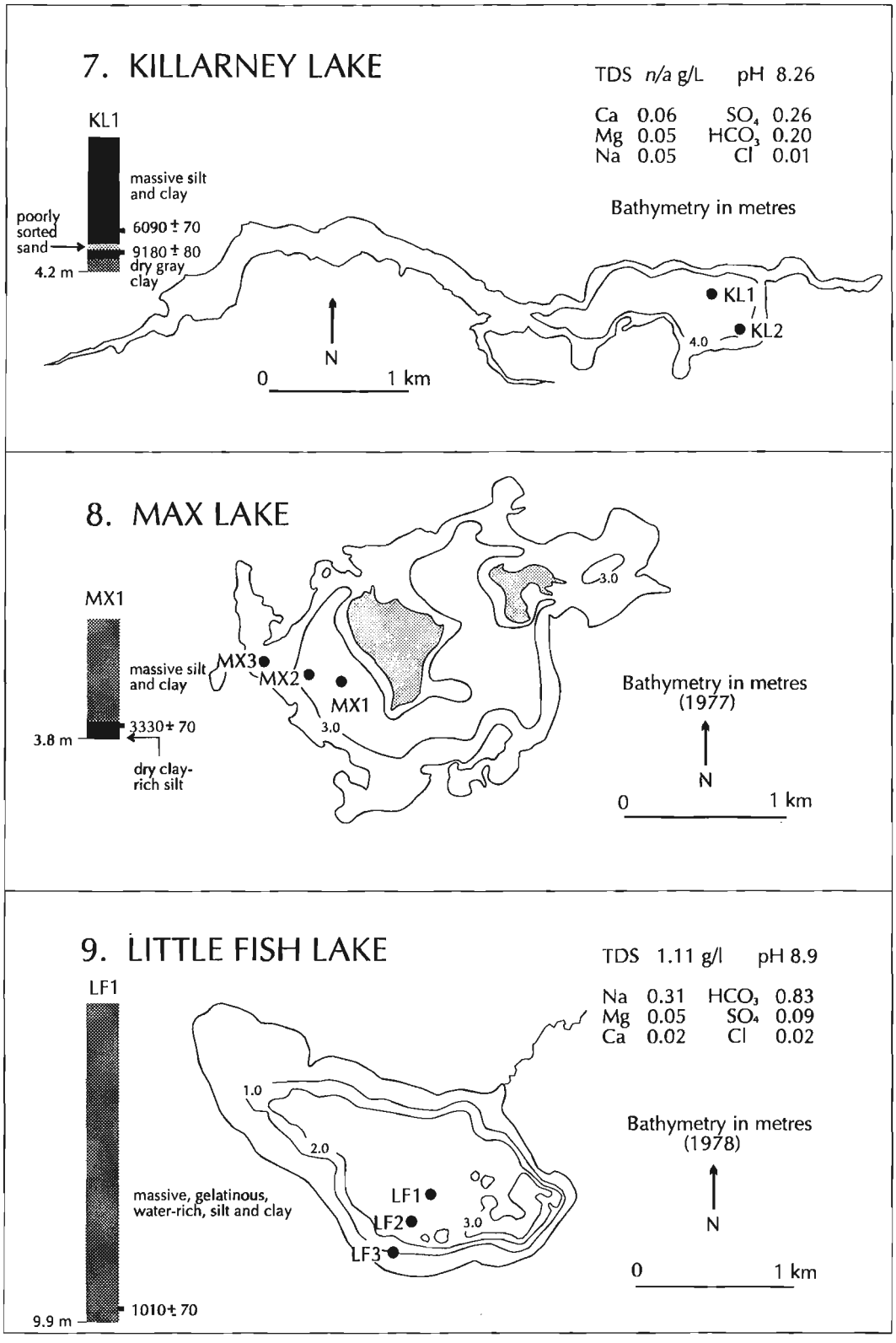

Figure 3. (cont.)

may relate to slope instability during the Little Ice Age, stimulated by climatic conditions similar to those of the cool, moist Neoglacial that increased the incidence of rotational landslides on the Cypress Hills (Goulden and Sauchyn, 1986).

In future, analyses of abundant gastropod and ostracode remains in these cores, along with continued plant macrofossil and mineralogical investigations, will be directed at documenting late Holocene lake-level and chemical variations, distinguishing periods of increased groundwater discharge and establishing a more precise chronology.

2. *Kenosee Lake*

Situated on a forested upland near the eastern limit of the Palliser Triangle, Kenosee Lake is now more saline than Elkwater Lake. Like Elkwater Lake, Kenosee Lake has become a popular recreation area, but declining lake levels and deteriorating water quality through the 1980s have created concern among land owners, provincial park officials and businesses established in the resort area at the north end of the lake (Aaston, 1983). Kenosee Lake is fed by groundwater and surface runoff. At present, outflow is restricted to groundwater discharge, as highway construction has blocked natural surface drainage to the southwest.

Three cores were retrieved from the deep southern embayment of Kenosee Lake in May 1992, and three near-shore cores were collected in March 1993. Four cores (KN1-4, Fig. 3.2) have been selected for detailed study. To date, preliminary analyses have been restricted to KN1. Macrofossil remains in this massive silty clay sequence (clay content increases and water content decreases with depth) indicate an early, high-salinity, low-water interval (ca. 4000-2700 BP), followed by lake freshening and a further water level rise in the upper 75 cm of the section. An attempt to date this most recent event resulted in an anomalously old date (the uppermost KN1 date, Fig 3.2). The error is again most likely the result of sampling ancient shoreline remains resuspended as water levels rose. Continued macrofossil and mineralogical study of these cores, complemented by diatom, ostracode and gastropod analyses, will be directed toward reconstructing paleohydrological conditions on the Moose Mountain upland, an important groundwater recharge feature of southeastern Saskatchewan (Różkowska and Różkowski, 1969).

3. *Chappice Lake*

The paleohydrology of Chappice Lake has been discussed in detail elsewhere (Vance, 1991; Vance et al., 1992, 1993). Recent investigations are focused on late Holocene events depicted in two cores (CP4 and CP5) collected in the area of highest known sedimentation rates in the basin (Fig. 3.3). Detailed macrofossil and mineralogical studies of CP4 are currently underway. In addition, mid-Holocene laminated carbonate sequences in core CP1 are being investigated to identify mechanisms involved in their genesis and stable isotope studies of this core are currently underway. Recent piezometer installations in the lake basin mark the first attempts to elucidate groundwater hydrodynamics in the watershed. Unfortunately, the highly alkaline water of the basin is not conducive to preservation of either diatoms or ostracodes, prohibiting the development of time stratigraphic sequences for these sensitive indicators of environmental change.

4. *Antelope Lake*

Situated on the southeastern margin of the Great Sand Hills, this relatively large, closed-basin saline lake may become one of the key basins in the Palliser IRMA, in terms of linking landscape processes and lake sedimentary sequences. Well defined layers of sorted fine sand in core AL2 raise the possibility of correlating these features to local dune activity. Detailed sedimentological investigations have been directed toward identifying the origin of these sand lenses. At the same time, water chemistry changes associated with lake-level dynamics depicted in plant macrofossil and lithostratigraphic records will provide a backdrop of climatic events associated with dune activity. As is the case in Chappice Lake, however, highly alkaline conditions prohibit diatom and ostracode studies.

5. *Harris Lake*

A single core was taken from a near-shore position in Harris Lake, a small groundwater discharge basin situated on the north flank of the east block of the Cypress Hills, to complement detailed pollen and lithostratigraphic analyses conducted on a central lake core from this basin (Sauchyn and Sauchyn, 1991; Last and Sauchyn, 1993). Plant macrofossil studies, mineralogical analyses and additional AMS radiocarbon dates on core HS1 will help delimit the magnitude and timing of lake-level fluctuations that accompanied Holocene environmental changes described by Sauchyn and Sauchyn (1991).

6. *Clearwater Lake*

Two cores have been extracted from the offshore area of this small, closed-basin lake originally investigated by Mott (1973). Although the lake has no inflowing stream or surficial outlet, the uncharacteristically low salinity of water in the basin (for an area of low precipitation and high evaporation rates), suggests that it is both receiving groundwater input (likely through subsurface springs in deeper sections of the lake) and discharging groundwater downslope to the north. A 9000 BP near-basal date on sedge seeds in CW2 and the finely laminated nature of the sediments suggest that development of a detailed, high resolution, long-term account of the lake's paleohydrology is possible. Moreover, excellent preservation of ostracodes, diatoms, and gastropods makes this an ideal site for analyzing multiple sensors. The record will complement ongoing plant macrofossil investigations of nearby early Holocene pond sediments by C. Yansa (University of Saskatchewan).

7. *Killarney Lake*

One other lengthy Holocene record from a freshwater lake on the eastern edge of the Palliser Triangle was recovered in March 1993. This elongate basin, occupying a glacier meltwater

channel, has recently been the subject of microfossil, pigment and chemical analyses to infer long-term trends in lake production (Richmond and Goldsborough, 1992). Detailed plant macrofossil and mineralogical analyses of the two new cores will complement this ongoing investigation by providing plant macrofossil and lithostratigraphic data pertinent to the basin's hydrological evolution, as well as outlining pace and amplitude of past climatic changes in southwestern Manitoba.

8. Max Lake

Situated 45 km southwest and 200 m above Killarney Lake on the Turtle Mountain Upland, Max Lake is a relatively large, freshwater, closed-basin lake. Its sedimentary record is a valuable complement to the Killarney Lake record, since Max Lake lies on the groundwater recharge feature closest to the groundwater discharge Killarney Lake site. The 3.8 m of massive mud collected at Max Lake is similar to the Kenosee Lake record from the nearby Moose Mountain Upland, both in terms of sediment type and temporal duration of the record. Moreover, preliminary macrofossil analyses indicate that an early low-water, high-salinity stand, like that evident in the Kenosee Lake record, also occurred at Max Lake. As at Killarney Lake, detailed macrofossil and mineralogical studies of the Max Lake cores will complement Richmond and Goldsborough's ongoing diatom and pigment studies.

9. Little Fish Lake

On the far western fringe of the Palliser Triangle, above the prairie floor on the Hand Hills upland, lies Little Fish Lake. This large (7 km^2) freshwater basin has been steadily declining in size through the 1980s, eliminating a once thriving fish population and reducing the lake's value as a recreation site. Three long cores were taken from the basin in January 1993. Core LF1 consists of gelatinous, water-rich, massive mud that is remarkably uniform in terms of grain size and mineralogy, and has an unusually low amount of plant macrofossil remains. A sedge seed recovered near the base of the 9.9 m sequence yielded an AMS radiocarbon age of *ca.* 1000 BP. This is an extremely young age for such deeply buried material and, together with the uniform composition and texture of the sediment, suggests that the lake is a site of vigorous groundwater discharge sufficient to redeposit and mix the sedimentary record. Thus, the Little Fish Lake sequence will not likely yield undisturbed, high-resolution data and no other analyses are planned. Hand Hills Lake, a shallow, ephemeral, closed-basin 10 km north of Little Fish Lake will be cored early in 1994 to provide a record from this area that currently constitutes a critical gap in coverage between sites in southeastern Alberta and the extensively studied Aspen Parkland of central Alberta (Schweger and Hickman, 1989).

Other study sites

Two additional lakes have been cored as part of Palliser Triangle IRMA field activities. Lake Manitoba lies beyond the northeastern margin of northern mixed-grass prairie, but is the only major drainage basin of the Palliser Triangle area that has previously been the subject of intensive study (Teller and Last, 1990). Analyses of the 4.8 m long core in collaboration with researchers involved in this ongoing investigation will help define hydrological responses in one of the region's major watersheds to late Holocene climatic change. Freefight Lake, on the other hand, lies in the heart of the driest portion of the Palliser Triangle. The 2.6 m long core recovered from this basin, the first retrieved from the offshore area of this deep (mean depth = 20 m), hypersaline, meromictic lake (Last, in press a), consists of finely laminated carbonate mud interbedded with massive salt deposits. Analyses of this sedimentary record will offer insights into the evolution of this unique lake as well as providing a high resolution record of hydrological change in the Great Sand Hills during the late Holocene.

In addition to coring Hand Hills Lake, the 1994 field season will be devoted to recovery of records in the Old Wives Lake drainage basin of southern Saskatchewan, filling another gap in geographic coverage. Cores of recent sediment will also be collected from two study sites for detailed analyses directed at relating recent stratigraphic variation in paleolimnological indices to historic events within each watershed.

CONCLUSIONS

Paleolimnological records in the southern Canadian prairies have been, until recently, an underutilized archive of detailed information on past hydrological and climatic change in this important but climatically sensitive agricultural region. In the century following European settlement, the area has been subjected to dramatic fluctuations in climate, from decades of devastating drought to periods of abundant rainfall. The application of new approaches and techniques to the recovery and analysis of numerous sedimentary records spanning this semi-arid grassland has opened the door to development of the first detailed record of past climate change for this economically important region of Canada. Coupled with documentation of geomorphic responses to climatic extremes, results of the Palliser IRMA will provide a much needed record of the varied landscape responses that the area has experienced over the last several millennia, giving land use planners and policy makers a realistic view of the range of extremes experienced in the past, their frequency of occurrence, and ultimately clues regarding the nature of changes western Canadian's face in future.

ACKNOWLEDGMENTS

We thank N. Alexander, M. Hay, T. Molnar and J. Wei for field and laboratory assistance. D.S. Lemmen's field assistance is gratefully acknowledged, as are his and J.V. Matthews critical reviews of the manuscript. In addition to able field and laboratory work, M. Birchard assisted in drafting figures. His endeavors over the past year are much appreciated. D.J. Sauchyn and L.G. Goldsborough kindly provided bathymetric and water chemistry data.

REFERENCES

Aaston, M.
1983: Report on Kenosee Lake and White Bear Lake water levels; unpublished report, Investigations Division, Hydrology Branch, Saskatchewan Environment, 35 p.

Barnosky, C. W., Grimm, E.C., and Wright, H.E., Jr.
1987: Towards a postglacial history of the northern Great Plains: a review of the paleoecologic problems; Annals of the Carnegie Museum, v. 56, p. 259-273.

Digerfeldt, G.
1986: Studies of past lake-level fluctuations; in Handbook of Holocene Palaeoecology and Palaeohydrology, (ed.) B.D. Berglund; John Wiley and Sons Ltd., p. 127-143.

Goulden, M.R. and Sauchyn, D.J.
1986: Age of rotational landslides in the Cypress Hills, Alberta-Saskatchewan; Géographie physique et Quaternaire, v. XL, p. 239-248.

Gullett, D.W. and Skinner, W.R.
1992: The state of Canada's climate: temperature change in Canada 1895-1991; State of the Environment Report No. 92-2, Atmospheric Environment Service, Environment Canada. 36 p.

Hammer, U.T.
1990: The effects of climate change on the salinity, water levels and biota of Canadian prairie saline lakes; Verhandlungen der Internationalen fur theoretische und angewandte Limnologie, v. 24, p. 321-326.

Karl, T.R. and Heim, R.R.
1991: The greenhouse effect in central North America: if not now, when?; in Symposium on the Impacts of Climatic Change and Variability on the Great Plains, (ed.) G. Wall; Department of Geography Publication Series, Occasional Paper No. 12, University of Waterloo, p. 19-29.

Last, W.M.
in press a: Geolimnology of Freefight Lake: an unusual hypersaline lake in the northern Great Plains of western Canada; Sedimentology, v. 40.
in press b: Paleohydrology of playas in the northern Great Plains: perspectives from Palliser's Triangle; in Paleoclimate and Basin Evolution of Playa Systems, (ed.) M.R. Rosen; Geological Society of America, Special Paper 289.

Last, W.M. and Slezak, L.A.
1988: The salt lakes of western Canada: a paleolimnological overview; Hydrobiologia, v. 158, p. 301-316.

Last, W.M. and Sauchyn, D.J.
1993: Mineralogy and lithostratigraphy of Harris Lake, southwestern Saskatchewan, Canada; Journal of Paleolimnology, v. 9, p. 23-39.

Lemmen, D.S., Dyke, L.D., and Edlund, S.A.
1993: The Geological Survey of Canada's Integrated Research and Monitoring Area (IRMA) Projects: a contribution to Canadian global change research; Journal of Paleolimnology, v. 9, p. 77-83.

Mott, R.J.
1973: Palynological studies in central Saskatchewan. Pollen stratigraphy from lake sediment sequences; Geological Survey of Canada, Paper 72-49, 18 p.

Mitchell, P. and Prepas, E.
1990: Atlas of Alberta Lakes; University of Alberta Press, 675 p.

Richmond, K.A. and Goldsborough, L.G.
1992: Paleolimnology of Killarney Lake in southwestern Manitoba: preliminary results; Abstract prepared for the Palliser Triangle Global Change Meeting, Regina.

Różkowska, A.D. and Różkowski, A.
1969: Seasonal changes of slough and lake water chemistry in southern Saskatchewan (Canada); Journal of Hydrology, v. 7, p. 1-13.

Sauchyn, M.A. and Sauchyn, D.J.
1991: A continuous record of Holocene pollen from Harris Lake, southwestern Saskatchewan, Canada; Palaeogeography, Palaeoclimatology, Palaeoecology, v. 88, p. 12-23.

Schweger, C.E. and Hickman, M.
1989: Holocene paleohydrology of central Alberta: testing the general-circulation model simulations; Canadian Journal of Earth Sciences, v. 26, p. 1826-1833.

Smith, D.G.
1992: Vibracoring: recent innovations; Journal of Paleolimnology, v. 7, p. 137-143.

Spry, I.M.
1968: The Papers of the Palliser Expedition 1857-1860; Robert MacLehose and Co. Ltd. at the University Press Glascow, 694 p.

Teller, J.T. and Last, W.M.
1990: Paleohydrological indicators in playas and salt lakes, with examples from Canada, Australia, and Africa; Palaeogeography, Palaeoclimatology, Palaeoecology, v. 76, p. 215-240.

Vance, R.E.
1991: A paleobotanical study of Holocene drought frequency in southern Alberta; unpublished Ph.D. thesis, Simon Fraser University, Burnaby, British Columbia, 180 p.

Vance, R.E., Mathewes, R.W., and Clague, J.J.
1992: 7000 year record of lake-level change on the northern Great Plains: a high-resolution proxy of past climate; Geology, v. 20, p. 879-882.

Vance, R.E., Clague, J.J., and Mathewes, R.W.
1993: Holocene paleohydrology of a hypersaline lake in southeastern Alberta; Journal of Paleolimnology, v. 8, p. 103-120.

Geological Survey of Canada Project 910013

Potassic magmatism in the Milk River area, southern Alberta: petrology and economic potential[1]

B.A. Kjarsgaard
Continental Geoscience Division

Kjarsgaard, B.A., 1994: Potassic magmatism in the Milk River area, southern Alberta: petrology and economic potential; in Current Research 1994-B; Geological Survey of Canada, p. 59-68.

Abstract: Potassic rocks of Eocene age known as the 'Sweet Grass Intrusives' outcrop as hypabyssal (dykes, plugs) intrusive rocks as well as extrusive rocks (agglomerates, lahars) in the Milk River area of southern Alberta. These rocks represent the northernmost extension of the 69-27 Ma Montana alkaline province. Combined whole-rock major and trace element chemistry, mineralogy, and mineral chemistry studies demonstrate that these rocks are minettes and that they are similar to other minettes (Highwood and Bearpaw mountains) from the Montana alkaline province. Minette pyroclastics at the Coulee 29 vent complex are the only known preserved extrusive rocks in the Sweet Grass area (Montana or Alberta). The economic potential (diamonds, gold, PGE) is considered to be low.

Résumé : Des roches potassiques d'âge éocène appelées «Intrusions de Sweet Grass» affleurent sous la forme de roches intrusives hypabyssales (dykes, culots) et de roches extrusives (agglomérats, lahars) dans la région de la rivière Milk, dans le sud de l'Alberta. Ces roches représentent le prolongement le plus septentrional de la province alcaline du Montana, qui date de 27 à 69 Ma. Les études combinées de la chimie, de la minéralogie et de la chimie minérale des éléments majeurs et des éléments traces de la roche entière montrent que ces roches sont des minettes et qu'elles ressemblent à d'autres minettes (minettes de Highwood et de Bearpaw Mountains) de la province alcaline du Montana. Les minettes pyroclastiques du complexe de cheminées volcaniques de la Coulée 29 sont les seules roches extrusives connues qui soient conservées dans la région de Sweet Grass (au Montana ou en Alberta). Le potentiel économique (diamants, or, ÉGP) est considéré comme très faible.

[1] Contribution to Canada-Alberta Agreement on Mineral Development (1992-1995), a subsidiary agreement under the Canada-Alberta Economic and Regional Development Agreement.

INTRODUCTION

Beginning in 1990, large tracts of land in Alberta were staked for diamond exploration, including the Milk River area of southern Alberta. This area is particularly interesting because potassic rocks known as the 'Sweet Grass Intrusives' outcrop locally and the regional geological setting (Archean basement of the Medicine Hat Block; Ross et al., 1991) is favourable. Early geological studies in the 1870s to 1920s considered the Sweet Grass Intrusives to be 'mica traps', or minettes (Dawson, 1884; Weed and Pirsson, 1895; Kemp and Billingsley, 1921). Modern petrological studies have included radiometric age determinations, establishing intrusive ages of 48 Ma (K/Ar biotite, quoted in Currie, 1976) and 49-52 Ma (K/Ar; Hearn et al., 1978) as well as tracer isotope systematics (Irving and O'Brien, 1991; Burwash and Cavell, 1992; Cavell and Burwash, 1993). The most recent study (Cavell and Burwash, 1993) suggests the Sweet Grass rocks have geochemical systematics transitional between lamproite and kamafugite, which infers that rock classification is problematic. If these rocks are bonafide lamproite (or kimberlite), they could have high diamond potential. Conversely, diamond potential would be considered low or nil if the rocks are minette. The current study began in late August, 1992 as a Federal Government component of the 1992-1996 Canada-Alberta Partnership on Minerals. Additional mapping and sampling was undertaken in August 1993. The main objectives of the project are to petrologically characterize the 'Sweet Grass Intrusives' and to evaluate their economic potential.

PREVIOUS GEOLOGICAL STUDIES

Potassium-rich magmatic rocks were discovered in the Milk River area of southern Alberta and northern Montana by G.M. Dawson in 1873 and 1874 during his assessment of the geology and resources of the 49th Parallel (British North American Boundary Commission, Montreal, 1875; cited in Dawson, 1884). The small intrusive masses and dykes in Alberta were described by Dawson (1884) as "mica-traps" and considered to be subordinate intrusions of the Sweet Grass Hills igneous complex to the south. Subsequent mapping of the geology of southern Alberta in the 1920s by Williams and Dyer (1930) and in the 1930s by Russell and Landes (1940) led to the discovery of additional outcrops in the Milk River area. All the sites were characterized as minette intrusions, with the exception of 'porphyritic andesite' at the westernmost locality. More recently, (Currie, 1976) described a sample from Black Butte. The mineral assemblage observed (biotite+augite+potassium feldspar+olivine) and the lamprophyric texture noted (Currie, 1976), is consistent with that of a minette.

DISTRIBUTION AND FIELD RELATIONSHIPS

There are seven outcrops of potassic rocks in the Milk River area: Black Coulee, Bear Creek, Coulee 29, Pakowki Coulee, Philp Coulee, Black Butte, and the 49th Parallel (Fig. 1). Two additional outcrops are listed in the literature, however, these are replicate references to the known outcrops. The intrusive Dawson (1884) refers to "about 2 miles off to the southeast (of the Pakowki Coulee dyke/plug) on the opposite side of the river" does not exist; this is a location error. The outcrop actually occurs to the southwest (Coulee 29), as illustrated in Map #172, which accompanies Dawson's (1884) report. The locality reported (but not found) by Williams and Dyer (1930) in "the upper part of Dead Horse Coulee" is suggested to be the "porphyritic andesite" observed in McTaggart Coulee by Russell and Landes (1940). Confusion has arisen because of historical name changes. McTaggart Coulee is in the upper part Dead Horse Coulee, however, this is shown as Black Coulee on the current Aden map sheet (72E/3).

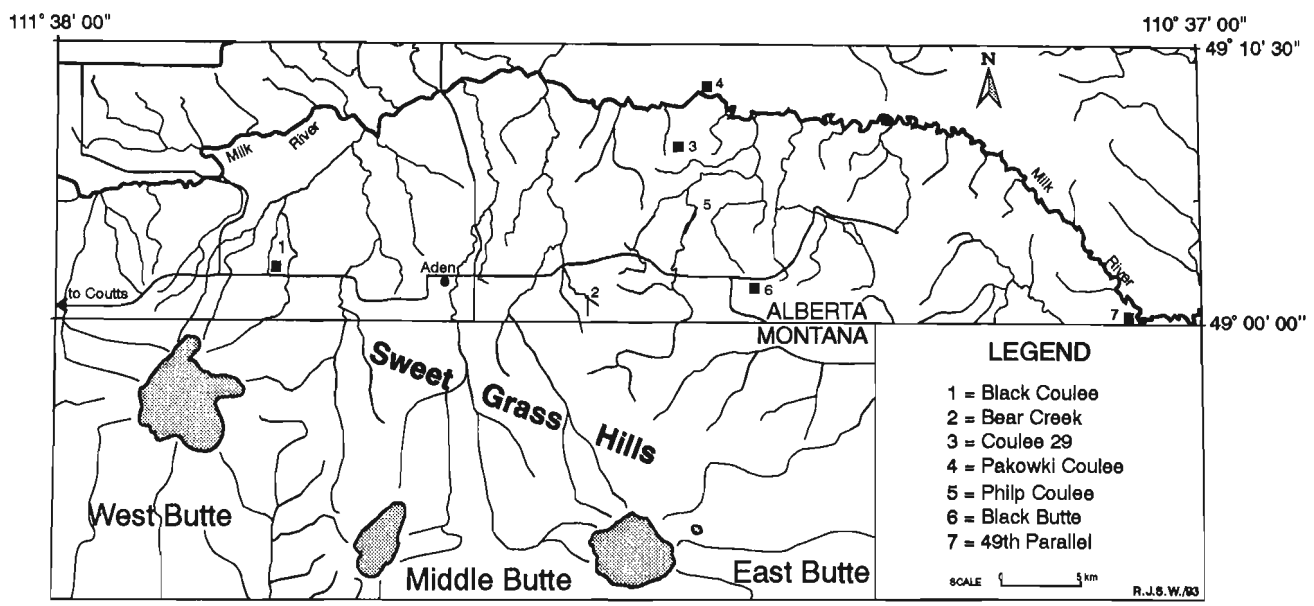

Figure 1. Location map of the Sweet Grass Intrusives in the Milk River area of southern Alberta in relation to the Sweet Grass igneous complex in Montana (from Kemp and Billingsley, 1921).

Black Coulee

The Black Coulee locality is an irregular mass of grey hypabyssal diorite porphyry that intrudes sedimentary rocks of the Milk River Formation. These rocks have a uniform appearance, with a weak trachytoid texture (defined by aligned 1-4 mm long hornblende crystals). The outcrop is located just below the eastern rim of the upper part of Black Coulee, approximately 250 m north of the Coutts-Aden road (Highway 500). Large blocks of diorite porphyry are also found in the bottom of the coulee, 80 m to the southwest from the above mentioned outcrop, but these do not appear to be in place. Russell and Landes (1940) interpreted these blocks to to be down-slumped from the coulee rim.

Bear Creek

The Bear Creek minette dyke strikes almost due north (ranging from 357° to 006°, with subvertical dips) and outcrops intermittently over 1100 m in shallow coulees to the east of Bear Creek. The dyke intrudes sedimentary rocks of the Foremost Formation. A trachytoid texture, defined by 2 mm to 1 cm (rarely to 3 cm) mica plates, is very pronounced (Fig. 2). The two best exposured segments of the dykes (both about 75 m in length) are of variable width, ranging from 1 to 2.5 m, but usually about 2 m. Along strike, notable changes in the proportions of phlogopite, olivine, and diopside phenocrysts were noted. Typical phenocryst modal abundances observed are: phlogopite, 20-40%; olivine, 3-15%; and diopside, 2-10%.

Coulee 29

At the southern edge of the Milk River valley rim, a deeply dissected coulee (called Coulee 29; R. Burwash, pers. comm., 1992) provides excellent outcrop exposures. The Coulee 29 locality is an irregulary shaped minette vent complex, formed by at least four distinct magmatic events, which intruded and/or are deposited on sedimentary rocks of the Pakowki and Foremost formations. The complex has maximum dimensions of approximately 450 m by 225 m, but the width is variable and on average is only 150 m.

The oldest observed magmatic rock type is a tan vent breccia (Fig. 3). This unit contains cognate magmatic clasts of diorite porphyry (andesite) and minette, plus a wide variety of broken (e.g., plagioclase) or bent (e.g., mica) phenocrysts from both of these rock types. Clinopyroxenite, phlogopite clinopyroxenite, glimmerite and mafic syenite cognate xenoliths (modal variants of phlogopite, diopside, apatite±alkali feldspar±carbonate) are also observed, but generally are rare. Locally derived sedimentary rocks (shales, sandstones, limestones) are common xenoliths, and in places abundant. Rare basement xenoliths (up to 1.5 m) are dominantly of tonalite gneiss.

The second phase of activity in the complex is extrusion of the brown minette proximal vent volcanic rocks, the only bonafide occurrence of extrusive rocks in the Sweet Grass Hills (Montana or Alberta). Angular, clast-supported scoria-fall and mass flow deposits, typical of Hawaiian-Strombolian volcanism (Fig. 4) are well preserved. The pyroclasts are dominated by highly vesicular minette lapilli and bombs (typically cowpat and spindle bombs; see Fig. 5), ranging from <1 cm to >100 cm in size. Associated with the pyroclastic rocks are massive, poorly sorted, matrix-supported epiclastic deposits, interpreted as proximal vent lahars (Fig. 6). These rocks contain a wide variety of rounded to subrounded clast types (minette bombs, local sedimentary and basement lithologies). The upper parts of both the pyroclastic and epiclastic rocks show evidence (crossbedded gravels) of fluvial reworking.

Closely associated with the brown minette pyroclastic phase are brown minette dykes which are phlogopite- and diopside-phyric. Olivine (generally pseudomorphed) is a minor to rare phenocryst. Crosscutting all previously described units is the final phase of magmatic activity, the black olivine minette dykes and sills. These rocks contain

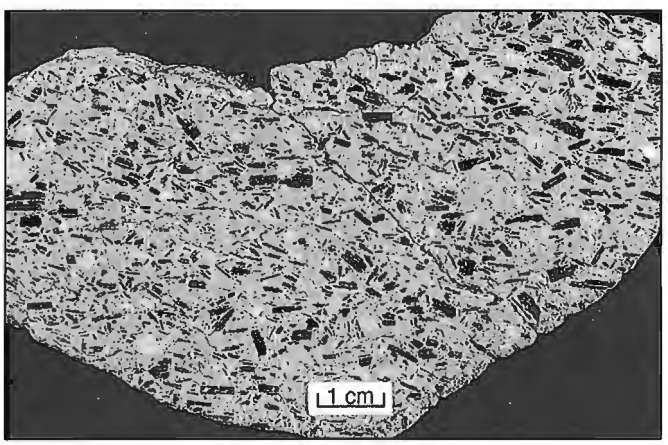

Figure 2. *Bear Creek minette (polished slab), showing aligned phlogopite phenocrysts. Subhedral to anhedral whitish-grey phenocrysts are pseudomorphs after olivine. GSC 1993-251B*

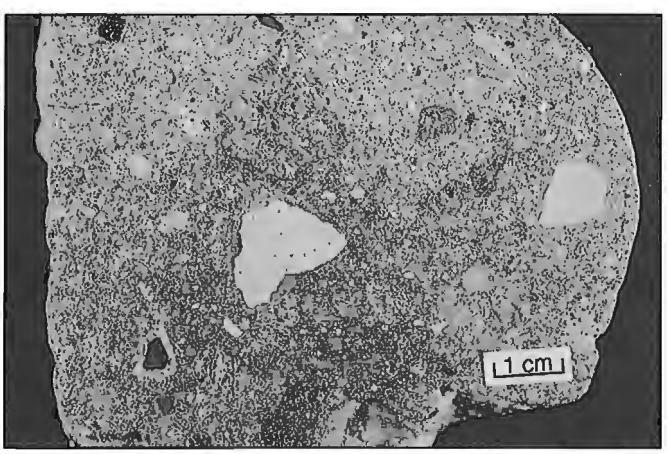

Figure 3. *Coulee 29 tan minette vent breccia (polished slab). Xenoliths include limestone and shale fragments from the local sedimentary sequences, plus cognate minette and diorite porphyry (andesite) clasts. GSC 1993-251A*

approximately equal proportions of olivine (fresh to completely altered), phlogopite, and diopside phenocrysts. The dykes or sills are generally less than 3 m thick, but in places reach 10 m.

Pakowki Coulee

The Pakowki Coulee minette dyke/plug, located on the north edge of the Milk River, is an irregular mass, approximately 25 m x 20 m in size, rising 10 m above the level of the river. It intruded sedimentary rocks of the Pakowki Formation. A brown minette breccia with abundant shale, sandstone, and limestone crustal xenoliths occupies the middle portion of the outcrop. Overlying this is a xenolith-poor brown minette, containing abundant carbonate veins. This minette is phlogopite- and diopside-phyric, with minor olivine phenocrysts and is quite similar to the brown minette intrusives at Coulee 29. Cutting both of the brown minette units is an olivine-rich, black minette sill and dyke, which again, is similar to the black minette intrusives at Coulee 29.

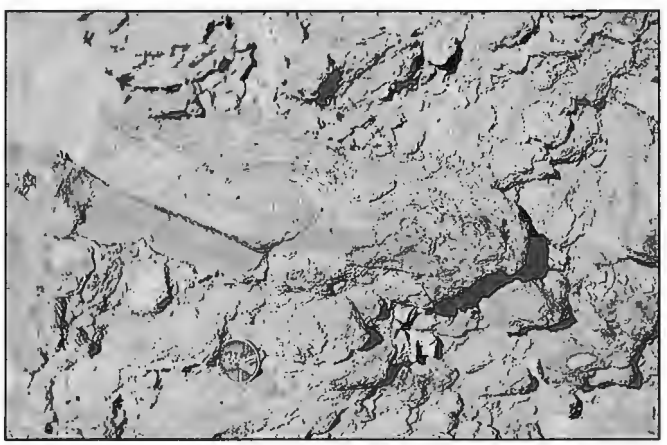

Figure 4. *Coulee 29 proximal vent agglomerate, with numerous brown minette bombs. GSC 1993-251J*

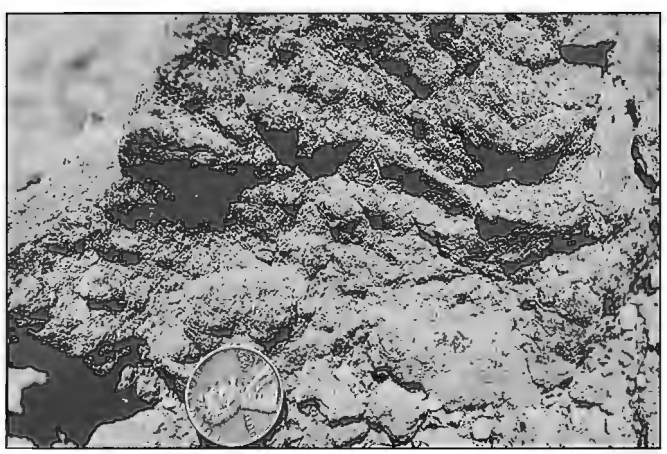

Figure 5. *Detail of minette spindle bomb in the proximal vent agglomerate at Coulee 29. GSC 1993-251K*

Philp Coulee

At Philp Coulee, a 1 to 3 m wide minette dyke has intruded sediments of the Oldman Formation in an en echelon fashion (left lateral offsets; see Fig. 7). No evidence for faulting is found associated with the offsets. The dyke strikes at 029°, with subvertical dips. The Philp Coulee dyke is well exposed (in 40-100 m long segments) at three locations from the southern end to the middle of the 700 m long dyke. The northern portion of the dyke is poorly exposed, however it is easily traced by a ridge of strongly hornfelsed sediments. Along strike, the dyke is quite variable in character, the total as well as relative proportions of phenocrysts (phlogopite+

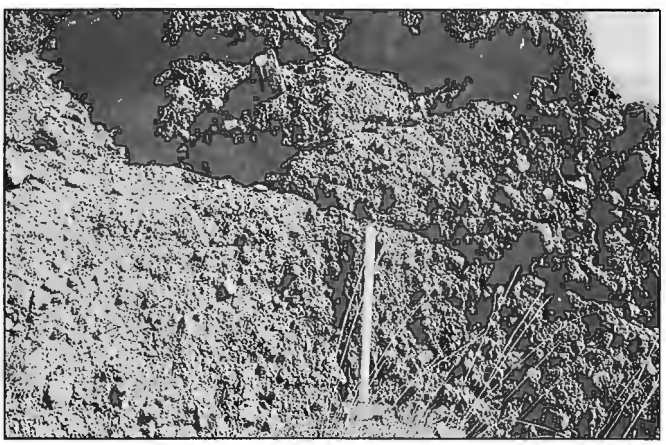

Figure 6. *Rounded to subrounded, matrix-supported clasts (dominantly minette), proximal vent lahar deposit, Coulee 29. GSC 1993-251L*

Figure 7. *Philp Coulee minette dyke, looking north, showing left lateral en echelon offset. GSC 1993-251I*

olivine+diopside) being quite variable (e.g., <10 to >30 modal% phenocryts). A moderately pronounced trachytoid texture is also observed, defined by 0.3-3 mm mica plates.

Black Butte

The Black Butte occurrence is a large, boss-like minette plug which rises about 30 m above the surrounding plain, intruding sediments of the Oldman Formation. In plan view, Black Butte has a stretched ovoid shape, long axis northeast/southwest. Maximum dimensions are approximately 400 m by 200 m, but the outcrop pinches out to the northeast where it is about 35 m in width. All exposed outcrops are dark to light grey minette intrusives; no extrusive rocks were recognized. Weak to moderate flow textures (aligned 0.2-2 mm mica crystals) are common. Basement xenoliths of tonalite and amphibolite gneiss up to 40 cm (long axis) and clinopyroxenite, phlogopite clinopyroxenite (e.g., Fig. 8), glimmerite, and mafic syenite cognate xenoliths up to 30 cm (long axis) are common at this locality.

49th Parallel

In the vicinity of the 49th Parallel at the Canada-United States border in the Milk River valley, four minette dykes intrude sedimentary rocks of the Foremost and Oldman formations. The main dyke (Fig. 9), striking 055° with subvertical dip, ranges from 1 to 2 m wide and is well exposed over a distance of 90 m, and then outcrops intermittently for another 110 m. Three thinner (0.5 to 1 m wide), minette dykes were found 10 to 50 m to the north with strikes (051° to 073°) subparallel to the main dyke. All the 49th Parallel minette dykes are light brown, fine grained, and have a pronounced trachytoid texture (defined by 0.3-1 mm mica crystals). The groundmass of these dykes is extremely rich in K-feldspar, with significant calcite also present.

MINERALOGY

Diorite

The Black Coulee diorite porphyry consists of phenocrysts of plagioclase (2-7 mm) and hornblende (1-4 mm) in a matrix of plagioclase and hornblende plus minor alkali feldspar and Fe-Ti oxide.

Tan vent breccia

The matrix of the Coulee 29 tan vent breccia consists of hornblende+plagioclase feldspar+diopside+salite+phlogopite+biotite phenocrysts (1-5 mm), in a fine grained groundmass of plagioclase and alkali feldspar+diopside+salite+biotite+magnetite+quartz. This assemblage consists of minerals associated with both of the rock types diorite and minette, suggestive of magma mixing.

Minette

All minette samples from the six outcrops have been divided into three groups, based on modal olivine and clinopyroxene phenocrysts (or there inferred pseudomorphs). Olivine-phyric assemblages (termed olivine minette) consist of olivine+phlogopite+diopside phenocrysts in a groundmass of mica (phlogopite-biotite$_{ss}$)+salite+sanidine+magnetite+apatite±analcime±calcite. Olivine-free assemblages, (termed minette) have similar mineral assemblages. Felsic minette has a similar mineral assemblage to minette, however, these rocks are salite-poor and consist mainly of phlogopite phenocrysts in a K-feldspar- and biotite-rich matrix. In general, mafic minerals in the olivine-free minettes have lower mg numbers. In both rock types, phlogopite and clinopyroxene phenocrysts are strongly zoned, showing normal, reverse, and oscillatory zoning. The presence of analcime is enigmatic, it potentially pseudomorphs primary leucite phenocrysts. Olivine minettes in the Highwood Mountains have preserved leucite inclusions

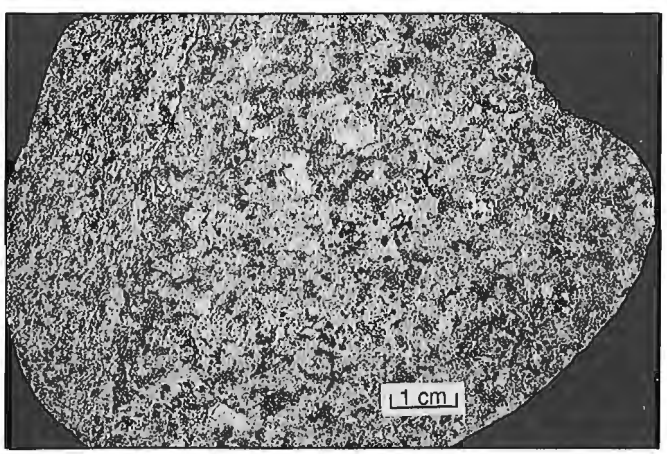

Figure 8. *Black Butte phlogopite clinopyroxenite cognate xenolith (polished slab). Note that this sample is layered, with a finer grained margin at the left side. Mineralogy is biotite+salite+apatite+dolomite. GSC 1993-251G*

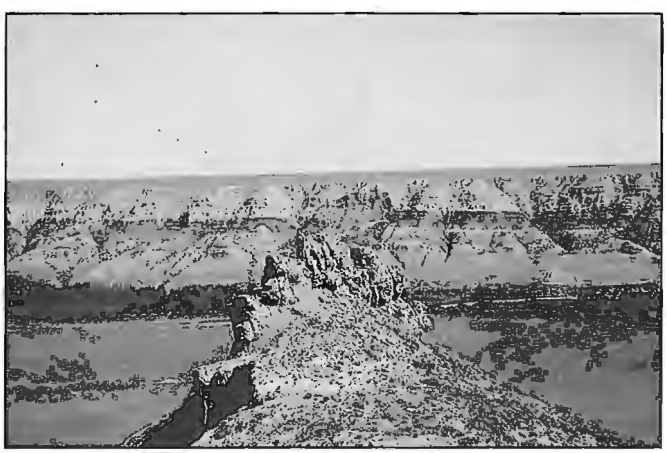

Figure 9. *The main 49th Parallel minette dyke, looking northeast with the Milk River valley and the Oldman and Foremost formations in the background. GSC 1993-251S*

within olivine and salite phenocrysts, however, these inclusions show partial and complete replacement by analcime in areas where fluids have gained access along fractures in the phenocrysts (O'Brien et al., 1989).

Minette cognate xenoliths

Coarse grained xenoliths (clinopyroxenite, phlogopite clinopyroxenite, glimmerite, and mafic syenite) recovered have varying modal proportions of the mineral assemblage mica (phlogopite or biotite)+clinopyroxene (diopside or salite)+apatite±K-feldspar±dolomite. This assemblage is the same as that observed in the minettes (with the exception of dolomite versus calcite), and the xenoliths are considered cognate. Minerals in the cognate xenoliths show minor or no compositional zoning.

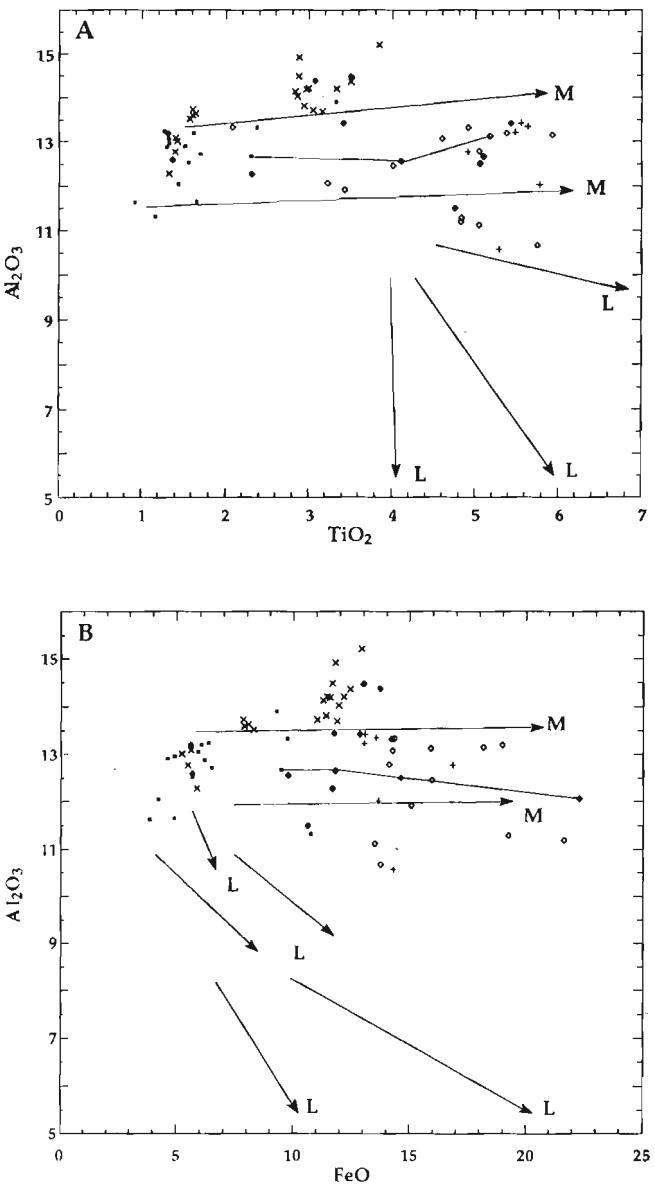

Figure 10. *Microprobe analysis of mica from the Sweet Grass minettes. A) Al_2O_3 versus TiO_2; B) Al_2O_3 versus FeO_t. Symbols as follows: X = cognate xenoliths; filled squares = phenocryst cores; filled diamonds = phenocryst middle; open diamonds = phenocryst rims; + = homogenous groundmass crystals. Lamproite (L) and minette (M) differentiation trends are indicated by arrows on the diagrams. Solid line joins analyses from a representative, zoned phenocryst.*

Mica chemistry

Phlogopite-biotite$_{ss}$ mica, a ubiquitous phase in the Sweet Grass minettes and associated cumulate xenoliths, exhibits a wide compositional range. Microprobe analyses of zoned mica phenocrysts (core, mid, rim) and homogeneous groundmass crystals from minette, plus coarse grained mica from cognate xenoliths are illustrated in Figure 10A (Al_2O_3 versus TiO_2) and 10B (Al_2O_3 versus FeO_t). The salient points to be observed from the two diagrams are: 1) compositions of mica from cognate xenoliths overlap the core and mid compositions of zoned phenocrysts, although Al_2O_3 contents may be slightly higher in the cognate samples; 2) zoning trends show increasing FeO_t and TiO_2 at essentially constant Al_2O_3 (i.e., the minette trend of Mitchell, 1986); and; 3) compositions fall within the known range for micas from minettes (cf. Mitchell and Bergman, 1991).

GEOCHEMISTRY

Whole-rock major and trace element chemistry have been completed on fresh samples from each locality. A representative analysis from each outcrop is listed in Table 1. Numerous major and trace element geochemical criteria have been suggested by various authors (summarized in Mitchell

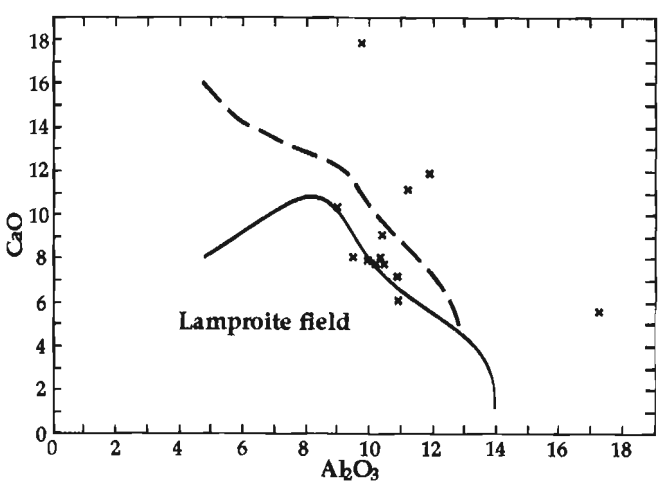

Figure 11. *Plot of CaO versus Al_2O_3 for rocks from the Sweet Grass area, southern Alberta. Discriminant boundaries for separating lamproites from other potassic rocks after Foley et al. (1987; solid line) and Mitchell and Bergman (1991; dashed line).*

Table 1. Whole-rock major and trace element chemistry for selected potassic rocks from the Milk River area, southern Alberta. Major elements by XRF fused disc, trace elements by XRF pressed powder, and ICP-MS at Department of Earth Sciences, Memorial University of Newfoundland; Au, Ag, and Ir by INAA at Activation Laboratories, Ancaster; F, Cl, S analyzed at GSC.

Sample#	KIA92 200A	KIA92 205	KIA92 217B	KIA92 221A	KIA92 222B	KIA92 224E	KIA92 225
Location	Coulee 29	Black Coulee	Black Butte	Philp Coulee	Bear Creek	Pakowki Coulee	49th Parallel
Type	olivine minette	diorite porphyry	minette	olivine minette	olivine minette	olivine minette	felsic minette
SiO2	48.74	60.71	50.93	51.90	46.15	47.39	45.01
TiO2	1.05	0.47	0.95	1.10	1.06	1.07	1.50
Al2O3	9.94	17.24	10.41	10.92	11.24	9.50	11.93
Fe2O3t	10.12	5.82	7.66	8.99	8.47	10.74	6.64
MnO	0.14	0.15	0.16	0.13	0.19	0.15	0.12
MgO	13.63	1.71	9.97	10.37	11.03	14.50	6.91
CaO	7.96	5.60	9.11	6.10	11.20	8.12	11.94
Na2O	1.14	4.03	1.62	1.64	0.62	0.74	1.19
K2O	4.43	2.71	6.14	5.99	7.15	4.70	8.56
P2O5	1.11	0.31	1.07	1.12	1.07	1.13	1.57
LOI	3.91	1.24	3.88	3.54	7.01	4.73	9.83
TOTAL	98.27	98.75	98.02	98.26	98.18	98.02	95.37
S	282	79	106	453	160	902	1727
F	2331	690	2800	3367	3463	2809	4768
Cl	186	208	278	277	232	170	246
Sc	21	10	22	16	19	20	20
V	209	73	154	181	188	206	190
Cr	1015	39	561	818	1436	1075	587
Ni	492	39	195	324	321	535	147
Cu	90	21	43	54	86	91	95
Zn	86	93	94	88	68	84	96
Li	58	21	24	31	14	52	12
Rb	141	65	172	179	237	140	330
Sr	902	1140	1999	1465	1069	1102	2026
Ba	3210	937	4771	3651	3730	3383	4943
Zr	224	122	271	359	158	221	351
Nb	12	11	14	18	10	11	22
Hf	6	3	7	9	4	6	11
Ta	0.7	0.7	0.8	0.9	0.6	0.9	0.3
Th	8.0	7.8	10.9	13.0	5.5	8.1	40.5
U	2.2	2.0	2.7	3.9	1.6	2.2	17.7
Pb	22.3	18.0	48.9	29.4	20.4	18.2	36.0
La	39	35	53	53	27	38	102
Ce	85	66	113	116	59	82	225
Pr	10	7	14	14	7	10	28
Nd	43	29	54	53	30	43	111
Sm	7.9	5.3	9.5	9.3	5.9	8.2	15.8
Eu	2.2	1.6	2.6	3.7	1.6	2.1	5.1
Gd	7.0	4.8	8.6	8.9	5.1	5.3	11.8
Tb	0.7	0.5	0.7	1.0	0.5	0.6	1.2
Dy	3.6	2.6	4.0	3.8	2.8	3.3	4.6
Ho	0.6	0.5	0.6	0.7	0.5	0.6	0.8
Er	1.6	1.3	1.6	1.7	1.3	1.5	1.9
Tm	0.2	0.2	0.2	0.2	0.2	0.2	0.2
Yb	1.2	1.3	1.2	1.7	1.0	1.2	1.6
Lu	0.2	0.2	0.2	0.2	0.2	0.2	0.2
Y	16	13	17	18	13	15	26
Ag	b.d.	b.d.	b.d.	b.d.	b.d.	b.d.	b.d.
Au	b.d.	b.d.	b.d.	b.d.	2	4	5
Ir	b.d.	b.d.	b.d.	11	b.d.	b.d.	12
La/Yb	22	18	29	21	18	21	44
K2O/Na2O	3.87	0.67	3.80	3.64	11.56	6.37	7.17
K/Al	0.48	0.17	0.64	0.59	0.69	0.54	0.78
Peralkalinity	0.67	0.55	0.89	0.84	0.78	0.66	0.94

and Bergman, 1991) to aid in recognizing lamproites, and to distinguish them from other potassic rocks. The Sweet Grass rocks are ultrapotassic (Na_2O/K_2O >3; observed range 2.75-11.56, average 5.61), typical of lamproites, however, they are not perpotassic (K/Al >1; observed range 0.45-0.78, average 0.60) nor are they peralkaline ([Na + K]/Al >1; observed range 0.66-1.00, average 0.80). Abundances of CaO and Al_2O_3 provide further useful major element discriminants. The Sweet Grass rocks (average wt.% CaO = 9.48; Al_2O_3 = 10.37) plot outside of Foley's lamproite field (Fig. 11). Mitchell and Bergman (1991) have suggested a different reference line which encompasses a larger area of $CaO-Al_2O_3$ space for the lamproite field, however, the Sweet Grass rocks still lie outside or at the margin of the lamproite field.

Additional lamproite/minette discrimination can be made on the basis of trace element chemistry. Rare-earth element (REE; normalization values from Nakamura, 1974) concentrations for six Sweet Grass minettes and the Black Coulee diorite are illustrated in Figure 12A, with the diorite having the lowest REE abundances. In Figure 12B, average REE from the Sweet Grass minettes (n = 12) are compared to average olivine minette from the Bearpaw and Highwood mountains, Montana. All Montana alkaline province minettes have similar REE patterns. Lamproites from Prairie Creek, Leucite Hills, and Smoky Butte have higher total REE, as well as steeper LREE-enriched patterns (expressed as La/Yb ratios) as compared to these minettes.

Multi-element spider-diagrams (normalization values from Thompson, 1982) for six Sweet Grass minettes and the Black Coulee diorite are illustrated in Figure 13A. The diorite sample has lower incompatible element concentrations than the minettes. Average incompatible element concentrations for the Sweet Grass minettes (n = 12) are similar to those of olivine minette from the Bearpaw and Highwood mountains,

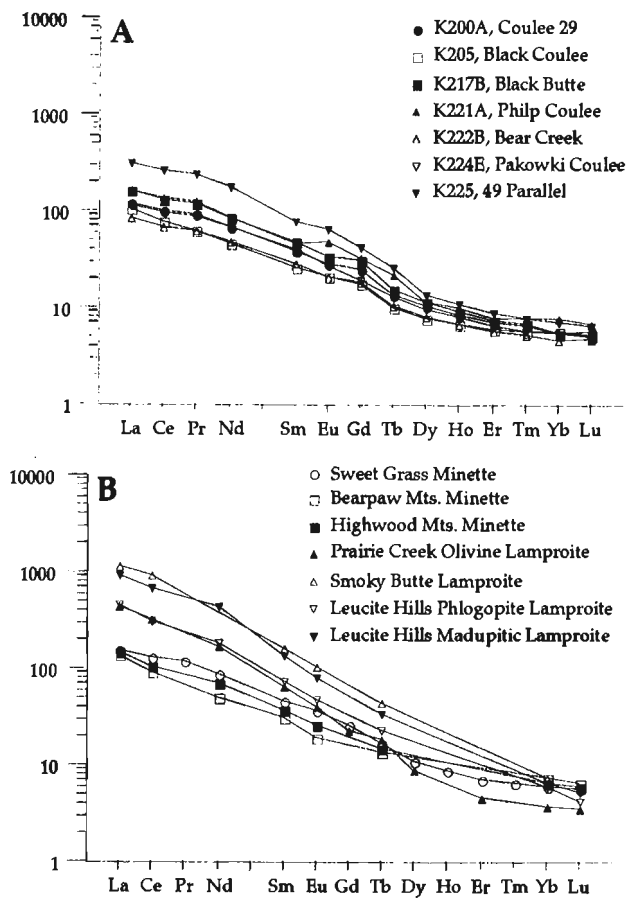

Figure 12. Chondrite normalized REE plots. A) REE for seven representative Sweet Grass samples; B) Comparison of REE in the Sweet Grass minettes with olivine minettes from the Bearpaw (Macdonald et al., 1992) and Highwood mountains (O'Brien et al, 1989), Montana, as well as lamproites from the Leucite Hills, Smoky Butte, and Prairie Creek (all lamproite data from Mitchell and Bergman, 1991).

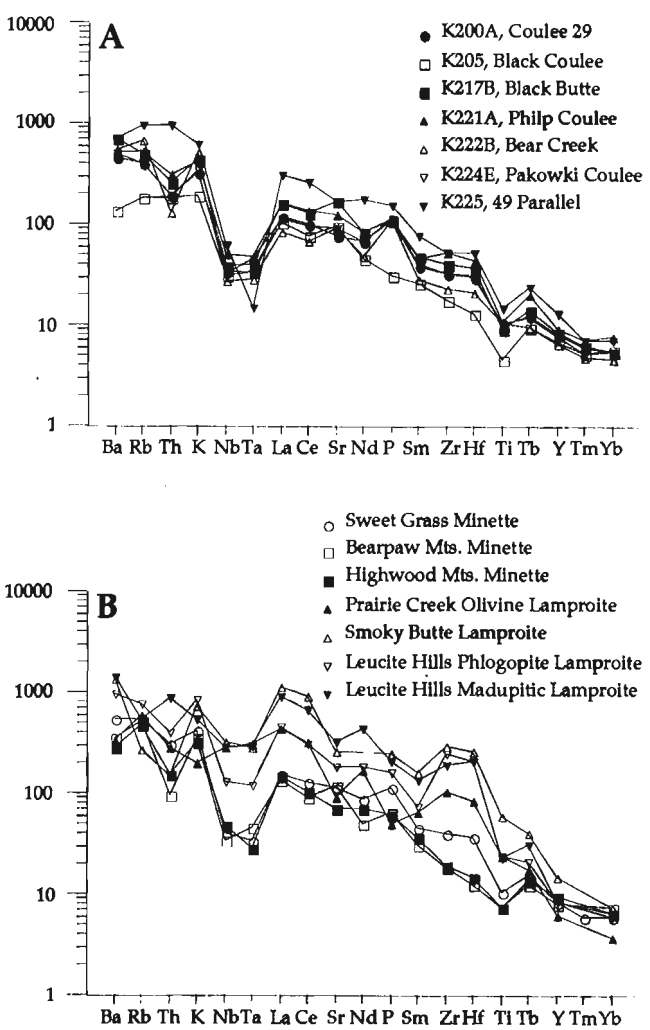

Figure 13. Incompatible element spider-diagrams; A) Incompatible elements for seven representative Sweet Grass samples; B) comparison of incompatible elements in the Sweet Grass minettes with olivine minettes from the Bearpaw and Highwood mountains, Montana, as well as lamproites from the Leucite Hills, Smoky Butte, and Prairie Creek. Data sources as per Figure 11B.

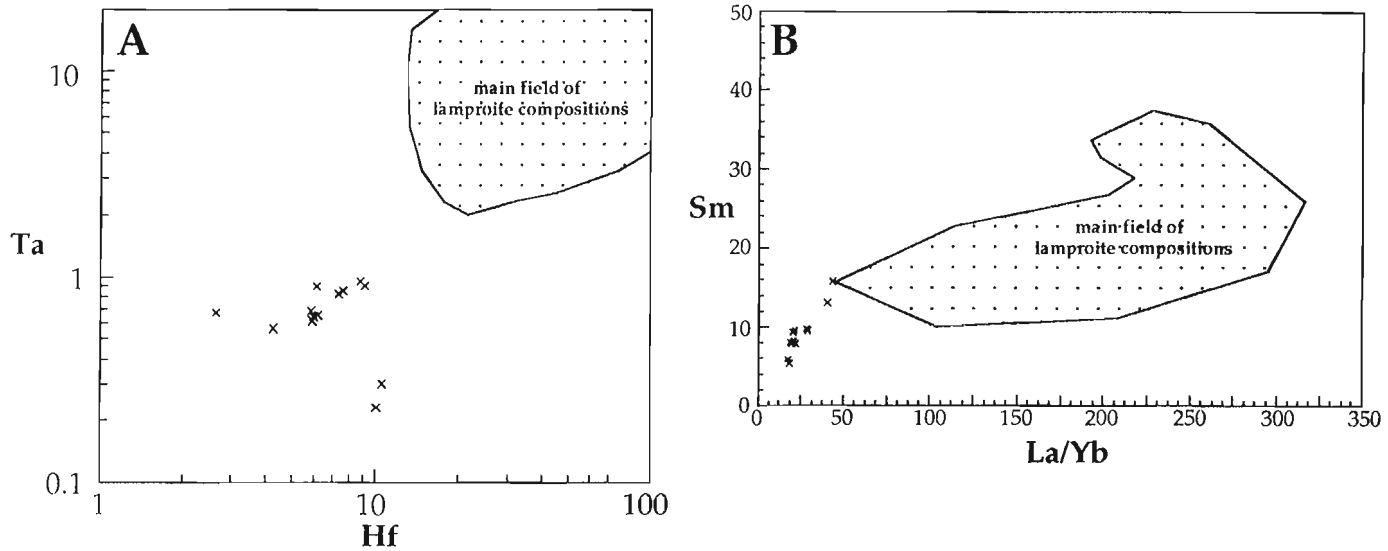

Figure 14. *Minette/lamproite trace element discrimination plots. Main field of lamproite compositions from Mitchell and Bergman (1991); X= all Sweet Grass data.* ***A)*** *Hf versus Ta diagram;* ***B)*** *Sm versus La/Yb. Note that all Sweet Grass data fall outside the main field of lamproite.*

Montana (Fig. 13B), although the Sweet Grass samples have slightly higher HFSE (high field strength elements). In Figure 13B, minette and lamproite samples can be differentiated on the basis of much lower concentrations of Ti, Nb, Ta, Zr, and Hf in the minettes. Furthermore, lamproites usually have higher concentrations of Ba, Rb, Th, K, Sr, P, and Y as compared to minettes, although these elements cannot be considered diagnostic on there own because of overlap (see Fig. 13B) between the two rock types.

DISCUSSION

On the basis of whole-rock major and trace element geochemical parameters, as well as zoning trends in mica phenocrysts, the potassium-rich magmatic rocks in the Milk River area are classified as minette (six eastern localities) and diorite porphyry (westernmost locality). This study illustrates that the field and petrographic studies of previous workers (i.e., Dawson, 1884; Kemp and Billingsley, 1921; Currie, 1976) correctly identified the rocks as minettes. However, these earlier studies did not recognize the extrusive rocks at the Coulee 29 vent complex.

The mineralogical and geochemical criteria for lamproite recognition as summarized by Mitchell and Bergman (1991) provide useful discriminants for separating minettes from lamproites. It is clear that a combined approach is necessary; from a petrographic standpoint alone, classification of a leucite-bearing, olivine-, phlogopite-, and diopside-phyric hypabyssal rock as a lamproite instead of a minette is highly probable. While a combined petrographic, mineral chemistry plus major and trace element geochemical approach to classifying any unknown potassic rocks would be optimum, this could be considered expensive at the grassroots exploration stage. In this respect, petrography plus whole-rock geochemistry (with neutron activation analysis [INAA] for partial trace element analysis) should suffice. Two simple, but exceptionally useful diagrams which can be generated from INAA data are Hf versus Ta (Fig. 13A) and Sm versus La/Yb ratio (Fig. 13B). In both of these diagrams, minette is clearly separated from the lamproite field.

Classification of the Sweet Grass intrusives as minette, and not lamproite or kimberlite indicates the diamond potential of these rocks is probably very low, as no diamonds have been recovered to date from any minette bulk sampled. This is consistent with thermobarometric studies of garnet peridotite xenoliths from minette. The deepest origin mantle xenoliths recovered from a minette (The Thumb, New Mexico; Ehrenburg, 1982) have a restricted range of pressures and temperatures between 35-46 kbar and 1075 - 1325°C. All xenoliths lie outside the diamond stability field in P-T space, suggesting minette magmas are generated at lower pressure and higher temperature conditions than those associated with diamond formation and stability.

Low potential for diamond-bearing minettes, however, does not preclude the occurrence of diamond-bearing lamproite or kimberlite in the Archean Medicine Hat Block. An important aspect of this problem is the potential for destruction of the diamond-bearing mantle root. In the Colorado/ Wyoming region, the mantle root is thought to have been destroyed by shallow subduction related to the Laramide orogeny (Helmstaedt and Gurney, in press). However, in the Eocene Missouri Breaks diatremes (Montana), P-T data from mantle xenoliths are consistent with a cool, conductive geotherm; from this Eggler et al. (1988) suggests the mantle root is intact. While it has been suggested (on the basis of characteristic Ti, Nb, Ta anomalies) that minette volcanism in the Montana alkaline province is subduction related

(e.g., O'Brien et al., 1989), thus supporting the model proposed by Helmstaedt and Gurney (in press), the evidence is equivocal. Eggler et al. (1988) has suggested back-arc related asthenospheric upwelling as the triggering mechanism for the minette volcanism, with the mantle root only being destroyed in the vicinity of the upwelling. Isotopic studies (Cavell and Burwash, 1993; Irving and O'Brien, 1991; Eggler et al., 1988) inidcate that the source region for the minette magmas was enriched in the Mid-Proterozoic. Thus the Ti, Nb, Ta subduction signature of Montana alkaline province potassic rocks could be a result of Mid-Proterozoic subduction related enrichment, i.e. not related to Cretaceous/Eocene subduction. This scenario favours the model of Eggler et al. (1988) and suggests that regions of the Medicine Hat Block in southern Alberta removed from Cretaceous/Eocene magmatism (i.e., north, east, and west of the Sweet Grass Hills) could be considered prospective for diamonds, as the mantle root should still be intact.

Potential for other types of economic deposits exist, as noted by Rock (1991), who has summarized the available data regarding the relationship between gold deposits and calc-alkaline lamprophyres (i.e., minettes). Of interest are the gold deposits at Middle and East Buttes, Sweet Grass Hills, Montana (Gavin, 1991). Results from neutron activation analysis for silver, gold, and iridium (used as an indicator for PGE) in general indicate low abundances (Table 1). Maximum values for 17 samples were 6 ppb Au and 12 ppb Ir, with most samples below detection limits (Au <2 ppb, Ir <5 ppb). Silver was below detection limits (5 ppb) in all samples.

ACKNOWLEDGMENTS

Ron Burwash is thanked for an introductory tour of the Coulee 29 locality. Pauline Orr is thanked for field assistance in 1992. Bill Davis and Gerry Ross assisted with the field work in 1993. Comments by Tony Peterson and critical review by Tony LeCheminant improved the manuscript. Robin J.S. Wyllie assisted in drafting the figures and proof-reading the manuscript.

REFERENCES

Burwash, R.A. and Cavell, P.A.
1992: Xenoliths in ultrapotassic rocks of the Sweetgrass Arch, Alberta: evidence of a Mid-Proterozoic mantle metasomatism; Rocky Mountain Section, Geological Society of America, Program with abstracts, v. 24, no. 6, p. 5.

Cavell, P.A. and Burwash, R.A.
1993: Enriched mantle beneath southern Alberta - isotopic evidence for a northern extension of the Wyoming Block into Canada; Geological Association of Canada/Mineralogical Association of Canada, Program with abstracts, p. A17.

Currie, K.L.
1976: The alkaline rocks of Canada; Geological Survey of Canada, Bulletin 239, 228 p.

Dawson, G.M.
1884: Geological Survey of Canada, Report of Progress 1982-83-84, part C; p. 16-17 and 45-47.

Eggler, D.H., Meen, J.K., Welt, F., Dudas, F.O., Furlong, K.P., McCallum, M.E., and Carlson, R.W.
1988: Tectonomagmatism of the Wyoming Province; Colorado School of Mines Quaterly, v. 83, no. 2, p. 24-40.

Ehrenburg, S.N.
1982: Petrogenesis of garnet lherzolite and megacrystalline nodules from the Thumb, Navajo volcanic field; Journal of Petrology, v. 23, p. 507-547.

Foley, S.F., Venturelli, G., Green, D.H., and Toscani, L.
1987: The ultrapotassic rocks: characteristics, classification and constraints for petrogenetic models; Earth Science Reviews, v. 24, p. 81-134.

Gavin, B.
1991: Precious-metal mineralization in the Sweet Grass Hills, north-central Montana; in Central Montana Alkalic Province Guidebook, (ed.) D.W. Baker and R.B. Berg; Montana Bureau of Mines and Geology, Special Publication No. 100, p. 55-62.

Hearn Jr., B.C., Marvin, R.F., Zartman, R.E., and Naeser, C.W.
1978: Ages of alkalic activity in north-central Montana; United States Geological Survey, Professional Paper No. 1100, p. 60.

Helmstaedt, H.H. and Gurney, J.J.
in press: Geotectonic controls on the formation of diamonds and their kimberlitic and lamproitic host rocks: application to diamond exploration; in Proceedings of the 5th International Kimberlite Conference, (ed.) H.O.A. Meyer and O.H. Leonardos; Companhia de pesquisa de Recurso Minerais, Brasilia.

Irving, A.J. and O'Brien, H.E.
1991: Isotopic and trace element characteristics of Late Cretaceous to Oligocene mafic volcanics from west-central Montana: implications for Tertiary tectonics and magma genesis; in Central Montana Alkalic Province Guidebook, (ed.) D.W. Baker and R.B. Berg; Montana Bureau of Mines and Geology, Special Publication No. 100, p. 140-142.

Kemp, J.F. and Billingsley, P.
1921: Sweet Grass Hills, Montana; Bulletin of the Geological Society of America, v. 32, p. 437-478.

Macdonald, R., Upton, B.G.J., Collerson, K.D., Hearn B.C. Jr., and James, D.
1992: Potassic mafic lavas of the Bearpaw Mountains, Montana: mineralogy, chemistry, and origin; Journal of Petrology, v. 33, p. 305-346.

Mitchell, R.H.
1986: Kimberlites; Plenum Press, New York, 442 p.

Mitchell, R.H. and Bergman, S.C.
1991: Petrology of Lamproites; Plenum Press, New York, 447 p.

Nakamura, N.
1974: Determination of REE, Ba, Mg, Na and K in carbonaceous and ordinary chondrites; Geochimica et Cosmochimica Acta, v. 38, p. 757-775.

O'Brien, H.E., Irving A.J., and MacCallum, I.S.
1989: Eocene potassic magmatism in the Highwod mountains, Montana: petrology, geochemistry, and tectonic implications; Journal of Geophysical Research, v. 96, p. 13 237-13 260.

Rock, N.M.S.
1991: Lamprophyres; Blackie & Son Ltd., Glasgow; 285 p.

Ross, G.M., Parrish, R.R., Villeneuve, M.E., and Bowring, S.A.
1991: Geophysics and geochronology of the crystalline basement of the Alberta basin, western Canada; Canadian Journal of Earth Sciences, v. 28, p. 512-522.

Russel, L.S. and Landes, R.W.
1940: Geology of the southern Alberta Plains; Geological Survey of Canada, Memoir 221, 223 p.

Thompson, R.N.
1982: Magmatism of the British Tertiary province; Scottish Journal of Geology, v. 18, p. 49-107.

Weed, W.H. and Pirsson, L.V.
1895: On the igneous rocks of the Sweet Grass Hills, Montana; American Journal of Science - Third Series, v. L, no. 298, p. 309-313.

Williams, M.Y. and Dyer, W.S.
1930: Geology of Southern Alberta and Southwestern Saskatchewan; Geological Survey of Canada, Memoir 163, 160 p.

Geological Survey of Canada Project 870008

Prairie NATMAP field work and field database structure[1]

R.J. Fulton, L.H. Thorleifson, G. Matile[2], and A. Blais
Terrain Sciences Division

Fulton, R.J., Thorleifson, L.H., Matile, G., and Blais, A., 1994: Prairie NATMAP field work and field database structure; in Current Research 1994-B; Geological Survey of Canada, p. 69-72.

Abstract : In this second year of the Prairie NATMAP project, field work was conducted in southeastern and southwestern Manitoba.

In the Virden area of southwestern Manitoba, field work has been completed to the stage where preliminary maps can be produced for 5 of the 16, 1:50 000 map sheets. The part of the area reported on this year is largely underlain by till, although glaciofluvial sediments suitable for aggregate are found in some of the numerous meltwater channels. The shale bedrock is not a significant surficial material but is responsible for a large number of slope failures where it has been intersected by the valley of Pipestone Creek.

In southeastern Manitoba, mapping field work in the eastern half of the area was completed. Crews led by both provincial and federal government staff addressed the distribution of sediments related to the action of Lake Agassiz, the limit of calcareous drift, and striation patterns.

Résumé : Au cours de cette deuxième année du projet sur les Prairies du CARTNAT, on a réalisé des travaux de prospection dans le sud-est et le sud-ouest du Manitoba.

Dans la région de Virden dans le sud-ouest du Manitoba, on a réalisé des travaux de prospection jusqu'au stade d'établissement de cartes préliminaires pour 5 des 16 coupures de cartes au 1/50 000. Dans la portion du secteur sur laquelle porte l'étude de cette année, le sous-sol se compose largement de till, mais l'on trouve aussi dans quelques-uns des nombreux chenaux d'eaux de fonte des sédiments fluvioglaciaires pouvant servir de granulat. Le substratum shaleux ne constitue pas un matériau superficiel important, mais il est à l'origine d'un grand nombre de glissements de terrain aux endroits où il est recoupé par la vallée du ruisseau Pipestone.

Dans le sud-est du Manitoba, on a complété les levés de terrain de la moitié est du secteur. Des équipes dirigées par le personnel des gouvernements provinciaux et fédéral ont examiné la distribution des sédiments associés à l'action du Lac Agassiz, la limite des sédiments glaciaires calcareux et la configuration des stries glaciaires.

[1] Contribution to the Prairie NATMAP project

[2] Geological Services Branch, Manitoba Department of Energy and Mines, 555-330 Graham Ave., Winnipeg, Manitoba R3C 4E3

INTRODUCTION

Objective of project

The objectives of the surficial/Quaternary studies on the Canadian Prairies (NATMAP) are to map, describe, and explain the surficial materials in the Virden map area (62F) and in southeastern Manitoba (52E west half and 62H east half), and to develop GIS and computer database handling techniques for storing, manipulating, and displaying surface and subsurface, surficial geology information. Mapping is being undertaken at a scale of 1:100 000.

Surficial geology information is required for many different activities in the Prairies and has many different users. In Canada's southern Prairie provinces, concerns have been expressed about such things as development and protection of groundwater resources, exploration for and extraction of petroleum and natural gas, waste disposal, soil fertility and degradation, engineering developments, and identification of natural and anthropogenic health hazards. Societal pressure is increasing across the Prairies to resolve these and other environmental issues in a manner that allows continued development and use of the resources while at the same time protecting the environment. A comprehensive understanding of the surficial geology of the Prairies is an essential component of the knowledge base upon which decisions about these issues will be made.

Areas being covered

The Virden map area (62F) lies on the Manitoba-Saskatchewan border (Fig. 1). It consists largely of flat to gently rolling terrain typical of the Interior Plains area of Canada with an area of hummocky terrain, Turtle Mountain, in the southeast corner of the map area. Agriculture is the dominant industry but the area includes significant oil and gas fields. In addition to many hamlets, villages, and towns, it includes the western outskirts of Brandon, the second largest city in Manitoba.

The southeastern Manitoba area (52E west half and 62H east half) reaches from Winnipeg to just east of the Ontario-Manitoba border (Fig. 1). It includes the eastern part of the flat glacial Lake Agassiz Plain, the rolling Sandilands area and a stretch of rocky Precambrian terrain along the Ontario-Manitoba border. The western part of the area supports intensive agriculture, the Sandilands area – largely forest reserve – is an important aquifer recharge area, and the eastern part of the area – mainly rock, bog, and lakes – is important as recreation land and for its mineral potential. The area includes the southeastern suburbs of Winnipeg, the thriving town of Steinbach, and many small towns and hamlets.

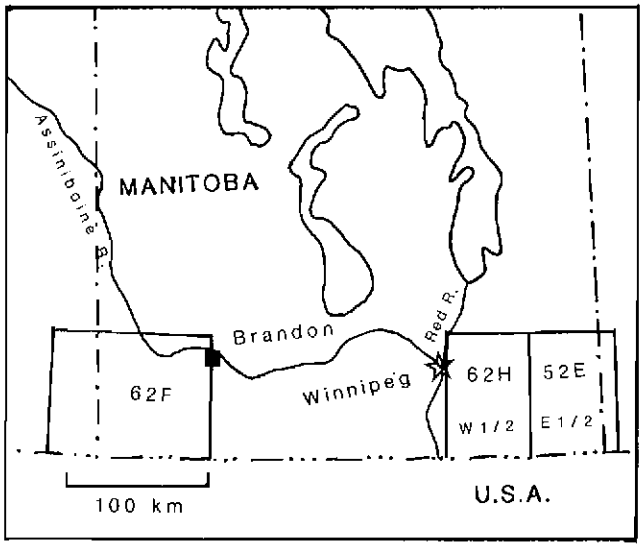

Figure 1. *Location of the two areas included in the Prairie NATMAP project.*

Purpose of field work

In response to the surficial data requirements of land uses such as agriculture, activities such as project engineering and aggregate extraction, and to providing data pertinent to subsurface topics such as hydrogeology and mineral exploration, the following objectives are being pursued: 1) production of surficial materials maps, 2) collection of samples to characterize surficial materials, 3) gathering of information pertinent to the Quaternary geological history of the areas, and 4) development and standardization of data collection techniques and protocols with emphasis on improving data collection, manipulation, and storage through use of computers.

SURFICIAL GEOLOGY DATABASE

A database structure has been developed for surficial geology information. This consists of a series of files which are linked in a relational database by a *station number* which is common to all files. The most important of the files is the **HEADER** file which contains the station number, site location, and general site information, and a record of the other data files which are available for that site. Other files are: **STRATLOG** – contains descriptive information pertaining to the surface material or a single stratigraphic unit and provides an entrance to other data files related to this unit (FLOWLOG, SAMPLOG, PEBCOUNT, PHOTOLOG); **FLOWLOG** – records ice flow direction measurements; **SAMPLOG** – contains information on samples which have been collected at the stations, and provides an entrance to analyses which have been run; **PEBCOUNT** – contains pebble count information; **PHOTOLOG** – contains information on photographs taken at the site; **ILLUSLOG** – contains digital copies of illustrations other than photographs; **COMMENTS** – contains additional information and comments which were not included in the other data files.

The surficial geology database files are stored in dBASE structure and the data is captured through an application referred to as TERACOMP. For data capture, TERACOMP uses *Toolbook*, a *Windows* program from *Asymetrix*, which constructs object linked applications. There are a number of advantages to using *ToolBook* rather than an application

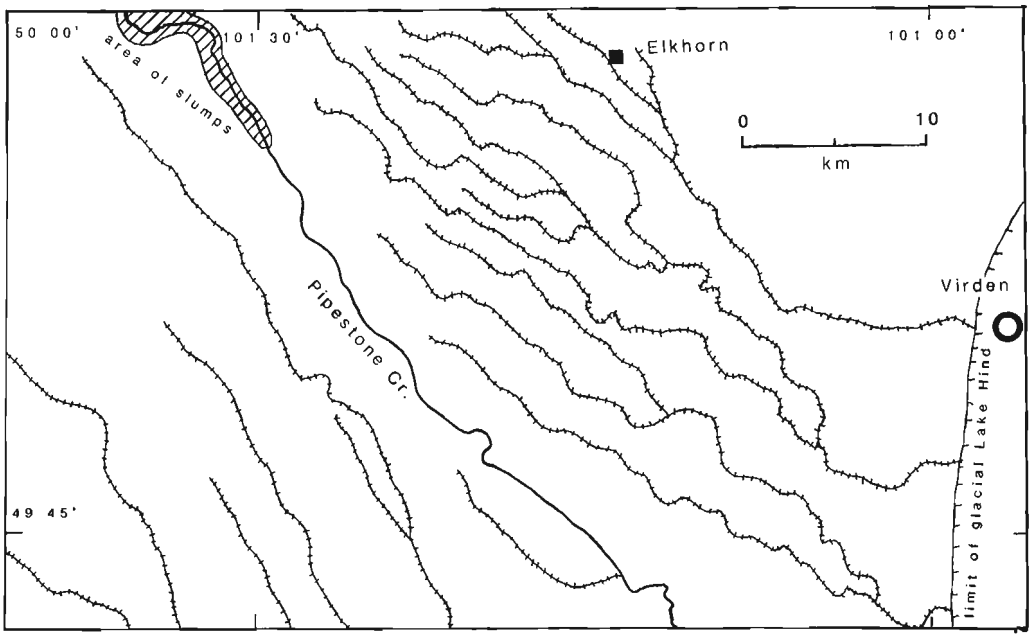

Figure 2. Subparallel meltwater channels west of Virden and area where slope failures have occurred in the Pipestone River valley.

developed within a specific relational database. First, *Toolbook* provides a common data capture platform so even though the user might manipulate the data in a specific relational database, the information will be available in a standard format for archiving in the Terrain Sciences divisional database and for manipulation by applications developed for the divisional database. Second, *Toolbook* applications run on *Windows* software and take less than a meg of disk space. Hence, it is not necessary to purchase expensive software or field computers with large hard disks. Third, from the scientists' point of view, most databases' software can import dBASE files so that the user can continue to use his favourite relational database to manipulate the data. Finally, because the *Toolbook* application and the software for plotting the data, were developed and are supported by Terrain Sciences Division personnel, the scientist is relieved of the burden of developing and supporting personal applications on his own database software.

COMMENTS ON THE FIELD DATA COLLECTION SYSTEM

The data form generated by the TERACOMP system worked well. The data form included most information collected during surficial mapping projects, and in addition provided ample space for free-form entry. Acceptance of the *Toolbook* application for data input was not universal. Even though the program was simple to use and robust it required some diligent practice before data could comfortably be entered into the system. In addition, a few minor bugs and quirks were found. In general however, revisions based on this summer's experience will provide an excellent system for input of field data.

Attempts to input data on the outcrop were less than satisfactory. The notebook computers are too cumbersome and difficult to manipulate for convenient use on site. There was considerable concern that the computers would not survive the rough handling, dust, and moisture endemic in field situations. Finally, there was a major problem reading the computer screen in full daylight. Data entry in the field vehicle bypassed some of the difficulties and concerns, but there too the logistics of working on the computer were trying, and lighting often made it difficult to read the screen. Data input on the outcrop is not feasible with the present system. It will only be workable with a data input system requiring an absolute minimum of keyboard or mouse input, on a moisture- and dust-proof computer which can be easily held in one hand.

VIRDEN FIELD WORK

The Virden area is generally flat with local relief of less than 5 m. Turtle Mountain in the southeast corner of the area stands almost 200 m above the level of the surrounding plains and the Assiniboine River, set in a valley up to 60 m deep, crosses the northeast corner of the area.

Three parties were active in the field in the Virden area. They were led by: S. Sun, Ph.D. candidate, University of Manitoba (3 months), R.J. Fulton (1 month), A. Blais (3 weeks). The field work conducted to date has consisted of checking of airphoto interpretation, collection of samples for materials characterization, and examination of stratigraphic sections. Data has been collected from more than 1000 points and 250 sample have been taken. Sufficient data are now on hand to complete preliminary maps of 5 of the 16 1:50 000 map sheets.

General information on the nature of the area, bedrock geology, and late glacial history, with emphasis on the northeast quarter of the map sheet, were given in last year's Current Research report (Sun, 1993). This year's report concentrates on 1:50 000 sheets 62F/13 and 14 in the northwest corner of the area.

These areas are dominantly till with very minor areas of glaciofluvial deposits and Holocene alluvium. Bedrock does not occur at the surface. Over most of the area the Cretaceous shale is covered by at least 10 m of drift (Betcher, 1983) except for the area east and north of Elkhorn where shale is encountered in dugouts (generally <5 m deep). A 12 km segment of the valley of Pipestone Creek at the northern edge of the map sheet has cut into the shale; the valley walls have failed and both slopes consist of flights of rotated slump blocks (Fig. 2).

Most till areas consist of gently undulating ground moraine plain but significant parts of the area are underlain by relatively closely spaced, broad till ridges with relief <10 m. These are an extension of the corrugated moraine area mapped by Klassen (1979) in the Riding Mountain map area to the north. Exposures generally are unavailable so it is difficult to obtain a clear picture of the structure and stratigraphy of surficial materials. The diamicton (till) generally has a silty matrix, contains little pebble sized material – but includes a variable number of boulders – and is grey to olive brown. Pebble composition ranges from 40-80% carbonates, 5-65% shale, 5-25% dark, fine grained metamorphic rock, 1-15% granitic rock, 2-10% quartzite, 0-5% sandstone, and 0-3% ironstone concretions with no apparent regional trend. In some of the places where till exposures were present, an approximately 1 m thick, relatively massive diamicton layer was underlain by diamicton containing lenses and boulders of sand and gravel or by stratified sediment with interbedded diamicton. Diamictons in the two units generally were similar in appearance but at some locations, diamictons in the lower unit were somewhat more sandy. In plain areas the stratified lenses were subhorizontal but where exposed in ridges, the lenses were moderately steeply dipping (10-45°). In several places boulder concentrations coincided with the base of the massive till. These might be poorly developed examples of the striated boulder pavements described by Elson (1956).

One of the more intriguing features of map area 62F/14 is the large number of subparallel meltwater channels (Fig. 2). Although in many areas the channel floors are underlain by a thin gravel and boulder lag, they locally contain low terraces which provide one of the few sources of aggregate in the area. In general the channels trend from northwest to southeast at roughly 45° to the north-south regional slope but swing to the east as they approach the former basin of glacial Lake Hind near the eastern edge of the map sheet. Channels are spaced at intervals of from 2 to 5 km and vary in depth from 2 to 25 m. The fact that these trend across rather than down the regional slope and have relatively normal down-valley gradients suggests that they are ice marginal in origin. However, a number of features, such as their uniform spacing, the local presence of ice contact gravel under till at the margins of valleys, and occurrence of kettles in deltaic deposits at the mouths of channels suggest they might have a subglacial origin. Determining the origin of these valleys has important glacial history implications. If they are ice marginal, they indicate the ice front retreated in a northeastward direction but if they are of subglacial origin, they would suggest northwestward ice retreat.

SOUTHEAST MANITOBA FIELD WORK

During the 1993 field season, two field parties were coordinated by G. Matile of Manitoba Geological Services Branch and H. Thorleifson of the GSC. The intent of this summer's work was to finalize mapping in the eastern half of the area. The work took into account previous field activities in the area by the former Manitoba Aggregate Resources Branch and the Geological Survey of Canada. All data collection followed the standardized format developed for surficial components of the NATMAP projects and data were entered and edited in a PC-based database.

Several topics were addressed, including the nature of thin surface sediments associated with the action of Lake Agassiz, the pattern of striations developed by southeastward ice flow associated with ice derived from the Red River valley and southwestward ice flow derived from the shield, and the eastern limit of carbonate-rich drift. From near surface observations along major roads, it was determined that the eastern limit of carbonate-rich drift was 20 km east of Whitemouth along Highway 44 and 4 km west of Falcon Lake along the Trans-Canada Highway. Although observations were shallow, drift thickness was seen to decrease dramatically to the east of the limit of carbonate-rich drift.

Road accessible bedrock outcrops were searched for glacial striae. A total of 35 outcrops were found to have measurable striae, including four sites that had crossing striae. Striations formed by shield derived ice were found on both sides of the eastern limit of carbonate-rich drift and trended approximately perpendicular to it (~235°). Striations formed by ice derived from the Red River valley were found on the west side of the eastern limit of carbonate-rich drift and ran approximately parallel to it (~130°). The age relationship between the two sets of striae, at the four sites which were found to have crossing striae, was not discernible.

REFERENCES

Betcher, R.N.
1983: Groundwater availability map series, Virden area (62F); Manitoba Natural Resources, Water Resources, scale 1:250 000.

Elson, J.A.
1956: Surficial geology of the Tiger Hills region, Manitoba, Canada; Ph.D. Thesis, Yale University, 316 p.

Klassen, R.W.
1979: Pleistocene geology and geomorphology of the Riding Mountain and Duck Mountain areas, Manitoba-Saskatchewan; Geological Survey of Canada, Memoir 396, 52 p.

Sun, S.
1993: Preliminary study of the surficial geology of Virden area, southwestern Manitoba; in Current Research, Part B; Geological Survey of Canada, Paper 93-1B, p. 57-61.

Geological Survey of Canada Project 910024

The distribution of cadmium in A horizon soils in the prairies of Canada and adjoining United States

Robert G. Garrett
Mineral Resources Division

Garrett, R.G., 1994: The distribution of cadmium in A horizon soils in the prairies of Canada and adjoining United States; in Current Research 1994-B; Geological Survey of Canada, p. 73-82.

Abstract: Data for Cd determined in the < 2 mm fraction of 1273 A_p horizon soils collected in 1992 across 850 000 km^2 of the Canadian Prairies and immediately adjoining United States are presented. Sampling was undertaken using a 7-level stratified random sampling design whose largest stratum was 80x80 km and included a level for the estimation of analytical variability. Cadmium was determined by flame AAS after dissolution of a 1 g sample with a HF-$HClO_4$-HNO_3 acid mixture, the detection limit was 0.2 ppm. The data range is < 0.2-3.8 ppm Cd, with an arithmetic mean of 0.28 ppm and a median of 0.3 ppm. An Analysis of Variance indicates that > 96% of the variability is at scales ≤ 20x20 km. However, there is a small (4%) but significant component of regional variation between the 80x80 km cell means, the range of which is < 0.2-0.73 ppm. It is concluded that the soils cannot be treated as a spatially homogeneous unit and that geological factors are influencing their composition.

Résumé : On présente dans cet article les données relatives au cadmium, déterminées pour la fraction granulométrique < 2 mm de 1 273 sols de l'horizon A_p recueillis en 1992 sur 850 000 km des Prairies du Canada et du territoire avoisinant des États-Unis. On a entrepris l'échantillonnage en mode aléatoire stratifié à sept niveaux, la strate la plus grande ayant pour dimensions 80 x 80 km et comportant un niveau pour l'estimation de la variabilité analytique. On a dosé le cadmium par spectrométrie d'absorption atomique par la flamme, après dissolution d'un échantillon de 1 g dans un mélange d'acides HF-$HClO_4$-HNO_3; la limite de détection était de 0,2 ppm. L'intervalle des données est < 0,2-3,8 ppm de Cd, avec une moyenne arithmétique de 0,28 ppm et une valeur médiane de 0,3 ppm. Une analyse de variance indique que > 96 % de la variabilité existe à des échelles de ≤ 20 x 20 km. Il y a toutefois une composante faible (4 %) mais significative de variation régionale entre la moyenne des cellules de 80 x 80 km où la gamme de concentrations est < 0,2-0,73 ppm. On en conclut que l'on ne peut traiter les sols comme une unité spatialement homogène et que des facteurs géologiques influencent leur composition.

INTRODUCTION

The recognition of kimberlites in central Saskatchewan in 1988, and therefore the potential for diamond, led to a significant increase in mineral exploration in southern Saskatchewan. This activity soon spread to Alberta and Manitoba, and the Canadian Prairies became a target for diamond exploration.

The region is predominantly covered by glacial deposits, mainly tills, glaciolacustrine deposits, and moraine complexes, etc.; a few small areas remained unglaciated. Heavy mineral, and to a lesser extent geochemical, surveys form a major part of the exploration activity. There was a notable lack of systematic data on the mineralogical and geochemical composition of prairie surficial materials in the public domain. This was particularly true for the glacial tills sampled in diamond exploration projects. The availability of systematic data would assist explorationists in recognizing mineralogically and geochemically abnormal areas within the prairies, and thus help direct exploration to the areas of highest potential.

In 1990 a project was proposed (R.G. Garrett and L.H. Thorleifson) for funding under the Saskatchewan-Canada (1991-95) Mineral Development Agreement (MDA) whose objective was to generate systematic mineralogical and geochemical data for prairie tills in Saskatchewan. This project was accepted and an orientation survey undertaken in 1991 (Garrett and Thorleifson, 1993). In the spring of 1992 a proposal for a similar survey in Alberta was submitted, and accepted, for funding under the Alberta-Canada (1992-95) Mineral Development Agreement. At about the same time Manitoba Energy and Mines offered to support a prairie-wide survey by undertaking sampling within the province of Manitoba to the survey specifications. The Geological Survey of Canada would provide the funds to process and analyze the Manitoba samples.

In the Saskatchewan, and subsequently the Alberta (in modified form), MDA project proposal documents the following section was included:

"Subsidiary Benefit of Regional Reconnaissance Survey:

> Governments and society are becoming more concerned with the environment in which we live and such problems as global change. The regional reconnaissance soil geochemical survey data would offer a "snapshot" of the environmental geochemistry of southern Saskatchewan in 1992 that would be a baseline against which future change could be measured. The geochemical survey would also provide data of interest to a wide range of agricultural and health scientists as it would define any major areas of elemental concentration or depletion. These in turn may have implications to crop productivity, animal husbandry or human health."

This report is a contribution to such environmental geochemical objectives, and describes the procedures followed and the results obtained for Cd in surface soils collected in the subsidiary soil survey noted above.

SAMPLING STRATEGY

Low density soil geochemical surveys based on 100x100 km grids had been used by the United States Geological Survey (USGS) to estimate geochemical baseline levels as early as the mid 1970s as a part of their "Geochemical Survey of the Western Energy Regions" project. The studies by Tidball and Severson (1976), and Severson and Tidball (1979) are particularly relevant, as is a study by Severson and Wilson (1990) undertaken in support of the Garrison Diversion Unit Reformulation Act (1986).

These USGS surveys were a radical departure from traditional mineral exploration soil surveys where sampling criteria are based on the necessity to detect the geochemical reflection of a small target, the anomalous (natural pollution) dispersion train from a mineral occurrence. Such mineral exploration surveys are characterized by high sample densities, often in the order of tens or hundreds of sites per square kilometre. In contrast, the objective of geochemical baseline surveys is to estimate the statistical parameters of the geochemical distribution, e.g., mean and variance, and determine if there are significant spatial variations. This is usually accomplished with a formal sampling design that permits the use of Analysis of Variance (ANOVA) procedures. Such surveys commonly employ low sampling densities of the order of 1 site per tens or hundreds of square kilometres. These contrasting sampling approaches and their design considerations have been discussed by Garrett (1983).

SAMPLING DESIGN

An unbalanced staggered stratified random sampling design that would permit the use of ANOVA procedures was employed in this study. On the basis of the 1991 orientation survey data and results reported by Severson and Tidball (1979) an 80x80 km cell was selected as the topmost stratification unit. Nested strata at 40x40 km, 20x20 km, and 10x10 km levels were also defined for sampling with randomly selected 1x1 km target cells (Fig. 1). Although all the 40x40 km cells are sampled a finite population correction is not required in the ANOVA as the sampling grid is laid over the study area in an effectively kinematically random manner (Garrett and Goss, 1978). Together with replication at smaller spatial scales this leads to an 80x80 km cell containing 12 geochemical samples for analysis. From the previous work it was expected that this number of randomly collected individuals within an 80x80 km cell would be sufficient so that, for the majority of elements, the regional geochemical variation patterns could be mapped.

The objective of the sampling design was to quantify the spatial and analytical variability at 7 levels (factors), i.e.:

between 80x80 km cells,
between 40x40 km cells in 80x80 km cells,
between 20x20 km cells in 40x40 km cells,
between 10x10 km cells in 20x20 km cells,
between 1x1 km cells in 10x10 km cells,
between samples <50 m apart at a 1x1 km site, and
between sample preparation and analysis duplicates.

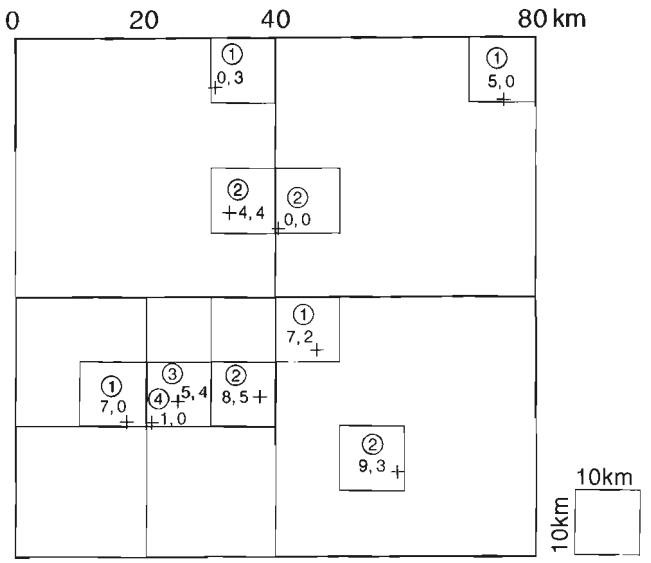

Figure 1. Survey unbalanced staggered stratified random sampling design; crosses and coordinates indicate random coordinates of 1x1 km target cells.

The ANOVA permits the partitioning of the data variability between these factors and permits a test at the topmost level as to whether the 80x80 km cells means are statistically different. If such is the case, at the least the lowest and highest cell means would be different at the stated significance level, and the preparation of a map demonstrating the regional variation patterns should be considered. Determining the cause of any significant differences in means would be the object of a subsequent interpretation exercise. Candidates for causative factors would include the variations in chemistry of the underlying soil parent material, regional differences in pedological processes, geological point sources of natural pollution, e.g., mineral occurrences, or possibly local anthropogenic causes.

FIELD PROCEDURES

All sample sites were randomly selected as 1x1 km target cells before the commencement of fieldwork within the framework of the overall design structure (Fig. 1). Alternate 1x1 km cell selection rules were prepared for use if the pre-selected target cell could not be occupied in the field. For example, a few cells fell in lakes and restricted access areas; but the preselected target cell could be occupied and soil samples collected in the majority of cases.

The sampling grid was located using the 10 km UTM grid printed on all Canadian and U.S. 1:250 000 scale topographic maps. The 80x80 km cells stepped out both westwards and eastwards from the central meridian of each of the 5 UTM zones (11-15 inclusively) that the survey fell within. The origin of the southernmost 80x80 km cells was 5 340 000 m north. This procedure led to some partially populated 80x80 km cells at the UTM zone boundaries, however, the logistical convenience of this procedure was considered to outweigh this disadvantage.

The limits of the soil survey were defined by the edge of contiguous ranch or farm land on the west, north, and east, and UTM northing 5 340 000 m some 80-90 km south of the Canada-U.S.A. border along the 49th parallel. Therefore, the survey area includes that part of North America known as the Canadian Prairies and part of the area in the United States known as the prairies and great plains. The survey area lies within the provinces of Alberta, Saskatchewan, and Manitoba (735 000 km^2) and in the states of Montana, North Dakota, and Minnesota (115 000 km^2) and totals 850 000 km^2.

The field sampling was undertaken between late May and early October, 1992, by contract staff from the Alberta Research Council (2 teams), the Saskatchewan Research Council (1 team), and Manitoba Energy and Mines (3 teams). Additional sampling in Manitoba, Alberta, and the U.S.A. was undertaken by the Geological Survey of Canada (2 teams). In the core three months, June to August, 90% of the sampling was completed. Only soils were sampled in the U.S.A. in co-operation with the United States Geological Survey in order that a data overlap existed that would facilitate the merging Canadian and U.S. soil data sets and the preparation of cross-border maps.

Two 2 kg soil samples were collected at each of 1273 field sites across the area outlined in Figure 2. The surface samples were collected by spade from the organic rich and stained portion of the pedon, usually the uppermost 20 cm and essentially the A_p horizon. Where the land was not ploughed, the organic rich and stained portion of the pedon, usually $\leq$ 20 cm, was collected and homogenized in the plastic sample bag. A C horizon sample was collected using a Dutch auger from between, on average, 40 to 65 cm below surface, but below any obvious organic staining or Fe/Mn hydroxide mottling.

Field data were recorded at each site, and the actual sampling site plotted on 1:250 000 topographic maps for later digitizing or manual UTM coordinate recovery. The field data provide information on the general sampling environment and observations on the colour, texture, moisture content, and mineralogy of the soil.

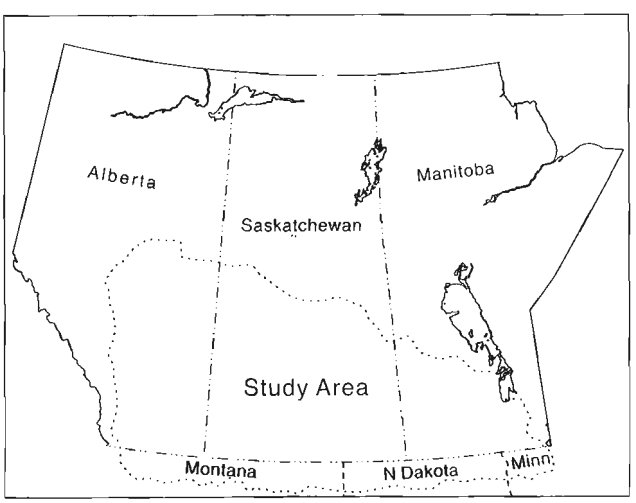

Figure 2. Location of survey area.

Samplers were instructed to select uninundated sites without preference for parent material or topographic position within the 1x1 km target cells. Sites were not to be selected in atypical minor stream valleys or peatland. However, if the entire target cell lay within a major river floodplain, that floodplain soil was to be sampled. The objective was to collect an unbiased statistical sample of the surface and C horizon soils in the study area. This would lead to a data subset, and subsequent statistics, weighted by the spatial frequency of the various soil environments across the study area, and so provide a valid basis for geochemical baseline level estimation.

SAMPLE PREPARATION, ANALYSIS AND QUALITY ASSURANCE

The soil samples were air dried at < 40°C and, following gentle disaggregation avoiding the crushing of rock and mineral grains, were screened using a 2 mm stainless steel sieve. The oversize was discarded and approximately 50 g of the retained fines was ground in an agate pestle and mortar to approximately < 100 μm and stored for analysis.

Prior to analysis, the samples, including 116 sample preparation duplicates, i.e., second cuts of 50 g of the < 2 mm fraction reduced to < 100 μm, 50 aliquots of a GSC internal prairie surface soil control sample, and 6 aliquots of the CANMET/Agriculture Canada international reference material SO-4, were randomized. The purpose of the randomization was to destroy any relationship between the order of analysis and the spatial location of the samples.

A 1 g aliquot of the < 100 μm sample was decomposed with a fuming $HF\text{-}HClO_4\text{-}HNO_3$ mixture to near dryness on a hot plate. The residue was taken into solution with concentrated HCl and, following dilution to a 1 M concentration, Cd was determined by flame atomic absorption spectrophotometry. The detection limit of the procedure was 0.2 ppm in the solid sample.

The insertion of both international and internal GSC standard reference materials and sample preparation and analysis duplicates permits the accuracy and the precision of the Cd analyses to be estimated. For the estimation of accuracy a recommended Cd working value for SO-4 of 0.34 ppm was employed (Govindaraju, 1989). The average of the six SO-4 determinations in this study is 0.37 ppm, representing an accuracy of +8%. The relative standard deviation (RSD) of the six determinations is 22.3%. In contrast, the RSDs for the 50 replicate analyses of the GSC internal control reference sample, and the 116 sample preparation and analysis duplicates are higher, 38% and 40% respectively.

An accuracy of +8% at 0.34 ppm Cd is satisfactory, especially when the proximity to the detection limit of 0.2 ppm is considered. Likewise, the RSDs of 38% and 40% are acceptable when the average levels of 0.29 ppm and 0.28 ppm respectively are viewed relative to the detection limit.

STATISTICAL DISTRIBUTION OF THE DATA

The data set used to compile the summary statistics (Table 1) is that for the 1273 field samples, i.e., not including the 116 sample preparation and analysis duplicates. Data values

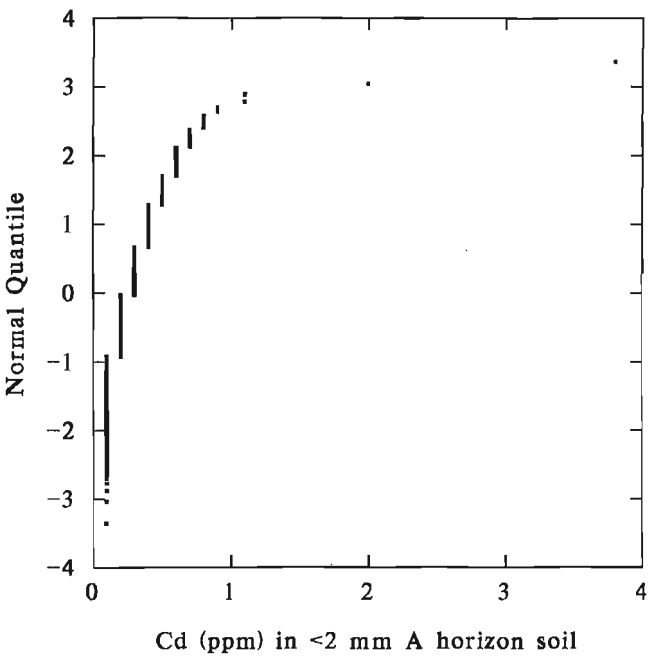

Figure 3. Normal quantile (probability) plot for field data set, N = 1273.

Table 1. Empirical percentiles and summary statistics for Cd (ppm).

Empirical Percentiles									
Minimum	5	10	25	50	75	90	95	99	Maximum
<0.2	<0.2	<0.2	0.2	0.3	0.4	0.5	0.5	0.7	3.8
Arithmetic Mean		Standard Deviation			Coefficient of Variation, %				Sample Size
0.28		0.1788			63.7				1273

below the detection limit of 0.2 ppm were arbitrarily set to a value of 0.1 ppm Cd. The arithmetic mean and the median of the data set are 0.28 and 0.3 ppm Cd respectively. The normal quantile (probability) plot for the data is presented in Figure 3. The data are positively skewed with two extreme values at 2.0 and 3.8 ppm Cd. Removal of these two outliers still leaves the distribution positively skewed (Fig. 4). Due to the presence of the outliers, the median, 0.3 ppm Cd, is preferred as a robust estimate of the average background level of Cd in prairie surface soils. The geological significance of the empirical frequency distribution and the outliers is discussed below.

SPATIAL ANALYSIS OF VARIANCE

Due to the mild positive skew of the data, the fact that 99% of the data span less than one order of magnitude, and the relative robustness of ANOVA to non-normality it was considered unnecessary to apply any transformations to the data prior to the analysis. For this procedure the 116 sample preparation and analysis duplicates were included for a total data set size of 1389. The computational procedures and software employed for the unbalanced ANOVA may be found in Garrett and Goss (1978, 1980), the results are presented in Table 2. In the Table, "80km Cells" refers to 80x80 km grid cells, etc., "10km Sites" refers to the variability between samples collected from 1x1 km cells within a 10x10 km cell. "Smpls at 3" and "Anals at 2" refer, respectively, to samples collected < 50 m apart in a single 1x1 km cell, and the duplicate sample preparations and analyses.

The ANOVA indicates (> 99.9% confidence level) that some 96% of the total variability is at scales ≤ 20x20 km. It should also be noted that 37% of the variability is due to subsampling and analytical variability, reflecting the RSDs obtained in the quality assurance procedures. From this, it is inferred that most of the variation in Cd is due to local (≤ 20 km) changes in soil chemistry, reflecting the composition of the underlying parent material and differences in local pedological processes, together with sampling and analytical variability, rather than broad prairie-wide factors.

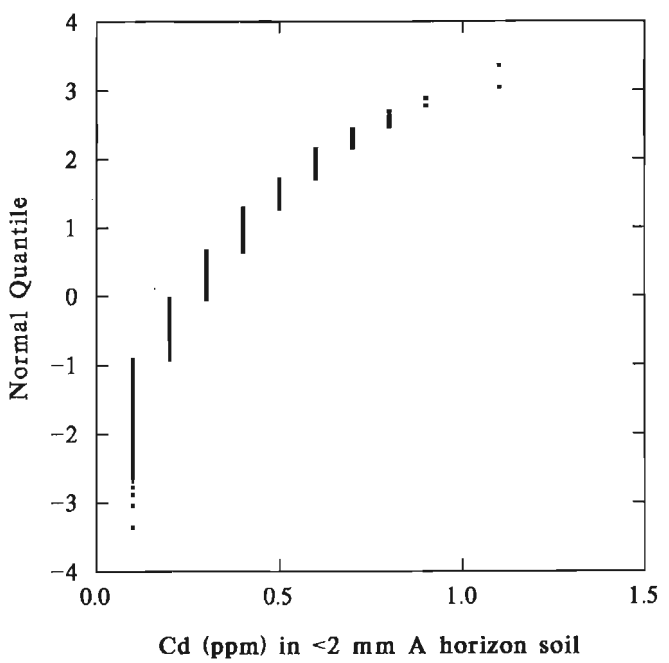

Figure 4. Normal quantile (probability) plot with two outliers ≥ 2 ppm removed, N = 1271.

However, there is a small (4%) but statistically significant (> 95% confidence level) component of variation at the topmost 80x80 km cell level. It might be argued that this is due to the effects of the two outliers and the skewed data distribution, however, for geological reasons, discussed below, the regional patterns are believed to be due to broader scale features of the prairie region's geological history.

The mean of the data, including the 116 sample preparation and analytical duplicates, is, as might be expected, unchanged from the smaller data set, i.e., 0.282 ppm Cd. The ANOVA does permit 95% confidence bounds to be placed on this mean employing the standard error from Table 1. The lower and upper bounds are respectively 0.267 and 0.297 ppm Cd. Realistically rounded off, the mean and limits become 0.28, and 0.27 and 0.30 ppm Cd, respectively.

GEOLOGICAL INTERPRETATION

The surface bedrock geology of the central continental basin, i.e., the prairies, may be crudely considered as a saucer. In the west, north, and east of the survey area, a Palaeozoic carbonate rim, partially missing in the north and west, forms the outer part. Within this lie Cretaceous shales, with sandstones becoming more common towards the northwest. Finally, a core that is dominantly composed of Cretaceous and Tertiary sandstones with minor conglomerates, shales, and coal beds, etc., lies at the centre of the basin and extends to the western edge of the survey area. This zoning is open to the south into the U.S.A. beyond the survey area. The glacial sediments on which most of the soils in the survey area have developed are in turn derived from these geological units, and Precambrian Shield materials in the north and east, and Alberta Foothills carbonates in the west. The following comments on possible geological causes of the observed data distribution are made within this general context. A full interpretation would require additional field and analytical work.

Skewed data distributions such as those presented (Fig. 3 and 4) have often been considered drawn from a single, possibly lognormal, distribution. Vistelius (1960) demonstrated that mixtures were a more likely cause of many of the observed skewed geochemical distributions. Garrett et al. (1980) concluded similarly on the basis of large amounts of regional geochemical stream and lake sediment data derived from the Canadian Uranium Reconnaissance Program (National Geochemical Reconnaissance) and the United States National Uranium Resource Evaluation Program. When the apparently lognormal regional reconnaissance data sets are subdivided on the basis of underlying geological units a series of normal, or only mildly skewed, distributions are observed.

The parent materials of the survey soils are dominantly glacially transported materials as described above. It is the mixing of the distributions associated with these sources that leads to the skewed data set (Fig. 4).

A total of 11 values exceed 0.7 ppm Cd, including the two outliers noted previously. A number of processes were considered that could have generated these data, including geological factors, eolian accumulation of fines, and anthropogenic causes, e.g., contamination or fertilizer application. Additional data generated in the project, both by atomic absorption spectrophotometry and instrumental neutron activation analysis for the A_p soils, not presented here, played an important part in this interpretation as the trace element associations provide useful insight to possible genesis. Eolian causes are not considered significant as this mechanical process would not have led to the chemical differentiation observed. There is a pattern in the geological association of most of these individuals, which is discussed below. Where locations are mentioned they are of the nearest habitation or mapped feature (see also Fig. 5).

Two of the highest values, 3.8 and 1.1 ppm, lie within 45 km of each other in Mountrail county, North Dakota. These sites are both in glaciated terrain, one (3.8 ppm, Tagus, A) in an area of terminal moraine, and the other (1.1 ppm, Lunds Valley, B) being in an area of thin till cover; both sites are underlain by Tertiary Sentinel Butte sandstones. The two samples exhibit unusually high values of Cd, Pb, Zn, and Au, and to a lesser extent Hg, Cu, Mn, As, Sb, and Ba. This trace element association is interpreted as having a sulphide mineral source. However, is the source local, or are the elevated values of transported (glacial) origin? The field data support the latter hypothesis. It was noted that the moraine material (3.8 ppm, Tagus, A) was a dark brown till that was possibly shale derived, while the thin till site (1.1 ppm, Lunds Valley, B) was characterized by a buff carbonate rich till.

Table 2. Seven-level unbalanced Analysis of Variance.

					Hypothesis Test No. 1 (Variance Component = 0)				
Level	Variation Between	Sums of Squares	DoF	Mean Square	Synthesized[1] M.S.	DoF	F Ratio	Prob[2] Value	
7	80km Cells	8.673	146	.059403	.04673	296.5	1.27	.957	*
6	40km Cells	11.80	348	.033901	.04156	351.2	.82	.029	ns
5	20km Cells	15.60	436	.035780	.01921	177.7	1.86	>.999	***
4	10km Cells	2.377	110	.021609	.01556	145.7	1.39	.968	*
3	10km Sites	1.856	116	.015998	.01278	148.6	1.25	.902	ns
2	Smpls at 3	1.482	116	.012772			1.00	.495	ns
1	Anals at 2	1.485	116	.012801					
Totals:		43.27	1388						

(1) Mean Squares and Degrees of Freedom synthesized after Satterthwaite (1946)
(2) ns = not significant, F ≤ 0.95
* = F > 0.95 ≤ 0.99
** = F > 0.99 ≤ 0.999
*** = F > 0.999

					Estimation of Variance Components		
Level	Variation Between	Sums of Squares	DoF	Mean Square	Unit Size	Variance Component	%_age
7	80km Cells	8.673	146	.059403	147	$.13428 \times 10^{-2}$	3.91
6	40km Cells	11.80	348	.033901	495	$-.30938 \times 10^{-2}$	.00
5	20km Cells	15.60	436	.035780	931	$.14230 \times 10^{-1}$	41.47
4	10km Cells	2.377	110	.021609	1041	$.37909 \times 10^{-2}$	11.05
3	10km Sites	1.856	116	.015998	1157	$.21485 \times 10^{-2}$	6.26
2	Smpls at 3	1.482	116	.012772	1273	$-.22099 \times 10^{-4}$	.00
1	Anals at 2	1.485	116	.012801	1389	$.12801 \times 10^{-1}$	37.31
Totals:		43.27	1388			$.34313 \times 10^{-1}$	

Estimated Population Mean = .282
Estimated Variance of Mean = $.45624 \times 10^{-4}$
Standard Error of Mean = .006755

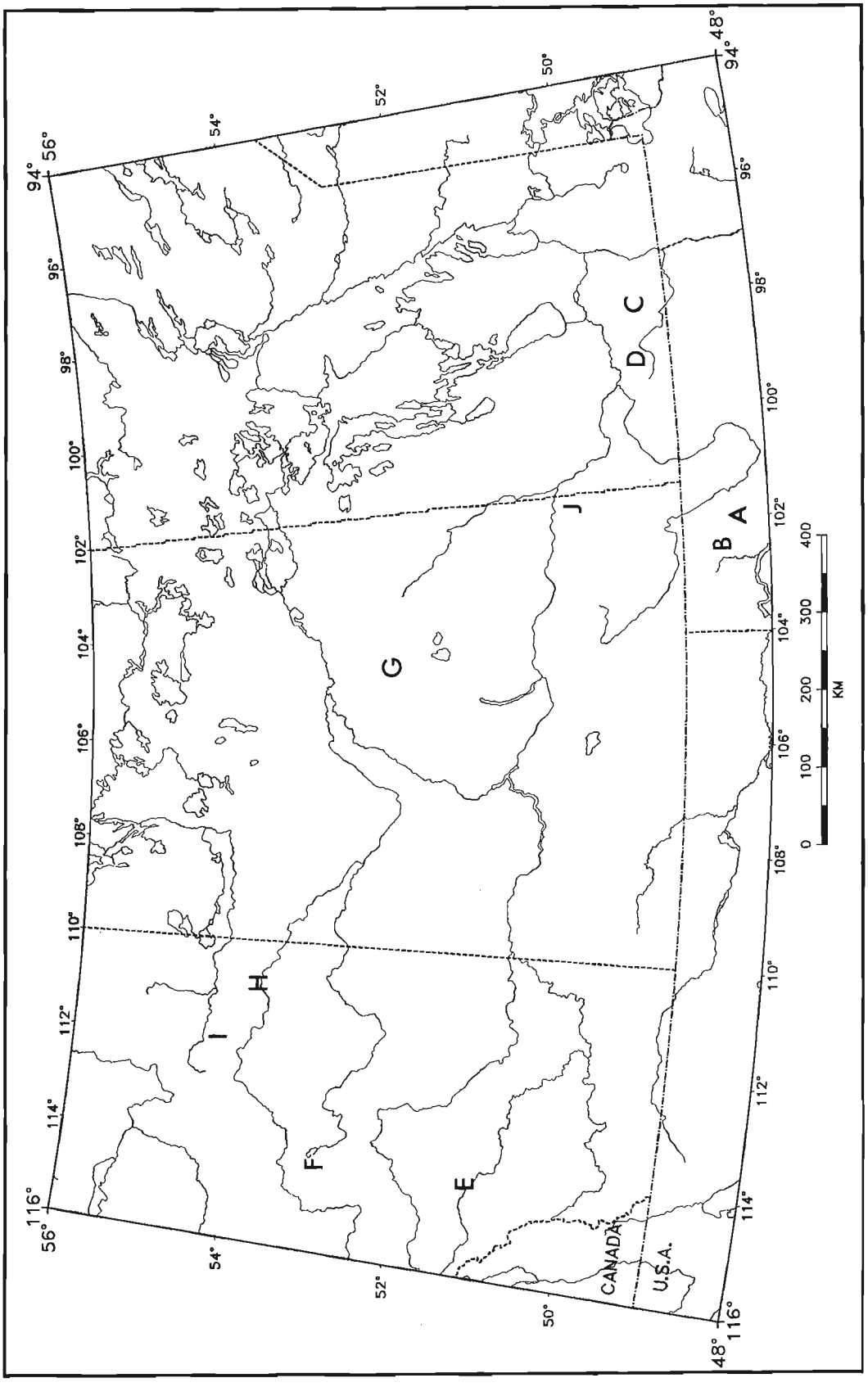

Figure 5. *Location of enhanced, ≥ 0.8 ppm, Cd sites.*

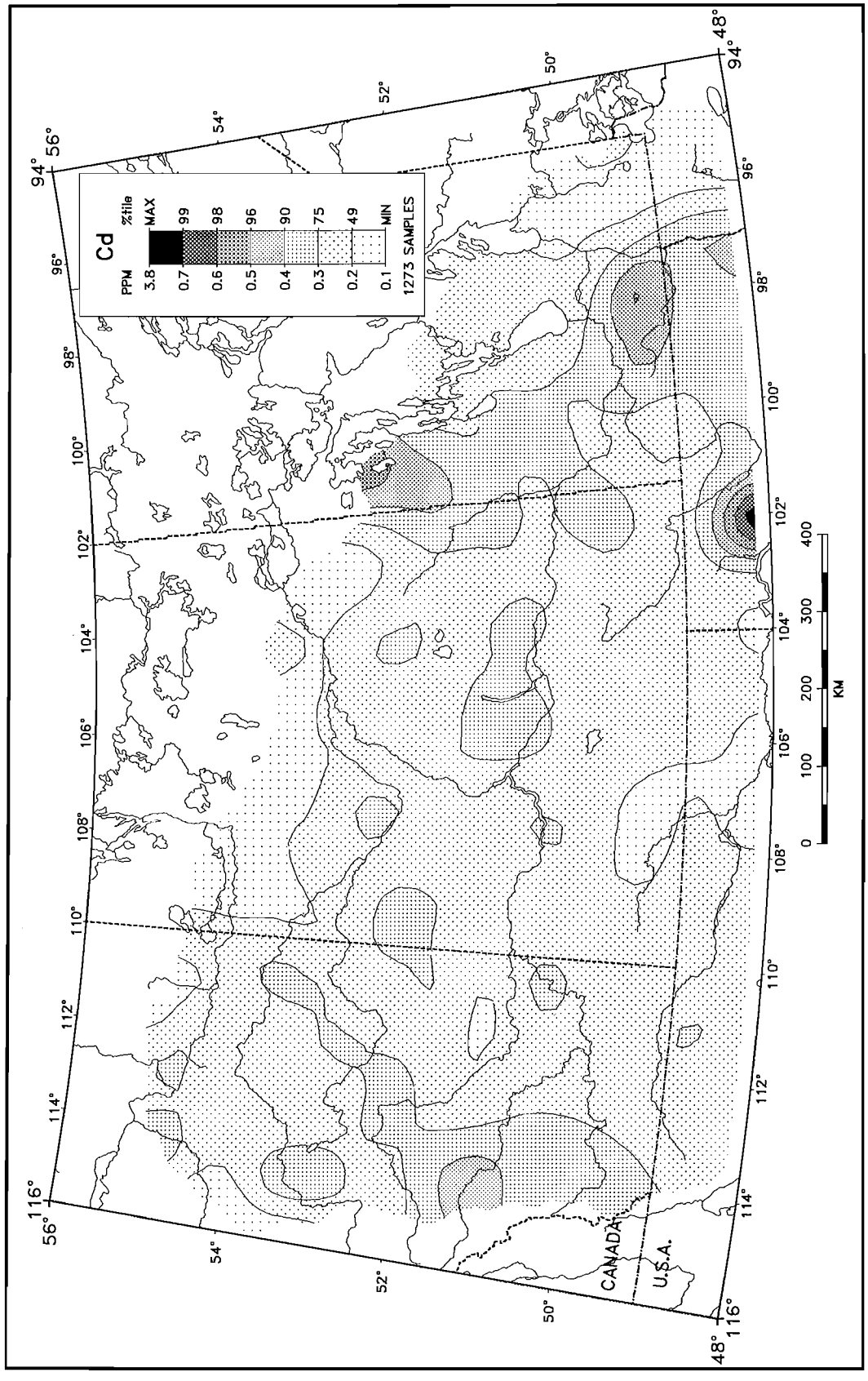

Figure 6. Regional distribution of Cd in prairie Ap horizon soils.

Both these glacial sediments are not what would be expected to overlie Sentinel Butte sandstones if they were of local origin. However, suitable source rocks do lie to the north and northeast as far away as Manitoba and the Precambrian Shield. This still begs the question as to why two of the highest values in A_p soils occur within 45 km of each other but are derived from different glacial parent materials. The explanation may relate to a minor local constituent of the parent material at both sites.

Five of the > 0.7 ppm Cd sites (0.8-2.0 ppm) occur in areas of Alberta, Saskatchewan, and Manitoba underlain by Upper Cretaceous Lea Park, Favel, and Riding Mountain shales (Fig. 5, C, D, H, I, J). Four of these soils are developed on glacial tills, and one on lacustrine sediments (Canada Soil Inventory, 1989). However, this last site (2.0 ppm, Miami, Manitoba, C) is close to the western boundary of glacial Lake Agassiz and is similar geochemically to another site (0.8 ppm, St. Alphonse, D) 65 km to the west. In the A_p soil samples some or all of the following elements are elevated in addition to Cd – Ni, V, Zn, Sb, Cu, and Se, while at some sites Mn, Cr, Co, As, and Br are also enhanced. Dunn and Irvine (1993) reported that in the Cretaceous White Speckled shale in central Saskatchewan, Ca, Cd, Mo, Se, U, and V, and to a lesser extent As, Cu, Ni, Sb, Sr, and Zn, are all enriched relative to other geological strata in the district. The trace element assemblage at these five sites is typical of black shale assemblages, and it is postulated that the elevated levels being discussed are due to background geochemical phenomena related to the concentration of trace elements in black shales. It is proposed that the higher values at the 2.0 ppm Cd (Miami, C) site are due to the relative concentration of the trace element rich "clay mineral" sized fraction in preference to the trace element poorer, coarser, quartz rich fraction at the margin of glacial Lake Agassiz.

Three sites with elevated Cd levels (0.8-1.1 ppm) occur in soils developed on glacial tills overlying Tertiary Paskapoo and Porcupine Hills sandstones in Alberta. There is a weak association of Cd with Zn, Ag, Cu, and Sb; again, this association is one usually indicative of sulphide minerals. The direction of glacial transport is from the north-northwest at the southern site (Porcupine Hills, 0.8 ppm, Bowness, E) and is in an area where the glacial tills are composed of both local, and Alberta Foothills derived carbonate rich, materials (Shetsen, 1984). Thus the trace elements could be locally derived or transported from the limestone Foothills terrain, which on geological grounds could host Zn mineral occurrences. The remaining two samples are for a site duplicate (< 50 m apart) underlain by Paskapoo sandstone (0.9 and 1.1 ppm, Pigeon Lake, F). Shetsen's study (1984) did not extend this far north, however they likely lie in her central domain where ice-flow was dominantly from the north. Volcanic tuffs have been mapped within the Paskapoo formation; the elevated Cd levels might be due to the local presence of sulphide bearing tuffs.

Lastly, a single high Cd site (0.9 ppm, Lac Vert, G) occurs in a soil developed on glaciofluvial materials in Saskatchewan in an area underlain by Cretaceous Riding Mountain shale. This site was not grouped with the shale assemblage noted above due to the fact that no other trace elements show elevated levels and that it occurs in soils developed from glaciofluvial materials. There is a possibility that the high Cd at this site has an anthropogenic source.

In order to illustrate the spatial variation in the data, a computer generated contour map was prepared (Fig. 6). Firstly, a 20x20 km grid was laid over the survey data, and where more than one point fell within a grid cell the separate values were replaced by their mean. Subsequent interpolation steps using a 60 km radius circle, the approximate radius of the circumscribing circle of an 80x80 km square, generated the smoothed map presented. The regional distribution of the Cd data (Fig. 6) reflects a number of regional geological features.

Firstly, the elevated Cd levels in eastern Saskatchewan, Manitoba, and North Dakota reflect Cretaceous shales, including the Riding Mountain, Vermilion River, Favel, Ashville, and Pierre shales. The lower black shale units, i.e., beneath and younger than the Riding Mountain, are generally thought to be the most heavy-metal enriched, and it is over and down-ice from these that the elevated Cd pattern is most marked. This pattern does not continue across central Saskatchewan in the area underlain by heavy-metal enriched shales, e.g., the White Speckled, within the Cretaceous shales. In much of central Saskatchewan the glacial deposits average some 100 m in thickness, and material reworked through the glacial sequence surfaces at diluted concentrations well down-ice from the source area. Thus, the Battleford Till on which the soils developed contains a significant Precambrian Shield and Palaeozoic carbonate component admixed with local shale derived material (B. Schreiner, pers. comm.), causing a dilution of the heavy-metal enriched shale geochemical signature. The scattered areas above the 0.3 ppm contour in central Saskatchewan are believed to be due to this phenomenon.

Secondly, the low Cd areas in the east and north of the survey area, and in the south-central area are related to natural geochemical abundance. In the east and northern margin areas the tills contain a large component of Precambrian Shield and/or Palaeozoic carbonate material that would be expected to be low in Cd relative to the shale units (Krauskopf, 1967). Similarly, in the southern area, the tills contain a significant Cretaceous and Tertiary sandstone component that would be expected to be similarly relatively low in Cd.

Thirdly, Cd levels rise in the west of the survey area, partly correlative with the Tertiary Paskapoo and Porcupine Hills sandstones, and at least in part with Alberta Foothills derived glacial material. The limestones of the Alberta Foothills could host Zn mineral occurrences, and if such was the case, elevated Cd levels would be expected to be associated with the Zn. Unfortunately, there is little available information on likely local geological sources for Cd in this area.

Lastly, a 300 km northeast-southwest linear feature runs from Elk Point, Alberta, to the Calgary area to connect to the above mentioned elevated Cd area. The head of this feature is one of the Cretaceous shale sites (0.8 ppm, Elk Point, H) discussed above. A point of interest is that a high Cd site (0.8 ppm, Whitefish Lake, I) lies some 90 km northwest along strike in the same uppermost part of the Lea Park shale. An

inspection of other available data for the A_p soils indicates that Zn, Ba, Se, Br, and, to a lesser extent Cu, exhibit a similar trend. This association could be due to a variety of processes, including, a shale-hosted base metal accumulation, and leakage to surface of subsurface brines. The possibility of a point source of metals northeast of Elk Point and that the linear feature is a glacial dispersal train, i.e., natural pollution, from a particular stratigraphic unit or mineral occurrence(s) is difficult to reconcile with late glacial ice direction data over the whole linear (Prest et al., 1968; Dyke and Prest, 1987). However, the linear feature generally coincides with a number of subsurface geological features, including the southwesterly extension of the Virgin River Domain, lying between the Western Craton and Mudjatik domains, at the southern margin of the Precambrian Shield; the Athabasca Axis gravity low described by Darnley (1982) and postulated to be a locus for "hot granites"; and the edge of the southern Alberta Devonian shelf. These subsurface phenomena, and the generally persistent but only slightly elevated level nature of the geochemical linear, offer a more likely avenue for further investigation.

CONCLUSIONS

In conclusion, while the overall average Cd content of the A_p horizon soils is 0.3 ppm there are regional heterogeneities, which are related to both broad geological scale features, such as the metal rich Cretaceous shales of the region, and to point sources of natural pollution.

In terms of environmental baselines, 0.3 ppm Cd would appear to be a useful working figure for the prairie region. With respect to the overall distribution, 95% of the data fall below 0.5 ppm Cd and 99% below 0.7 ppm Cd. Setting action levels below these figures is likely to raise several per cent of false alarms that are due to geological processes. The cost of investigating such sites has to be offset against possible benefits of setting a low action level. On the basis of these data, and experience around known mineral deposits elsewhere in Canada, it is realistic to expect that higher levels than 0.7 ppm Cd will arise due to natural geological processes. It would be futile and a prohibitively expensive task to attempt to "clean up" an area of natural geological pollution that has been equilibrating with its environment since the retreat of the continental ice-sheet.

ACKNOWLEDGMENTS

This work derives from a joint project with L.H. Thorleifson, Terrain Sciences Division, with whom many stimulating hours have been spent discussing various aspects of prairie geology. However, the author takes full responsibility for the ideas expressed in this report. Secondly, the assistance of Wendy Spirito in working to determine the optimal contouring parameters used in, and preparing, Figures 5 and 6 is gratefully acknowledged.

REFERENCES

Canada Soil Inventory
1989: Soil landscapes of Canada – Manitoba; Land Resource Research Centre, Research Branch, Agriculture Canada, Agriculture Canada Publication 5242/B, 22 p. and 1:1 million scale map.

Darnley, A.G.
1982: 'Hot granites': some general remarks; in Uranium in Granites, (ed.) Y.T. Maurice; Geological Survey of Canada, Paper 81-23, p. 1-10.

Dunn, C.E. and Irvine, D.G.
1993: Relevance of a lithogeochemical database to epidemiological studies in central Saskatchewan, Canada; Applied Geochemistry, Supplementary Issue No. 2, p. 215-222.

Dyke, A.S. and Prest, V.K.
1987: Paleogeography of northern North America, 18,000 to 5,000 years ago; Geological Survey of Canada, Map 1703A, scale 1:12 500 000.

Garrett, R.G.
1983: Sampling Methodology; in Statistics and Data Analysis in Geochemical Prospecting, Chapter 5, (ed.) R.J. Howarth; Handbook of Exploration Geochemistry, Vol. 2, Elsevier, Amsterdam, p. 83-110.

Garrett, R.G. and Goss, T.I.
1978: The evaluation of sampling and analytical variation in regional geochemical surveys; in Geochemical Exploration 1978, (ed.) J.R. Watterson and P.K. Theobald; Association of Exploration Geochemists, Toronto, p. 371-383.
1980: UANOVA: A Fortran IV program for unbalanced nested analysis of variance; Computers and Geoscience, v. 6, no. 1, p. 35-60.

Garrett, R.G. and Thorleifson, L.H.
1993: Prairie Kimberlite Study – Soil and till geochemistry and mineralogy, low density orientation survey traverses, Winnipeg-Calgary-Edmonton-Winnipeg, 1991; Geological Survey of Canada, Open File 2685, 1 3.5" 1.4MB diskette containing ASCII files.

Garrett, R.G., Kane, V.E., and Zeigler, R.K.
1980: The management and analysis of regional geochemical data; Journal of Geochemical Exploration, v. 13, no. 2-3, p. 115-152.

Govindaraju, K.
1989: 1989 compilation of working values and sample description for 272 geostandards; Geostandards Newsletter, v. 13, Special Issue, 113 p.

Krauskopf, K.B.
1967: Introduction to geochemistry; McGraw-Hill Book Co., New York, 721 p.

Prest, V.K., Grant, D.R., and Rampton, V.N.
1968: Glacial map of Canada; Geological Survey of Canada, Map 1253A, scale 1:5 000 000.

Satterthwaite, F.E.
1946: An approximate distribution of estimates of variance components; Biometrics, v. 2, no. 2, p. 110-114.

Severson, R.C. and Tidball, R.R.
1979: Spatial variation in total element concentration in soil within the Northern Great Plains coal region; U.S. Geological Survey Professional Paper 1134-A, p. A1-A18.

Severson, R.C. and Wilson, S.A.
1990: Assessment of geochemical variability and a listing of geochemical data for surface soils of Eastern North Dakota and parts of Northeastern South Dakota and Northwestern Minnesota; U.S. Geological Survey, Open File Report 90-310, 58 p.

Shetsen, I.
1984: Application of till pebble lithology to the differentiation of glacial lobes in southern Alberta; Canadian Journal of Earth Sciences, v. 21, no. 8, p. 920-933.

Tidball, R.R. and Severson, R.C.
1976: Chemistry of Northern Great Plains soils; in Geochemical Survey of the Western Energy Regions, Third Annual Progress Report, July 1976. U.S. Geological Survey, Open File Report 76-729, p. 57-81.

Vistelius, A.B.
1960: The skew frequency distributions and the fundamental law of the geochemical processes; Journal of Geology, v. 68, no. 1, p.1-22.

Geological Survey of Canada Project 790004

Cambrian and Ordovician volcanic rocks in the McKay Group and Beaverfoot Formation, Western Ranges of the Rocky Mountains, southeastern British Columbia

B.S. Norford and M.P. Cecile
Institute of Sedimentary and Petroleum Geology, Calgary

Norford, B.S. and Cecile, M.P., 1994: Cambrian and Ordovician volcanic rocks in the McKay Group and Beaverfoot Formation, Western Ranges of the Rocky Mountains, southeastern British Columbia; in Current Research 1994-B; Geological Survey of Canada, p. 83-90.

Abstract: Basic volcaniclastics and volcanic or subvolcanic amygdaloidal rocks (flows and/or sills) are present within the Upper Cambrian part of the McKay Group and within the basal Beaverfoot Formation (Upper Ordovician) in the Hughes Range of the western Rocky Mountains north of Cranbrook. The McKay rocks had been thought to be Late Silurian or Devonian and mapped as the SDs unit. The evidence of marine volcanism within the McKay Group of the White River Trough invites comparison with analogous depositional environments in the Selwyn Basin where similar volcanic and intrusive activity is considered to be the key factor in the formation of several rich lead-zinc-barite deposits. The McKay Group is widely distributed within the western Rocky Mountains of southeastern British Columbia and, because of the presence of the volcanics, has the potential to contain significant base metal deposits.

Résumé : Il y a des roches volcanoclastiques basiques et des roches amygdaloïdes volcaniques ou subvolcaniques (coulées, filons-couches ou les deux) dans le Cambrien supérieur du Groupe de McKay et dans la formation basale de Beaverfoot (Ordovicien supérieur) dans le chaînon Hughes des Rocheuses occidentales au nord de Cranbrook. On pensait que les roches du Groupe de McKay dataient du Silurien tardif ou du Dévonien, et elles ont été cartographiées sous le vocable d'unité SDs. Les indications d'un volcanisme marin au sein du Groupe de McKay dans la dépression de White River invitent à faire la comparaison avec des milieux de dépôt analogues dans le bassin de Selwyn, où une activité volcanique et intrusive semblable est considérée comme le facteur déterminant dans la formation de plusieurs gisements riches en plomb-zinc-barytine. Le Groupe de McKay est largement répandu dans les Rocheuses occidentales du sud-est de la Colombie-Britannique et, à cause de la présence des roches volcaniques, il pourrait contenir d'importants gisements de métaux communs.

INTRODUCTION

Complex folding and faulting are characteristic of the Western Ranges of the southern Rocky Mountains (Fig. 1). Resistant Lower Paleozoic carbonate formations are prominent but there are some recessive shaly units, argillaceous carbonate units, and evaporitic units. Dykes and diatremes are known from specific localities (Leech, 1979; Mott et al., 1986; Helmstaedt et al., 1988). Reconnaissance mapping of the Hughes Range was completed by Leech (1958, 1960) when access was difficult and before the ready availability of helicopter support. Leech recognized a thick succession of undetermined age near Ruault Lake. These rocks included volcaniclastic rocks, sills, and possible flows. He mapped them as stratigraphically above the Beaverfoot Formation (Upper Ordovician-Lower Silurian) and reported fossiliferous boulders of the Beaverfoot Formation within their basal beds. Höy and Carter (1988) and Welbon and Price (1992a, 1992b, 1993) similarly mapped these rocks as within the core of an overturned syncline, referring to them as the SDs unit of Silurian-Devonian(?) age. The same SDs unit was mapped farther south, near the headwaters of Tanglefoot Creek, directly overlying the Cambrian part of the McKay Group, but now these occurrences are thought to be sills within the McKay (R.A. Price, pers. comm., 1993).

In 1992, volcaniclastic rocks were recognized by Norford at Mt. Dingley (Fig. 2) at the upper limit of the rocks that Leech (1958, 1960) mapped as McKay Group and below the Beaverfoot Formation. Detailed examination by Cecile and Norford in 1993 found that the volcaniclastics were directly associated with the upper part of a diatreme exposed in the northern face of Mt. Dingley. An apparently unrelated thin layer of volcanic or subvolcanic rock was discovered within McKay rocks cut by the Mt. Dingley diatreme and a tuff was found within the basal part of the Beaverfoot Formation. The McKay Group is intruded by another igneous pipe just northwest of Sparkle Lake. Mt. Dingley is only 7 km north of Ruault Lake, where the SDs unit was described. Cecile, Norford, H.H. Helmstaedt, and R.A. Price visited the Ruault Lake area in 1993 and recognized the SDs unit as the McKay Group. The present authors ran a detailed traverse across the structurally complex outcrops west and north of Ruault Lake.

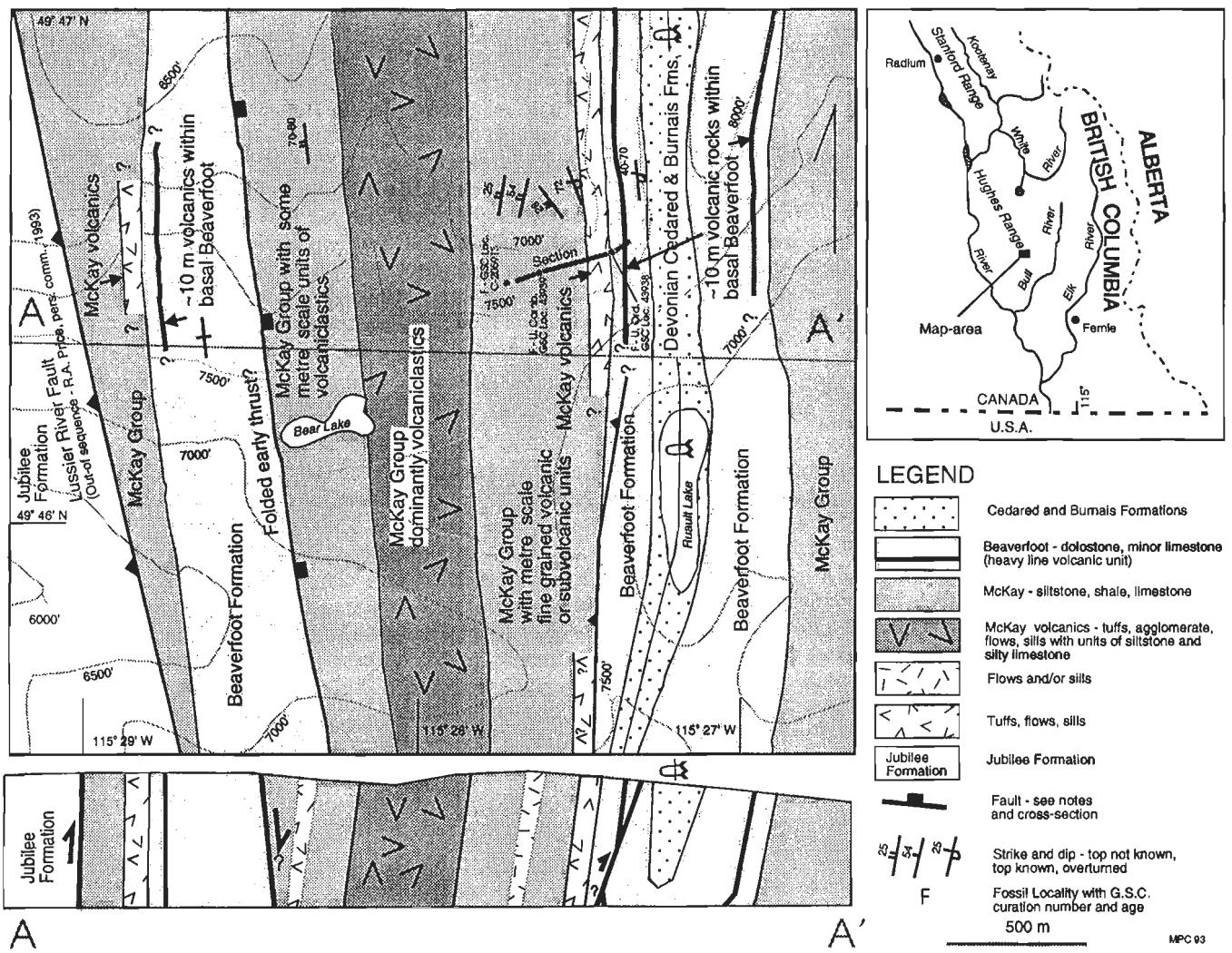

Figure 1. Locality map, geological sketch map, and cross-section of the study area.

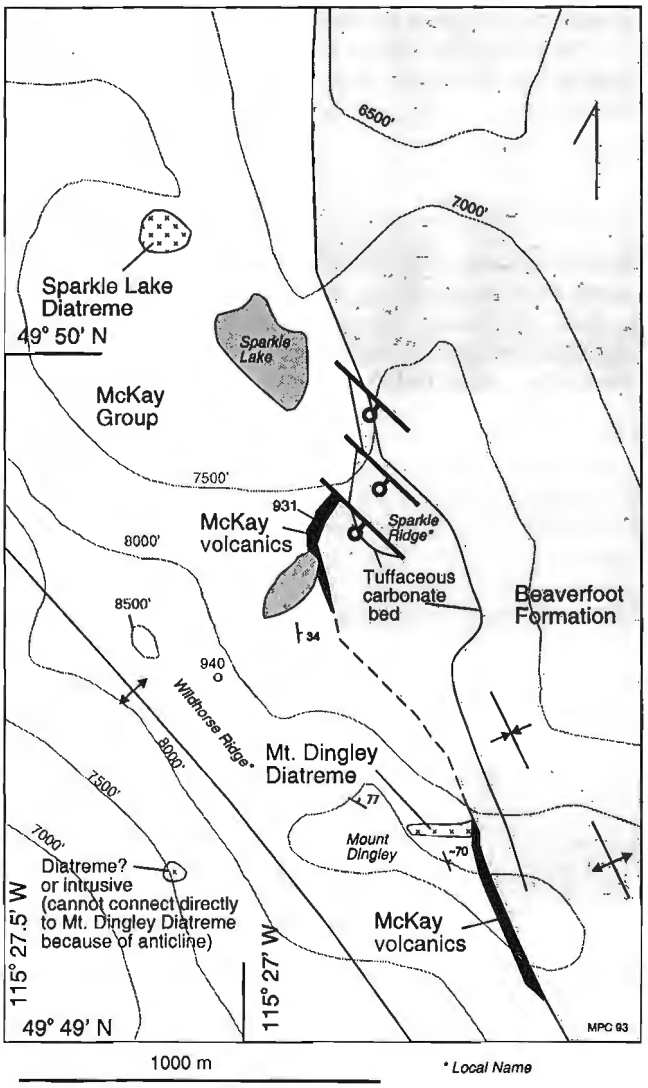

Figure 2. Geological sketch map, Mt. Dingley area, just north of the area indicated on the locality map in Figure 1.

GEOLOGICAL SETTING

The McKay Group is a very thick sequence of carbonates and shales deposited within the White River Trough (Norford and Jackson, 1989) of the southern Rocky Mountains during the Late Cambrian and Early Ordovician (Cecile and Norford, 1992). Within the Hughes Range, carbonates of the Upper Ordovician and Lower Silurian Beaverfoot Formation rest on an erosion surface cut deeply into the McKay Group (Franconian to Ibexian). North of the Hughes Range, the Beaverfoot directly overlies the Jubilee Formation (Upper Cambrian, Dresbachian) in the western Stanford Range with the McKay Group completely missing (Henderson, 1954; Norford, 1969). Recessive Devonian rocks (basal Devonian unit, Cedared, Burnais, and younger formations) overlie the Beaverfoot. Although stocks, dykes, and sills have been recognized within the McKay Group (Leech, 1958, 1960, 1979; Mott et al., 1986; Helmstaedt et al., 1988) and flows have been reported from directly above the McKay (Pell, 1987), no contemporaneous igneous activity has been reported within the McKay Group. In younger rocks, agglomerates and tuffs are present within the lower part (Upper Ordovician) of the Beaverfoot Formation (including the fossiliferous conglomerate reported by Leech, 1960) and flows have been reported from the basal Mount Forster Formation (Middle Devonian) on the Purcell Arch west of the southern Rocky Mountains (Root, 1987).

STRUCTURE

Leech (1958, 1960) originally interpreted the structure in the Ruault Lake area as a complex, broad syncline outlined by east and west panels of Beaverfoot Formation facing west and east respectively. This interpretation was continued by subsequent workers but the present study makes substantial revisions. Now the east panel of Beaverfoot Formation is recognized as a very tight, almost vertical, syncline with a core of Cedared and Burnais formations exposed on the ridge crest due north of Ruault Lake (Fig. 1, 3). The west panel of Beaverfoot Formation stratigraphically overlies the McKay Group and is an almost complete succession of the formation with the upper beds facing east where they are faulted against the McKay Group (Fig. 4). The fault laterally cuts out beds of both the McKay Group and the Beaverfoot Formation. The pattern of the bedding plane cutoffs along the fault indicates that it is a thrust fault. The sense of motion that can be interpreted from the exposures south of Bear Lake (Fig. 1, 4) is down on the east, implying that it may be a folded thrust (D.G. Cook, pers. comm., 1993). There is virtually continuous outcrop of the McKay Group between this west panel of Beaverfoot and the tight Beaverfoot syncline to the east. Deformation is intense locally, with phyllitic cleavage. Small contorted folds are present within the informal stratigraphic units that can be recognized locally within the McKay. Structurally, these outcrops of the McKay Group

Figure 3. Tight syncline north of Ruault Lake (ISPG 4196-6).

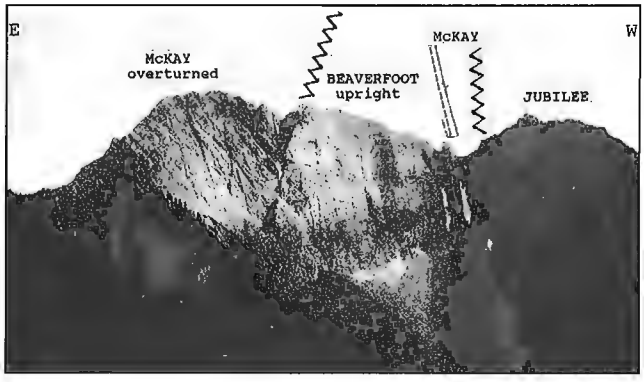

Figure 4. *Faulted contact between McKay and Beaverfoot, north side of ridge about 2 km south of Bear Lake (ISPG 4196-10).*

between the two panels of Beaverfoot comprise the west limb of a large syncline which includes the tight Beaverfoot syncline, and forms the axial zone trending north through Ruault Lake.

STRATIGRAPHY

Figure 5 indicates six informal thick units within the McKay Group of the Hughes Range, two of which are not present in the Bear Lake-Ruault Lake area. The lowermost unit represents lower beds of the McKay Group which are faulted out beneath the westernmost panel of Beaverfoot Formation (Fig. 1, 4). The uppermost unit is missing beneath the sub-Beaverfoot unconformity. Elsewhere this unit represents a considerable succession of higher beds of the McKay Group that is present in places where the sub-Beaverfoot unconformity does not cut down as deeply as at Ruault Lake. Informal units 3 and 5 are dominated by volcanics and units 2 and 4 contain volcaniclastics. Mapping indicates that the stratigraphic thickness of units 2 to 5 is estimated to be 700 to 900 m, with

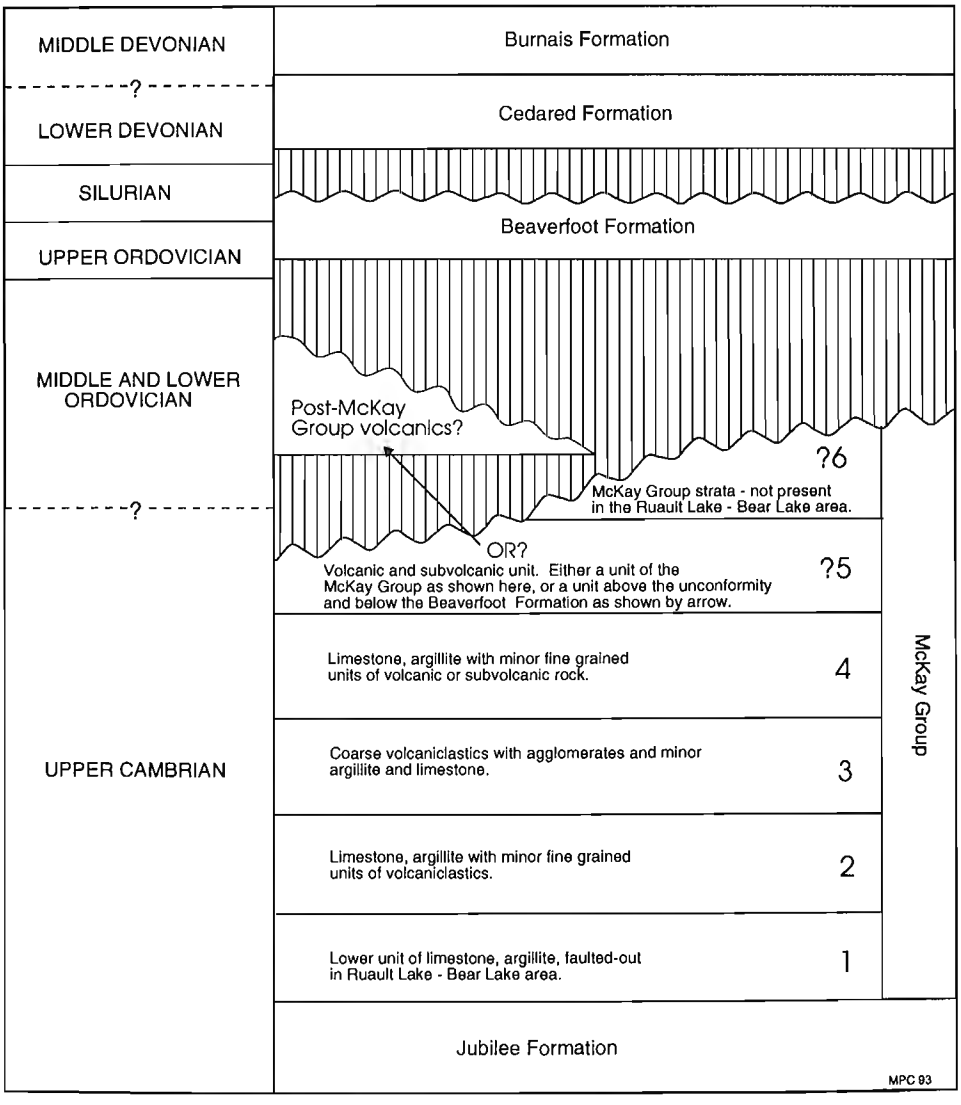

Figure 5.

Stratigraphic units, Ruault Lake area.

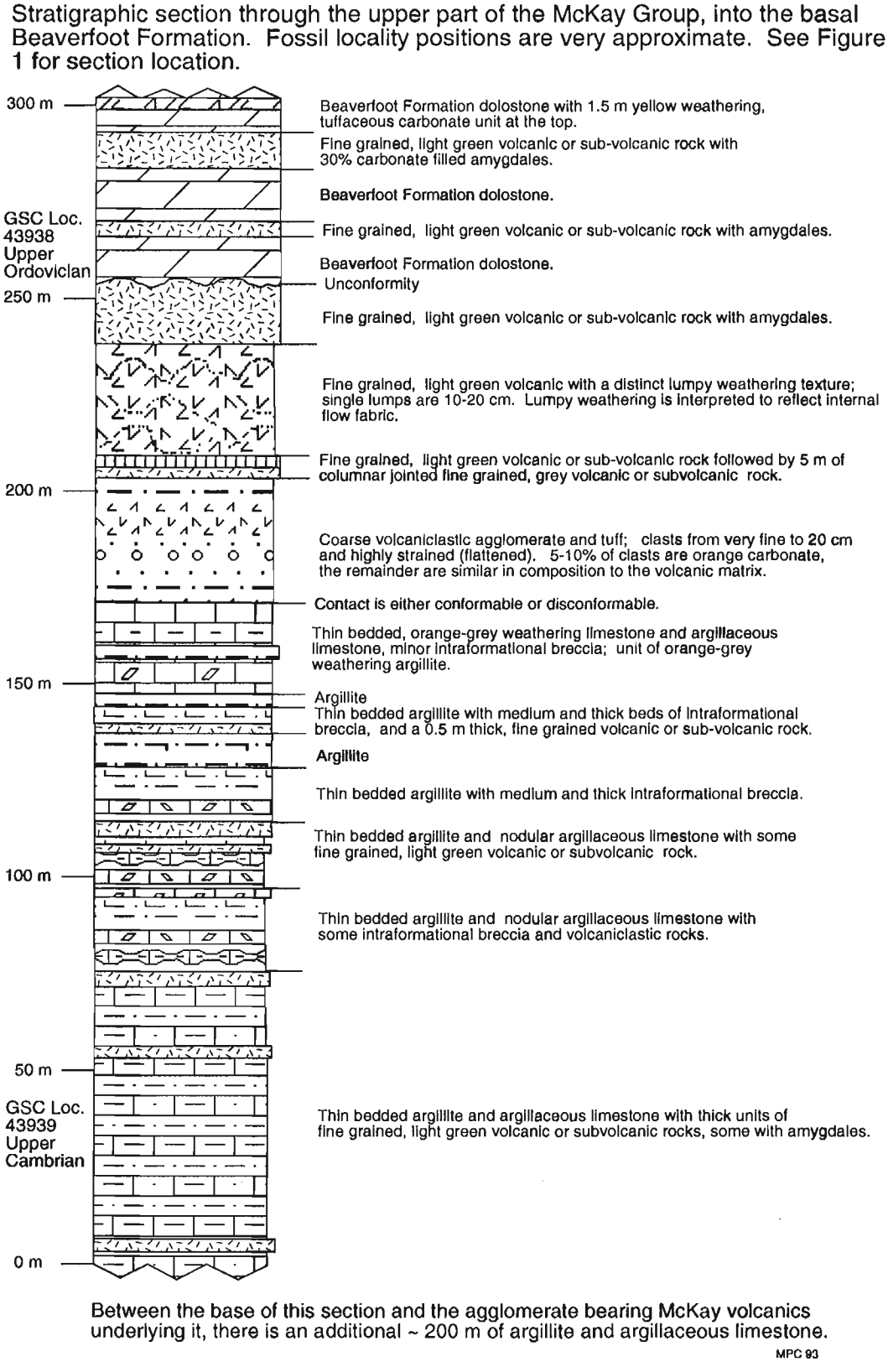

Figure 6. Schematic stratigraphic section through upper part of McKay Group (informal unit 5 and part of unit 4), ridge northwest and west of Ruault Lake.

unit 5 being 85 m. However, these are rough estimates of the true stratigraphic thicknesses because clasts in many of the agglomerates are intensely strained (flattened into cleavage planes that approximately parallel compositional layering that has depositional origins). Only unit 5 and the upper part of unit 4 could be examined in any detail during the traverse and Figure 6 outlines the stratigraphy of these rocks.

The McKay Group is about 880 m thick near Sharktooth Mountain near the northern end of the Hughes Range, about 36 km north-northwest of Ruault Lake (Leech, 1954, p. 10-11; 1958, p. 13). Leech described the McKay as a lower division (about 360 m thick) of shales and limestones and an upper division (about 520 m thick) dominated by resistant, cliff-forming limestones. The lower division contains Upper Cambrian (Franconian) fossils and most of the upper division is Lower Ordovician (Ibexian trilobite zone E is the youngest documented horizon). Resistant McKay limestones are not present near Ruault Lake and Leech's upper division is thought to be missing entirely because of downcutting of the sub-Beaverfoot unconformity. Informal units 1 to 5 are thought to fall within Leech's lower division but are thickened because of the presence of the volcanic rocks.

VOLCANIC ROCKS

Three different sets of Lower Paleozoic volcanics can be recognized and mapped locally (Fig. 1, 5, 6): one set within McKay informal units 2 to 4, another set (informal unit 5) stratigraphically either within the McKay or between the McKay and the Beaverfoot, and the youngest set within the basal Beaverfoot. The oldest set consists of metre-scale units of volcanic and subvolcanic rocks together with coarse agglomerates (Fig. 7) and tuffs. These rocks are interpreted as being close to a volcanic centre. Volcanics in this stratigraphic position have not been recognized outside the Bear Lake-Ruault Lake area, encouraging the suggestion that these are local deposits associated with a vent located very close to the outcrops. This set of volcanics underlies Upper Cambrian fossils (GSC loc. 43939).

The second set of volcanic rocks near Ruault Lake lies stratigraphically between the McKay Group and the Beaverfoot Formation but for convenience is mapped as McKay informal unit 5 and assumed to be older than unit 6. The rocks are agglomerates, tuffs, and fine grained, light green volcanic or subvolcanic rocks. One of the volcanic beds weathers with a lumpy texture that can be interpreted to result from some form of flow fabric. X-ray diffraction (by J.N.Y. Wong, GSC, Calgary) of a single sample (GSC loc. C-237815 3-5R2) of volcanic rock from this lumpy bed shows the following composition:

Chlorite	22%
Calcite	14%
Magnesio hornblende/tremolite	14%
Albite	13%
Mica (phlogopite?)	11%
Magnetite	7%
Potassium feldspars	6%
Quartz	5%
Siderite	3%
Dolomite	trace
Unknown	5%

A thick columnar jointed subvolcanic unit is also present and could be either a sill or a flow (Fig. 8). This second set of volcanic rocks is above McKay rocks dated as Upper Cambrian and below Beaverfoot rocks dated as Upper Ordovician.

Volcaniclastic rocks occupy a similar supra-McKay, sub-Beaverfoot stratigraphic position near Mt. Dingley (6 km north-northeast of Ruault Lake; Fig. 2). These volcaniclastics are directly associated with the layered upper phase of a pre-Beaverfoot diatreme. Outcrops of volcaniclastics 1 km northwest of Mt. Dingley may well represent a less proximal

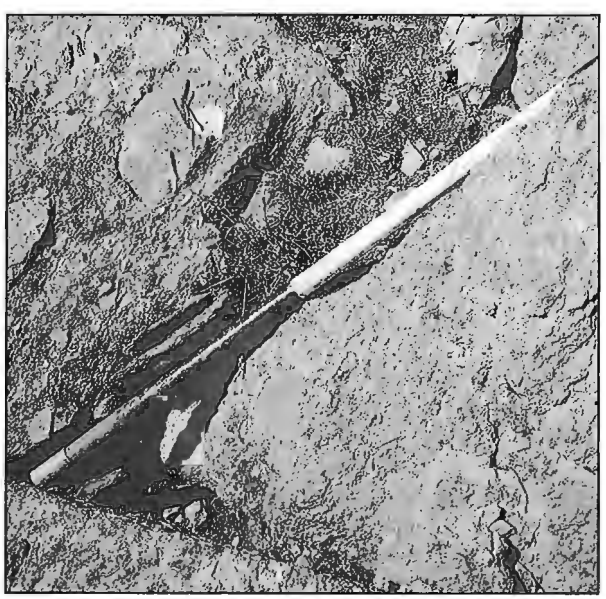

Figure 7. *Agglomerate within McKay Group west of Ruault Lake; staff calibrated in half metres (ISPG 4176-22).*

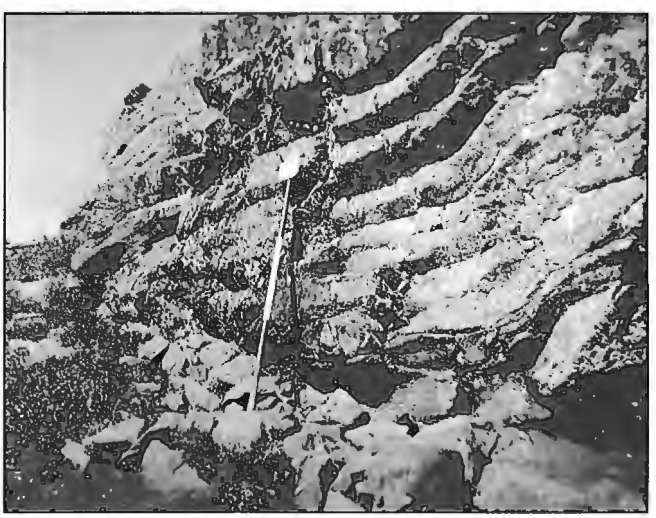

Figure 8. *Columnar jointing in subvolcanic rock north of Ruault Lake; staff calibrated in half metres (ISPG 4196-1).*

facies of the same rocks. These latter outcrops are interstratified with olistostromal-like deposits with McKay boulders that are likely to be debris flows from a submarine elevation formed by the diatreme.

Sub-Beaverfoot volcanic rocks have also been reported from the Swan claims, about 23 km northeast of Ruault Lake, and include flows (Pell, 1987). These volcanics are immediately beneath a few metres of quartzites and shales that represent the feather edge of the Mount Wilson Quartzite and possibly the Glenogle Formation beneath the Beaverfoot Formation (Leech, 1960). Pell reports that the central portions of green volcanic rocks appear to be pillowed. These structures could be similar to the lumpy weathering aspect of the volcanic rocks near Ruault Lake. The flows were reported by Pell to be olivine melilitites but later she commented (J. Pell, pers. comm., 1991) that some of the rocks discussed in her 1987 report were misidentified as melilitites.

The third set of volcanic rocks in the Bear Lake-Ruault Lake area consists of two separate stratigraphic units (6 and 10 m thick) within the basal part of the Beaverfoot Formation. The rocks include fine grained, light green amygdaloidal volcanic or subvolcanic rocks and tuffaceous carbonates. These rocks are exposed on the west limb of the tight syncline with the axis trending through Ruault Lake. On the east limb of the same syncline there is a 10 m thick succession of tuffs and carbonates commencing 15 to 20 m above the base of the Beaverfoot. The volcanic succession of the west limb includes one bed with well developed fiamme indicating that it was deposited as an ash-flow tuff (possibly subaqueously).

Volcanic rocks were seen from a distance within the basal Beaverfoot Formation west of Bear Lake (Fig. 1) and used (together with the stratigraphic character of the upper Beaverfoot outcropping at the lake itself) to establish the facing direction of the Beaverfoot Formation at this location. There is a fault between the Beaverfoot at the lake and the McKay Group to the east (Fig. 4). In the Mt. Dingely area, the only volcanic rock noted within the basal Beaverfoot Formation was a single tuffaceous carbonate bed (Fig. 2).

AGE

Echinoderm fragments are abundant in some pebbles within limestone conglomerates in the McKay Group and trilobite debris can be found in some of these pebbles. The only known identifiable macrofossil is a fragmentary Late Cambrian trilobite collected by G.B. Leech and identified by W.H. Fritz:

GSC loc. 43939 (see Fig. 1) — *Briscoia?* sp.
age: Late Cambrian, Franconian or Trempealeauan

A sample was taken in search of conodonts from a horizon thought to be at least a hundred metres below 43939, but no conodonts were found in the etched residues:

GSC loc. C-205913 (see Fig. 1) — echinoderm debris
trilobite fragments
age: Late Cambrian or younger

Macrofossils are present in the basal beds of the Beaverfoot Formation and G.B. Leech collected a typical Late Ordovician fauna:

GSC loc. 43938 (see Fig. 1) — echinoderm debris
Catenipora cf. *C. delicatulus* (Wilson)
Streptelasma sp.
age: Late Ordovician, probably *Bighornia-Thaerodonta* Fauna

COMPARISON WITH OTHER AREAS

Somewhat similar volcaniclastic rocks have been described from the Northern Cordillera in the District of Mackenzie, where several Proterozoic to Devonian volcanic complexes have been reported (Cecile, 1982). Alkalic basalt flows, dykes, and sills are present together with tuffs and breccias, conglomerates, and sandstones that include limestone clasts in addition to volcanic material.

MINERAL DEPOSIT POTENTIAL

An extensive complex of platform-margin basins and intraplatformal embayments and troughs was situated at the western and northwestern margin of the cratonic carbonate platform of ancestral North America during much of early Paleozoic time. The White River Trough (Norford and Jackson, 1989; Cecile and Norford, 1992) was a site of slope and basin deposition from Late Cambrian to Middle Ordovician time accumulating about 3000 m of sediments of the McKay Group and the overlying Glenogle Formation. Regional unconformities below the Mount Wilson Quartzite and below the Beaverfoot Formation mark the end of this depositional feature.

Volcanic rocks are present within the Lower Paleozoic successions of most of the basins, embayments and troughs, including: the Nasina and Selwyn basins, the Misty Creek and Prairie Creek embayments and the Kechika Trough. Now volcanic rocks are also recognized within the White River Trough. Significant syndepositional exhalative zinc and lead deposits have been discovered in the Selwyn Basin (Anvil District and Howards Pass; Dawson et al., 1992). The discovery of volcanic rocks within the White River Trough invites comparison with similar rocks in the Selwyn Basin and the Misty Creek Embayment. The presence of volcanic rocks increases the potential for mineral deposits within this region of the southern Rocky Mountains.

ACKNOWLEDGMENTS

The volcaniclastic rocks at Mt. Dingley were examined during co-operative field work on the Beaverfoot Formation by the Royal Tyrrell Museum of Palaeontology and the Geological Survey of Canada. G.B. Leech kindly provided copies of relevant parts of his field notes and discussed the interpretations of the field data. W.H. Fritz identified the trilobite, G.S. Nowlan searched etched residues for

conodonts, and B.S. Norford identified the corals. D.G. Cook and D.W. Morrow reviewed early drafts of the manuscript. The topographic names used in Figures 1 and 2 include names used on topographic maps and by the B.C. Parks Service and two informal names: Bear Lake (Fig. 1) due west of Ruault Lake, and Sparkle Ridge (Fig. 2) just south of Sparkle Lake.

REFERENCES

Cecile, M.P.
1982: The Lower Paleozoic Misty Creek Embayment, Selwyn Basin, Yukon and Northwest Territories; Geological Survey of Canada, Bulletin 335.

Cecile, M.P. and Norford, B.S.
1992: Ordovician and Silurian assemblages; in Geology of the Cordilleran Orogen in Canada, (ed.) H. Gabrielse and C.J. Yorath; Geological Survey of Canada, Geology of Canada (7th. edition), no. 4, p. 184-197, 210-217.

Dawson, K.M., Panteleyev, A., Sutherland Brown, A., and Woodsworth, G.J.
1992: Regional metallogeny, Chapter 19; in Geology of the Cordilleran Orogen in Canada, (ed.) H. Gabrielse and C.J. Yorath; Geological Survey of Canada (7th edition), Geology of Canada, no. 4, p. 709-768.

Helmstaedt, H.H., Mott, J.A., Hall, D.C., Schulze, D.J., and Dixon, J.M.
1988: Stratigraphic and structural setting of intrusive breccia diatremes in the White River-Bull River area, southeastern British Columbia; British Columbia, Ministry of Energy, Mines and Petroleum Resources, Paper 1988-1, p. 363-368.

Henderson, C.G.L.
1954: Geology of the Stanford Range of the Rocky Mountains, Kootenay District, British Columbia; British Columbia, Department of Mines, Bulletin 35.

Höy, T. and Carter, G.
1988: Geology of the Fernie W1/2 Map Sheet (and part of Nelson E1/2) (NTS 82G W1/2 and 82F E1/2); British Columbia, Ministry of Energy, Mines and Petroleum Resources, Open File Map 1988-14.

Leech, G.B.
1954: Canal Flats, British Columbia; Geological Survey of Canada, Paper 54-7.
1958: Fernie Map-area, west half, British Columbia, 82G W 1/2; Geological Survey of Canada, Paper 58-10 and Map 20-1958.
1960: Geology, Fernie (west half), Kootenay District, British Columbia; Geological Survey of Canada, Map 11-1960.
1979: Kananaskis, West Half (82J W1/2) Map-area; Geological Survey of Canada, Open File 634 (compiled with the assistance of R.I. Thompson).

Mott, J.A., Dixon, J.M., and Helmstaedt, H.
1986: Ordovician stratigraphy and structural style at the Main Ranges-Front Range boundary near Smith Peak, British Columbia; Geological Survey of Canada, Paper 86-1B, p. 457-465.

Norford, B.S.
1969: Ordovician and Silurian stratigraphy of the southern Rocky Mountains; Geological Survey of Canada, Bulletin 176.

Norford, B.S. and Jackson, D.E.
1989: Ordovician stratigraphy and graptolite faunas of the Glenogle Formation, southeastern British Columbia; Geological Association of Canada and Mineralogical Association of Canada, Program with Abstracts, v. 14, p. A28.

Pell, J.
1987: Alkaline ultrabasic rocks in British Columbia: carbonatitites, nepheline syenites, kimberlites, ultramafic lamprophyres and related rocks; British Columbia, Ministry of Energy, Mines and Petroleum Resources, Open File 1987-17.

Root, K.G.
1987: Geology of the Delphine Creek Area, southeastern British Columbia; Ph.D. thesis, University of Calgary, Calgary, Alberta.

Welbon, A.I. and Price, R.A.
1992a: Stratigraphic dating of fault systems of the central Hughes Range, southeast British Columbia (82G/12); British Columbia, Geological Survey Branch, Paper 1992-1, p. 21-26.
1992b: Geology of the central Hughes Range, British Columbia, NTS 82G/11, 12, 13, 14; British Columbia, Geological Survey Branch, Open File 1992-17.
1993: Geology of the Wild Horse River-Lussier River area, S.E. British Columbia, NTS 82G/11, 12, 13, 14; British Columbia, Geological Survey Branch, Open File 1993-7.

Geological Survey of Canada Project 910004

Author Index

NOTE TO CONTRIBUTORS

Submissions to the Discussion section of Current Research are welcome from both the staff of the Geological Survey of Canada and from the public. Discussions are limited to 6 double-spaced typewritten pages (about 1500 words) and are subject to review by the Chief Scientific Editor. Discussions are restricted to the scientific content of Geological Survey reports. General discussions concerning sector or government policy will not be accepted. All manuscripts must be computer word-processed on an IBM compatible system and must be submitted with a diskette using WordPerfect 5.0 or 5.1. Illustrations will be accepted only if, in the opinion of the editor, they are considered essential. In any case no redrafting will be undertaken and reproducible copy must accompany the original submissions. Discussion is limited to recent reports (not more than 2 years old) and may be in either English or French. Every effort is made to include both Discussion and Reply in the same issue. Current Research is published in January and July. Submissions should be sent to the Chief Scientific Editor, Geological Survey of Canada, 601 Booth Street, Ottawa, Canada, K1A 0E8.

AVIS AUX AUTEURS D'ARTICLES

Nous encourageons tant le personnel de la Commission géologique que le grand public à nous faire parvenir des articles destinés à la section discussion de la publication Recherches en cours. Le texte doit comprendre au plus six pages dactylographiées à double interligne (environ 1500 mots), texte qui peut faire l'objet d'un réexamen par le rédacteur scientifique en chef. Les discussions doivent se limiter au contenu scientifique des rapports de la Commission géologique. Les discussions générales sur le Secteur ou les politiques gouvernementales ne seront pas acceptées. Le texte doit être soumis à un traitement de texte informatisé par un système IBM compatible et enregistré sur disquette WordPerfect 5.0 ou 5.1. Les illustrations ne seront acceptées que dans la mesure où, selon l'opinion du rédacteur, elles seront considérées comme essentielles. Aucune retouche ne sera faite au texte et dans tous les cas, une copie qui puisse être reproduite doit accompagner le texte original. Les discussions en français ou en anglais doivent se limiter aux rapports récents (au plus de 2 ans). On s'efforcera de faire coïncider les articles destinés aux rubriques discussions et réponses dans le même numéro. La publication Recherches en cours paraît en janvier et en juillet. Les articles doivent être envoyés au rédacteur en chef scientifique, Commission géologique du Canada, 601, rue Booth, Ottawa, Canada, K1A 0E8.

Geological Survey of Canada Current Research, is released twice a year, in January and July. The four parts published in January 1994 (Current Research 1994- A to D) are listed below and can be purchased separately.

Recherches en cours, une publication de la Commission géologique du Canada, est publiée deux fois par année, en janvier et en juillet. Les quatre parties publiées en janvier 1994 (Recherches en cours 1994-A à D) sont énumérées ci-dessous et sont vendues séparément.

Part A: Cordillera and Pacific Margin
Partie A : Cordillère et marge du Pacifique

Part B: Interior Plains and Arctic Canada
Partie B : Plaines intérieures et région arctique du Canada

Part C: Canadian Shield
Partie C : Bouclier canadien

Part D: Eastern Canada and national and general programs
Partie D : Est du Canada et programmes nationaux et généraux